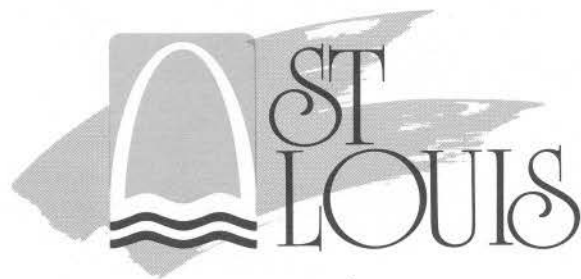


**GEOLOGICAL
SOCIETY OF AMERICA
1989
FIELD TRIP GUIDEBOOK**

*Gateway to the Future
. . . Frontiers in Geoscience*



Annual Meeting and Geoscience Exposition

St. Louis, Missouri

November 6-9, 1989



**MISSOURI DEPARTMENT OF NATURAL RESOURCES
DIVISION OF GEOLOGY AND LAND SURVEY
P.O. Box 250, Rolla, Missouri 65401**



**GEOLOGICAL
SOCIETY OF AMERICA
1989
FIELD TRIP GUIDEBOOK**

**Compiled by
Jerry D. Vineyard
and
W. Keith Wedge**



**MISSOURI DEPARTMENT OF NATURAL RESOURCES
DIVISION OF GEOLOGY AND LAND SURVEY
P.O. Box 250, Rolla, Missouri 65401
(314) 364-1752**

ISSN 1046-0594

Missouri Classification Number MO/NR. Ge 21:5

*Vineyard, Jerry D., and Wedge, W. Keith (compilers), 1989, GEOLOGICAL SOCIETY OF AMERICA 1989
FIELD TRIP GUIDEBOOK: Missouri Department of Natural Resources, Division of Geology and Land Survey,
Special Publication 5, 194 p., 63 figs., 3 tables.*

TABLE OF CONTENTS

	Page
Field Trip No. 1 ARCHAEOLOGICAL GEOLOGY AND GEOMORPHOLOGY IN THE CENTRAL MISSISSIPPI-LOWER ILLINOIS VALLEY REGION, ILLINOIS AND MISSOURI <i>Edwin R. Hajic et al.</i>	1
Field Trip No. 2 LATE PENNSYLVANIAN AND EARLY PERMIAN CYCLIC SEDIMENTATION, PALEOGEOGRAPHY, PALEOGEOLOGY, AND BIOSTRATIGRAPHY IN KANSAS AND NEBRASKA <i>Roger K. Pabian, and Robert F. Diffendal, Jr.</i>	5
Field Trip No. 3 DEPOSITIONAL ENVIRONMENTS AND GEOLOGY OF COALS OF LOWER PENNSYLVANIAN OF THE WESTERN PART OF THE APPALACHIAN BASIN AND THE EASTERN PART OF THE ILLINOIS BASIN IN KENTUCKY, INDIANA, AND ILLINOIS <i>James C. Cobb et al.</i>	7
Field Trip No. 4 GEOLOGY AND HYDROGEOLOGY OF THE PROPOSED NUCLEAR WASTE REPOSITORY AT YUCCA MOUNTAIN, NEVADA, AND SURROUNDING AREA <i>Steven R. Mattson et al.</i>	9
Field Trip No. 5 REGIONAL STRATIGRAPHY, FACIES, AND PALEOENVIRONMENTS IN THE CAMBRIAN OF SOUTHERN MISSOURI <i>Vincent E. Kurtz and James R. Palmer</i>	45
Field Trip No. 6 SURFACE EFFECTS OF THE 1811-1812 NEW MADRID EARTHQUAKE SEQUENCE AND SEISMO-TECTONICS OF THE NEW MADRID SEISMIC ZONE, WESTERN TENNESSEE, NORTHEASTERN ARKANSAS, AND SOUTHEASTERN MISSOURI <i>Eugene S. Schweigg, III and Randall W. Jibson</i>	47
Field Trip No. 7 HYDROGEOLOGY OF SHALLOW KARST GROUND-WATER SYSTEMS IN SOUTHEASTERN MISSOURI <i>James E. Vandike et al.</i>	69
Field Trip No. 8 "OLYMPIC DAM-TYPE" DEPOSITS AND GEOLOGY OF PRECAMBRIAN ROCKS IN THE ST. FRANCOIS MOUNTAINS TERRANE, MISSOURI <i>Eva B. Kisvarsanyi et al.</i>	87
Field Trip No. 9 CENTRAL UNITED STATES EARTHQUAKES AND THE ST. LOUIS UNIVERSITY SEISMIC NETWORK <i>Sean T. Morrissey</i>	89
Field Trip No. 10 THE GEOLOGIC STORY OF THE ST. LOUIS RIVERFRONT (A Walking Tour) <i>Arthur W. Hebrank</i>	91

CONTENTS (cont.)	Page
Field Trip No. 11 ENGINEERING GEOLOGY AND INDUSTRIAL MINERALS ASPECTS OF THE GREATER ST. LOUIS- ILLINOIS AREA <i>Paul B. DuMontelle et al.</i>	93
Field Trip No. 12 DIGITAL CARTOGRAPHY, MAP LIBRARY, AND DATA BASE MANAGEMENT SYSTEMS OF WASH- INGTON UNIVERSITY'S DEPARTMENT OF EARTH AND PLANETARY SCIENCES <i>Raymond E. Arvidson and Clara McLeod</i>	101
Field Trip No. 13 AEROSPACE CENTER, U.S. DEFENSE MAPPING AGENCY <i>Ron Blouse and Captain Dale Hotzaphel</i>	103
Field Trip No. 14 ENGINEERING AND ENVIRONMENTAL GEOLOGY OF THE ST. LOUIS AREA, MISSOURI <i>Mimi Garstang et al.</i>	105
Field Trip No. 15 TRANSITION FROM PASSIVE MARGIN TO FORELAND BASIN SEDIMENTATION: THE ATOKA FOR- MATION OF THE ARKOMA BASIN, ARKANSAS AND OKLAHOMA <i>David W. Houseknecht et al.</i>	121
Field Trip No. 16 QUATERNARY LOESS AND GLACIAL RECORD OF SOUTHWESTERN ILLINOIS <i>Leon R. Fallmer et al.</i>	139
Field Trip No. 17 CYCLIC STRATA OF THE LATE PENNSYLVANIAN OUTLIER, EAST-CENTRAL ILLINOIS <i>C. Pius Weibel et al.</i>	141
Field Trip No. 18 SELECTED ECONOMIC MINERAL DEPOSITS OF CENTRAL ARKANSAS <i>J. Michael Howard et al.</i>	171
Field Trip No. 19 MISSISSIPPI VALLEY-TYPE MINERALIZATION OF THE VIBURNUM TREND, MISSOURI <i>Richard D. Hagni and Raymond M. Coveney, Jr.</i>	185

Field Trip No. 1
(Guidebook Published Separately)

**ARCHAEOLOGICAL GEOLOGY AND
GEOMORPHOLOGY IN THE
CENTRAL MISSISSIPPI-LOWER ILLINOIS
VALLEY REGION,
ILLINOIS AND MISSOURI**

Edwin R. Hajic
Department of Geology
University of Illinois
Urbana, Illinois 61801

**Michael D. Wiant, Russel W. Graham, Bonnie W. Styles,
and Steven R. Ashler**
Illinois State Museum
Springfield, Illinois 62708

William R. Iseminger
Cahokia Mounds State Park
Cahokia, Illinois 62206

E. Arthur Bettis, III
Iowa Department of Natural Resources
Iowa City, Iowa 52242

and

Toby A. Morrow
Center for American Archaeology
Kampsville, Illinois 62053

FIELD TRIP SUMMARY

One of the richest concentrations of prehistoric cultural remains in the United States is found in the vicinity of St. Louis, in the central Mississippi Valley, where the Illinois River and Missouri River enter the Mississippi Valley within kilometers of each other. The region is known for excellent preservation of stratified Archaic sites, abundant Woodland habitation and mortuary sites, and the center of Mississippian period culture, the Cahokia Mounds. Although the region has a rich heritage of archaeological research extending back to the last century, sometimes including the rudiments of stratigraphy, it was not until the early 1970's and implementation of the "New Archeology" that geological involvement in archaeological research extended beyond brief site visits by interested or curious geologists. Much current archaeological research is focused on identifying changes in environments and cultural adaptations through the Holocene, and identifying settlement and subsistence patterns (cf. Brown, 1985; McMillan and Klipple, 1981). It is only in the last two decades that integrated archaeological and geological investigations have contributed significantly to understanding these relationships, patterns, and controlling factors. Prior to this time, it is fair to say Holocene deposits were undifferentiated (cf. Willman and Frye, 1970), probably as a result of the scale at which Quaternary geologists in the region were working. Little if any attempt was made to distinguish even basic characteristics or age of alluvial units in tributary or principal valleys. However, predictable and temporally constrained consequences and effects of the late Pleistocene and Holocene evolution of the central Mississippi and lower Illinois Valleys, on identification and interpretation of the archaeological record, are now emerging from these joint investigations.

The primary purposes of the trip are to (1) outline the late Pleistocene and Holocene depositional and geomorphic history of the central Mississippi and lower Illinois Valleys, and outline the prehistoric culture chronology and apparent cultural trends and patterns of the region; (2) critically discuss apparent cultural trends and patterns and a fluctuating resource base within geologic and paleoenvironmental contextual relationships; (3) examine the lithology, stratigraphy, and age of deposits at some of the most significant excavated sites that have

contributed to geoarchaeological understanding of the region; and, (4) discuss strengths and weaknesses of specific approaches and techniques used to decipher the interrelationships among geologic history and process, prehistoric cultures, and the archaeological record.

Exposures and cores will be examined to provide evidence and data to discuss the relationships of late Pleistocene and Holocene valley depositional and geomorphic history, paleoenvironments, archaeological site preservation, settlement patterns, and cultural adaptations. Stops in the American Bottom, central Mississippi Valley, are at Barnhart mastodon site, Jefferson County, Missouri (vertebrate paleontology, alluvial stratigraphy, late Pleistocene terraces, discussion of mastodon—Paleo-Indian association at the nearby Kimmswick site) (Graham, 1986; Graham et al., 1981); the deeply stratified Modoc Rock Shelter, a National Historic Landmark in Randolph County, Illinois (Early Archaic through Late Woodland archaeology, stratigraphy of alluvial fan, colluvial and eolian valley margin deposits, geochronology, vertebrate paleontology, southern American Bottom geomorphology) (Fowler and Winters, 1956; Fowler, 1959; Styles et al., 1983); and, the Cahokia Mounds State Park, a World Heritage site, Madison County, Illinois (Mississippian ceremonial center with largest prehistoric earthwork in the Western Hemisphere, northern American Bottom geomorphology and alluvial stratigraphy) (cf. Fowler, 1969; Fowler and Hall, 1975).

Investigations of lower Illinois Valley geology and archaeology suggest both similarities and differences to the central Mississippi Valley in the relationships between landscape evolution, paleoenvironments, archaeology, and archaeological contexts. The trip compares and contrasts these aspects between the two major valleys, emphasizing different relationships with successive cultural periods and between valley subenvironments. In the lower Illinois Valley stops include the deeply stratified Koster Site, listed on the National Register of Historic Places, Greene County, Illinois (Early Archaic through Mississippian archaeology, colluvial and alluvial fan stratigraphy and sedimentology, geochronology, paleoenvironmental change and cultural adaptation, Holocene valley margin sedimentation patterns and archaeo-

logical implications) (Houart, 1971; Brown and Vierra, 1983; Brown, 1985; Butzer, 1977; Wiant et al., 1983; Hajic, 1981, in press); the Twin Ditch site, Greene County, Illinois (Paleo-Indian — Early Archaic Thebes component archaeology, shallowly buried flood plain contexts, outline of lower Illinois Valley Holocene stratigraphy, sedimentology, and geomor-

phology) (Morrow, 1988); and, Sievers South Quarry, Calhoun County, Illinois (late Pleistocene Savanna [Deer Plain] Terrace and related glaciofluvial, fluvial, and lacustrine sediments and age, Mississippi River-Illinois River interactions, fluvial environments contemporaneous with regional Paleo-Indian occupation) (Hajic, 1986).

REFERENCES CITED

- Brown, J.A., 1985, Long-term trends to sedentism and the emergence of complexity in the American Midwest, in Price, T.D., and Brown, J.A., eds., Prehistoric hunter-gatherers: The emergence of cultural complexity: Academic Press, New York, p. 201-231.
- _____, and Vierra, R.K., 1983, What happened in the Middle Archaic? Introduction to an ecological approach to Koster Site archaeology, in Phillips, J.L., and Brown, J.A., eds., Archaic hunters and gatherers in the American Midwest: Academic Press, New York, p. 165-196.
- Butzer, K.W., 1977, Geomorphology of the lower Illinois Valley as a spatial-temporal context for the Koster Archaic site: Illinois State Museum Reports of Investigations No. 34.
- Fowler, M.L., 1959, Summary report of Modoc Rock Shelter: 1952, 1953, 1955, 1956: Illinois State Museum Reports of Investigations 8, Springfield, Illinois.
- _____, 1969, The Cahokia site, in Fowler, M.L., ed., Explorations into Cahokia archaeology: Illinois Archaeological Survey Bulletin 7, Urbana, Illinois, p. 1-30.
- _____, and Hall, R.L., 1975, Archaeological phases at Cahokia, in Brown, J.A., ed., Perspectives in Cahokia archaeology: Illinois Archaeological Survey Bulletin 10, Urbana, Illinois, p. 1-14.
- Fowler, M.L., and Winters, H., 1956, Modoc Rock Shelter: preliminary report: Illinois State Museum Reports of Investigations 4, Springfield, Illinois.
- Graham, R.W., 1986, Stratigraphy and taphonomy of faunal sequences at Barnhart, Missouri, in Graham, R.W., Styles, B.W., Saunders, J.J., Wiant, M.D., McKay, E.D., Styles, T.R., and Hajic, E.R., Quaternary records of southwestern Illinois and adjacent Missouri: Field Guide, American Quaternary Association, Ninth Biennial Meeting, Urbana, Illinois, p. 45-55.
- _____, Haynes, C.V., Johnson, D.L., and Kay, M., 1981, Kimmswick: a Clovis-mastodon association in eastern Missouri: Science, v. 213, p. 1115-1117.
- Hajic, E.R., 1981, Geology and paleopedology of the Koster archeological site, Greene County, Illinois: unpublished Masters thesis, Department of Geology, University of Iowa, Iowa City.
- _____, 1986, The late Wisconsin Deer Plain Terrace in the lower Illinois River Valley, in Graham, R.W., Styles, B.W., Saunders, J.J., Wiant, M.D., McKay, E.D., Styles, T.R., and Hajic, E.R., Quaternary records of southwestern Illinois and adjacent Missouri: Field Guide, American Quaternary Association, Ninth Biennial Meeting, Urbana, Illinois, p. 80-89.
- _____, in press, Stratigraphy and intravalley relationships of the Koster archaeological site: Center for American Archaeology, Kampsville Archaeological Center, Research Series.
- Houart, G.L., 1971, Koster: A stratified Archaic site in the Illinois Valley: Illinois State Museum Reports of Investigations No. 22.
- McMillan, R.B., and Klippel, W.E., 1981, Environmental changes and hunter gatherer adaptations in the southern Prairie Peninsula: Journal of Archaeological Science 8, p. 215-245.
- Morrow, T.A., 1988, Early Archaic tasks and technology at the Twin Ditch Site, Greene County, Illinois (abstr.): Midwest Archaeological Con-

ference, Thirty-third Annual Meeting, Program and Abstracts, p. 15.

Styles, B.W., Ahler, S.R., and Fowler, M.L., 1983, Modoc Rock Shelter revisited, *in* Archaic hunters and gatherers in the American Midwest: Academic Press, New York, p. 261-297.

Wiant, M.D., Hajic, E.R., and Styles, T.R., 1983, Napoleon Hollow and Koster Site stratigraphy:

Implications for Holocene landscape evolution and studies of Archaic Period settlement patterns in the lower Illinois River Valley, *in* Phillips, J.L., and Brown, J.A., eds., Archaic hunters and gatherers in the American Midwest: Academic Press, New York, p. 147-164.

Willman, H.B., and Frye, J.C., 1970, Pleistocene stratigraphy of Illinois: Illinois State Geological Survey Bulletin 94.

Field Trip No. 2

(Guidebook Published Separately)

**LATE PENNSYLVANIAN AND
EARLY PERMIAN CYCLIC SEDIMENTATION,
PALEOGEOGRAPHY, PALEOGEOLOGY, AND
BIOSTRATIGRAPHY IN
KANSAS AND NEBRASKA**

Roger K. Pabian and R.F. Diffendal
Conservation and Survey Division
University of Nebraska
Lincoln, Nebraska 68588-0517

Lynn Watney and Chris Maples
Kansas Geological Survey
Lawrence, Kansas 66044

Philip H. Heckel
University of Iowa
Iowa City, Iowa 52240

Ron West and R. Matsumoto
Kansas State University
Manhattan, Kansas 66502

Royal H. Mapes and Gene Mapes
Ohio University
Athens, Ohio 45701

Hans-Peter Schulze
University of Kansas
Lawrence, Kansas 66044

Ted Huscher
University of Nebraska
Lincoln, Nebraska 68588

Peter Holterhoff
University of Cincinnati
Cincinnati, Ohio 45202

and

R.M. Joeckel
University of Florida
Gainesville, Florida 32602

FIELD TRIP SUMMARY

The trip will begin with examination of classic Pennsylvanian cyclic depositional sequences in the Kansas City area. Participants will become familiarized with nearshore shales, transgressive limestones, offshore or "core" shales, and regressive limestones, and how to recognize these deposits in the field in the open marine facies belt. Emphasis will be placed on conodont occurrences in the Iola and Wyandotte cyclothems. In addition to observing classic cyclothems, participants will observe some dramatic facies and thickness variations over short distances.

Older cyclothems to be observed include the Swope and Dennis cycle, both of which show phosphatic, black core shales. Evidence for subaerial exposure at the top of the Swope cycle and minor cyclothems in the Dennis will also be examined. The Bronson escarpment that is held up by Dennis, Swope, and Hertha Limestones overlying Pleasanton prodeltaic shales will be examined. Facies changes in the Critzer Limestone into a thick unit, informally called the Bourbon flags, and a greatly thickened Pleasanton-Hertha interval farther down the Middle Pleasanton delta slope will also be observed.

Phylloid algal mound complexes in the Raytown, Captain Creek, and Stoner limestones, and facies changes along the north side of a contemporaneous marine channel in the Captain Creek Limestone will be observed. Positions of absent core shales will be demonstrated by conodont occurrences. Stanton channel facies near the axis of a marine channel and Plattsburg off-mound facies complete this portion of the trip.

The enigmatic stratigraphy, flora, and fauna of the Hamilton Quarries will be observed. This includes nonmarine and marginal marine vertebrate and invertebrate faunas and unusual lithologies and associations.

Tidal flat deposits with their associated sedimentary structures and trace fossils, trails, burrows, and lag accumulations are to be seen in the Doniphan Shale Member of the Lecompton Formation. These show, in detail, one portion of a large-scale transgressive-regressive cycle in dominantly non-marine to marginal marine facies.

A non-typical cyclothem sequence and facies mosaic that records numerous small-scale events occurs in the Pony Creek shale, and the Pennsylvanian-Permian boundary is observed in the last Kansas stop.

The oldest cyclothem to be seen in the Nebraska part of the trip contains a regressive limestone, the Howard. Younger cycles contain very poorly developed or no regressive limestones and this is possibly due to glaciation on the Gondwanaland paleocontinent. During this interval, the regressive sequences are generally marked by influxes of clastics that appear to be overlain by transgressive limestones. Regressive limestones again develop in Early Permian deposits, beginning in the Hughes Creek Shale member of the Foraker Formation. Excellent examples of paleosols in the Eskridge Shale of Nebraska are to be examined.

In all, the cyclothem in many different disguises will be observed.

Field Trip No. 3

(Guidebook Published Separately)

**DEPOSITIONAL ENVIRONMENTS AND GEOLOGY
OF COALS OF THE LOWER PENNSYLVANIAN
OF THE WESTERN PART OF THE
APPALACHIAN BASIN AND THE EASTERN PART
OF THE ILLINOIS BASIN IN
KENTUCKY, INDIANA, AND ILLINOIS**

**James C. Cobb, Coordinator,
Donald R. Chestnut, Jr., and Stephen F. Greb**
Kentucky Geological Survey
228 Mining and Mineral Resources Building
University of Kentucky
Lexington, Kentucky 40506-0107

Erik P. Kvale
Indiana Geological Survey
611 North Walnut Grove
Bloomington, Indiana 47405

Joe Devera and C. Pius Weibel
Illinois State Geological Survey
615 East Peabody Drive
Champaign, Illinois 61820

FIELD TRIP SUMMARY

The purpose of this guidebook is to present the results of recent research on the geology of Lower Pennsylvanian rocks in the Illinois and Central Appalachian Basins. The preparation of this field trip and guidebook was a cooperative effort of the Kentucky, Illinois, and Indiana Geological Surveys. This guidebook reflects the great interest in the origin of Lower Pennsylvanian strata represented by the Lee and Caseyville formations of the Central Appalachians and Illinois Basins.

There are two distinct parts to this field trip. Part one is a field excursion that explores the sedimentology of several outstanding exposures of Lower Pennsylvanian rocks on the western side of the Central Appalachian Basin. The exposures of Lower Pennsylvanian sandstones in the Central Appalachian Basin offer an exciting opportunity to observe a wide variety of sedimentary sequences, including bay fill, tidal estuary, sand flats, mouth bar, fluvial channels, mass flows, and peat swamps.

Part two is a field conference on the Illinois Basin. Many of the best exposures of Pennsylvanian rocks

in the Illinois Basin have been well covered by previous field trips. The long travel times between new exposures of interest were considered unacceptable for this 3-day field trip; therefore, new geological findings from outcrops and cores from the Illinois Basin will be brought to field trip participants in the form of a field conference. Historic New Harmony, Indiana, which was the center of geologic research in North America in the middle of the last century, will be the backdrop for the second part of the trip. In the Illinois Basin the role of marine depositional processes in the Lower Pennsylvanian has been a major focus of research, both in Illinois and in Indiana. New and exciting findings will be discussed, including the recognition of tidal depositional processes and a greater degree of marine influence than was previously recognized. Moreover, core and trace-fossil workshops will be presented.

We hope the combination of field and conference formats will give to all the trip participants the best possible geologic experience.

Field Trip No. 4

GEOLOGY AND HYDROGEOLOGY OF THE PROPOSED NUCLEAR WASTE REPOSITORY AT YUCCA MOUNTAIN, NEVADA AND THE SURROUNDING AREA

Steven R. Mattson

¹Science Applications International Corporation
Suite 407, 101 Convention Center Drive
Las Vegas, Nevada

David E. Broxton

²Los Alamos National Laboratory
Los Alamos, New Mexico

Bruce M. Crowe

³Los Alamos National Laboratory
Suite 860, 101 Convention Center Drive
Las Vegas, Nevada

Anthony Buono

⁴U.S. Geological Survey
Suite 860, 101 Convention Center Drive
Las Vegas, Nevada

and

Paul P. Orkild

⁵U.S. Geological Survey
Denver, Colorado

Field Trip Leader Affiliations:

⁶Consultant with Sandia National Laboratory, Albuquerque, New Mexico

⁷U.S. Bureau of Reclamation, Denver, Colorado

⁸Department of Energy, Yucca Mountain Project Office, 101 Convention Center Drive, Las Vegas, Nevada

⁹Lawrence Livermore National Laboratory, Livermore, California

¹⁰University of New Mexico, Albuquerque, New Mexico

¹¹U.S. Geological Survey, Menlo Park, California

¹²U.S. Geological Survey, Mercury, Nevada

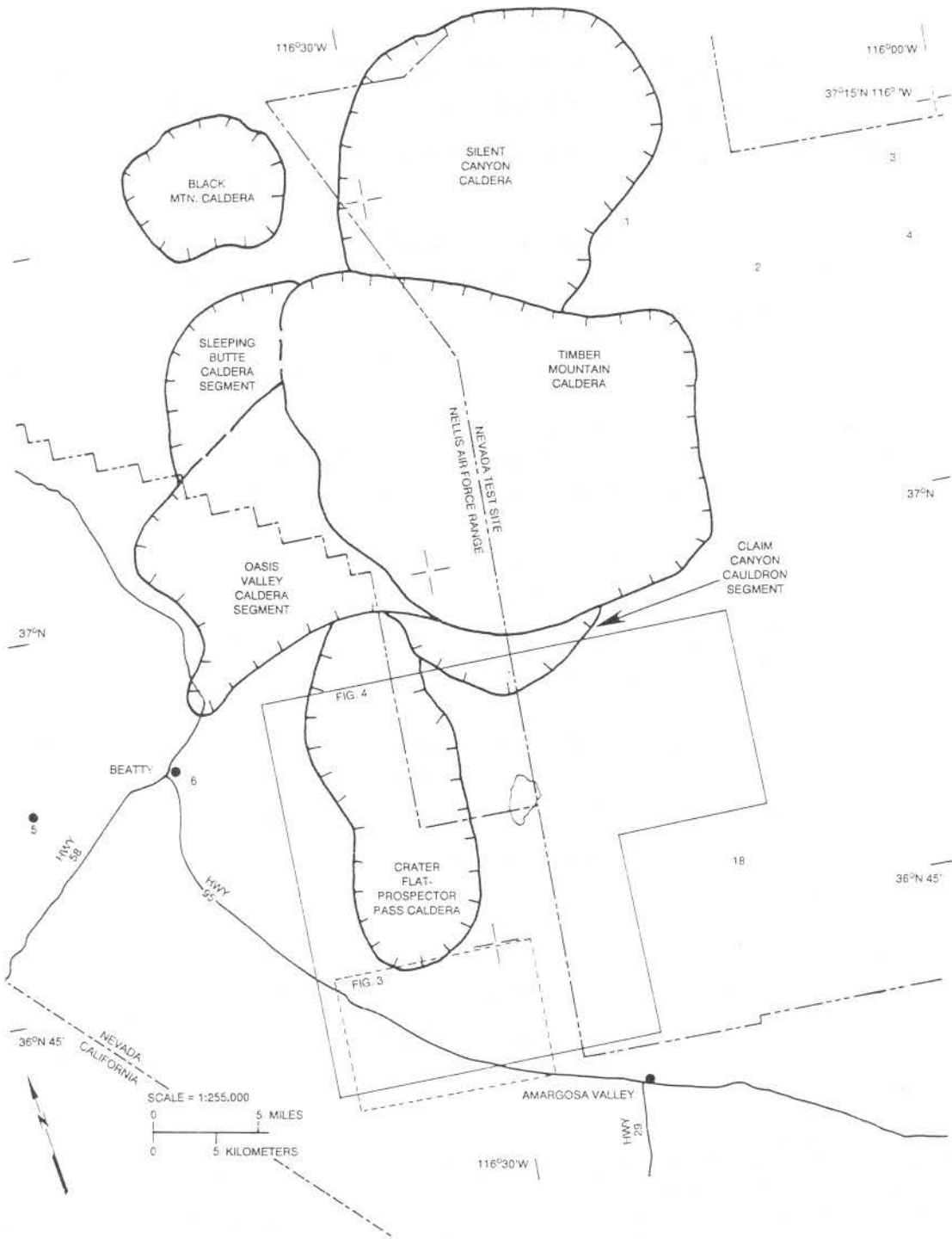


Figure 1 — Index map showing stop and caldera locations. Stop locations marked, except where they are found on other figures.

Day 1 INTRODUCTION

In late 1987 Congress issued an amendment to the Nuclear Waste Policy Act of 1982 which directed the characterization of Yucca Mountain, Nevada as the only remaining potential site for the nation's first underground high-level radioactive waste repository. The evaluation of a potential underground repository is guided and regulated by policy established by the Department of Energy (DOE), Nuclear Regulatory Commission (NRC), Environmental Protection Agency (EPA), Department of Transportation (DOT), and the U.S. Congress. The Yucca Mountain Project is the responsibility of the DOE. The purpose of this field trip is to introduce the present state of geologic and hydrologic knowledge concerning this site.

The potential high-level radioactive waste site at Yucca Mountain is approximately 160 km by road northwest of Las Vegas, Nevada, in an arid desert region. The location of Yucca Mountain, the surface site of the proposed underground repository, and other maps are shown on figure 1. The potential repository is beneath land controlled by three Federal agencies, principally the Bureau of Land Manage-

ment, but also by the DOE (Nevada Test Site) and the U.S. Air Force (Nellis Air Force Range). Yucca Mountain stratigraphy includes a sequence of ash-flow tuff, with minor bedded tuff and volcanoclastic sediments. The stratigraphic section for Yucca Mountain and the region are shown on table 1. The proposed repository horizon is in densely welded silicic ash-flow tuff of the lower Topopah Spring Member of the Paintbrush Tuff (Tertiary). The repository is designed to be in the unsaturated zone approximately 400 to 300 m below the land surface and has a planned area of approximately 6.5 km². The water table is approximately 300 to 200 m below the repository horizon.

Important geologic and hydrologic topics of concern for site characterization are 1) tectonics of the site, including the rates of recent faulting and the geometry of extensional faulting; 2) recurrence rates, location, volume, and nature of Pliocene and Quaternary basaltic volcanism as close as 8 km to the potential site; and 3) hydrologic processes occurring and expected to occur in the unsaturated

Formation, Member	Inferred Volcanic Center	General Composition	Approximate Age (m.y.)
Modified from Orkild, 1982; Dockery et. al., 1984; Carr, et. al., 1986.			
YOUNGER BASALTS	NUMEROUS	Basalt (hawaiite)	0.3-7
THIRSTY CANYON TUFF	BLACK MOUNTAIN CALDERA	Trachytic soda rhyolite	7-9
RHYOLITE OF SHOSHONE MTN.	SHOSHONE MOUNTAIN	High-silica rhyolite	9
BASALT OF SKULL MOUNTAIN, EMAD	JACKASS FLAT(?)	Quartz-bearing basaltic andesite	10
TIMBER MOUNTAIN TUFF Intracaldera ash-flow tuffs Ammonia Tanks Member Rainer Mesa Member	TIMBER MOUNTAIN CALDERA	Rhyolite to quartz latite	10-12
PAINTBRUSH TUFF Intracaldera ash-flow tuffs Tiva Canyon Member Yucca Mountain Member Pah Canyon Member Topopah Spring Member	CLAIM CANYON CALDERA	Rhyolite to quartz latite	12-13
WAHMONIA AND SALYER FORMATIONS	WAHMONIE-SALYER CENTER	Dacitic tuffs and lavas	13-13.5
CRATER FLAT TUFF (coeval Prow Pass Member Bullfrog Member Tram Member)	CRATER FLAT (?). Calderas buried under basalt and alluvium	Rhyolite (coeval with tuffs of Area 20)	13.5-14
STOCKADE WASH TUFF	UNCERTAIN (coeval with Crater Flat Tuff)	Rhyolite	14
BELTED RANGE TUFF Grouse Canyon Member Tub Spring Member	SILENT CANYON CALDERA	Peralkaline Rhyolite	14-15
TUFF OF YUCCA FLAT	UNCERTAIN	Rhyolite	15
REDROCK VALLEY TUFF	UNCERTAIN	Rhyolite	16
FRACTION TUFF	CATHEDRAL RIDGE CALDERA	Rhyolite	17
ROCKS OF PAVITS SPRING	DISPERSED (underlies Crater Flat Tuff)	Tuffaceous sediments	14-?
HORSE SPRING FORMATION	DISPERSED	Mostly sediments	30

Table 1 — Principal Cenozoic volcanic and sedimentary units.

and saturated zone at Yucca Mountain. The geologic and hydrologic processes of concern will be projected and modeled for the next 10,000 years based on the Quaternary geologic record (2.0 Ma). Many other geologic and hydrologic investigations are planned during site characterization over the next six years.

STOP 1: TIMBER MOUNTAIN CALDERA

F.M. Byers, Jr.², W.J. Carr⁶, and P. Orkild⁵.

The Timber Mountain-Oasis Valley caldera complex (fig. 1), the central and largest volcanic feature of the Miocene SW Nevada volcanic field (Byers et al., 1976a; Christiansen et al., 1977), consists of a thick sequence of volcanic rocks that has several major cycles of ash-flow tuff and lava of calcalkaline and peralkaline compositions (Broxton et al., 1989; Sawyer and Sargent, 1989). Tuff and lava cycles, which extend from about 16 to 9 Ma (Marvin et al., 1970), were erupted, not only from Timber Mountain caldera, but also from the contiguous Silent Canyon and Crater Flat-Prospector Pass caldera complexes (Carr, W.J. et al., 1986). A younger ash-flow tuff and lava sequence, also included in the volcanic field, was erupted from the Black Mountain and Stonewall Mountain calderas northwest of Timber Mountain (Noble et al., 1984). A review of volcanological investigations in the southwest Nevada volcanic field during the past 30 years is given in Byers et al. (1989).

A stop will be made to view the Timber Mountain caldera part of the complex at an overlook outside the caldera on the edge of Pahute Mesa (fig. 1). The Timber Mountain-Oasis Valley caldera complex is about 40 km in diameter (fig. 1). The caldera and its central resurgent dome are elongate northwestward. Topographically expressed caldera structures are related to the eruptions of the Timber Mountain Tuff, which consists of two widespread members, the Rainier Mesa (11.6 Ma) and the Ammonia Tanks (11.3 Ma).

Two major subsidences of the Timber Mountain caldera occurred: the first resulted from eruption of more than 1,250 km³ of the Rainier Mesa Member; the second from about 1,000 km³ of the Ammonia Tanks Member. The Rainier Mesa collapse was the larger of the two; the Ammonia Tanks caldera is mostly nested within the central part of the complex. During eruption of both members there was some

collapse of the Oasis Valley western segment of the complex (Byers et al., 1976b).

The resurgent dome of the caldera, about 15 km in diameter, is composed of more than 900 m of magmatically uplifted Ammonia Tanks, radially and longitudinally faulted (Carr and Quinlivan, 1968). The caldera moat contains caldera fill debris, reworked tuff, rhyolite lava, and Thirsty Canyon Tuff from the Black Mountain caldera, about 30 km to the northwest, and younger basalt (2.8 Ma).

Rim of Pahute Mesa

This stop provides a view of the eastern part of the Timber Mountain caldera and the exposure of the base of the Rainier Mesa Member of the Timber Mountain Tuff. About 4 km to the south, cuestas of Ammonia Tanks Member dip into the caldera, and the Stockade Wash Tuff and the Grouse Canyon Member of the Belted Range Tuff form much of the wall of the caldera and the valley floor between this viewpoint and the edge of the caldera (Byers et al., 1976a). On the skyline, about 30 km to the south, the rhyolite of Shoshone Mountain (about 9 Ma) overlies the southeastern caldera rim. Rainier Mesa is on the left (east), capped by the Rainier Mesa Member; resistant cap rocks below the mesa are the Rainier Mesa of the Timber Mountain tuff and the Tiva Canyon Member of the Paintbrush Tuff. Several faults in that area drop the section down toward the caldera.

A vitric bedded tuff, exposed in the adjacent roadcut, is overlain unconformably by about 3 cm of ash-fall and pyroclastic surge deposits of the Rainier Mesa Member. The Paintbrush Tuff is absent here and the Rainier Mesa Member thickens northward, and thereby indicates that the edge of Pahute Mesa was topographically high at the time of eruption of the Paintbrush and Timber Mountain Tuffs.

Just to the northwest of this viewpoint is the limit of another major volcano-tectonic feature (fig. 1), the Silent Canyon caldera (Orkild et al., 1968; 1969), which is largely beneath Pahute Mesa and is not topographically expressed. Although it is essentially hidden by younger tuff, it is well defined gravimetrically and by numerous drill holes. The major outflow tuff sheet from the Silent Canyon caldera is the Grouse Canyon Member of the Belted Range Tuff. Peralkaline tuff and lava associated with the

Silent Canyon caldera intertongue with calkalkaline tuff and lava, such as the bedded tuff exposed in the adjacent roadcut (tuffs of Area 20; table 1). Airfall and nonwelded tuff of the Crater Flat Tuff (Carr, W.J. et al., 1986) also occur in the Pahute Mesa area (Warren, 1983).

STOP 2: G-TUNNEL, RAINIER MESA, NEVADA TEST SITE

E.L. Hardin¹.

G-tunnel is a long entry adit and a complex of drifts driven into the side of Rainier Mesa, at about 2,034 m elevation. The tuff sequence comprises predominantly rhyolitic air-fall and welded/non-welded ash-flow tuff and volcanoclastic beds that have been tilted gently and overlain discordantly by the Rainier Mesa Member of the Timber Mountain Tuff. Suitability of the nonwelded units for excavation by mechanical and other means was a principal factor in the selection of the mesa for nuclear testing. Five underground nuclear tests were conducted in G-tunnel during the 1960's under the auspices of Sandia National Laboratories. These test drifts are now sealed and isolated from the frequented openings.

The ride into G-tunnel ends at the bottom of an incline that leads upward in the section into the welded Grouse Canyon Member of the Belted Range Tuff. The densely welded portion of this unit, about 13 m thick, is similar to the Topopah Spring Member at Yucca Mountain, in physical, thermal, and mechanical characteristics. Near the bottom of the unit are two distinct vitrophyres and a rubble zone 1.0 to 1.3 m thick. Several near-vertical normal faults trend in the direction of structural dip and can be traced from the Demonstration Drift in the welded Grouse Canyon to the parallel drifts below, in the nonwelded Tunnel Bed #5. Another interesting feature is a perched water reservoir created by a fault that downdropped the moderately fractured welded unit against underlying nonwelded beds. A small seep can be observed in the roof, about halfway up the long access incline. Perched water has not been detected at Yucca Mountain and is expected to be less common because the elevation is more than 610 m lower and the mean annual precipitation (~16 cm/yr) is less than half that at Rainier Mesa (35 cm/yr).

Since 1979, the G-tunnel underground facility (GTUF) has been used by Sandia National Laboratories (SNL) for Project-sponsored prototype field-scale testing. Experiments have evaluated the mechanical and thermomechanical rock mass response, including a heated block experiment, borehole heater tests, and a mine-by experiment. SNL has used the GTUF for refining equipment and instrumentation, including cutting slots in welded tuff using a chain saw, and high-pressure flatjack development and tests. Prototype experiments, including a thermal stress and rock mass response tests, are in progress.

In addition, other laboratories participating in the Project have used the GTUF for proof-of-concept or prototype testing, such as the crosshole VHF EM tomography experiment performed by Lawrence Livermore National Laboratory. The GTUF has been the location of a prototype testing program, whereby test methods specifically planned for the Yucca Mountain Exploratory Shaft Facility have been implemented. These prototype tests have included the following (some may still be underway): dry drilling and coring with dust hazard evaluation, hydrologic drill hole instrumentation, blast effects on instrumentation, intact fracture sampling methods, tracer diffusion test, high-pressure flatjack testing, engineered barrier (near-field) design testing, cross hole hydraulic and pneumatic flow testing, and photogrammetric mapping technology. Additional information on the latter two tests is provided below.

Prototype Underground Geologic Mapping at G-Tunnel

M.H. McKeown⁷, G.M. Fairer⁵, S.C. Beason⁷.

The U.S. Geological Survey (USGS) and the U.S. Bureau of Reclamation (USBR) are developing equipment and techniques for geologic mapping of exposures in the proposed Exploratory Shaft Facility (ESF) and associated drifts at Yucca Mountain. Prototype geologic mapping in G-tunnel is one of the pre-excavation tests of plans, equipment, and techniques that will be used in drift mapping; other prototype tests are planned for shaft mapping. For both kinds of mapping, a computerized analytical plotter will be used to provide complete and accurate

data. Information for use on the plotter will be obtained from a) close-range stereoscopic photographs, b) measurements and descriptions of features along detailed line surveys, and c) on-site observations by geologists. Maps and data-sets will be used to understand hydrologic characteristics of the unsaturated zone in which the proposed repository will be located.

During prototype testing, stereoscopic photographs were taken of washed-down surfaces in a selected segment of G-tunnel to provide film positives for close-range photogrammetric geologic mapping. Detailed line surveys were completed and additional geologic notes were recorded as necessary. Geologic mapping from combined data shows discontinuities such as faults, fractures, and breccia zones, as well as lithology and stratigraphy.

Six instruments developed for mapping include 1) stereogrammetric camera mount, 2) strike-rail goniometer, 3) right-angle prism goniometer, 4) laser goniometer, 5) prism beam splitter, and 6) geogyroscope. These new techniques and instruments were developed to increase underground mapping accuracy and precision.

Cross-hole Pneumatic and Hydraulic Prototype Test

R.C. Trautz⁵.

Cross-hole pneumatic and hydraulic tests, commonly referred to as interference tests in the petroleum industry, evaluate formation properties such as permeability and storativity, determine location of structural features such as faults and no-flow and recharge boundaries, and determine if reservoirs or fractured aquifers exhibit permeability anisotropy (Earlougher, 1977; Hsieh and Neuman, 1985; and Hsieh et al., 1985). Cross-hole testing is a methodology requiring at least one active (producing or injecting) well and at least one observation well. Gas or water is injected into or produced from an isolated test interval within a drill hole and formation response to fluid pressure change is monitored in nearby observation holes. Test results, namely active and observation well fluid pressures, temperatures and injection or production flow rates, are used to calculate permeability. Analysis of test results depends upon flow domain boundary conditions, the type of fluid injected into

the formation (water or gas), the formation saturation state, and the type of test conducted (e.g., steady state, transient, or instantaneous injection). The primary objective of the pneumatic and hydraulic cross-hole prototype test is to develop and/or refine field equipment (hardware), software, quality assurance technical procedures, and determine optimum testing configuration.

STOP 3: CLIMAX STOCK AND THE HIGH-LEVEL SPENT FUEL TEST

W.T. Hughes⁸ and S.R. Mattson¹.

The Cretaceous (93 Ma) Climax quartz monzonite and granodiorite intrudes Paleozoic and Precambrian sedimentary strata (Maldonado, 1977) at the northern end of Yucca Flat. The granodiorite is light gray to greenish medium gray and equigranular; it averages 28 percent quartz, 16 percent potassium feldspar, 45 percent plagioclase, and 9 percent biotite. The quartz monzonite is light to medium gray and is highly porphyritic with respect to potassium feldspar (5 percent) and quartz (10 percent); it has an average modal analysis of 28 percent quartz, 25 percent potassium feldspar, 40 percent plagioclase, and 6 percent biotite (Houser and Poole, 1961; Maldonado, 1977).

The Climax stock is part of the Oak Spring Mining District which produced mainly tungsten. Surface workings visible from the Climax headframe are part of the mining district that began operating in 1937. Because of conflicts with the nuclear testing program, the Atomic Energy Commission bought out the mining interests in the 1960's. Mineralization and hydrothermal alteration comprise clay minerals, feldspars, quartz, epidote, pyrite, scheelite, and chalcocopyrite. This mineralized area will be one of many considered in evaluating the potential of Yucca Mountain to contain economic resources (see Stop 13b).

Spent Fuel Test Climax

The Climax stock was the host rock for two nuclear weapons tests, Hard Hat and Piledriver, in the 1960's. From 1980 to 1983, as part of the Spent Fuel Test at Climax (SFT-C), spent fuel from a commercial nuclear reactor was emplaced in drifts mined from the previously developed Piledriver shaft. The SFT-C work was operated by DOE under the technical direction of Lawrence Livermore National

Laboratory. The main objectives of the SFT-C were to demonstrate and evaluate safe and reliable waste packaging, transport, and storage of nuclear spent fuel in a geologic medium, and demonstrate the ability to retrieve spent fuel canisters. In addition, the test provided information on the suitability of crystalline rock a repository host medium. The tests were conducted at the 427-m level, in quartz monzonite.

By 1980 the central emplacement drift and two parallel heater drifts had been constructed. For maximum stability they were perpendicular to the main joint set (N30°E) and parallel to another joint set (N60°W). Instrumentation emplaced in the heater drifts evaluated the effects of mining and heating of the central drift.

Eleven spent fuel canisters were emplaced in the central drift. At both ends of this drift, three heaters were alternated with the spent fuel canisters. The heat and radiation effects produced by spent fuel were compared to the effects of heat alone on the rock. Heaters were emplaced in the drifts on either side of the central drift to simulate, for the middle of the central drift, the interior environment of a large repository grid containing 8,000 canisters. Predictive models based on a 15.2 m (50 ft) square cell were compared to measurements made in the middle portion of the central drift.

Extensive testing included thermal load heater tests, natural cool down of the granitic rocks after waste removal, post-test sampling of the granitic rocks for detecting heat or radiation effects, geomechanical tests, and stress/strain instrumentation (e.g., Isherwood et al., 1982; Patrick et al., 1983; Montan and Bracken, 1984). The maximum canister temperature recorded was 145°C, and a peak rock temperature recorded was 85°C, both within 3-4° of modeling predictions. When installed, the canisters provided approximately 1,500 watts of thermal power and generated 650 watts of thermal power when removed. Studies of the rocks detected no changes in strength or deformability, and no increases in the number of microcracks in the rocks. Thermal expansion elevated the central drift floor 3 mm, close to predicted values.

Underground

The stainless steel spent fuel canisters were transported to the SFT-C site by surface transport

vehicle, then lowered down the spent fuel access hole into the cylindrical shielding cask on the underground rail car. The remotely operated rail car weighs 130,000 lbs, of which 80,000 lbs is due to the shielding cask. The rail car transported each canister along the drift and lowered it into one of eleven steel-lined boreholes, then covered the hole with a 5,000 lb concrete floor plug. An unshielded fuel assembly would deliver a lethal dose in less than one minute, but with the cement floor plug in place the radiation levels were less than background (approximately 0.02 millirem/hour) from the granitic rocks.

The water table at this location is 145 m below the drift. Water observed in the shaft results from condensation and/or surface infiltration. At one time, one of two parallel shear zones toward the end of the main emplacement drift produced about a gallon of water per day, which was pumped out because of instrumentation corrosion problems. Clay alteration is evident in the lower shear zone that did not seep water. Displacements of a few hundredths of a millimeter were observed across the shear zone during the experiments.

STOP 4, SEDAN CRATER

H.L. McKague⁹.

Both high explosive and nuclear cratering experiments were conducted principally during the period 1960 to 1970, as part of a program designed to assess the peaceful uses of thermonuclear devices. Several experiments of both types were conducted in alluvium and in bedrock in Frenchman Flat, Yucca Flat, and Pahute Mesa, the largest of which was the Sedan experiment in Yucca Flat.

The Sedan crater was formed on July 6, 1962, by a thermonuclear explosion (70 percent fusion, 30 percent fission) having a yield equivalent to 100 kt of TNT at a depth of 193.5 m. The seismic energy released was 2.45×10^{18} ergs, equivalent to an earthquake magnitude of 4.8. The maximum depth of the crater was 98.5 m; the average radius was 185.3 m. The crater volume was about 5×10^6 m³. The crater lip is 5.5 to 29 m above pre-shot levels. Ejecta were found as far as 1,770 m from ground zero. Observed overturning of the alluvium strata in the lower part of the lip is similar to that at the Teapot-Ess nuclear created crater, about 0.8 km

south of here (Shoemaker, 1960). Winograd (1980) proposed consideration of radioactive waste disposal in unsaturated alluvial deposits of the Great Basin. He discussed waste burial in Sedan crater as an example of the potential use of the unsaturated zone

for waste isolation. This paper was one of several factors that influenced the DOE decision, in the early 1980's, to consider exploration studies to include sites in the unsaturated zone, such as Yucca Mountain, Nevada.

DAY 2

STOP 5: DETACHMENT FAULTING AND MINERALIZATION AT BULLFROG MOUNTAIN, BULLFROG HILLS AREA

*Florian Maldonado*⁵.

The Bullfrog Hills, a structurally extended terrane, contains two detachment faults overlain by a complex system of listric and planar rotational normal faults (Ransome et al., 1910; Maldonado, 1985a, 1988; and Maldonado and Hausback, in press). The detachment faults separate three groups of rocks. The lower detachment fault separates metamorphosed upper Proterozoic rocks from overlying lower and middle Paleozoic clastic and carbonate rocks. The Paleozoic rocks are brecciated, commonly not metamorphosed, and the stratigraphic section is incomplete and highly attenuated. The upper detachment fault separates these Paleozoic rocks from overlying Miocene volcanic, volcanoclastic, and sedimentary rocks. The Miocene and Paleozoic rocks are allochthonous relative to the underlying metamorphic rocks and will be referred to as upper and lower plates, respectively.

Upper plate rocks form most surface exposures and dip moderately to steeply into the upper detachment fault, or, where the lower plate has been tectonically removed, into the lower detachment fault. Upper plate rocks are broken, tilted, and repeated in blocks bounded by normal faults that terminate against, or flatten and merge into the upper detachment fault. Normal faults in the upper plate are listric faults that form imbricate, oval, and horseshoe map patterns and planar rotational faults that form imbricate map patterns. These upper-plate faults have extended the upper plate more than 100 percent and possibly more than 275 percent locally. The dip direction of the normal faults (predominantly west) and the repetition and dip direction (predominantly east) of the Miocene rocks indicate that extension, at least of the upper plate, was west-northwest and occurred between about 8 and 10

Ma and not younger than about 7.5 Ma as previously indicated (Maldonado, 1985a, 1988). This constraint on extension is based on the age of the youngest deformed unit, a latite lava flow dated at 10 Ma (Maldonado and Hausback, in press) and the oldest undeformed unit, a basalt lava flow dated at 8 Ma (Maldonado, in press).

The stop at Bullfrog Mountain shows a partial section of the Miocene succession underlain by the upper detachment fault. The mountain, a rotated block, contains essentially conformable hydrothermally altered strata dipping about 40° to 60° into the upper detachment fault. The block forms an oval map pattern, bounded on the west and below by the upper detachment fault and on the east by a normal fault that separates the Bullfrog Mountain block from the block eastward by about 3,000 m of apparent stratigraphic separation. This fault is interpreted to merge into or be truncated by the upper detachment fault. The lower plate, below the upper detachment fault, is comprised of slivers of brecciated Paleozoic rocks. Below the Paleozoic rocks the lower detachment fault separates Paleozoic rocks from Proterozoic metamorphic rocks. However, on the southwest edge of Bullfrog Mountain, Paleozoic rocks have been tectonically eliminated; therefore, Miocene rocks lie on metamorphic rocks. The metamorphic rocks are penetratively foliated and lineated and consist of mylonitic quartzofeldspathic gneiss, biotite schist, marble, and amphibolite dikes of amphibolite facies (Carr and Monsen, 1988). These rocks have been correlated with the late Proterozoic Johnnie (?) Formation (B.W. Troxel, oral commun., 1986).

Gold mineralization at Bullfrog Mountain is in a quartz vein complex in the Miocene succession; it has been referred to as the "Original Bullfrog Vein" (Ransome et al., 1910). This complex, truncated by the upper detachment fault, is intensely brecciated, and contains disseminated gold along with frag-

ments of the Eleana Formation, quartz latite lava flow(?), and the Lithic (?) Ridge Tuff. Gold along faults at other localities in the upper plate suggests that some gold mineralization and hydrothermal alteration are probably coeval with extension.

STOP 6: NORTHERN BARE MOUNTAIN, FLUORSPAR CANYON

Yucca Mountain Project Staff.

Bare Mountain exposes a faulted, folded, generally northward dipping section of upper Proterozoic and Paleozoic miogeoclinal sedimentary rocks (figs. 1 and 3) (Carr and Mosen, 1988). Bare Mountain is bordered on the east by Crater Flat, filled with as much as 3.5 km of Cenozoic volcanic and sedimentary rocks (Ackermann et al., 1988), on the southwest by the northern Amargosa Desert, a broad alluvial valley filled by less than 1 km of Cenozoic deposits (Healey and Miller, 1972), and to the north by a complexly faulted terrane of middle Miocene volcanic and sedimentary rocks (Carr and Mosen, 1988).

The Fluorspar Canyon fault forms the saddle on the south flank of Beatty Mountain (middle Miocene rocks) and is near the northwest flank of Bare Mountain (upper Proterozoic and Cambrian meta-sedimentary rocks) (Mosen, 1983). The fault has been interpreted by Carr and Mosen (1988) as part of a regional low-angle normal fault system that propagated to the surface during the late Miocene. The regional low-angle normal fault system extends from the Bullfrog Mountain area (Stop 5) eastward to the head of Fluorspar Canyon. Whether the Fluorspar Canyon fault continues to the east is questionable (Carr and Mosen, 1988). Additional studies of the structural setting of this area will occur as site characterization of Yucca Mountain continues.

STOP 7: STEVES PASS, CRATER FLAT OVERLOOK

Yucca Mountain Project Staff.

The eastern flank of Bare Mountain and the western flank of Yucca Mountain are visible from this location. Based on gravimetric and magnetic data, Crater Flat has been interpreted as an asymmetric graben extending southward into the Amargosa Desert (Synder and Carr, 1984). The conspicuous surface expression of this graben is

confined to Crater Flat (Carr and Mosen, 1988). The structure of Crater Flat and western Yucca Mountain has been variously interpreted to be either the result of movement along faults of the Crater Flat-Prospector Pass caldera (Carr, W.J. et al., 1986) or as part of a listric and normal fault pattern that soles into low-angle normal faults (Scott, 1986, 1988; Scott and Rosenbaum, 1986).

To the east, Yucca Mountain is a remnant of a volcanic plateau that was subsequently dissected by erosion along numerous steeply westward-dipping faults (see Stop 13a for discussion). Westward, Bare Mountain is bounded by the north-south trending Bare Mountain fault, which has been active during the Quaternary (Reheis, 1988). In many locations, the Bare Mountain fault dips steeply eastward and has components of dip-slip and right-lateral strike slip (Reheis, 1988; Carr and Mosen, 1988). The gold producing Sterling Mine is on the eastern flank of Bare Mountain, at or near the intersection of two thrust faults (Tingley, 1984; DOE, 1988) (see Stop 13b) that displace miogeoclinal Paleozoic strata. The volcanic centers of Little Cones, Red Cone, Black Cone, and northernmost cone are visible from south to north, respectively, forming part of a northwestern trend of basaltic volcanism (see Stops 10 and 13b).

STOP 8: SPRING DEPOSITS OF THE NORTHERN AMARGOSA DESERT

W.C. Swadley⁵.

Marl and limestone exposures along U.S. 95, near the north end of the Amargosa Desert, are part of a widespread group of similar deposits over much of the Amargosa Desert basin. These outcrops are the northernmost of a discontinuous band of marl, siltstone, and limestone exposures that extend about 60 km southeastward. They have been attributed to deposition in a Pliocene-Pleistocene lake, informally called Lake Amargosa (Swadley and Carr, 1987). However, the deposits are more likely the result of deposition in discontinuous marshes and small ponds fed by carbonate-rich springs similar to springs at Ash Meadows in the southern part of the basin (Hay et al., 1986). The deposits are thus analogous to the spring and marsh deposits of Las Vegas Valley (Quade, 1986).

The spring deposits crop out north of U.S. 95, approximately 19 km northwest of the town of

Amargosa Valley (formerly Lathrop Wells). Most of the exposure consists of pale-yellowish-gray to light-greenish-gray marl that weathers white to very light gray. It is sandy, locally tuffaceous, thin bedded to massive, and weathers to low rounded mounds. Several prospect pits offer good exposures. The marl contains vertebrate remains (including fragments of mammoth teeth), gastropods, plant stems, and diatoms. Downslope from the conspicuous white marl exposures, an exposure of light-gray, hard, fine-grained, crystalline Pliocene or Pleistocene, limestone that weathers yellowish gray. The limestone forms low ledges that are partly covered by alluvium and windblown sand. No spring vents have been recognized in the deposits. The exposures are surrounded and partly covered by late Holocene alluvial deposits derived from the nearby hill slopes and the stratigraphic relation of the spring deposits to the underlying bedrock is unknown. A sinkhole-like opening in coarse fan alluvium 0.3 km northwest of the outcrop appears to be fault related, but no connection between this feature and a possible fault controlling the location of the spring deposits has been established.

Spring deposits north of U.S. 95 are similar in lithology and occurrence to more extensive claystone and carbonate deposits of the Amargosa Flat and Ash Meadows areas. These two areas were studied by Hay et al. (1986) who described deposits of calcareous claystone, chalky to crystalline limestone, and sandy, silty, and tuffaceous mudstone. Based on detailed field relations and chemical and X-ray diffraction clay mineral analyses, they concluded the sediments are a mixture of playa deposits and marsh and pond deposits. Carbonate minerals and various Mg-clays constitute much of the deposits precipitated from ground water supplied by fault controlled springs. The ponds and marshes were fresh to slightly saline. Radiometrically determined ages of volcanic-ash interbeds range from 3.2 to 2.4 Ma.

Correlation of deposits north of U.S. 95 with those analyzed by Hay et al. (1986) at Amargosa Flat is based on similarities in lithology and the presence of similar deposits exposed discontinuously in the area between these two exposures. In the southern part of the Lathrop Wells Quadrangle (Swadley, 1983), spring-related deposits are well exposed and are continuous with those of the Amargosa Flat area. Correlation has been extended northwestward

through the Big Dune Quadrangle (Swadley and Carr, 1987), but it is somewhat less certain because of increasingly larger gaps between exposures.

Age of the northern deposits is indicated by the presence of vertebrate remains (*Mammuthus* sp.) that C.A. Repenning (U.S. Geological Survey, written commun., 1982) considers to be less than 2 Ma. This age is younger than the radiometric ages reported by Hay et al. (1986) and suggests that spring-related deposition sites may have occurred at various times over much of the Amargosa basin during the late Pliocene and Quaternary. Similar spring deposits are currently forming in the Ash Meadows area, where several large springs discharge carbonate-rich ground water.

STOP 9: TYPE SECTION OF THE CRATER FLAT TUFF

W.J. Carr⁶ and F.M. Byers, Jr.²

The main stratigraphic and lithologic units (fig. 2) from the base of the exposure upward are (1) vitric ash fall tuff, containing a thick boulder fluvial and/or debris-flow deposit; (2) Bullfrog Member of the Crater Flat Tuff; (3) vitric nonwelded to partially welded unit of the Bullfrog resting in a scour or pocket on the main Bullfrog; (4) a coarse breccia of welded Bullfrog clasts; and (5) the Prow Pass Member of the Crater Flat Tuff. The lowest member, the Tram, is not present here. This is the only section where the Crater Flat Tuff is essentially unaltered.

The lowest exposed volcanic unit comprises several hundred feet of very light-gray bedded ash, and reworked tuff. Some of the tuff contains conspicuous biotite and hornblende and may be related to a group of dacitic to rhyolitic lavas that mostly underlie the Crater Flat Tuff in the Crater Flat region (Carr, W.J. et al., 1986). One such lava, a quartz latite, in this general stratigraphic position, is exposed 9 km northwestward (unit Tql, fig. 2; after Swadley and Carr, 1987).

In the upper part of the vitric bedded tuff unit is a resistant, pale yellowish-green lens of crudely bedded coarse to massive bouldery gravel about 30 m thick. The clasts are rounded, as much as 2 m in diameter, and apparently consist of only three rock types: porphyritic and non-porphyritic densely welded tuff of the Grouse Canyon Member of the Belted Range Tuff, and welded tuff of the Tram

Member of the Crater Flat Tuff. The tuff matrix contains small pumice fragments, especially in the lower part. The closest Grouse Canyon exposures are more than 50 km northward; no Grouse Canyon is present in the deep drill holes at Yucca Mountain, 20 km northward. To account for transport of such large boulders over a long distance, Carr, W.J. et al. (1986) suggested the deposit was a catastrophic debris flow. However, the rounded clasts, the locally pumiceous matrix, and the crude bedding may indicate a fluvial origin.

The Crater Flat Tuff is well exposed in the canyon about 0.8 km east of the vitric tuff described above. It consists of three compositionally similar ash-flow tuff members characterized by subequal modal plagioclase, sanidine, and quartz, with minor biotite, hornblende, and rare clinopyroxene (Byers et al., 1976b; Carr, W.J. et al., 1986). Quartz is strongly resorbed in the Bullfrog and Prow Pass Members. At this locality the Tram Member is not present.

The Bullfrog Member has a prominent dark vitrophyre about 5 m thick near the base, where welding increases abruptly upward. The member is moderately welded and devitrified in much of this section and is about 150 m thick. The average of four K-Ar age determinations of the Bullfrog, obtained from biotite and sanidine, is 13.5 Ma.

Two unusual units are present near the head of the canyon, where the top of the Bullfrog is well exposed. A lens of gray, mostly vitric nonwelded ash-flow tuff of Bullfrog composition is in a large scour or pocket directly on top of the welded devitrified Bullfrog. This unit resembles a thickened nonwelded vitric top that is occasionally found preserved as a thick cap on a normally zoned ash-flow. Here the unit is unusually thick and has a sharp lower contact. In equally sharp contact above the gray vitric tuff is a lens of purplish-gray monolithologic breccia that is exposed laterally for nearly 2 km (fig. 2). The breccia blocks consist entirely of welded Bullfrog. The blocks are unlike any other Bullfrog exposed in the area. Carr (1988) suggested the breccia slid into this position, perhaps caused by tectonic movements accompanying nearby caldera collapse.

Above the breccia is a thin bedded tuff overlain by about 50 m of orange-brown and cavernous-weathering Prow Pass Member of the Crater Flat Tuff. The Prow Pass at this location is a simple

cooling unit that is nonwelded to partially welded. It has fewer mafic phenocrysts than the Bullfrog and contains minor orthopyroxene and rare to sparse biotite and hornblende. The Topopah Spring and Tiva Canyon Members of the Paintbrush Tuff are on the ridge above the Prow Pass.

On the basis of topography, structure, geophysics, and other evidence (fig. 2; Carr, W.J. et al., 1986), the source of the Crater Flat Tuff was the Crater Flat-Prospector Pass caldera complex, the southern edge of which is about 3 km north of this locality. Other workers (e.g., Scott, 1988) interpret the basin under Crater Flat as a basin-range graben underlain by a detachment fault. Two drill holes in central Crater Flat show that the structural depression is mostly older than the Paintbrush Tuff (Carr, 1988), but the holes are not deep enough to resolve the structural genesis of Crater Flat.

STOP 10: LATHROP WELLS VOLCANIC CENTER

Bruce M. Crowe³, F. Perry¹⁰, S. Wells¹⁰, L. McFadden¹⁰, C. Harrington³, D. Champion¹¹, B. Turrin¹¹.

The Lathrop Wells volcanic center, the youngest of a group of five small volume Quaternary basaltic centers in and adjacent to Crater Flat (fig. 3), is 20 km south of the Yucca Mountain exploration block. It is an asymmetric (elongate NW-SE) scoria cone flanked eastward, north and south, by blocky aa lava flows.

The age of the Lathrop Wells center has proven problematic. An original age estimate of 270 ka (DOE, 1986) was based on K-Ar age determinations from the lava flows and from a bomb from the summit of the main cone. This age appeared inconsistent with the degree of preservation of the main scoria cone and some of the lava flow units. It was originally assumed the center formed during a single pulse of magmatic activity (monogenetic volcanic center). Lava flow age determinations were believed to indicate the age and duration of volcanic activity; however, subsequent detailed work shows this is incorrect.

The volcanic center has been newly mapped at a scale of 1:4,000 (Crowe et al., 1988). There are at least two to as many as four episodes of eruptive activity from spatially separate vents and fissure systems. Local soils with partial horizon development

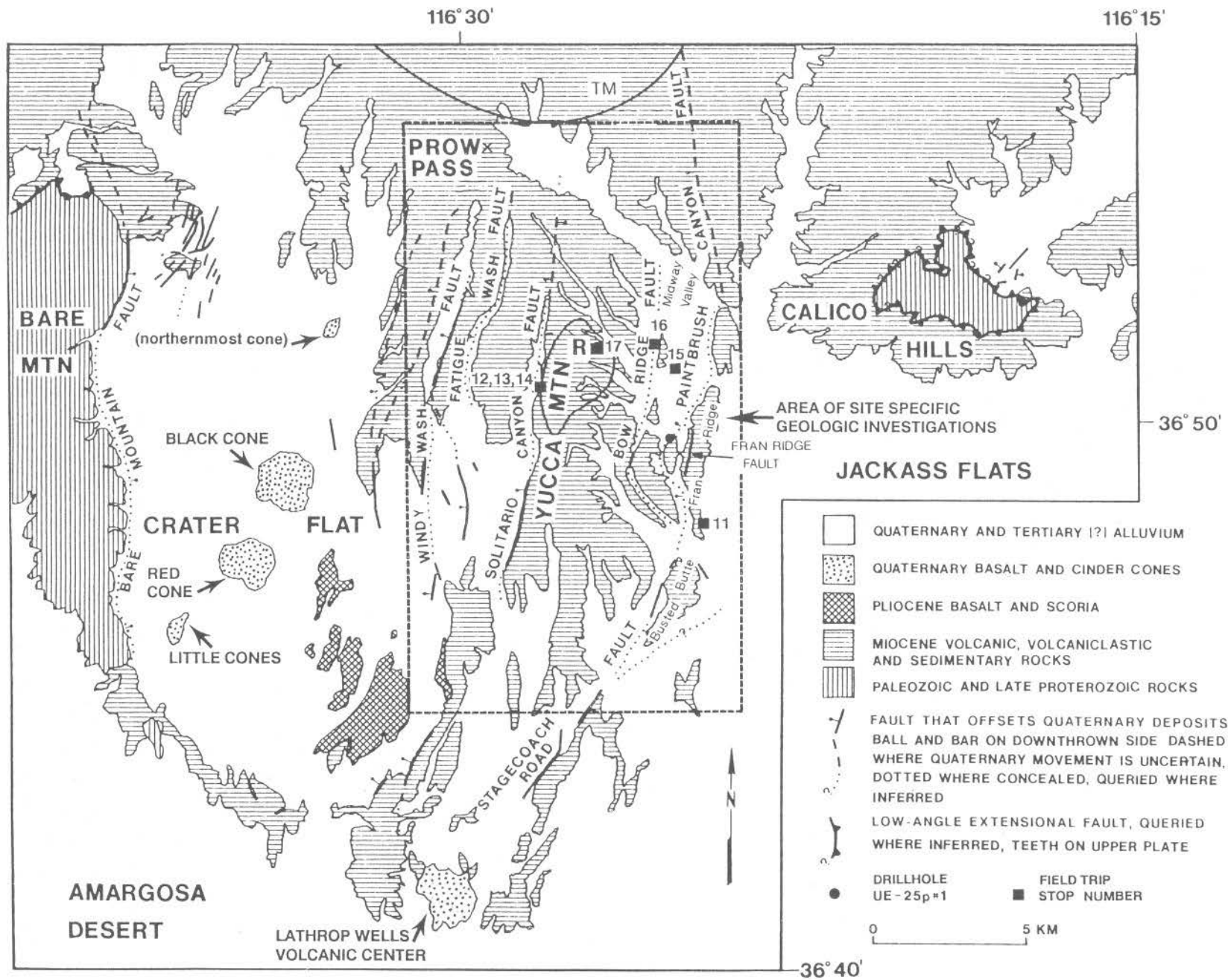


Figure 3 — Generalized geologic map of Yucca Mountain and vicinity showing selected stratigraphic and structural framework features (TM, approximate southern boundary of the Timber Mountain-Oasis Valley caldera complex; R, approximate extent of the candidate repository. Geology modified from Swadley et al. (1984).

between eruptive units and the differing degrees of geomorphic preservation of the deposits require a lengthy eruptive history. Analysis and comparison of geomorphic and pedologic properties of the Lathrop Wells scoria cone with those of the Cima volcanic field (Wells et al., 1988) indicate the Lathrop Wells cone is most similar to the youngest cone of the Cima field, which is about 15 ka, based on various direct and indirect dating techniques. Features indicative of a Late Pleistocene or Holocene age of the final eruptions of the Lathrop Wells volcanic center include 1) cone slopes near the angle of repose (29°), 2) the absence of development of a cone-slope apron at the base of the cone, 3) paucity of rilling and mass wasting features on cone slopes, and 4) poor horizon development of soils on the tephra. The major uncertainty in calibrating the age of the final scoria eruptions of the scoria cone are the rates of erosional degradation and soil formation in an area of high eolian flux. Rock varnish studies show lava flow surfaces contain heavy mineral components derived from volcanic ash in the upper varnish sequence. The position and presence of minerals is consistent with introduction from a young scoria-fall eruptive event (Harrington, 1988).

Studies of the direction of remnant magnetism of volcanic units of the Lathrop Wells center show two distinct field directions. The north and northeast lava flows have a field direction that differs from the older fissure system that is inferred as the source of the southwest lava flows. A currently unresolved inconsistency is the pole position for bombs from the main scoria cone rim. This preliminary field direction appears to match that of the older fissure system. There are several possibilities for these data: 1) the preliminary field direction for bombs from the cone rim is incorrect, a possibility that will be clarified with additional data; 2) field directions of the cone rim and older fissure units are identical, but they represent separate eruptive events; and 3) the measured field direction from the cone rim is the same event as the older fissure system, a matter that requires a complex cone growth history.

Sixteen new K-Ar age determinations and re-evaluation of existing K-Ar data indicate the lava flows are younger by at least a factor of two than the reported age of 0.27 Ma. Weighted averages of 34 K-Ar age determinations from the lavas that correspond to the two distinct magnetic field

directions yield 0.133 ± 0.010 Ma for the younger flow unit and 0.115 ± 0.012 Ma for the older flow unit. The ages are inverted from the observed stratigraphic relations, but are identical at the 95 percent confidence level. Based on analysis of the reported analytical precision, differences in ages between the two lava flow units are less than or equal to approximately 0.030 Ma. K-Ar ages are consistent with the uranium trend chronology and stratigraphy of the surficial alluvial units in the Yucca Mountain region (Swadley et al., 1984); however, geomorphic preservation of the younger flow unit and the topographic position of the younger flows compared to modern alluvial surfaces are permissive with a significantly younger age than indicated by K-Ar. The K-Ar ages of the lava flows of the Lathrop Wells center will be compared with studies of other isotopic systems: U-Th disequilibrium measurements using solid source mass spectrometry, $^4\text{He}/^3\text{He}$ surface exposure ages, thermal luminescence, and $^{40}\text{Ar}/^{39}\text{Ar}$ measurements.

A new finding from the study of the Lathrop Wells volcanic center is the complex eruptive history and long duration for activity at this small volume center; these observations are supported by preliminary studies of two other Quaternary centers (Little Black Peak and Hidden cones) 47 km northwest of Yucca Mountain. All the centers exhibit the following features: 1) multiple eruptions from closely spaced volcanic vents, 2) intermittent eruptive activity over time spans exceeding 10^5 yrs, and 3) decreased magma volume and increase in the ratio of scoria/lava of successive eruptions. Preliminary studies of other Quaternary volcanic centers in the Yucca Mountain region, in the Lunar Crater, and Cima volcanic fields indicate that small-volume centers commonly exhibit the same patterns of eruptive activity. Polycyclic volcanic eruptions may be a common characteristic of basaltic centers of the southern Great Basin.

These observations imply several significant implications. First, petrologic studies of small volume basaltic centers are generally incomplete. Samples are normally collected and analyzed only for lava flows, because these rocks tend to be less vesicular and less altered; hence, the complete range of magma compositions in the centers is unstudied. Second, repeated basalt magma eruption from adjacent vents requires structural control of

subsurface magma feeder pathways; this suggests the initial magma pulse may create a preferential subsurface pathway for later pulses. Third, the long duration and complex eruptive history of the volcanic

centers must be considered in assessing potential volcanic hazards to the proposed Yucca Mountain repository.

DAY 3

STOP 11: GEOLOGIC FEATURES AT FRAN RIDGE

R.W. Spengler⁵ and W.R. Page⁵.

Natural and man-made exposures at Fran Ridge provide opportunities to study in detail lithologic and structural characteristics of the Paintbrush Tuff, particularly the Topopah Spring Member, near the eastern margin of a 230 km² area, referred to as the area of site specific geologic investigations (fig. 3). Fran Ridge is one of several north-trending east-tilted ridges typical of the Yucca Mountain area (fig. 3). Jackass Flats and Midway Valley are east and west of the ridge, respectively. Busted Butte is the conspicuous outcrop directly southward.

Stratigraphy

The Paintbrush Tuff comprises the Topopah Spring, Pah Canyon, Yucca Mountain, and Tiva Canyon Members, in ascending order (Byers et al., 1976b). The Topopah Spring Member reaches a maximum thickness of about 350 m beneath the northern half of the proposed repository site (Spengler and Fox, in press). At Fran Ridge, the member is about 250 m thick, based on interpolation between boreholes. At this stop, only 30 m of the upper part of the member is exposed. Southward, along the northern flank of Busted Butte, a nearly complete section of the cliff-forming Topopah Spring and Tiva Canyon Members, separated by a slope-forming interval of bedded tuff, can be seen. At Fran Ridge this bedded tuff sequence is about 14 m thick and mostly comprises ash-fall material.

Almost all the rock within the Topopah Spring Member is moderately to densely welded, except for zones a few meters thick, near the top and base, which are nonwelded to partially welded. In ascending order, the member includes three distinctive and mappable depositional units within the site area: lithic-poor rhyolite, lithic-rich rhyolite, and quartz latite caprock (Spengler et al., 1987). The rhyolite units are phenocryst poor and distinguishable on the basis of type, size, and abundance of lithic

clasts. Within the site area, the lithic-poor rhyolite is the thickest depositional unit and can be divided into five mappable zones. Except for a basal vitric zone, mappable zones are primarily differentiated on the basis of relative abundance of lithophysal cavities and include, in ascending order, the lower non-lithophysal, lower lithophysal, middle nonlithophysal, and upper lithophysal zones. Lithophysal cavities, generally 1-3 cm in diameter, formed during early stages of ash-flow tuff crystallization. The cavities increase the bulk porosity of the rock and, in the proposed repository area, may influence the thermal response, stability, and hydrologic characteristics of the rock mass.

Rock exposed at the drill collar of a horizontal hole UE25-H1, continuously cored in a westerly direction, is the middle nonlithophysal zone and contains few lithophysae (Norris et al., 1986). The proposed repository would be excavated in rock lower in the section, but which has similar physical and structural characteristics.

Above the drill pad, lithophysae increase progressively. At Fran Ridge, the lithophysae-rich rock, about 11 m thick, is referred to as the upper lithophysal zone. Volumetric estimates of lithophysal cavities, derived from core holes along a north-south section through the proposed repository, suggest that most rock within the upper lithophysal zone consistently contains between 20 percent and 30 percent lithophysal cavities.

Up slope, the uppermost depositional unit, a quartz latite caprock forms a conspicuous bench; it typically contains abundant phenocrysts (5 percent near the base to about 15 percent near the top).

Structural Characteristics, Faults

The western flank of Fran Ridge is cut by the Paintbrush Canyon-Fran Ridge fault zone, one of the longest Quaternary fault zones in the site area. The Paintbrush Canyon fault merges with the Fran Ridge fault along the western edge of Fran Ridge, and may

extend northward to the southern boundary of the Timber Mountain caldera and southward to the Stagecoach Road fault, directly south of Busted Butte (fig. 3). If the Paintbrush Canyon-Fran Ridge fault zone connects with the Stagecoach Road fault, their combined length would exceed 30 km. The Paintbrush Canyon fault displaces Miocene strata almost 400 m at the northern end of Fran Ridge. West-dipping strata have been mapped between the Paintbrush Canyon and Fran Ridge fault planes (Scott and Bonk, 1984). Detailed mapping elsewhere in the area suggests that west-dipping strata are common within major north-trending fault zones (Scott and Bonk, 1984). The conspicuous fault "busting" the center of Busted Butte probably is a splay of the Paintbrush Canyon fault.

Fractures

Surface studies of hydraulically cleared outcrops, between 200 and 300 m² in size, reveal two-dimensional patterns of complexly anastomosing, steeply dipping fractures in welded units of the Tiva Canyon and Topopah Spring Members (Barton and Larsen, 1985). A hydraulically cleared outcrop, at the southern end of Fran Ridge, displays a two-dimensional fracture system in the middle non-lithophysal zone of the Topopah Spring Member (Barton and Hsieh, 1989). Fractures over 2 m in length are preferentially oriented north-northwest and dip westward. This information and the abundance of moderately dipping fractures in core from the 120-m horizontal core hole UE25-H1 (Norris et al., 1986), suggest that the attitude of the fracture system in the middle nonlithophysal zone at Fran Ridge coincides with the attitude of mapped faults in the immediate vicinity (Scott and Bonk, 1984).

Vertical variations of fracture density in core samples have been estimated by calculating fracture densities for a unit volume of 1 m³ (Scott et al., 1983). Most fractures occur in the moderately to densely welded section of the Topopah Spring Member, where 28 to 42 fractures per 1 m³ were estimated in core holes USW G-4 and USW GU-3/G-3, within or near the proposed repository area (Spengler and Chornack, 1984; Scott and Castellanos, 1984). Fracture density in nonwelded to partially welded zones below the Topopah Spring rarely exceeds four fractures per 1 m³.

Within the upper part of the Topopah Spring Member, most fracture surfaces are uncoated or

partially coated with silica; calcite is locally abundant. In the lower Topopah Spring Member, zeolites and minor amounts of manganese oxides partially coat fractures. Coatings of zeolites and manganese and/or iron oxide minerals are prevalent along fracture surfaces in the underlying tuffaceous beds of Calico Hills and the Crater Flat Tuff. Below the Crater Flat Tuff, most fractures are filled with calcite, clay, and zeolite minerals. Fracture fillings, as much as 1 to 5 mm thick, rarely cover the entire fracture surface in core samples of units within the Paintbrush Tuff. However, in stratigraphic units below the Topopah Spring, fillings appear to have completely resealed many (20 percent to 80 percent) of the fractures (Spengler and Chornack, 1984).

STOP 12: CREST OF YUCCA MOUNTAIN; THE POST-ERUPTION HISTORY OF YUCCA MOUNTAIN

D.T. Vaniman².

The history of alteration and of possible past variations in fluid flux, transport directions, and transport mechanisms is partially recorded in the post-eruption mineralogic and petrologic features of tuff at Yucca Mountain. The petrologic record above the water table indicates no major alteration of the candidate host rock since ~11.5 Ma. Some fracture minerals (e.g., calcite and clay minerals) at relatively shallow depths indicate a small amount of ongoing transport and deposition, in at least the uppermost part of the tuff sequence.

The major alteration observed in the unsaturated tuff below the potential repository horizon is zeolitization of glasses within 80 to 200 m above the present water table (the bottom of the vitric zone in fig. 4). This zeolitization occurred before 11.6 Ma, based on the pre-Timber Mountain age of tectonic tilting recorded by geopetal features of tuff that formed toward the end of major zeolitization. The last major alteration below the water table occurred at 11 Ma, based on K-Ar illite determinations (Aronson and Bish, 1987), when a hydrothermal system developed during waning stages of volcanism in the nearby Timber Mountain caldera.

Exceptions to these predominantly middle- to late-Miocene alteration ages appear to be few. Relatively young calcite (perhaps 26 to 310 ka) occurs in fractures 34 to 330 m deep in or near the exploration

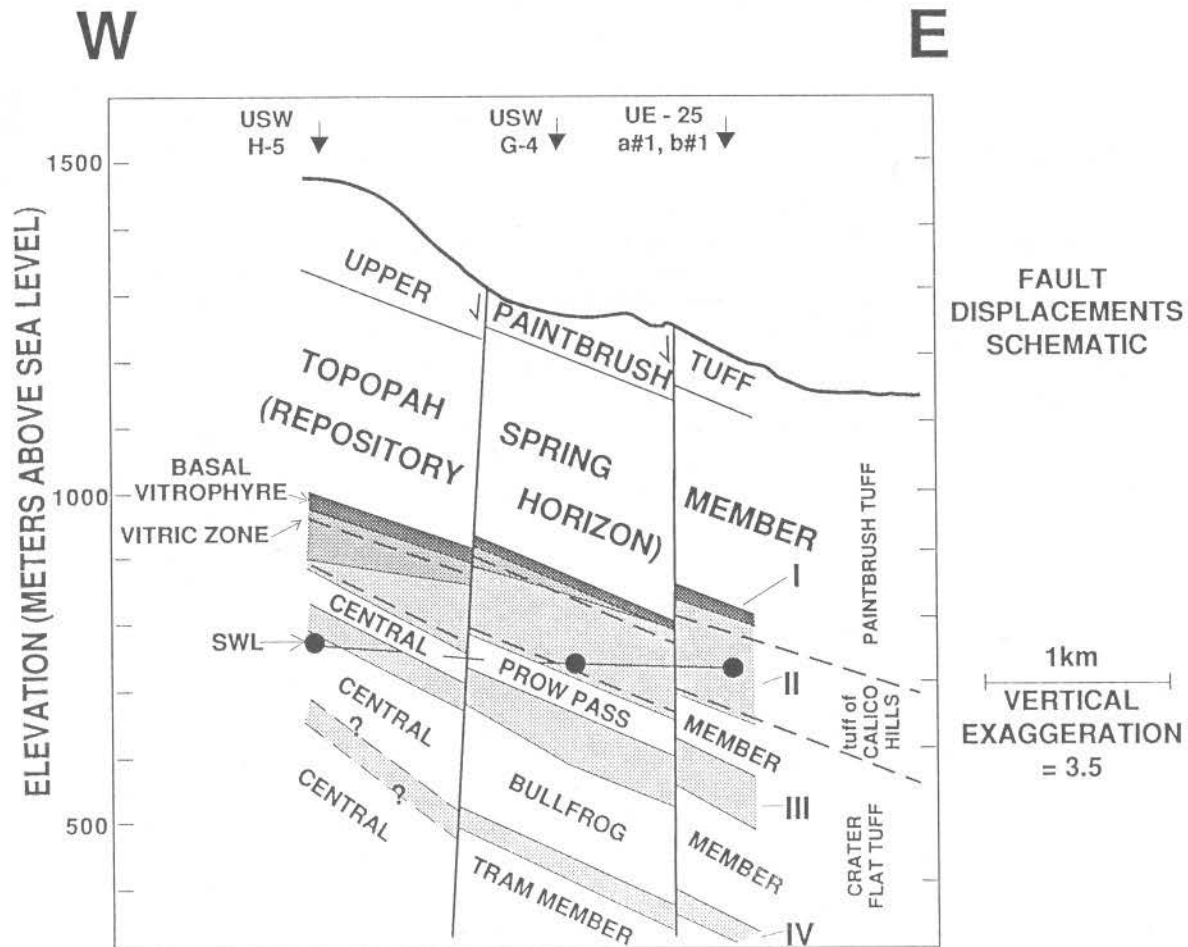


Figure 4 — Cross-section of Yucca Mountain showing the major volcanic units and distribution of clinoptilolite-rich zeolitized horizons. Numbers I to IV indicate major stratigraphically contained zones of zeolitization: 1) heulandite zone about the basal vitrophyre of the Topopah Spring Member; II) zeolitized interval including the nonwelded base of the Topopah Spring Member, the Calico Hills, and the nonwelded top of the Prow Pass Member; III) zeolitized interval including the nonwelded base of the Prow Pass Member and the nonwelded top of the Bullfrog Member; IV) zeolitized zone spanning the upper Tram and lower Bullfrog Members of the Crater Flat Tuff. The cross section is based on drill holes indicated at the top of the figure.

block at Yucca Mountain (uranium-series ages by Szabo and Kyser, 1985). Other fracture mineral ages are poorly constrained.

The stratified layers of devitrified (mostly quartz plus feldspar) and nonwelded (mostly glass or zeolite) tuff beneath the proposed host rock are the major coarse-scale mineralogic variability at Yucca Mountain (fig. 4). Clinoptilolite is the most abundant zeolite. There are subordinate amounts of mordenite. As noted above, the highest zone of pervasive zeolitization is about 80 to 200 m above the present water table. This is also the elevation above which porous glass (in nonwelded and unaltered glassy tuff) is preserved. This glass would be mostly dissolved or altered if it were beneath the water table. Paleo-

lake shorelines (and/or paleo-marshes, see Stop 8) in the Amargosa Valley support a past rise in water table of about 80 m beneath Yucca Mountain (W. Dudley, written commun., 1988). The top of the pervasive zeolitized zone II in figure 4 may be close to the maximum sustained rise in paleo-water table beneath Yucca Mountain.

Stop 13a: OVERVIEW OF STRATIGRAPHY; STRUCTURE, AND TECTONICS FROM THE CREST OF YUCCA MOUNTAIN

R.W. Spengler⁵ and K.F. Fox, Jr.⁵

Yucca Mountain reaches an elevation of 1,800 m, at the Prow, directly north of us. The mountain is bordered on the west, south, and east by the broad

intermontane alluvial basins of Crater Flat, Amargosa Desert, and Jackass Flats, respectively, and they range from 800 to 1,200 m in altitude.

The crest of Yucca Mountain is near the western edge of the proposed repository block (fig. 3). Bedrock within the proposed repository area, as well as, in the surrounding site-specific geologic investigations area (fig. 3) consists of Miocene tuff and lavas that in places exceed 2.5 km in thickness. An unsaturated lithologic sequence of welded ash-flow tuff underlain by nonwelded zeolitic ash-flow and bedded tuff dominates the more than 500 m of rock above the static water level. These unsaturated rocks may provide natural barriers to radionuclide migration.

Stratigraphy

Sedimentary strata exposed outside the area of site-specific geologic investigations comprise late Proterozoic and Paleozoic (600 to 300 Ma) limestone, dolomite, shale, argillite, and quartzite (Waddell et al., 1984). The most extensive exposure of a nearly complete north-dipping sequence of Paleozoic rocks flanks Crater Flat, directly westward at Bare Mountain; outcrops of Paleozoic rock also occur to the east at the Calico Hills, and about 10 km to the southeast, at Striped Hills.

Drill hole UE-25p#1, west of Fran Ridge and about 3 km southeast of Stop 13, provides the only direct subsurface information about the distribution of Paleozoic rocks beneath the site area. At this locality, dolomite was encountered at depths of 1,240 m to 1,807 m (Carr, M.D. et al., 1986).

Miocene Volcanic Rocks

Most of the tuff and lava underlying Yucca Mountain erupted between 14 and 11 Ma (Byers et al., 1976b) from sources associated with the Timber Mountain-Oasis Valley caldera complex, immediately north (figs. 1 and 3) of the site specific geologic investigation area. Chocolate Mountain, the high peak to the north, consists of caprock lithology of the Tiva Canyon Member of the Paintbrush Tuff and is within the Claim Canyon cauldron segment of the caldera complex. The volcanic rocks are 1.25 km thick at the western edge of Fran Ridge (Carr, M.D. et al., 1986). They thicken to at least 1.8 km beneath Stop 13 and to the north (Spengler et al., 1981; Scott and Castellanos, 1984). The rocks are probably as much as 3.2 km thick beneath central

Crater Flat (Snyder and Carr, 1984; Ackermann et al., 1988; and Hoffman and Mooney, 1984). The volcanic section thins significantly southward, toward the Amargosa Desert (Carr, M.D. et al., 1986).

The sequence of rocks underlying Yucca Mountain is mostly rhyolitic ash-flow tuff intercalated with thin beds of volcanoclastic rock. The ash-flow tuff consists of an alternating sequence of nonwelded to densely welded rock.

Major stratigraphic units are continuous across most of the site area. As observed at Fran Ridge (Stop 11), rocks in the upper half of the section (the Paintbrush Tuff) are mostly densely welded. Rocks in the lower part of the volcanic section (Lithic Ridge Tuff; Tram, Bullfrog, and Prow Pass Members of the Crater Flat Tuff; and tuffaceous beds of Calico hills) are typically porous partially welded tuffs, that have been pervasively altered to clay and zeolite.

The tuffaceous beds of Calico Hills and the upper part of the Prow Pass Member are more than half of the 100 to 300 m interval between the proposed level of the proposed repository drifts and the static water level (Waddell et al., 1984). Both units contain abundant zeolites that may influence rock permeability and sorptive capacity; therefore, they may be an important natural barrier to the migration of some radionuclides (Broxton et al., 1987). This interval appears to form a continuous blanket of zeolite-rich rock beneath the northeastern half of the proposed repository site; however, the tuffaceous beds of Calico Hills are mostly vitric tuff beneath the southwestern half of the proposed repository site, whereas, rhyolite lava occurs to the northeast of the proposed repository.

Structure, Faults between the Paleozoic and Miocene Sections

Low-angle extensional faults that partly separate the Paleozoic and Miocene rocks are recognized at two localities within 20 km of this stop: at the northern end of Bare Mountain (Carr and Monsen, 1988) and in the central Calico Hills (Simonds and Scott, 1987).

At Calico Hills, discontinuously exposed low-angle faults have been mapped in the Paleozoic sequence, in the Miocene sequence, and between the two sections (Maldonado, 1985). These exposed faults appear to be part of an anastomosing network of

interconnected low-angle extensional features that coincide crudely with the contact between Paleozoic and Miocene sequences (Simonds and Scott, 1987). A fault between the Paleozoic and Miocene sections has also been inferred within the site area in drill hole UE-25p#1 (Carr, M.D. et al., 1986). However, the attitude of this fault is uncertain.

Faults in the Miocene Volcanic Section

Volcanic strata at Yucca Mountain area series of fault-bounded blocks, 1 to 4 km wide. The central block of Yucca Mountain, which includes the proposed repository area, is tilted 5° to 10° eastward. Like many structural blocks at Yucca Mountain, the central block is elongate north-south and bounded by westward dipping high-angle faults (Scott and Bonk, 1984). Structural complexities increase to the south and east of the central block, where faults tend to increase in abundance and amount of displacement. Major faults offset strata (100 to 200 m) vertically; however, Solitario and Paintbrush Canyon fault segments displace strata more than 400 m (Carr, 1984; fig. 3). The dip of strata increases as much as 20° south and east of the proposed repository (Scott and Bonk, 1984; Scott and Rosenbaum, 1986).

Faults along the western edges of major blocks form highly brecciated zones, as wide as 500 m. In addition to overturned blocks that are several hundreds of meters in size, these fault zones commonly enclose west-dipping strata, as mapped along the Paintbrush Canyon-Fran Ridge and Solitario fault zones (Scott and Bonk, 1984). The western parts of blocks are relatively intact; however, internally, blocks grade eastward to broken zones characterized by abundant subparallel, west-side-down, west-dipping faults (Scott and Bonk, 1984; Spengler and Fox, in press). Individual faults in the broken zones displace strata only a few meters; however, a characteristic feature of these zones is that the dip of strata between the faults progressively steepens eastward toward the extreme eastern edges of broken zones (Scott and Bonk, 1984).

Paleomagnetic studies, in conjunction with field mapping, indicate the southern end of Yucca Mountain has been rotated about 30° clockwise, relative to the northern end, about 25 km away (Scott and Rosenbaum, 1986). North to south, broken zones appear to increase in width at the expense of intact parts of blocks, possibly indicating that deeper

structural levels are exposed toward the southern part of Yucca Mountain.

Broken zones are absent in areas north of the proposed repository, where a change in structural style occurs. In this area, all rock units dip 5° southeastward and several faults, coincident with northwest-trending drainages, show evidence of strike-slip movement. Lateral displacement along these faults is uncertain, but is probably minor as inferred from little or no apparent offset of upper stratigraphic units.

Geometry of Structures in the Miocene Volcanic Rocks

Tectonic models to explain the near-surface geometry of Yucca Mountain structures include the basic modes of extension in extensional terranes outlined by Wernicke and Burchfiel (1982). These modes are 1) extension by rotational planar normal faulting (Carr, M.D. et al., 1986), 2) imbricate listric (concave upward) normal faulting with reverse drag (Scott et al., 1983), and 3) listric normal fault bounding a series of planar fault blocks (Scott and Bonk, 1984).

Cross sections, constructed by Scott and Bonk (1984), show major blockbounding fault zones as two subparallel curvilinear fault planes enclosing west-dipping strata that are similar to western Colorado Plateau structures described by Hamblin (1965); however, the numerous west-side-down faults within broken zones have been interpreted (Scott and Bonk, 1984) as more steeply dipping planar features that terminate against the major curvilinear block-bounding structures.

Many structural elements of the extensional fault model described by Hamblin (1965) and the clay model experiments by Cloos (1968) on the development of "down-to-basin" faults in the Gulf Coast region appear remarkably similar to structural elements currently recognized in the volcanic section at Yucca Mountain. In general, these similarities include 1) evidence of reverse drag flexures and subparallel west-dipping curvilinear block-bounding fault planes; 2) abundant west-dipping subparallel faults with progressive eastward increase in strata rotation, presumably to accommodate eastward increase in the reverse drag flexure; 3) increase in the abundance of west-dipping subparallel faults at deeper structural levels; and 4) appearance of a horst

and graben pattern, possibly indicating the western edge of each reverse drag flexure.

These similarities support the hypothesis that major high-angle blockbounding faults and broken zones at Yucca Mountain form listric geometries at depth (Scott, 1986; Spengler and Fox, in press).

Tectonics

At the previously described localities (Stops 6 and 7) where Late Proterozoic and Paleozoic rocks are exposed, and presumably below Yucca Mountain, the basement rocks consist of imbricated thrust sheets, stacked during one or more episodes of Mesozoic thrust faulting. These rocks were buried in late Oligocene and early Miocene intermontane basins by thick deposits of siltstone, claystone, fresh-water limestone, tuff, and conglomerate, and finally buried by the silicic ash-flows and intercalated bedded tuff directly beneath us. This sequence and the underlying basement rock were faulted during a catastrophic episode of crustal extension that culminated during or shortly after eruption of 14 to 11 Ma tuff and 10 Ma basalt flows, which locally cap the tuff. Study of the geomorphic evolution of the Amargosa River (which flows southward through the Amargosa Desert, south of our vantage point) and Fortymile Wash (east of Yucca Mountain) suggests that the distribution and structural geometry of geologic formations, at Yucca Mountain and its immediate vicinity, and perhaps even much of the landscape, were established in approximately their present form by about that time (Huber, 1987).

Many of the faults that formed during middle and late Miocene have also been active in the Pleistocene and even the Holocene. These faults include the north-trending Windy Wash, Fatigue Wash, and Solitario Canyon faults to the west, the Bow Ridge and Paintbrush Canyon faults to the east, and the northeast-trending Stagecoach Road fault to the southeast (fig. 3).

The Windy Wash fault, 4 km west, is marked by a west-facing scarp that locally reaches 4 m in height (Swadley et al., 1984). The fault exhibits, through progressive offset of surficial deposits, at least seven episodes of movement during the Quaternary, including four within the last 0.3 Ma (Whitney et al., 1986). The most recent movement displaced a 3.5 to 6.5 ka silt deposit less than 10 cm (Whitney et al., 1986).

The Solitario Canyon fault, flanking the west side of Yucca Mountain at Stop 13, and the Bow Ridge fault (Stop 16), on the east side of Yucca Mountain, are of special interest, because trenches expose fissure-filled calcium carbonate and silica veins deposited in the fault zone. The vein in the Solitario Canyon fault zone is a wedge-shaped body, thinly layered to laminated, tapering downward from a thickness of about 2 m near the surface, to about 1 m at a depth of 2 m. At the Bow Ridge fault, steeply dipping, upwardly bifurcating veins are filled by carbonate-silica deposits, as are low-angle veins which intersect them. The vein material is conspicuously laminated parallel to vein walls, indicating repeated opening and filling of the fissures (Taylor and Huckins, 1986).

One or more episodes of ground breakage and fault dilation is also recorded along segments of the Windy Wash (Fault M of Swadley et al., 1984), Solitario Canyon, and Bow Ridge faults by a fissure within the fault zone that is filled with uncemented, reworked black volcanic ash. The ash is chemically and petrographically similar to the basaltic ashes erupted approximately 1.2 Ma at the cones in Crater Flat (Vaniman et al., 1982), and also to the much younger basaltic ash at Lathrop Wells center that apparently formed in several eruptive stages during the late Pleistocene and Holocene (Crowe et al., 1988).

The north-trending Quaternary faults at Yucca Mountain have been postulated to be listric normal faults that flatten at depth and merge with a detachment fault, forming the contact between the volcanic and volcanoclastic strata of Yucca Mountain and subjacent Paleozoic rocks, or possibly with other detachment faults within the basement rock (Scott, 1986). As yet, the Quaternary movement on the detachment fault(s), which is implied by this hypothesis, has been neither demonstrated nor refuted.

STOP 13b: BASALTIC VOLCANISM

Bruce M. Crowe³

Pliocene and Quaternary basaltic volcanic rocks are exposed west of Yucca Mountain, in Crater Flat. Vaniman et al. (1982) divided these rocks into three episodes including 1) 3.7 Ma basalt cropping out in the southeast side of Crater Flat, 2) a series of four 1.2 Ma volcanic centers extending across Crater Flat,

and 3) the Lathrop Wells volcanic center described previously (Stop 10).

The 3.7 Ma basalt of Crater Flat occurs as deeply dissected scoria cones and associated lava flows (fig. 3) and as more extensive lava flows with no recognized scoria vents (southeast Crater Flat). The deposits retain no original scoria cone slopes; they are preserved only where overlapped by lava flows or where feeder dikes have preserved the erosional resistance of the deposits. Dike trends are radial and concentric adjacent to original scoria vents. Away from vents, dikes trend north-northeast, parallel to faults in Yucca Mountain. Erosion highly modified lava flows and modified all topography created by flow fronts and primary flow features. Aeromagnetic data are interpreted to indicate that the 3.7 Ma lavas are not continuous in subsurface; they probably formed at and adjacent to surface scoria cones, similar to other Quaternary basalt centers. Basalt flows, dated 3.7 Ma and encountered at shallow depth in drill hole VH-1 just north of the outcrop area of the 3.7 Ma basalt, are moderately porphyritic; total phenocryst content ranges from 12 to 20 modal percent. Olivine (Fo^{80-75}) is the major phenocryst phase with lesser amounts of plagioclase (An^{82-68}), clinopyroxene and iron-titanium oxides (Vaniman et al., 1982). Phlogopite is present in the groundmass of basalt and as a vein-fill in dike rocks. All measured 3.7 Ma basalt outcrops have reversed magnetic polarity.

The 1.2 Ma basalts include, northeast to southwest, northernmost cone (not visible from Yucca Mountain), Black Cone, Red Cone, and Little Cones. Each center comprises a partially dissected main scoria cone, several satellite scoria cones, and multiple aa flows. K-Ar ages for the centers average about 1.2 Ma (Vaniman et al., 1982); however, preliminary field studies of Little Cones, Red Cone, and Black Cone centers indicate that each center exhibits multiple time-separate volcanic events. Their eruptive history is probably similar to the polycyclic patterns of the Lathrop Wells volcanic center (Stop 10).

Wells et al. (1988) described scoria cone geomorphology of Crater Flat and noted the cones have geomorphic features comparable to Cima volcanic field cones, dated at about 1 Ma. Red Cone and Black Cone have summit craters filled with coarse spatter that mantles the inward dipping crater walls. Aa flow

fronts from the centers are well preserved; erosion has completely modified primary flow surface topography. The northernmost center is significantly more erosionally incised than the other centers. Scoria deposits are only locally preserved and alluvial deposits have overlapped the lava flow fronts. Basalts of the 1.2 Ma eruptive event are aphyric to sparsely porphyritic; olivine is the main phenocryst mineral (Fo^{77-62}) and plagioclase is a microphenocryst mineral (An^{70} and greater) (Vaniman et al., 1982). All measured basalt outcrops have reversed magnetic polarity.

MINERAL AND ENERGY RESOURCES OF THE YUCCA MOUNTAIN REGION

S.R. Mattson¹.

Mineral and energy resources will be assessed to evaluate the potential for inadvertent human intrusion or interference with functioning of a high-level nuclear waste repository. The possible occurrence of natural resources that could attract human activity (i.e., mining or drilling) now or in the foreseeable future must be evaluated during site characterization to determine if human activity could lead to a loss in waste isolation. A key feature for resource evaluation is comparison of the surrounding area with the site to determine if the Yucca Mountain site would have a real or perceived mineral resource potential.

Mineral Resources

There are over 182 drill holes and 23 trenches within 10 km of the site. Numerous mapping projects have covered the area, and the portion on BLM land has been open for exploration until recently. During these activities no mineral resources, except zeolites, of possible industrial potential, have been identified. The abundant zeolites at Yucca Mountain are not considered economically important now or in the future. Trillions of tons of zeolites occur in playa lakes and volcanoclastic sediments that would likely be mined before bedrock sources became economically important (DOE, 1988). Continuing mineral resource evaluation includes geochemical analyses for elements for which no analyses currently exist (e.g., Hg) and for elements for which only limited data are available (e.g., Au) (DOE, 1988). For example, 106 analyses are available for gold that exhibit concentrations at, near, or below crustal average (0.004 ppm) with a single reported exception of 0.06 (+ 15 percent) ppm gold from drill hole USW G-2

(515 m deep) (Mattson, 1988). More than 200 additional analyses performed for land withdrawal should be available from the Nevada Bureau of Mines and Geology by the time of this field trip.

Joint mining (Sterling Mine and Mother Lode property) is operating in the area, approximately 13 km and greater from the site, on the eastern flank and interior of Bare Mountain, in a host of thrustured Paleozoic siltstones and dolomites. Open-pit/underground gold mines, heap-leach pad, and a tailings pile are visible from the top of Yucca Mountain. In 1980, the Sterling Mine was estimated to have produced 500,000 tons, with an average grade of 0.25 oz/t gold (Bonham, 1984) and unreported reserves; the new Mother Lode property has sulfide reserves of 1.6 million tons of 0.049 oz/t gold and 3.3 million tons of 0.057 oz/t gold (Lockard, written commun., 1989). The Bond Gold Bullfrog and Montgomery-Shoshone deposits, 3.3 km west of Beatty, Nevada, with reserves of 17.4 million tons of 0.103 oz/t gold and 0.240 oz/t silver (Jorgensen et al., 1989a, 1989b), began operations in late 1988. These deposits are in highly altered ash-flow units of the same age as those in the Yucca Mountain area. Additional deposits may exist in the Bare Mountain Paleozoic rocks or at depth in the Paleozoic rocks in the region beneath the sedimentary cover and volcanics. Paleozoic rocks underlie the Yucca Mountain site but are probably deeper than 3.0 km.

Historical mine sites include the Silicon Mine (silica source from 1918-1929), in northwestern Yucca Mountain; the Thompson Mine, in northwestern Yucca Mountain; the Tip Top Mine, at Bare Mountain; the Telluride or Harvey Mine (all with less than 100 flasks of mercury production), at Bare Mountain; and fluorspar production at the Daisy Mine and other localities at Bare Mountain (DOE, 1988). The Daisy Mine was the largest fluorspar producer in Nevada (Smith et al., 1983). In addition to these historical mining sites, several exploratory pits and workings are known in Crater Flat, Frenchman Flat, and the Calico Hills, all with no known production. The Horn Silver Mine, more than 20 km to the northeast, produced gold in the 1920's to 1930's. Industrial minerals are mined south of Yucca Mountain, at the Lathrop Wells cinder cone (Stop 10), where volcanic cinders and pumice are mined for aggregate in foundation block and decorative cover in the Las Vegas area (DOE, 1988).

Geothermal Resources

Down-hole temperatures at Yucca Mountain (19 wells) vary from a low of 21°C (102 m) to a high of 65°C (1,006 m) (Garside and Schilling, 1979; Trexler et al., 1979; Benson and McKinley, 1985; Sass et al., 1988). Heat flow in the region around Yucca Mountain varies from 0.6 to 3.1 HFU (Heat Flow Units) (Sass et al., 1980; Sass and Lachenbruch, 1982). Heat flow determinations at Yucca Mountain consist of four values: 1.25, 1.1, 1.3 and 1.6 HFU (average: 1.3 HFU) (Sass et al., 1980; Sass et al., 1988), and are demonstrably low compared to the Nevada average (2.0 HFU). Regional geothermal resources are considered low-temperature (<90°C) and of limited economic use (DOE, 1988). Further down-hole temperature measurements, temperature gradient information, heat flow determinations, and geochemical work are planned during site characterization to 1) assess the presence of geothermal resource potential and 2) to assess the causes of local variations observed in heat flow determinations over short lateral distances.

Oil and Gas Resources

No known oil or gas fields are in the Death Valley region (Bedinger et al., 1984) or southern Nye County, despite the drilling of some 60 unsuccessful exploration holes (Brady, 1984a, 1984b). At Yucca Mountain the Paleozoic rocks are deeper than approximately 3.0 km below most of the repository area and have likely passed the thermal maturity to produce oil and gas (DOE, 1988); however, further evaluation is planned during site characterization because of the following: 1) in central Nevada the Railroad Valley field contains the largest producing well in the continental United States (4,000 barrels a day) (Fritz, 1987) and wells have produced oil from ash-flow tuff in central Nevada (Garside et al., 1977); 2) although most Paleozoic rocks in the Yucca Mountain region are known to be past the gas producing maturity as determined from Conodont Alteration Index (CAI) data (Harris et al., 1980), new CAI data from a drill hole (UE-25p#1) revealed a CAI of 3 (140° to 180°C) in the gas producing range (Carr, M.D. et al., 1986). The drill hole is 3 km from the candidate site and penetrated Silurian rocks at a depth of 1.2 km. It is planned to assess site oil and gas resource potential, including new maturation data; geochemistry and organic geochemistry data; and to assess possible source rocks, reservoir rocks, and structural traps and seals (DOE, 1988).

STOP 14: SATURATED AND UNSATURATED ZONE HYDROGEOLOGY

Characterization of Unsaturated-Zone Infiltration

Alan L. Flint¹²

Objectives of the unsaturated-zone infiltration studies at Yucca Mountain are 1) to determine the effective hydraulic conductivity, storage properties, and transport properties as a function of moisture content or potential, and 2) to determine the present and estimate the future spatial distribution of infiltration rates of surficial materials covering Yucca Mountain. Four activities are planned to collect the required data for these objectives: laboratory analysis of matrix hydrologic properties, evaluation of natural infiltration, characterization of hydrologic properties of surficial materials, and artificial infiltration studies.

Analysis of matrix hydrologic properties is designed to support unsaturated-zone infiltration studies and vertical boreholes studies. The objectives are 1) to characterize the flux-related matrix hydrologic properties of major unsaturated-zone hydrogeologic units through laboratory testing of geologic samples from near-surface boreholes and excavations, and from boreholes drilled in the exploratory shaft, and 2) to use statistical and geostatistical methods to calculate, with known uncertainties, the values of flux-related matrix hydrologic properties in the rock beneath Yucca Mountain. The geostatistical methods will consist of a three-dimensional multivariate analysis using a variety of kriging techniques (e.g., simple kriging, cokriging, disjunctive kriging, and universal kriging) to estimate hydrologic properties and state variables at specific points or blocks, depending on the specific needs of the finite element or finite difference flow models.

The calculation of natural infiltration is to characterize the upper flux boundary condition for Yucca Mountain under present climatic conditions, in order to model flow through the thick unsaturated-zone beneath Yucca Mountain. Four major studies will determine boundary conditions. Neutron access hole studies will monitor natural infiltration in about 100 shallow boreholes. Studies using artificial infiltration control plots will monitor natural infiltration in major surficial hydrogeologic units. These plots will be instrumented to monitor water

content and water potentials automatically, by use of a variety of instrumentation (e.g., tensiometers, psychrometers, time domain reflectometers, and heat-dissipation probes). Tritium-profiling studies will determine flow velocities averaged over approximately the last 35 years by analyzing tritium produced by nuclear weapons testing. Water budget studies will calculate net infiltration by mass balance methods, will use intensive meteorological measurements of energy balance components, and direct measurements of evapotranspiration.

Methods designed to characterize the hydrologic properties of surficial materials include sampling, testing, and mapping; remote sensing; nuclear borehole geophysical logging; shallow surface seismic exploration; and geotomography studies. The main purpose of these tests is to help characterize the infiltration-related hydrologic properties of the surficial materials of Yucca Mountain. Surficial hydrogeologic units and geostatistical analysis will then be used to model infiltration processes on Yucca Mountain.

Artificial infiltration tests will be conducted on surficial materials covering Yucca Mountain to characterize near-surface water movement. Water fluxes, flow velocities, and flow pathways will be characterized in the major hydrogeologic surficial units. The main purpose of these tests is to determine the upper flux boundary conditions for Yucca Mountain under present and simulated wetter climatic conditions. A series of different types of artificial infiltration studies is proposed: portable infiltrometer studies, ponding studies, and rainfall-simulation studies, where each type of study increases in complexity and builds on the results of previous studies.

Site Vertical Boreholes — Unsaturated Zone Percolation

J.P. Rousseau⁵

Seventeen vertical boreholes will be drilled from the surface of Yucca Mountain through the repository block and into the underlying Calico Hills unit and will terminate at the water table. These boreholes will be used to test various hypothetical models of fluid flow in the unsaturated zone, as presented by Montazer and Wilson (1984). Drilling will provide access to (1) define structure and stratigraphy of rocks penetrated; (2) characterize the spatial variability of the hydrologic and geologic

properties associated with each geohydrologic unit; (3) recover core and drill-bit cuttings for laboratory measurement of hydrologic and physical properties of the rock matrix; (4) determine saturation of each geohydrologic unit as a function of depth; (5) perform in situ pneumatic and hydraulic tests to evaluate bulk permeability of the combined matrix and fracture system; (6) recover matrix pore-water and in situ gases for age dating and hydrochemical analysis; (7) measure and monitor in situ the potential field in which unsaturated flow occurs; (8) visually observe and record the density and orientation of fractures with depth; (9) evaluate tracer travel times using gas-tracer tests; and (10) conduct geophysical logging.

An important component of the borehole drilling program is the in situ measurements of fluid flow potential. Each borehole will be permanently instrumented with sensors designed to measure and monitor the various components (liquid, gas, vapor) of the total-fluid potential field. In situ instrumentation and stemming provide a means of (1) evaluating the dynamic stability of each component of the total-fluid potential field; (2) measuring those components of the total-fluid potential field that incorporate the contributions of larger-scale heterogeneities and anisotropies of the conductive media than is possible from core analysis alone; (3) isolating discrete rock intervals to characterize potentials associated with abrupt physical changes in rock conductive properties (i.e., joints, faults, shear zones, and fractures versus matrix), features that may not be conducive to physical sampling and laboratory tests; (4) isolating and containing mobile pore gases and water vapor for subsequent sampling and hydrochemical analysis without excessive mixing and contamination in the borehole; (5) evaluating the effects of diurnal and seasonal variations in surface temperature and pressure with depth; and (6) tracking the downward propagation of recharge resulting from individual storms. This monitoring program will have an estimated duration of 3 to 5 years.

Gaseous Phase Flow and Transport Through Yucca Mountain

R.C. Trautz⁵ and E.P. Weeks⁵

Because the proposed nuclear waste repository would be in the unsaturated zone, the potential exists

for radionuclide release to the environment through air-filled voids, particularly fractures. Topographic and barometric effects are observed when wells UZ6 and UZ6S are open to the atmosphere. Three mechanisms for air and water vapor circulation through Yucca Mountain have been proposed by United States Geological Survey researchers: (1) air flow due to density differences created by geothermal gradients in thick fractured units (Montazer and Wilson, 1984); (2) topographically induced air (Weeks, 1987); and (3) barometric pumping (Weeks, 1987). The topographic effect occurs when an area has substantial topographic relief, such as Yucca Mountain. The column of air extending from a fractured-rock outcrop on the side of the mountain to its crest will be colder, drier, and therefore more dense during cold weather than the column of air within the mountain between the crest and the outcrop elevation. The warmer, less dense formation air will tend to rise to the crest of the mountain while cooler, denser air enters along the mountain flanks. The air flow reverses direction in summer, when atmospheric air is warmer than formation air. When air pressure in the mountain lags behind changing atmospheric pressure, the topographic effect is superimposed upon the barometric effect; therefore, a pressure gradient forms that causes formation gas to flow. It is believed that such air flow will occur throughout the mountain. Gas-injection tests at several locations will characterize fracture permeability and storativity of the hydrologic units. These data may be used to model air flow throughout the mountain for both natural and repository conditions.

Regional and Local Flow Systems near Yucca Mountain, Nevada

J.B. Czarnecki⁵ and R.R. Luckey⁵

Yucca Mountain overlies a ground-water subbasin extending from about the edge of the Timber Mountain caldera (about 30 km from the design repository area) in the north, to a ground-water divide between Fortymile Wash and Ash Meadows in the east, to Eagle Mountain to the south, and to the Funeral Mountains and Greenwater Range to the west. Water may flow across subbasin boundaries, especially along the northern boundary. Water levels within the subbasin range from more than 1,100 m above sea level north of Yucca Mountain to about 600 m near the south end at Franklin Lake playa.

Subbasin ground-water flow is generally north to south. Within this subbasin, water flows in alluvium, tuff, and carbonate rocks of Tertiary age and younger.

Sources of inflow to the subbasin are believed to be under flow derived from recharge on Pahute and Rainier Mesas, under flow from the northwestern edge of the Amargosa Desert, periodic flooding along Fortymile Wash and the Amargosa River, and possibly precipitation on the Funeral Mountains and Greenwater Range. Minor recharge from precipitation is believed to occur elsewhere in the subbasin, including Yucca Mountain. Discharge occurs primarily as evapotranspiration at Franklin Lake playa, where depths to water are less than 3 m and upward hydraulic gradients are as much as 1.6. Evapotranspiration rates at the playa are estimated to range from 1 to 3 mm per day.

Earlier conceptual models of subbasin flow included spring discharge near Furnace Creek Ranch in Death Valley. A refined conceptual model now attributes this discharge to a separate, deeper flow system in Paleozoic carbonate rocks (Czarnecki, 1987). This model indicates that less water flows beneath Yucca Mountain; hence, ground-water travel times are longer than in previous conceptual models.

Hydraulic-head and temperature data from deep holes in the Amargosa Desert indicate an upward gradient and possible upward leakage from an underlying Paleozoic carbonate aquifer.

The local flow system at Yucca Mountain is arbitrarily defined as the flow system within about 5 km of the proposed designed repository. The local system includes a large hydraulic gradient to the north, where the water-level altitude changes about 300 m in less than 3 km in the vicinity of Yucca Wash, and a small gradient to the south where water level altitude changes less than 0.3 m in 3 km. The local flow system also contains a substantial change in water levels near the Solitario Canyon Fault. The water level is about 35 m higher on the west side of the fault compared to that on the east side of Yucca Mountain.

In some areas of the local flow system, there is a pronounced upward gradient. At test well UE-25

p#1, completed in the underlying Paleozoic carbonates rocks, the water level is about 22 m above that in the overlying tuff. At test well USW H-3 on the crest of Yucca Mountain, the water level in the lower tuff is about 40 m higher than that in the upper tuff. Water levels are being continuously monitored in 28 test wells completed in the local flow system. These test wells are monitored to provide data for mapping the potentiometric surface, to determine any long-term water-level cycles or trends, to determine vertical and horizontal gradients, and to obtain data to estimate flow system hydraulic properties.

Water levels at Yucca Mountain are as much as 750 m below land surface. These depths present special problems for accurately measuring water levels. Measurements must be adjusted for borehole deviation from vertical, deformation due to equipment weight, and down-hole temperature. Because of the extremely small hydraulic gradient south and east of Yucca Mountain, the measurements must be accurate to determine flow direction. To estimate hydraulic properties of the flow system by use of barometric fluctuations and earth tides, the water-level monitoring network must provide accurate water-level data without interruption for many months.

Future work in the subbasin includes expansion of water-level monitoring network in the Amargosa Desert and Fortymile Wash. This network will include data from mining company boreholes and two new boreholes in Crater Flat drilled specifically for this study. Additional work will be done to improve estimates of ground-water discharge by evapotranspiration.

Large hydraulic gradients at the north end of Yucca Mountain and at Solitario Canyon will be further characterized through additional drilling, hydraulic testing, and geophysical surveys. Flow and chemical transport in fractured tuff will be studied by conducting hydraulic and tracer tests within test wells UE-25 c#1, UE-25 c#2, and UE-25 c#3. Data from these test wells and geohydrologic characterization activities within the regional and local flow systems will be synthesized through refinement and development of numerical models of ground-water flow.

STOP 15: SURFACE FACILITIES*R.C. Murray¹, A.C. Matthusen¹, S.R. Mattson¹*

Proposed surface facilities are currently planned to be in Midway Valley. Central surface facilities will include areas for receiving and repackaging waste shipments, site operations, and general logistical support. These facilities would occupy approximately 75 acres directly eastward of Exile Hill, on a gently sloping alluvial fan area. The period of operation of the surface facilities may vary, but it will probably be 50 yrs or longer. Geologic siting criteria leading to selection of this site include surface slope (grade of 2.6 percent), protection from flash flooding, location of structural features such as major faults, and proximity to rock outcrops that could be used for a waste emplacement ramp portal.

Drilling and outcrop information indicate that the surface facilities site is on an alluvium wedge, the thickness of which is zero at the margins of Exile Hill to 27 m at UE-25 RF-3 (approximately 500 m eastward), to approximately 50 m on the east side of the valley at UE-25 WT-5 (Scott and Bonk, 1984). The proposed site lies above the flood zone for a predicted 100-yr flood, although the northern margin is in the 500-yr flood zone for Drill Hole Wash. Flood control measures are not anticipated to present major engineering difficulties or costly additions to facility design and construction.

The main siting and design concern is damage potential from seismic activity that could result in the release of radionuclides to the accessible environment. Preliminary studies indicate the annual probability of exceeding a peak ground acceleration of 0.4 g to be ≤ 0.0005 . Such low probability results from relatively long return periods for events on local faults and resulting low rate of regional seismicity. The site overlies an imbricate normal fault zone proposed by Scott and Bonk (1984), a north-south trending belt of closely spaced, high-angle normal faults. The offset along individual faults in this zone may be minor, but cumulative vertical displacement across the zone is believed to be on the order of 100 m. Strata within the zone have been rotated up to dips of 50°, compared to the 5° to 15° dip in Exile Hill, as evidenced by drill hole and core measurements in Midway Valley. Planned trenching studies in the proposed site area will investigate surface-fault rupture hazards; these study results will help determine the final facility location.

STOP 16: TRENCH 14*E.M. Taylor⁵, J.S. Stuckless⁵, and S.S. Levy²*

Geologic investigations at Yucca Mountain, Nevada, have exposed near vertical veins containing carbonate, opaline silica, sepiolite, and fine-grained sediments in a fault intersected by Trench 14 (fig. 5). Concern arose whether these deposits were precipitated from downward percolating water, as in a soil environment, or from ascending spring waters.

Trench 14 exposes, east to west, (1) fractured bedrock, (2) a fault zone of discrete near-vertical veins in brecciated bedrock, and (3) colluvium adjacent to the bedrock beyond the main fault zone. The north wall exposes a nonwelded tuff, stratigraphically between the 11.3 Ma Rainier Mesa Member of the Timber Mountain Tuff and the 12.6 Ma Tiva Canyon Member of the Paintbrush Tuff. On the south wall, the nonwelded tuff is absent. The brecciated Tiva Canyon bedrock has been locally recemented by both secondary carbonate and silica, especially within the main fault. The fault zone, approximately 2.5 m wide on the north wall, is characterized by prominent banded carbonate and opaline silica veins and splays into a zone with five main veins, approximately 4 m wide on the south wall. The adjacent well-cemented colluvium is sandy, with a large component of angular rock fragments. Soil formed in the colluvium has a well-developed K horizon cemented by secondary carbonate and opaline silica. The colluvium and the vein fillings are unconformably overlain by a finer grained depositional unit composed of slopewash with eolian additions.

Secondary carbonate concentrated at the bedrock-colluvial contact decreases with distance from the fault zone in Trench 14. The near-vertical bands exposed in the vein fillings were precipitated from calcium- and silica-enriched water moving along fractures. A basaltic ash is present in fractures in the veins. Carbonate in fault fillings and colluvium has a microcrystalline structure. The colluvial deposit is laterally persistent, the concentration of secondary carbonate decreases with depth, and there are discrete soil horizons. Clasts within the sediments have been jacked apart by the secondary carbonate. Sepiolite has been identified in vein fillings and colluvium. A few charophytes and chrysophyte cysts have been noted in sediment samples from Trench

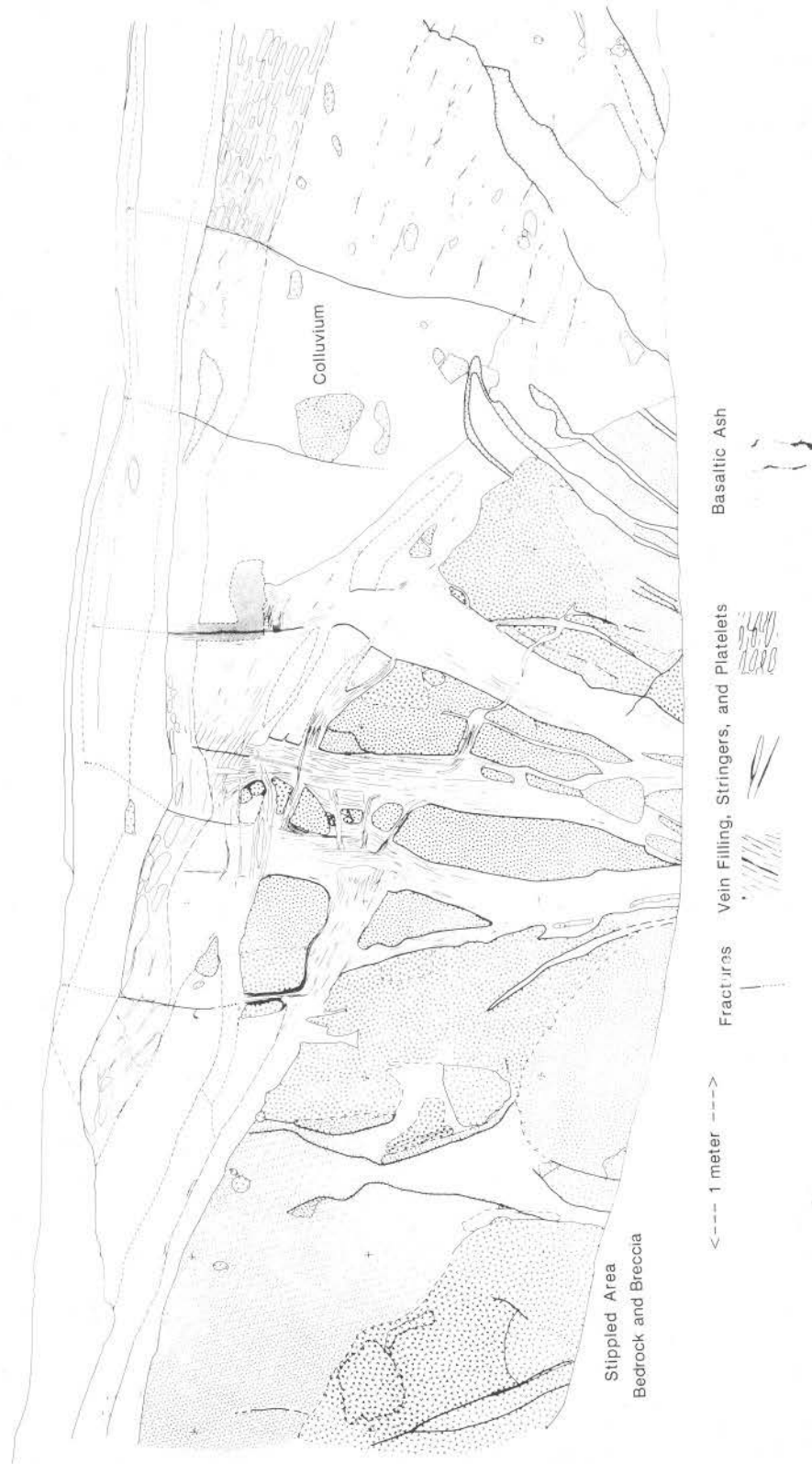


Figure 5 — Simplified map of the south wall of Trench 14, Nevada Test Site.

14. No ostracodes have been found (R.M. Forester, USGS, written commun., 1985; J.P. Bradbury, USGS, oral commun., 1985).

The vein fillings and colluvium in Trench 14 contain opal-CT and opal-A (Vaniman et al., 1988). Preliminary $^{18}\text{O}/^{16}\text{O}$ data for the opaline silica (J.R. O'Neil, USGS, written commun., 1985) are similar to values reported for low-temperature quartz. These values are also consistent with precipitation at about 15°C from water isotopically similar to ground water at the Nevada Test Site today (Claassen, 1985). Opal-C (typical of hydrothermal veins) has not been reported.

Trench 14 exposes at least three distinct silica deposits, in addition to the vein-filling, in which calcite is a minor constituent or locally absent. These deposits include (1) drusy quartz and chalcedony lining fractures and lithophysal cavities in the Tiva Canyon bedrock, (2) silica cementation of fault breccia in the Tiva Canyon bedrock, and (3) chalcedony and (or) opaline silica in the nonwelded tuff. Preliminary $^{18}\text{O}/^{16}\text{O}$ data suggest the drusy quartz probably formed at somewhat higher temperatures than the opaline silica. Although breccia cement is predominantly silica, other secondary minerals, such as calcite and sepiolite, are locally abundant.

Restriction of in situ drusy quartz to the Tiva Canyon bedrock suggests quartz formation predates fault juxtaposition of the Tiva Canyon bedrock against the nonwelded tuff exposed in the trench walls. The matrix of the brecciated tuff contains fragments of drusy quartz and silica cement, as well as undisturbed silica cement. This indicates that there have been multiple episodes of brecciation. Age relationships among episodes of brecciation, faulting, and silica deposition have not yet been established.

Field, chemical, mineralogical, biological, petrographic, and isotopic data are consistent with a pedogenic origin for the vein fillings (Taylor and Huckins, 1986); thus, the possibility of origin by ascending waters seems quite unlikely. Sepiolite, common in pedogenic deposits (Hay and Wiggins, 1980; Callen, 1984; Hay et al., 1986), also occurs in low-temperature spring-type and playa deposits in the Amargosa Desert (Khoury et al., 1982; Hay and Stoessell, 1984). Ostracodes are indigenous to

all modern springs near the NTS, and they are ubiquitous in the fossil record of springs and other shallow ground-water deposits. Chrysophyte cysts and perhaps charophytes could be introduced as windblown debris. Other eolian material, such as volcanic ash, has washed into near-vertical cracks in the Trench 14 deposit, and biological materials are known to exist in eolian materials throughout the region. Conversely, because gyrogonites (of the charophytes) float and because chrysophytes are very abundant in modern springs, sparse fossils of each could be preserved near the margin of the body of water without other aquatic organisms. The choice between these two alternatives will have to be based on detailed sampling, but at present, existence of a standing body of cold water in the vicinity of Trench 14 seems less likely.

Vertically and horizontally laminated carbonate and opaline silica deposits are common in Quaternary sediments throughout the arid and semiarid parts of the southwestern United States. Carbonate leached from the surface and upper horizons of the soil by downward percolating meteoric water subsequently precipitates in lower soil horizons at a depth controlled by soil moisture and texture (McFadden and Tinsley, 1985). Because so little carbonate is in the parent material, carbonate precipitated in the vein filling must be derived almost exclusively from eolian additions (Gile et al., 1966, 1981; Bachman and Machette, 1977). A very small contribution to the carbonate may be derived from in situ leaching of the parent material and carbonate reprecipitation. Studies elsewhere in southern Nevada have shown that rainwater can transport eolian-derived carbonate to depths of more than 3 m (Lattman and Simonberg, 1971).

STOP 17: EXPLORATORY SHAFT

E.L. Hardin¹ and S.R. Mattson¹

The Exploratory Shaft Facility (ESF), a statutory requirement of the Nuclear Waste Policy Act (NWPA) of 1982, as amended in 1987, was considered by NWPA architects as a necessary part of site characterization, owing to intrinsic limitations of surface-based drill hole testing. As currently planned (DOE, 1988), the Yucca Mountain ESF will be two shafts connected by workings at the proposed repository level which is about 364 m deep. Drill-blast-muck methods will be used to mine each shaft,

which will be lined with approximately 0.3 m of nonreinforced concrete to a depth of ~25 m below the repository level. The shaft collars for ES-1 will be approximately 218 m N50°E of USW G-4 and ES-2 will be collared 91 m N75°E of ES-1; both will be on the north side of Coyote Wash, near the canyon mouth. The shaft collars will therefore be above the calculated probable maximum-flood crest for the location (Fernandez et al., 1988). The two-shaft plan allows for extensive scientific work in Exploratory Shaft-1 (ES-1), concurrent with expedited penetration and development of the main test level that will use ES-2.

The stratigraphy at the location has been sampled at drill hole USW G-4, near the middle of Coyote Wash. The Tiva Canyon Member, exposed at the surface, is 43 m thick at G-4. Beneath this are about 27 m of bedded, nonwelded ash-flow tuff, including the Yucca Mountain Member and the Pah Canyon Member of the Paintbrush Tuff. Underlying this is about 360 m of the Topopah Spring Member, consisting of partially welded and densely welded ash-flow tuff, with sub-zones containing lithophysal cavities (Stop 11). The proposed repository horizon lies in the lower nonlithophysal zone of the Topopah Spring Member. Beneath the thick vitrophyre at the base of Topopah Spring Member are tuffaceous beds of the Calico Hills, consisting of about 107 m of altered nonwelded tuff with intercalated ash-flows and ash-falls. At the ESF location, the water table lies near the base of the Calico Hills unit, which has been extensively zeolitized throughout most of its thickness.

The in situ testing program in shaft ES-1 and at the main test level will address various geomechanical and hydrologic objectives, and include extensive mapping and sampling. Approximately 13,000 m of drilling is to be associated with the underground testing program. Monitoring holes will be drilled without liquid prior to shaft construction to obtain certain hydrologic and hydrochemical data under relatively undisturbed conditions. During excavation, the rock mass and the concrete liner geomechanical response will be monitored at several locations. A series of radial boreholes will be drilled from the shaft to sample and test hydrologic conditions, particularly at interfaces between welded and nonwelded units where capillary barrier effects and lateral diversion of moisture flux may be observed.

A test room for monitoring will be excavated at about 183 m in a highly lithophysal portion of the Topopah Spring Member. A series of experiments using drill holes parallel to the shaft will investigate construction effects on the rock mass hydrologic characteristics.

Many geomechanical tests are planned at the main test level (DOE, 1988) including heater tests, a heated block test, a mine by experiment, and a long-term heated room test simulating repository thermoelastic stress conditions. Geomechanical testing will investigate ground support requirements for the repository and other conditions necessary to maintain worker safety and retrievability of waste canisters for 50 yrs after emplacement. A series of in situ scaled heater tests will characterize the near-field waste canister environment for such conditions as temperature, moisture effects, and chemistry. Planned hydrologic tests include an in situ infiltration experiment, bulk permeability test, and diffusion experiment. In situ hydrologic testing objectives will characterize processes and phenomena. Long drifts at the main test level will intercept, observe, and characterize structural features such as the Ghost Dance fault to the west, Drill Hole Wash fault to the northeast (an inferred fault), and an imbricate normal fault zone to the east-southeast.

STOP 18: SAMPLE MANAGEMENT FACILITY (SMF)

Donna Sinks¹, E.D. Davidson¹, and H.A. Perry¹

The DOE operates a SMF which processes, documents, and preserves Yucca Mountain Project geologic samples to satisfy quality assurance requirements for licensing a geologic repository. In addition to management, quality assurance, and operations staff, the SMF includes the physical facility designed to process and preserve samples. A main staff responsibility is to document a sample from the time it is collected in the field, through transport, processing, analysis, storage, and archiving. The SMF restricts access to project samples, so that an accurate record is made of every person who comes into contact with each sample. Samples and specimens are identified and tracked by a bar code system. Sample information is entered into a Curatorial Sample Inventory and Tracking System (CSITS), a computer data base that tracks all Project

geotechnical samples and the associated records under control of the SMF.

The SMF is in Area 25 of the Nevada Test Site, about 10 km west of the potential site. There are physical facilities to handle the following: (1) shipping and receiving of geological samples and specimens of these samples; (2) processing of

samples, including logging, marking, cutting, crushing, splitting, washing and drying of drill cuttings, microscopic examination of core and cuttings, photography, and packaging; (3) viewing of core and samples; (4) storage of research and archive samples, specimens, remnants, and related records; and (5) administration.

REFERENCES

- Ackermann, H.D., Mooney, W.D., Snyder, D.B., and Sutton, V.D., 1988, Preliminary interpretation of seismic-refraction and gravity studies west of Yucca Mountain, Nevada and California, *in* Carr, M.D., and Yount, J.C., eds., *Geologic and hydrologic investigations of a potential nuclear waste disposal site at Yucca Mountain, southern Nevada*: U.S. Geological Survey Bulletin 1790, p. 23-33.
- Aronson, J.L., and Bish, D.L., 1987, Distribution, K/Ar dates, and origin of illite/smectite in tuffs from cores USW G-1 and G-2, Yucca Mountain, Nevada, a potential high-level radioactive waste repository [abs.], *in* Clay Minerals Society 24th Annual Meeting: Socorro, New Mexico, p. 25.
- Bachman, G.O., and Machette, M.N., 1977, Calcic soils and calcretes in the southwestern United States: U.S. Geological Survey Open-File Report 77-794, 163 p.
- Barton, C.C., and Hsieh, P.A., 1989, Physical and hydrologic-flow properties of fractures, *in* International Geologic Conference Field Trip Guide T-385: American Geophysical Union, 36 p.
- Barton, C.C., and Larsen, E., 1985, Fracture geometry of two-dimensional fracture networks at Yucca Mountain, southwestern Nevada, *in* Proceedings, the International Symposium on Fundamentals of Rock Joints: Bjorkliden, Sweden, p. 77-84.
- Bedinger, M.S., Sargent, K.A. and Langer, W.H., 1984, Studies of geology and hydrology in the Basin and Range Province, southwestern United States, for isolation of high-level radioactive waste: characterization of the Death Valley Region, Nevada and California: U.S. Geological Survey Open-File Report 84-743, 173 p.
- Benson, L.V., and McKinley, P.W., 1985, Chemical composition of ground water in the Yucca Mountain area, Nevada, 1971-84: U.S. Geological Survey Open-File Report 85-484, 10 p.
- Bonham, H.F., Jr., 1984, Reserves, host rocks, and ages of bulk-mineable, precious-metal deposits in Nevada, *in* The Nevada mineral industry — 1983: Nevada Bureau of Mines and Geology Special Publication MI-1983, University of Nevada, Reno, p. 15-16.
- Brady, B.T., 1984a, Mineral and energy resources, *in* Bedinger, M.S., Sargent, K.A., and Langer, W.H., eds., *Studies of geology and hydrology in the Basin and Range Province, southwestern United States, for isolation of high-level radioactive waste*: U.S. Geological Survey Open-File Report 84-743, p. 118-173.
- _____, 1984b, Selected geologic and hydrologic characteristics of the Basin and Range Province, western United States: coal, oil and gas wells, seeps and tar sandstone occurrences: U.S. Geological Survey Miscellaneous Investigations Series Map I-1522-E, Map Scale 1:2,500,000.
- Broxton, D.E., Bish, D.L. and Warren, R.G., 1987, Distribution and chemistry of diagenetic minerals at Yucca Mountain, Nye County, Nevada: *Clays and Clay Minerals*, v. 35, p. 89-110.
- Broxton, D.E., Warren, R.G., Byers, F.M., Jr., and Scott, R.B., 1989, Chemical and mineralogical trends within the Timber Mountain-Oasis Valley caldera complex, Nevada: evidence for multiple cycles of chemical evolution in a long-lived silicic magma system: *Journal of Geophysical Research*, v. 94, no. B5, p. 5961-5985.
- Byers, F.M., Jr., Carr, W.J., and Orkild, P.P., 1989, Volcanic centers of southwestern Nevada: evolution of understanding, 1960-1988: *Journal of Geophysical Research*, v. 94, no. B5, p. 5908-5924.

- Byers, F.M., Jr., Carr, W.J., Christiansen, R.L., Lipman, P.W., Orkild, P.P., and Quinlivan, W.D., 1976a, Geologic map of the Timber Mountain caldera area, Nye County, Nevada: U.S. Geological Survey Miscellaneous Geologic Investigations Map I-891, scale 1:48,000.
- Byers, F.M., Jr., Carr, W.J., Orkild, P.P., Quinlivan, W.D., and Sargent, K.A., 1976b, Volcanic suites and related cauldrons of Timber Mountain Oasis Valley caldera complex: U.S. Geological Survey Professional Paper 919, 70 p.
- Callen, R.A., 1984, Clays of the palygorskite-sepiolite group—depositional environment, age, and distribution, *in* Singer, A., and Galan, E., eds., Palygorskite-sepiolite occurrences, genesis and uses, Elsevier, New York, N.Y., p. 1-37.
- Carr, M.D., and Monsen, S.D., 1988, A field trip guide to the geology of Bare Mountain, *in* Weld, D.L., and Faber, M.L., eds., This extended land-geological journeys in the southern Basin and Range: Geological Society of America, Cordilleran Section, Field Trip Guidebook, p. 50-57.
- Carr, M.D., Waddell, S.J., Vick, G.S., Stock, J.M., Monsen, S.A., Harris, A.G., Cork, B.W., and Byers, F.M., Jr., 1986, Geology of drill hole UE25p#1: a test hole into pre-Tertiary rocks near Yucca Mountain, southern Nevada: U.S. Geological Survey Open-File Report 88-175, 87 p.
- Carr, W.J., 1984, Regional structural setting of Yucca Mountain, southwestern Nevada, and Late Cenozoic rates of tectonic activity in part of the Southwestern basin, Nevada and California: U.S. Geological Survey Open-File Report 84-854, 109 p.
- _____, 1988, Volcano-tectonic setting of Yucca Mountain and Crater Flat, southwestern Nevada, *in* Carr, M.D., and Yount, J.C., eds., Geologic and hydrologic investigations of a potential nuclear waste disposal site at Yucca Mountain, southern Nevada: U.S. Geological Survey Bulletin 1790, p. 35-49.
- _____, and Parrish, L.D., 1985, Geology of drill hole VH-2, and structure of Crater Flat, southwestern Nevada: U.S. Geological Survey Open-File Report 85-475, 41 p.
- Carr, W.J., and Quinlivan, W.D., 1968, Structure of Timber Mountain resurgent dome, Nevada test site, *in* Eckel, E.B., ed., Nevada Test Site: Geological Society of America Memoir 110, p. 99-108.
- Carr, W.J., Byers, F.M., Jr., and Orkild, P.P., 1986, Stratigraphic and volcano-tectonic relations of Crater Flat Tuff and some older volcanic units, Nye County, Nevada: U.S. Geological Survey Professional Paper 1323, 28 p.
- Christiansen, R.L., Lipman, P.W., Carr, W.J., Byers, F.M., Jr., Orkild, P.P., and Sargent, K.A., 1977, Timber Mountain-Oasis Valley caldera complex of southern Nevada: Geological Society of America Bulletin, v. 88, p. 943-959.
- Claassen, H.C., 1985, Sources and mechanisms of recharge for ground water in the west-central Amargosa Desert, Nevada — a geochemical interpretation: U.S. Geological Survey Professional Paper 712-F, 31 p.
- Cloos, E., 1968, Experimental analysis of Gulf Coast fracture patterns: American Association of Petroleum Geologists Bulletin, v. 52, p. 420-444.
- Crowe, B., Harrington, C., McFadden, L., Perry, F., Wells, S., Turrin, B., and Champion, D., 1988, Preliminary geologic map of the Lathrop Wells volcanic center: Los Alamos National Laboratory Report LA-UR-88-4155, 7 p.
- Czarnecki, J.B., 1987, Should the Furnace Creek Ranch — Franklin Lake playa ground-water subbasin simply be the Franklin Lake playa ground-water subbasin? [abs]: EOS (Transactions American Geophysical Union), v. 68, p. 1292.
- DOE, 1986, Final environmental assessment: Yucca Mountain Site, Nevada Research and Development Area, Nevada, DOE/RW-0073: Washington, D.C.
- _____, 1988, Site characterization plan, Yucca Mountain site, Nevada Research and Development Area, Nevada, DOE/RW-0199: U.S. Department of Energy, Office of Civilian Radioactive Waste Management, Oak Ridge, Tennessee.
- Earlougher, R.C., Jr., 1977, Advances in well test analysis, Henry L. Doherty series, Monograph 5,

- 2nd printing: Society of Petroleum Engineers of AIME, 264 p.
- Fernandez, J.A., Hinkebein, T.E., and Case, J.B., 1988, Analysis to evaluate the effect of the exploratory shaft on repository performance of Yucca Mountain: Sandia National Laboratory Report SAND85-0598, 284 p.
- Fritz, F., 1987, Good fortune found in Nevada: American Association of Petroleum Geologists Explorer, January, p. 14-15.
- Garside, L.J., and Schilling, J.H., 1979, Thermal waters of Nevada: Nevada Bureau of Mines & Geology Bulletin 91, University of Nevada, Reno, 163 p.
- Garside, L.J., Weimer, B.S. and Lutsey, I.A., 1977, Oil and gas developments in Nevada, 1968-1976: Nevada Bureau of Mines & Geology Report 29, University of Nevada, Reno, 32 p.
- Giles, L.H., Peterson, F.F., Grossman, R.B., 1979, The desert project soil monograph: Soil Conservation Service, U.S. Department of Agriculture, 984 p.
- _____, 1981, Soils and geomorphology in the Great Basin and Range area of southern New Mexico — guidebook to the desert project: New Mexico Bureau of Mines and Mineral Resources, Memoir 39, 222 p.
- Hamblin, W.K., 1965, Origin of "reverse drag" on the downthrown side of normal faults: Geological Society of America Bulletin, v. 76, p. 1145-1163.
- Harrington, C.D., 1988, Recognition of components of volcanic ash in rock varnish and the dating of volcanic ejecta plumes: Geological Society of America Abstracts with Programs, v. 20, p. 167.
- Harris, A.G., Wardlaw, B.R., Rust, C.C., and Merrill, G.K., 1980, Maps for assessing thermal maturity (conodont color alteration index maps) in Ordovician through Triassic rocks in Nevada and Utah and adjacent parts of Idaho and California: U.S. Geological Survey Miscellaneous Investigation Series Map I-1249.
- Hay, R.L., and Stoessell, R.K., 1984, Sepiolite in the Amboseli Basin of Kenya — a new interpretation, in Singer, A., and Galan, E., eds., Palygorskite-sepiolite occurrences, genesis and uses, Elsevier, New York, N.Y., p. 125-136.
- Hay, R.L., and Wiggins, B., 1980, Pellets, ooids, sepiolite and silica in three calcretes of south-western United States: Sedimentology, v. 27, p. 125-136.
- Hay, R.L., Pexton, R.E., Teague, T.T., and Kyser, T.K., 1986, Spring related carbonate rocks, Mg clays, and associated minerals in Pliocene deposits of the Amargosa Desert, Nevada and California: Geological Society of America Bulletin, v. 97, p. 1488-1503.
- Healey, D.L., and Miller, C.H., 1972, Gravity survey of the Amargosa Desert area of Nevada and California: U.S. Geological Survey Report 474-136, 32 p.
- Hoffman, L.R., and Mooney, W.D., 1984, A seismic study of Yucca Mountain and vicinity, southern Nevada; data report and preliminary results: U.S. Geological Survey Open-File Report 83-588, 50 p.
- Houser, F.N., and Poole, F.C., 1961, Age relations of the Climax composite stock, Nevada Test Site, Nye County, Nevada, in Short papers in the geologic and hydrologic sciences: U.S. Geological Survey Professional Paper 424-B, p. B176-B177.
- Hsieh, P.A., and Neuman, S.P., 1985, Field determination of the three-dimensional hydraulic conductivity tensor of anisotropic media: 1. Theory: Water Resources Research, v. 21, p. 1655-1665.
- Hsieh, P.A., Neuman, S.P., Stiles, G.K., and Simpson, E.S., 1985, Field determination of the three-dimensional hydraulic conductivity tensor of anisotropic media: 2. Methodology and application of fractured rocks: Water Resources Research, v. 21, p. 1667-1676.
- Huber, N.K., 1987, Late Cenozoic evolution of the upper Amargosa River drainage system, southwestern Great Basin, Nevada and California: U.S. Geological Survey Open-File Report 87-617, 26 p.
- Isherwood, D., Raber, E., Stone, R., Lord, D., Rector, N., and Failor, R., 1982, Engineering test plan for field radionuclide migration experiments in Climax

- Granite: Lawrence Livermore National Laboratory Report UCRL-53286, 72 p.
- Jorgensen, D.K., Rankin, J.W., and Wilkins, J., Jr., 1989a, The geology, alteration, and mineralogy of the Bullfrog Gold Deposit, *in* 118th Annual proceedings of the American Institute of Mining Engineers, February 27-March 3, 1989, Las Vegas, Nevada, p. 117.
- Jorgensen, D.K., Rankin, J.W., and Wilkins, J., Jr., 1989b, The geology, alteration and mineralogy of the Bullfrog gold deposit, Nye County, Nevada, *in* Abbott, E.W., ed., Northern Nevada Section-AIPG 1989 Field Trip March 19-21: American Institute of Professional Geologists-Nevada Section, Reno, 113 p.
- Khoury, H.N., Ebert, D.D., and Jones, B.F., 1982, Origin of magnesium clays from the Amargosa Desert, Nevada: *Journal of Sedimentary Petrology*, v. 41, p. 327-336.
- Lattman, L.H., and Simonberg, E.M., 1971, Case-hardening of carbonate alluvium and colluvium, Spring Mountains, Nevada: *Journal of Sedimentary Petrology*, v. 41, p. 274-81.
- Maldonado, F., 1977, Summary of the geology and physical properties of the Climax Stock, Nevada Test Site: U.S. Geological Survey Open-File Report 77-356, 25 p.
- _____, 1985a, Late Tertiary detachment faults in the Bullfrog Hills, southwestern Nevada: *Geological Society of America Abstracts with Programs*, v. 17, p. 651.
- _____, 1985b, Geologic map of the Jackass Flats area, Nye County, Nevada: U.S. Geological Survey Miscellaneous Investigations Series Map I-1519, scale 1:48,000.
- _____, 1988, Geometry of normal faults in the upper plate of a detachment fault zone, Bullfrog Hills, southern Nevada: *Geological Society of America Abstracts with Programs*, v. 20, p. 178.
- _____, *in press*, Geologic map of the northwest quarter of the Bullfrog 15-minute Quadrangle, Nye County, Nevada: U.S. Geological Survey Miscellaneous Investigations Map I-1985, scale 1:24,000.
- _____, and Hausback, B.P., *in press*, Geologic map of the northeast quarter of the Bullfrog 15-minute Quadrangle, Nye County, Nevada: U.S. Geological Survey Miscellaneous Investigations Map I-2049, scale 1:24,000.
- Marvin, R.F., Byers, F.M., Jr., Mehnert, H.H., Orkild, P.P., Stern, T.W., 1970, Radiometric ages and stratigraphic sequence of volcanic and plutonic rocks, southern Nye and western Lincoln Counties, Nevada: *Geological Society of America Bulletin*, v. 81, p. 2657-2676.
- Mattson, S.R., 1988, Mineral resource evaluation: implications of human intrusion and interference on a high level nuclear waste repository, *in* Post, R.G., and Wacks, M.E., eds., *Waste Management Eighty Eight*, February 28 to March 3, University of Arizona, p. 915-924.
- McFadden, L.D., and Tinsley, J.C., 1985, Rate and depth of pedogenic carbonate accumulation in soils: formation and testing of a compartment model, *in* Weide, D.L., ed., *Soils and Quaternary geology of the southwestern United States: Geological Society of America Special Paper 203*, p. 23-41.
- Monsen, S.A., 1983, Structural evolution and metamorphic petrology of the Precambrian-Cambrian strata, northwestern Bare Mountain, Nevada: unpublished M.S. Thesis, University of California, Davis, California.
- Montan, D.N., and Bradkin, W.E., 1984, Heater test 1, Climax Stock Granite, Nevada: Lawrence Livermore National Laboratory Report UCRL-53496, 56 p.
- Montazer, P., and Wilson, W.E., 1984, Conceptual hydrologic model of flow in the unsaturated zone, Yucca Mountain, Nevada: U.S. Geological Survey Water-Resources Investigations Report 84-4345, 55 p.
- Noble, D.C., Vogel, T.A., Weiss, S.I., Erwin, J.W., McKee, E.H., and Younker, L.W., 1984, Stratigraphic relations and source areas of ashflow sheets of the Black Mountain and Stonewall Mountain volcanic centers, Nevada: *Journal of Geophysical Research*, v. 89, no. B10, p. 8593-8602.

- Norris, A.E., Byers, F.M., Jr., and Merson, T.J., 1986, Fran Ridge horizontal coring summary report hole UE25h#1, Yucca Mountain area, Nye County, Nevada: Los Alamos National Laboratory Report LA-10859-MS, 78 p.
- Orkild, P.P., Byers, F.M., Jr., Hoover, D.L., and Sargent, K.A., 1968, Subsurface geology of Silent Canyon caldera, Nevada Test Site, Nevada, *in* Eckel, E.B., ed., Nevada Test Site: Geological Society of America Memoir 110, p. 77-86.
- Orkild, P.P., Sargent, K.A., and Snyder, R.P., 1969, Geologic map of Pahute Mesa, Nevada Test Site and vicinity, Nye County, Nevada: U.S. Geological Survey Miscellaneous Geologic Investigations Map I-567, scale 1:48,000.
- Patrick, W.C., Ballou, L.B., Butkovich, T.R., Carlson, R.C., Durham, W.B., Hage, G.L., Majer, E.L., Montan, D.N., Nyholm, R.A., Rector, N.L., Wilder, D.G., and Yow, J.L., Jr., 1983, Spent fuel test-Climax: Technical Measurements Interim Report, Fiscal Year 82: Lawrence Livermore National Laboratory Report UCRL-53294-82, 120 p.
- Quade, J., 1986, Late Quaternary environmental changes in the upper Las Vegas Valley, Nevada: *Quaternary Research*, v. 26, p. 340-357.
- Ransome, R.L., Emmons, W.H., and Garrey, G.H., 1910, Geology and ore deposits of the Bullfrog district, Nevada: U.S. Geological Survey Bulletin 407, 130 p.
- Reheis, M.C., 1988, Preliminary study of Quaternary faulting on the east side of Bare Mountain, Nye County, Nevada, *in* Carr, M.D., and Yount, J.C., eds., Geologic and hydrologic investigations of a potential nuclear waste disposal site at Yucca Mountain, southern Nevada: U.S. Geological Survey Bulletin 1790, p. 103-112.
- Sass, J.H., and Lachenbruch, A.H., 1982, Preliminary interpretation of thermal data from the Nevada Test Site: U.S. Geological Survey Open-File Report 82-973, 30 p.
- Sass, J.H., Lachenbruch, A.H., and Mase, C.W. 1980, Analysis of thermal data from drill holes UE24a-3 and UE25a-1, Calico Hills and Yucca Mountain, Nevada Test Site: U.S. Geological Survey Open-File Report 80-826, 25 p.
- Sass, J.H., Lachenbruch, A.H., Dudley, W.W., Jr., Priest, S.S., and Munroe, R.J., 1988, Temperature, thermal conductivity, and heat flow near Yucca Mountain, Nevada: some tectonic and hydrologic implications: U.S. Geological Survey Open-File Report 87-649, 118 p.
- Sawyer, D.A., and Sargent, K.A., 1989, Petrologic evolution of divergent peralkaline magmas from the Silent Canyon caldera complex, southwestern Nevada volcanic field: *Journal of Geophysical Research*, v. 94, no. B5., p. 6021-6040.
- Scott, R.B., 1986, Extensional tectonics at Yucca Mountain, southern Nevada: *Geological Society of America Abstracts with Programs*, v. 18, p. 411.
- _____, 1988, Tectonic setting of Yucca Mountain, Nevada: *Geological Society of America Abstracts with Programs*, v. 20, p. 229.
- _____, and Bonk, J., 1984, Preliminary geologic map of Yucca Mountain, Nye County, Nevada, with geologic sections: U.S. Geological Survey Open-File Report 84-494, scale 1:12,000.
- Scott, R.B., and Castellanos, M., 1984, Stratigraphic and structural relations of volcanic rocks in drill holes GU-3 and USW G-3, Yucca Mountain, Nye County, Nevada: U.S. Geological Survey Open-File Report 84-491, 121 p.
- Scott, R.B., and Rosenbaum, J.G., 1986, Evidence of rotation about a vertical axis during extension at Yucca Mountain, southern Nevada [abs]: *EOS (Transactions American Geophysical Union)*, v. 67, p. 358.
- Scott, R.B., Spengler, R.W., Diehl, S., Lappin, A.R., and Chornack, M.P., 1983, Geologic character of tuffs in the unsaturated zone at Yucca Mountain, southern Nevada, *in* Mercer, J.W., Rao, P.S.C., and Marine, I.W., eds., Role of the unsaturated zone in radioactive and hazardous waste disposal: Ann Arbor Science Publishers, Butterworth Group, Ann Arbor, Michigan, p. 289-335.
- Shoemaker, E.M., 1960, Brecciation and mixing of rock by strong shock, *in* Short papers in the geological sciences: U.S. Geological Survey Professional Paper 400-B, p. B423-B425.
- Simonds, F.W., and Scott, R.B., 1987, Detachment faulting and hydrothermal alteration in the Calico

- Hills, SW Nevada [abs]: EOS (Transactions, American Geophysical Union), v. 60, p. 1475.
- Smith, P.L., Tingley, J.V., Bentz, J.L., Garside, L.J., Papke, K.G., and Quade, J., 1983, A mineral inventory of the Esmeralda-Stateline resource area, Las Vegas district, Nevada: Nevada Bureau of Mines and Geology Open-File Report 83-11, University of Nevada, Reno, 180 p.
- Snyder, D.B., and Carr, W.J., 1984, Interpretation of gravity data in a complex volcano-tectonic setting, southwestern Nevada: Journal of Geophysical Research, v. 89, no. B12, p. 10,193-10,206.
- Spengler, R.W., and Chornack, M.P., 1984, Stratigraphic and structural characteristics of volcanic rocks in core hole USW G-4, Yucca Mountain, Nye County, Nevada, with a section on geophysical logs by D.C. Muller and J.E. Kibler: U.S. Geological Survey Open-File Report 84-789, 77 p.
- Spengler, R.W., Byers, F.M., Jr., and Warner, J.B., 1981, Stratigraphy and structure of volcanic rocks in drill Hole USW-G1, Yucca Mountain, Nye County, Nevada: U.S. Geological Survey Open-File Report 81-1349, 49 p.
- Spengler, R.W., and Fox, K.F., Jr., in press, Stratigraphic and structural framework at Yucca Mountain, in Special Issue of Radioactive Waste Management and the Fuel Cycle: An International Journal.
- Spengler, R.W., Kornreich, S.K. and Diehl, S.F., 1987, Proximal depositional features of a regional ash-flow sheet—The Topopah Spring Member of the Paintbrush Tuff, Nevada, in Hawaii Symposium on how Volcanoes Work, Abstract Volume: Geology Club, University of Hawaii at Hilo, p. 239.
- Swadley, W.C., 1983, Map showing surficial geology of the Lathrop Wells Quadrangle, Nye County, Nevada: U.S. Geological Survey Miscellaneous Investigations Series Map I-1361, scale 1:48,000.
- Swadley, W.C., and Carr, W.J., 1987, Geologic map of the Quaternary and Tertiary deposits of the Big Dune Quadrangle, Nye County, Nevada and Inyo County, California: U.S. Geological Survey Miscellaneous Investigations Series Map I-1767, scale 1:48,000.
- Swadley, W.C., Hoover, D.L., and Rosholt, J.N., 1984, Preliminary report on late Cenozoic faulting and stratigraphy in the vicinity of Yucca Mountain, Nye County, Nevada: U.S. Geological Survey Open-File Report 84-788, 42 p.
- Szabo, B.J., and Kyser, T.K., 1985, Uranium, thorium isotopic analyses and uranium-series ages of calcite and opal, and stable isotopic compositions of calcite from drill cores UE25a#1, USW G-2, and USW G-3/GU-3, Yucca Mountain, Nevada: U.S. Geological Survey Open-File Report 85-224, 25 p.
- Taylor, E.M., and Huckins, H.E., 1986, Carbonate and opaline-silica fault-filling on the Bow Ridge fault, Yucca Mountain, Nevada — deposition from pedogenic processes or upwelling ground water?: Geological Society of America Abstract with Programs, v. 18, p. 418.
- Tingley, J.V., 1984, Trace element associations in mineral deposits, Bare Mountain (fluorine) mining district, southern Nye County, Nevada: Nevada Bureau of Mines and Geology Report 39, 28 p.
- Trexler, D.T., Flynn, T., and Koenig, B.A., 1979, Assessment of low-to-moderate temperature geothermal resources of Nevada, final report for the period April 1978-June 1979: Nevada Bureau of Mines and Geology Report NVO/01556-1, 31 p.
- Vaniman, D.T., Bish, D.L., and Chipera, S., 1988, A preliminary comparison of mineral deposits in faults near Yucca Mountain, Nevada, with possible analogs: Los Alamos National Laboratory Report LA-11289-MS, 54 p.
- Vaniman, D.T., Crowe, B.M., and Gladney, E.S., 1982, Petrology and geochemistry of hawaiite lavas from Crater Flat, Nevada: Contributions to Mineralogy and Petrology, v. 80, p. 341-357.
- Waddell, R.K., Robinson, J.H., and Blankennagel, R.K., 1984, Hydrology of Yucca Mountain and vicinity, Nevada-California—investigative results through mid-1983: U.S. Geological Survey Water-Resources Investigations Report 84-4267, 72 p.
- Warren, R.G., 1983, Geochemical similarities between volcanic units at Yucca Mountain and Pahute Mesa: evidence for a common magmatic

- origin for volcanic sequences that flank the Timber Mountain caldera [abs.]: EOS (Transaction American Geophysical Union), v. 64, p 896.
- Weeks, E.P., 1987, Effect of topography on gas flow in unsaturated fractured rock, *in* Evans, D.D., and Nicholson, T.J., eds., Concepts and observations, in flow and transport through unsaturated fractured rocks: Geophysical Monograph 42, American Geophysical Union, p. 165-170.
- Wells, S.G., McFadden, L.D., and Renault, C., 1988, A geomorphic assessment of Quaternary volcanism in the Yucca Mountain Area, Nevada Test Site, Southern Nevada: Geological Society of America Abstracts with Programs, v. 20, p. 242.
- Wernicke, B., and Burchfiel, B.C., 1982, Modes of extensional tectonics: Journal of Structural Geology, v. 4, no. 2, p. 105-115.
- Whitney, J.W., Shroba, R.R., Simonds, F.W., and Harding, S.T., 1986, Recurrent Quaternary movement on the Windy Wash fault, Nye County, Nevada: Geological Society of America Abstracts with Programs, v. 18, p. 787.
- Winograd, I.J., 1981, Radioactive waste disposal in thick unsaturated zones: Science, v. 212, no. 4502, p. 1457-1464.

Field Trip No. 5
(Guidebook Published Separately)

**REGIONAL STRATIGRAPHY, FACIES,
AND PALEOENVIRONMENTS IN
THE CAMBRIAN OF
SOUTHERN MISSOURI**

Vincent E. Kurtz
Southwest Missouri State University
Box 87, 901 S. National
Springfield, Missouri 65804-0089

and

James R. Palmer
Missouri Department of Natural Resources
Division of Geology and Land Survey
P.O. Box 250
Rolla, Missouri 65401-0250

FIELD TRIP SUMMARY

Earliest Paleozoic rocks are 4,700 ft thick at the failed margin of the northeast-striking, apparently complete graben of the Reelfoot Rift in extreme southeastern Missouri, and thin gradually to 700 ft in the western Ozarks. Regional facies tracts in the Upper Cambrian carbonate shelf are reflected in four distinct stratigraphic sequence types: a rift graben basin, with 2,500 ft of shales that grade upward to limestones and dolostones; graben marginal St. Francois Mountain — regional carbonate shelf margin, with limestone-dolostone cycles; a north-east-trending ramp and platform 60-120 mi wide, dominantly dolostones; and broad intrashelf basin areas with limestones and shales that grade upward to dolostones. The small- and large-scale transgressive-regressive cycles in these strata present a complex picture of eustatic versus local tectonic controlled sedimentation.

The earliest sediments, of uncertain age, are alluvial fan deposits around locally rugged basement highlands. These grade laterally and upward to braided fluvial plain sandstones. The initial marine transgression in the middle to upper part of the basal clastic sequence may be as old as late Middle Cambrian. Carbonate shelf deposition began in the early Dresbachian. Shelf drowning and intrashelf basin formation occurred during two episodes, one in the early Dresbachian, and the second at the

Dresbachian-Franconian boundary. The largest intrashelf basins appeared in the early Franconian, and covered at least 25,000 square miles in southern Missouri. The last Upper Cambrian intrashelf basin shoaled around the end of the Franconian.

The outcrop examples of depositional facies that serve as a window into this Cambrian shelf include (1) alluvial fan conglomerates and sandstones; (2) braided fluvial plain sandstones; (3) burrowed marine carbonates and interbedded fan-delta sandstones (the above three facies in the lower quarter of the section); (4) intrashelf basin shales and carbonates, the latter containing a variety of matrix- and clast-supported carbonate lithoclast conglomerates that have local thrombolite crusts and mounds; (5) deep- to shallow-carbonate ramp thrombolite-stromatolite buildups; (6) homoclinal carbonate ramp "ribbon rock" and shoal sequences; and (7) large-scale platform cycles with bases of "ribbon rock" that grade upward to tidal flat carbonates and local dolomitized paleokarsted limestones.

Post-depositional features observed in outcrops are limestone-dolostone interfaces; collapse breccias; former redbeds reduced to pale-olive green sandstones and dolostones; vuggy porosity with a variety of cements from quartz to dolomite and sulfides; and faults and fractures.

Field Trip No. 6

**SURFACE EFFECTS OF THE
1811-1812 NEW MADRID EARTHQUAKE SEQUENCE
AND SEISMOTECTONICS OF THE
NEW MADRID SEISMIC ZONE,
WESTERN TENNESSEE, NORTHEASTERN ARKANSAS,
AND SOUTHEASTERN MISSOURI**

Eugene S. Schweig, III
Center for Earthquake Research
Memphis State University
Memphis, Tennessee

and

Randall W. Jibson
U.S. Geological Survey
922 National Center
Reston, Virginia

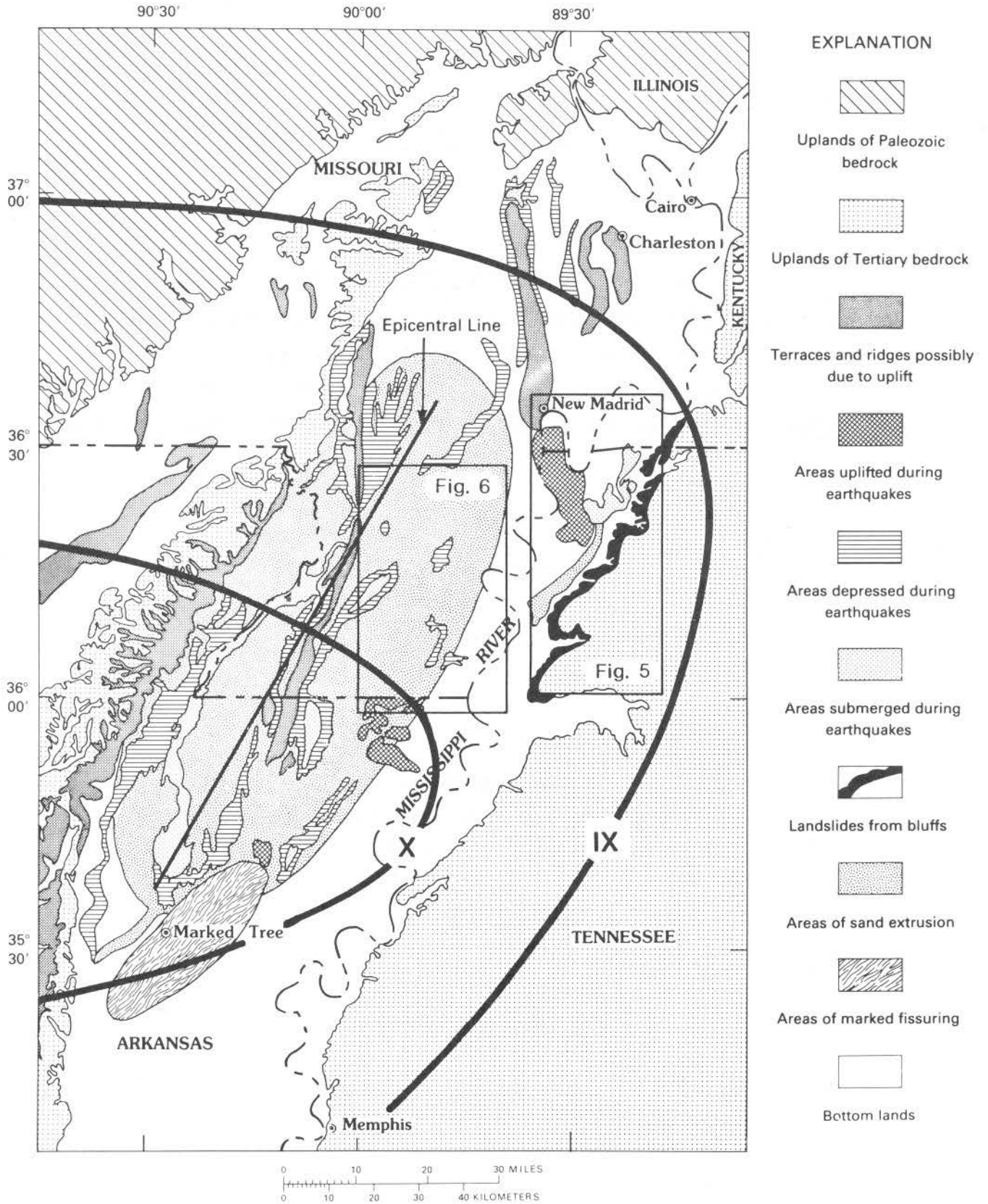


Figure 1 — Map showing generalized geology, ground failures, and other disruptions of the ground surface in the epicentral region of the 1811-12 New Madrid earthquake sequence (adapted from Fuller, 1912). Generalized Modified Mercalli Intensity isoseismals for the first earthquake on December 16, 1811 from Nuttli (1973).

INTRODUCTION

During the winter of 1811 and 1812, the region of southeastern Missouri, northeastern Arkansas, and western Tennessee was the site of the largest historical earthquakes in the central and eastern United States, the New Madrid earthquake sequence. Although no major ($m_b > 6.0$) earthquake has occurred in the region since 1895, hundreds of microearthquakes occur each year; the zone is the most seismically active area in the central and eastern United States (Nuttli, 1982). On this field trip we will visit sites exhibiting the effects of the New Madrid earthquake sequence, including landslides, liquefaction, and surface faulting.

THE NEW MADRID EARTHQUAKES AND THE NEW MADRID SEISMIC ZONE

The first New Madrid earthquake occurred at 2:15 a.m., December 16, 1811; Street and Nuttli (1984) recently concluded from contemporary accounts that a second major earthquake occurred on December 16 at 8:15 a.m. Other great earthquakes occurred on January 23 and February 7, 1812. All four earthquakes had estimated body-wave magnitudes m_b greater than seven, which corresponds to surface wave magnitudes (M_S) greater than eight (Nuttli, 1982; Nuttli and Herrmann, 1984). Epicentral Modified Mercalli Intensities (MMI) ranged from X to XII (Street and Nuttli, 1984), indicating near total destruction of structures. Because of the low attenuation of seismic waves in the central United States, these four earthquakes had felt areas of at least 5,000,000 km² (Nuttli, 1982) and were felt as far away as Boston, Mass. (1,690 km). Nuttli (1973) estimated that 2,500,000 km² were affected at MMI \geq V, the threshold of structural damage, and that 600,000 km² were affected at MMI \geq VII, the threshold of major damage (fig. 1). For comparison, during the 1906 San Francisco earthquake of similar magnitude, 150,000 km² were affected at MMI \geq V and 30,000 km² at MMI \geq VII (Nuttli, 1973). In addition to the main shocks, thousands of aftershocks were associated with the New Madrid earthquake sequence, many of which caused damage and were felt along the eastern seaboard (Street and Nuttli, 1984).

Seismic networks operated by Saint Louis University and the Center for Earthquake Research and Information at Memphis State University have shown that modern microseismicity is concentrated in several linear arms collectively known as the New Madrid seismic zone (fig. 2), which extends from Marked Tree, Arkansas to near Cairo, Illinois. Since 1812 at least 20 damaging earthquakes having body-wave magnitudes between 3.8 and 6.2 have struck the region (Nuttli, 1982). The linear arms of seismicity do not correlate with any known faults that intersect the surface; however, they do correlate with some subsurface faults.

The New Madrid seismic zone lies in the mid-plate province of Zoback and Zoback (1989), a region of fairly uniform compressive stress with the average maximum horizontal stress oriented about east-northeast. Structural features formed during Precambrian and Mesozoic rifting have been reactivated under this stress regime. Seismic-zone focal mechanisms indicate that strike-slip and thrust earthquakes are occurring (Herrmann and Canas, 1978; O'Connell et al., 1982), indicating similar magnitudes for intermediate and minimum principal stresses (Zoback and Zoback, 1980).

The return time for great $m_b \geq 7.0$ earthquakes in the New Madrid seismic zone is not well constrained. Trenching of the Reelfoot scarp (Stop B) in northwestern Tennessee by Russ (1979) indicates a maximum recurrence interval of about 900 yr. Johnston and Nava (1985), using frequency-magnitude data for post-1812 historical events, along with 10 yr of instrumental data, estimate a recurrence interval between 550 and 1,100 yr for a New Madrid-type event (fig. 3). More paleoearthquake data is needed to assess realistically the potential for great earthquakes in the New Madrid seismic zone.

Although the exact epicenters of the New Madrid earthquakes are unknown, their relationship to the New Madrid seismic zone is strongly suggested by the isoseismal maps compiled from historical accounts (Nuttli, 1973; Street and Nuttli 1984) and the distribution of ground failures, particularly liquefaction (Fuller, 1912; Heyl and McKeown, 1978;

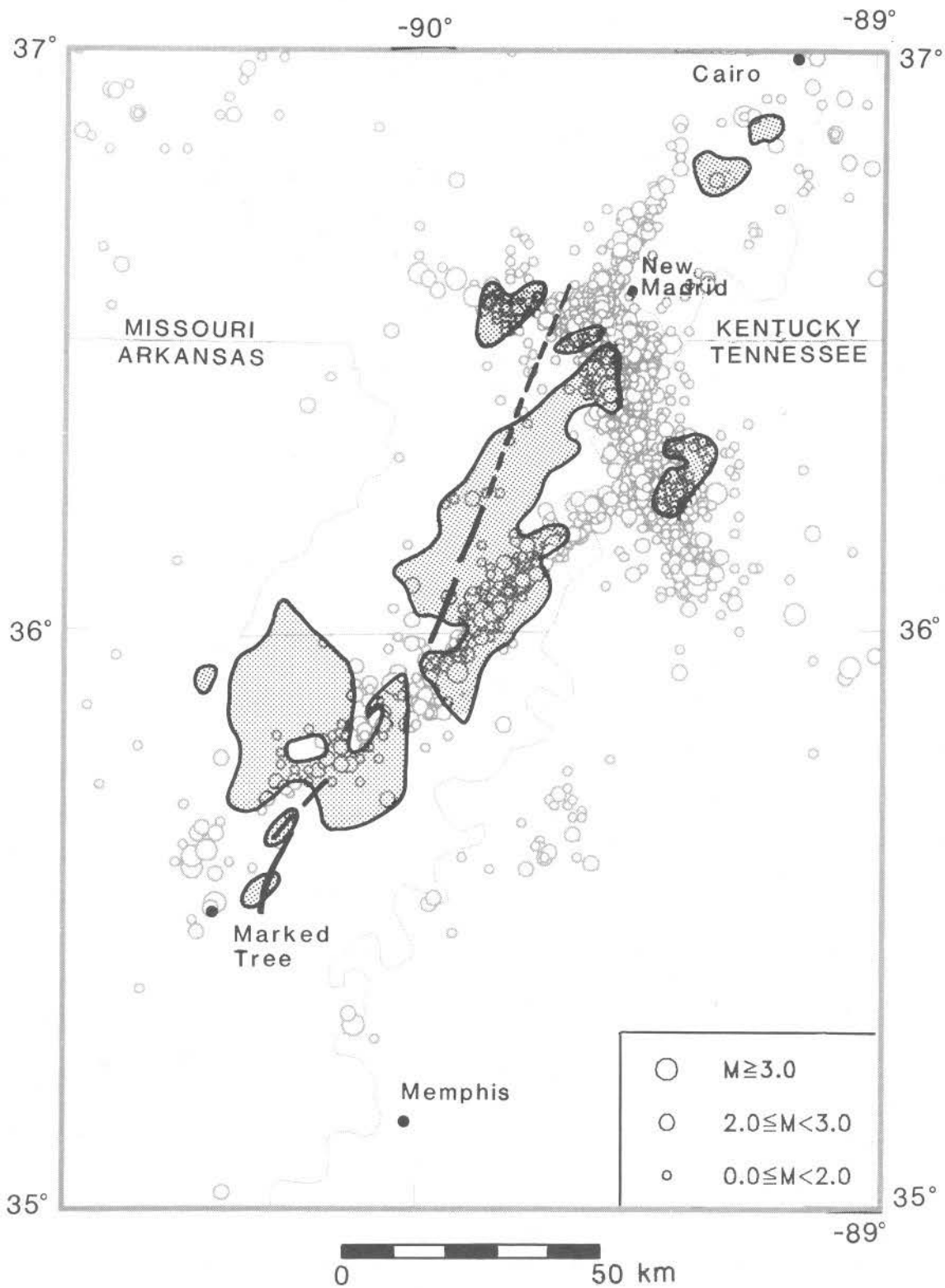


Figure 2 — New Madrid seismic zone earthquakes for the period July 1974 to March 1987. Shaded area is the region of alluvium covered more than 25 percent by liquefaction deposits (Obermeier, 1984). Bold lines in Missouri and Arkansas represent segments of the Bootheel lineament.

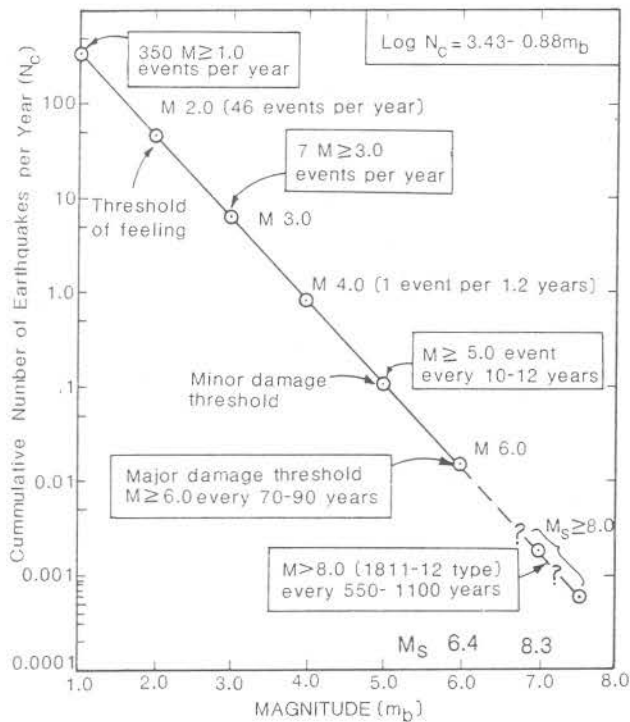


Figure 3 — Average behavior of the New Madrid seismic zone adapted from Johnston and Nava (1985). Magnitude (m_b) is plotted against the number of events per year (N_c) greater than or equal to that magnitude. The line is based on post-1812 historical data combined with the instrumental record from 1974-1983.

Obermeier, 1984) and earthquake-induced landslides (Jibson and Keefer, 1988, 1989) (fig. 1).

The total area affected by ground failure in 1811-12 including fissures, sandblows, landslides, and subsidence was about 48,000 km² (Street and Nuttli, 1984). Figure 1 shows the distribution of these and other geologic phenomena. In the epicentral region, uplift and subsidence on the order of a couple of meters occurred over hundreds of square kilometers (Fuller, 1912; Russ, 1982). Liquefaction of subsurface sand layers ejected sand, water, and other materials through fissures, some several kilometers long and many tens of meters wide (Fuller, 1912). Saucier (1977) has estimated that 10,500 km² was inundated by as much as one meter of ejected sand and water. Massive bank failures along the Mississippi River precipitated large tracts of land into the river channel, which was reported to have been choked with trees and the wreckage of boats (Penick, 1981). At two locations, one upstream and one

downstream from New Madrid (Johnston, 1982), waterfalls or rapids formed in the Mississippi River channel; these disturbances in the soft sediments of the riverbed were eroded and obliterated rapidly. Landslides along the bluffs bordering the Mississippi River alluvial valley occurred from near Cairo, Illinois, at least to about 20 km north of Memphis, Tennessee (Fuller, 1912; Jibson and Keefer, 1988). Eyewitnesses describe the epicentral region land surface as being disrupted and in many places uninhabitable (Penick, 1981).

GEOLOGIC FRAMEWORK

The New Madrid seismic zone is in the northern Mississippi embayment, a broad south-southwest-plunging syncline whose axis roughly coincides with the Mississippi River. Embayment sedimentation has been largely controlled by a rift that formed in latest Precambrian and Early Cambrian time and has been intermittently active since then (Braile et al., 1982, 1984). This failed rift, called the Reelfoot rift, developed in Middle Proterozoic igneous basement rocks of the eastern granite-rhyolite province (Bickford, 1988). The Reelfoot rift was first identified and named by Ervin and McGinnis (1975), using regional gravity data, and it was the first crustal feature to be correlated with the regional seismic activity. Presence of this subsurface rift was later confirmed by Kane et al. (1981), Hildenbrand et al. (1982), and Hildenbrand (1985) using more detailed gravity measurements and aeromagnetic data.

The Reelfoot rift began with incipient rift development with normal faulting and deposition of upper Precambrian or Lower Cambrian syn-rift alluvial fans (Weaverling, 1987). Thick Upper Cambrian and Ordovician carbonate rocks and some shales were deposited over the subsiding rift structure (Weaverling, 1987). By Silurian time the locus of deposition for the region had migrated northward to southern Illinois, where it remained until at least Late Mississippian time (Buschbach and Schwalb, 1984).

Uplift and erosion occurred in late Paleozoic or early Mesozoic time and any sediments that may have been deposited from Early Permian to Late Cretaceous have been removed (Buschbach and Schwalb, 1984). The most prominent feature associated with this uplift is the Pascola arch, in southeastern Missouri and northwestern Tennes-

see. It is estimated that nearly 3,700 m of sediment was eroded from the crest of this feature during uplift. Faults in the Reelfoot rift region were reactivated at this time, and plutons were intruded near the rift margins. Since Late Cretaceous time, subsidence of the region has filled the Mississippi embayment with shallow marine and fluvial sediments, which are about 1,000 m thick at the latitude of Memphis, Tennessee (Buschbach and Schwalb, 1984).

Quaternary sedimentation and geomorphology of the New Madrid seismic zone largely reflects shifting glacial and interglacial climates and associated glacial outwash and sea-level changes (e.g., Saucier, 1974; Autin et al., 1989). Glacial periods generally are correlated with lower sea level, increased discharge of the Mississippi River and its tributaries, valley incision, and deposition of loess sheets. Interglacial periods correlate with high sea level and aggradation of the Mississippi alluvial valley.

The stratigraphy seen in the bluffs along the Mississippi Valley on Stops E and F is shown in figure 4. The Eocene Jackson Formation (Conrad, 1856) is at the base of the bluffs in most of the study region; exposures are as thick as 50 m. Its composition is highly variable; it generally comprises discontinuous layers of shallow-water marine clays and silts that are a few centimeters to tens of meters thick. In some areas the Jackson Formation contains clean uncemented sands more than 10 m thick interbedded with soft clays. Some clay layers are saturated; others are desiccated and fissured. The clays are

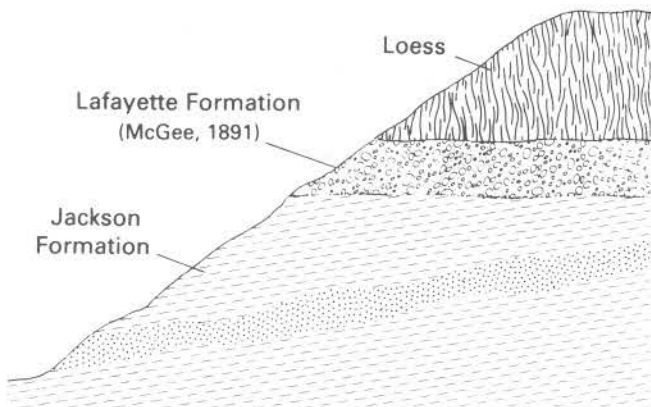


Figure 4 — Generalized structure and stratigraphy of the bluffs east of the Mississippi River, in the field trip area (Jibson and Keefer, 1988).

subjected to seasonal fluctuations in ground-water level near the bluffs. East of the Mississippi River, the Jackson Formation generally dips a few degrees westward, out of the bluff face.

The Pliocene Lafayette gravel (McGee, 1891; Potter, 1955) lies unconformably on the Jackson Formation. These fluvial gravels and sands are as thick as 20 m but pinch out locally. The deposits are uncemented in many areas, but a few localities contain concretionary beds as thick as 2 m. This unit is locally saturated where water tables are perched and is subject to large seasonal fluctuations in ground-water conditions. Autin et al. (1989) consider "Lafayette gravel" an obsolete term and include this unit in their Upland Complex. For the sake of consistency with past reports on this region, however, the term "Lafayette gravel" will be used in this field guide.

The bluffs are capped by 3 to 45 m of Pleistocene loess, which lies unconformably on the Jackson Formation and the Lafayette gravel; the average thickness is about 15 m. Loess is silt deflated from active and recently abandoned valley trains of early and late Wisconsin and earlier glacial cycles (Autin et al., 1989). It commonly forms vertical faces that are supported because of a clay binder, calcareous cement, or both (Krinitzky and Turnbull, 1967). The loess pinches out 100 to 200 km east of the bluffs.

GEOLOGIC HIGHLIGHTS EN ROUTE

Most of the route from St. Louis, Missouri to Dyersburg, Tennessee is along Interstate 55. Between St. Louis and Cape Girardeau, Missouri the rocks in roadcuts are Ordovician through Mississippian limestones with subordinate shale and sandstone. In southern Ste. Genevieve County the highway crosses the Ste. Genevieve fault zone, which has as much as 900 m of displacement down to the northeast; it is partly Devonian and partly Carboniferous in age (Nelson and Lumm, 1985). South of Cape Girardeau, the route is in the Mississippi embayment and is underlain by Cretaceous and younger sands, gravels, and clays. Near Sikeston, Missouri and south, the highway is on Mississippi River Holocene alluvium. For a detailed road log of the route, see Thacker and Satterfield (1977).

SITE DESCRIPTIONS

Stops A through F in northwestern Tennessee (fig. 5) examine surface faulting at Reelfoot scarp (Stops A and B), regional subsidence at Reelfoot Lake (Stop C), sand blows (Stop D), and earthquake-generated landslides (Stops E and F). Stops G and H are north and south of the border between Arkansas and the Missouri bootheel (fig. 6). Stop G shows liquefaction features in drainage-ditch exposures, and Stop H is along the Bootheel lineament.

All of the stops are on or along the edge of the Mississippi River floodplain; stops G and H are on braided stream terraces. The Mississippi River changed from a braided to a meandering regime by about 9,500 yr B.P. in the upper Mississippi embayment (R.T. Saucier, oral commun., 1989). Stops A through D are on the modern meander belt of the river. Stops E and F are along the bluffs east of the floodplain.

STOP A: REELFOOT SCARP ON TENNESSEE HIGHWAY 78 AND THE LAKE COUNTY UPLIFT

Stop A is 2.8 mi north of Tennessee 22 on Tennessee 78 (fig. 5).

Reelfoot scarp is formed on Holocene Mississippi River alluvium. Southeast of the highway, the scarp is clearly visible in the fields and forms the western margin of Reelfoot Lake. Northwest of the highway, the scarp generally trends north to the Mississippi River for a total length of at least 7 km. The scarp faces east, is 3 to 9 m high, and has slope angles ranging from less than 1° to nearly 3° ; it is significant and visible on the smooth alluvial plain (Russ, 1979, 1982). West of the scarp, the Tiptonville dome, rising as much as 10 m above the surrounding floodplain, is the highest part of the areally larger Lake County uplift (Stearns, 1979), which has maximum dimensions of 50 km by 23 km (fig. 5).

Russ (1982) argues convincingly that the Lake County uplift is of tectonic origin. He cites four lines of evidence: (1) the uplift surface is higher than any naturally occurring landform in the modern meander belt; (2) surveyed longitudinal profiles indicate warping of abandoned river channels to the extent that slope directions have been reversed; (3) an

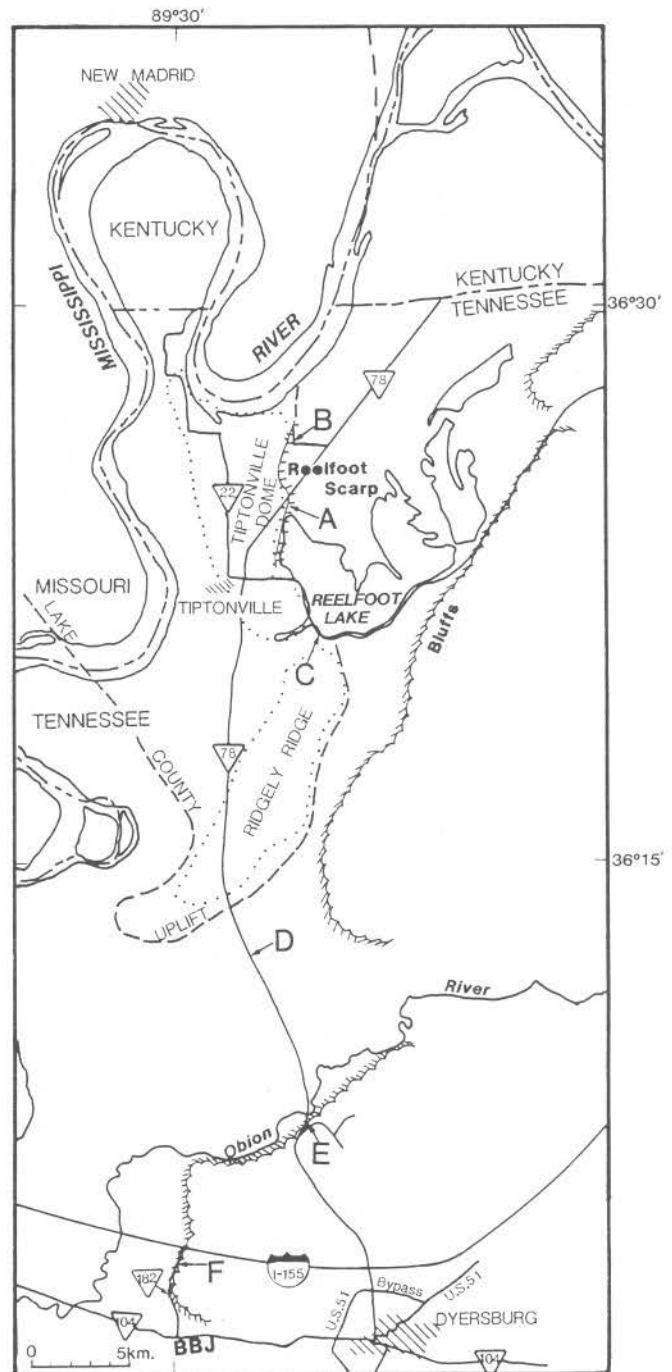


Figure 5 — Generalized map of features to be seen in the area of stops A through F. Lake County uplift (dashed line), Tiptonville dome (dotted line), Ridgely ridge (dotted line), and Reelfoot scarp from Russ (1982). BBJ represents Big Boy Junction.

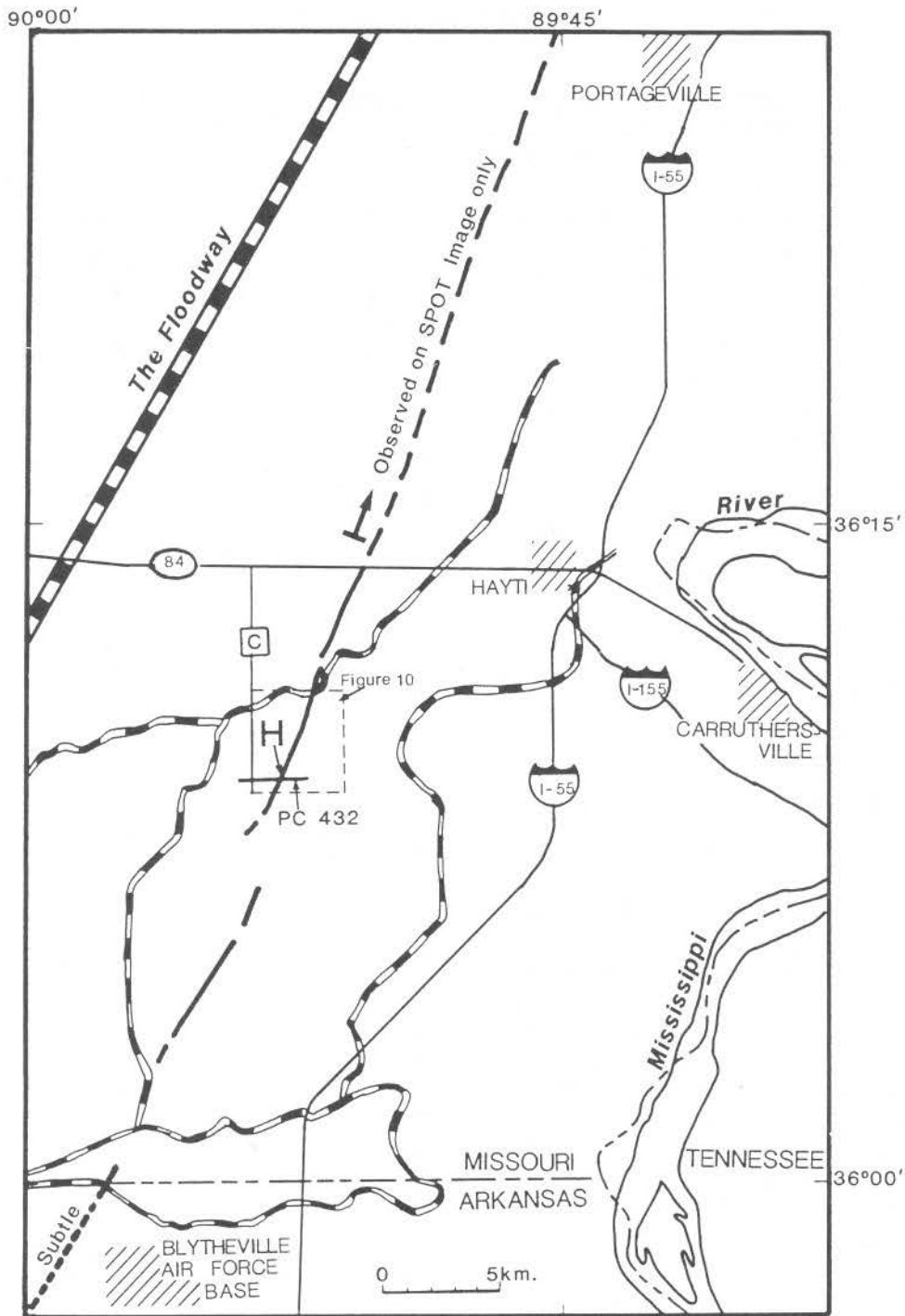


Figure 6 — Generalized map of features to be seen on stops G and H. The Boot-heel lineament is shown as an irregularly broken bold line extending north-northeastward from the southeast corner of the map. Thick dashed lines are Corps of Engineers drainage ditches. The ditch north of Blytheville Air Force Base was widened in April and May of 1989. PC 432 is Pemiscot County Road 432. Also shown is the outline of the areal photograph in figure 10.

exploratory trench along Reelfoot scarp demonstrated that most of the scarp is a monoclinial flexure developed in sediments; and (4) seismic reflection profiles show that Late Cretaceous to Eocene reflectors are arched over the uplift.

STOP B: REELFOOT SCARP AT USGS TRENCH SITE

Continue 2.1 mi northeast of Stop A on Tennessee 78; turn at the third left (west) across the railroad tracks. The road turns right (north) after 1.2 mi. Park about 0.2 mi north of the turn (fig. 5).

Here Reelfoot scarp is higher and steeper than to the south. This is the former location of a 260-m-long trench excavated across the scarp in 1977 and described by Russ et al. (1978) and Russ (1979). The trench exposed Holocene silty sands and subordinate clays and sands deposited in point bar, natural levee, and crevasse environments. These materials were warped and faulted into a broad monocline mimicking the geometry of Reelfoot scarp. In addition, small-scale monoclines, anticlines, and synclines, and nearly 100 normal and reverse faults having displacements of 0.5 m and less were observed in the upper third of the scarp. Liquefied sand was injected along the fault planes. The single most significant structure observed in the trench was a 0.5-m-wide normal fault zone exposed near the scarp base. Beds were displaced more than 3 m in the zone. Russ (1979) argued that the Reelfoot scarp structures are tectonic; he particularly cites a fault identified by Zoback (1979), using seismic reflection profiling. This fault apparently offsets Paleozoic through Tertiary strata beneath Reelfoot scarp and may be continuous with it.

Relationships shown in figure 7 indicate at least two separate episodes of faulting in the trench. Faults at 232.5 m were cut by a crevasse channel that was, in turn, cut by a low-angle fault extending from 228.5 m to 231.5 m. None of the faults was observed cutting the young overbank deposits along the scarp. Russ (1979) points out that these deposits are more than several hundred years old; therefore, the faulting must pre-date A.D. 1800. Russ (1979) also used a radiocarbon date from gastropod shells to constrain the age of the trench sediments to less than about 2 ka; therefore, with the sequence of events in 1811-12 and at least two events in the

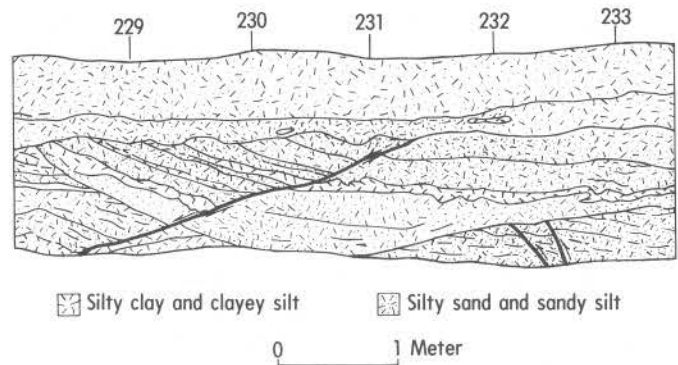


Figure 7 — Sketch of part of trench across Reelfoot scarp showing multiple episodes of faulting. Faults at 232.5 m were cut by crevasse channel that subsequently was offset by the low-angle fault extending from 228.5 m to 231.5 m (from Russ, 1982).

preceding 2 ka, the maximum average return time for earthquakes large enough to cause faulting and liquefaction is about 900 yr. Interestingly, Russ (1979) saw no evidence for movement on Reelfoot scarp during the 1811 and 1812 events.

STOP C: REELFOOT LAKE AT BLUE BANK

Stop C is at the Reelfoot Lake Public Park, on Tennessee 22, 3.4 mi east of Tennessee 78 (fig. 5).

Perhaps the feature most commonly associated with the 1811-12 earthquakes is Reelfoot Lake in northwestern Tennessee (fig. 5); it fills a broad, shallow, irregular depression about 20 km long (measured southwest to northeast) by about 6 km wide. Maximum lake depths are about 5 m; the average depth is only about 2 m. The lake and surrounding marshes cover approximately 100 km².

Although several historical accounts attribute the formation of Reelfoot Lake to the 1811-12 earthquakes (Fuller, 1912; Lyell, 1849; McGee, 1892; Owen, 1856; Usher, 1837), the association of the lake with old river channels and the presence of discontinuous bayou levees indicates that much of the region was probably covered by remnants of oxbow lakes before 1811 (Russ, 1982); however, Russ (1982) cites drowned cypress trees, partially eroded Indian mounds, and submerged trees marking old land-grant boundaries as evidence that the lake enlarged significantly during the 1811-12 earthquakes.

Several causes for the enlargement of Reelfoot Lake have been proposed. Owen (1856) suggested that sandblows (caused by earthquake-induced liquefaction) blocked Reelfoot Creek drainage, caused lake water damming and impoundment, and deflected the basin drainage outlet to the south end. This scenario is unlikely because large amounts of subsurface sand extrusion probably would have been accompanied by an equivalent amount of subsidence. In addition, loose extruded sand is easily eroded and probably would not have formed a permanent drainage barrier. Glenn (1933) suggested that compaction of Holocene channel clays during the earthquakes enlarged the lake; this could have been a contributing factor but probably could not account for the regional extent of the submergence. Fuller (1912) hypothesized that a combination of tectonic subsidence of the Reelfoot basin and uplift of the Tiptonville dome along the southern and western lake margins created the lake. Although Russ' (1982) indicated evidence is insufficient to isolate the causative mechanism(s), he concluded that the formation of Reelfoot Lake was at least partly associated with Reelfoot scarp and Tiptonville dome; as stated earlier, however, no evidence of 1811-12 displacement was observed in the USGS trench.

STOP D: LARGE SAND BLOWS IN FIELDS

Stop D is east of road 0.3 mi south of Obion-Dyer County line on Tennessee 78. Pull off where convenient (fig. 5).

The most visible effects of the New Madrid earthquake sequence are those related to liquefaction-induced ground failure. Over many thousands of square kilometers (figs. 1 and 2) these ground failures were manifested as sandblows, lateral spreads, curvilinear fissures, and ground surface warping (Fuller, 1912). The sandblows are visible in the field and on aerial photographs as light-colored, commonly irregular shapes against the finer grained dark brown soils of the Mississippi alluvial lowlands. Linear sand patches commonly parallel modern and relict stream channels and are probably due to liquefaction and lateral spreading of river banks toward the channels.

Liquefaction is a major concern in New Madrid seismic zone hazard evaluation. If earthquakes similar to those of 1811-1812 were to occur today, liquefaction-induced ground failure would probably

render the interstate highway system and other roads in the region impassable at many places (Obermeier, 1988). Other structures and buried utilities also would be badly damaged. Widespread flooding from extruded sand and water would pose a severe problem.

Liquefaction is defined as "the transformation of a granular material from a solid to a liquefied state as a consequence of increased pore pressures" (Youd, 1973). Liquefied material behaves as a fluid mass and consequently loses shear strength and stiffness (Committee on Earthquake Engineering, 1985). Liquefaction occurs during almost all large earthquakes; cyclic shear-stresses induced by earthquake ground motions cause buildup of pore pressure. Such conditions in saturated cohesionless soils cause loosely packed grains to become more closely packed if pore water can drain. During the relatively brief period of earthquake shaking, however, drainage is impeded, pore pressures increase, and effective intergranular stresses decrease. Eventually, increased pore pressure may exceed the confining pressure and lead to loss of shear strength and flowage (Obermeier, 1988).

Sir Charles Lyell (1849), among the first geologists to describe liquefaction phenomena related to the New Madrid earthquakes, described the still relatively fresh fissures, sandblows, and landslides. Fuller (1912) completed the first systematic description and map of liquefaction features. He cited contemporary accounts of fissures 8 km long and more than 200 m wide. The creation of the fissures commonly was associated with ejection of water, sand, mud, and gas through sandblows; resulting oval to linear sand patches reach lengths of 60 m.

At this stop two large 20 m by 30 m sandblows are elongate northeast-southwest. The subsurface geometry of similar features will be examined at Stop G. Blythe (1986) considers sandblows in this area to be associated with the Ridgely fault, which has been noted on seismic sections and apparently bounds an elevated area known as Ridgely Ridge. The fault and ridge also trend northeast-southwest.

STOP E: STEWART LANDSLIDE

Drive 0.8 mi south of the Obion River on Tennessee 78. Make a sharp left at Harness Road. Continue

on the paved road for 0.8 mi and park at the Bledsoe Cemetery on the left. To reach the landslide it will be necessary to go through the fence, walk around the deep gully on the left, and climb down the face of the bluffs (fig. 5).

One of the most dramatic effects of the New Madrid earthquakes of 1811-12 was the formation of numerous landslides along the bluffs bordering the Mississippi River alluvial plain in western Tennessee and Kentucky. In his report of a field investigation of the New Madrid earthquakes conducted in 1904, Fuller (1912, p. 59) stated,

Probably no feature of the earthquake is more striking than the landslides developed in certain of the steeper bluffs * * *. From the vicinity of Hickman in southwestern Kentucky at least to the mouth of the Obion River, about halfway across the State of Tennessee * * * the landslides are a striking feature. Skirting the edge of the bluffs, in the vicinity of Reelfoot Lake, a characteristic landslide topography is almost constantly in sight * * *.

Recent studies by Jibson (1985) and Jibson and Keefer (1988) described and cataloged more than 220 large (more than 60 m wide) landslides along the bluffs forming the eastern edge of the Mississippi alluvial plain from Cairo, Illinois to Memphis, Tennessee. Three major classes of landslides (classification after Varnes, 1978) are present along the bluffs (Jibson and Keefer, 1988). Young rotational slumps (11 percent of the landslides) are associated with fluvial erosion and occur on oversteepened bluffs; they have relatively small amounts of rotation, single slump blocks, and fresh features. Old coherent slides (65 percent of the landslides), which are single- and multiple-block rotational slumps and translational block slides, have eroded and revegetated features, and normally large amounts of rotation or translation; translation commonly appears to have occurred along gently dipping shear surfaces. Earth flows (24 percent of the landslides) have more subtle features and form a gently hummocky topography. Most earth flows are covered by dense forest, are inactive, and have eroded features, but some of them have active lobes where vegetation has been cleared.

The only landslides present in areas where the river has impinged on the bluffs since about 1820 are large, deep-seated rotational slumps; neither translational block slides nor earth flows are present in such areas. In addition, these near-river portions

of the bluffs are the only places where deep-seated landslides have fresh features; thus, it appears that under aseismic conditions large, deep-seated landslides along the bluffs form only where fluvial erosion oversteepens the toe of the bluffs and triggers rotational slumps. Although the 1811-12 earthquakes probably caused landslides on the bluffs bordering the river channel, fluvial erosion and consequent landsliding have probably destroyed evidence of earthquake-induced landslides.

If the old coherent slides and earth flows in the area were triggered by fluvial erosion and oversteepening of the bluffs, we would expect to see (1) continuous variation in landslide ages corresponding to the length of time since the river impinged on different parts of the bluffs, and (2) active analogues forming along bluffs currently being undercut by the Mississippi River. Neither situation occurs; most earth flows and old coherent slides (both translational and rotational) appear to be of similar age. As stated above, the only landslides forming along near-river bluffs—young rotational slumps—are morphologically distinct from all other types of landslides in the area; therefore, most or all of the old coherent slides and earth flows probably were triggered by a single event unrelated to fluvial activity.

Previous investigations, historical accounts, and present field evidence all indicate that old coherent slides and earth flows in the area formed during the 1811-12 earthquakes. Fuller (1912) and McGee (1892) established absolute ages of some landslides that correspond to the 1811-12 earthquakes, by tree-ring dating and supporting geomorphic evidence. Present landslide features are much more degraded than those described by McGee (1892) and Fuller (1912); this suggests that those features were geomorphically young when they were investigated (1891 and 1904) and have been significantly degraded in the last 80 to 100 yr. If the landslides were several hundred or thousand years old, the geomorphic changes over this time period would probably not be as pronounced as those observed. Historical accounts from local inhabitants suggest that the landslide features date at least to the 1850's and that they were geomorphically young at that time. Jibson and Keefer (1988) examined tree cores that indicated minimum ages of some landslides consistent with triggering in the 1811-12 sequence.

Historical topographic maps and air photos showed that the old coherent slides and earth flows mapped in 1983 (Jibson, 1985) are all present on the oldest photos and maps, dating to 1874. Many young rotational slumps, however, are not visible on the older maps and photos.

Two statistical techniques, discriminant analysis, and multiple linear regression, were used to relate regional landslide distribution to geology, distance from seismic sources, and topography (Jibson, 1985; Jibson and Keefer, 1989). These analyses indicate that the locations of young rotational slumps correlate best to increased slope angle, probably related to fluvial undercutting of the near-river bluffs. Distribution of old coherent slides and earth flows correlates most strongly with slope height, but the minimum distance and the sum of the distances to the estimated hypocenters of the 1811-12 earthquakes, the direction to the epicenters, and the slope aspect of the bluff, also relate to the distribution of these landslides; thus, statistical analyses indicate that the distribution of old coherent slides and earth flows is influenced by factors related to the 1811-12 earthquakes.

The Stewart landslide, studied in detail as a representative of old coherent slides in the area (Jibson, 1985), is a translational block slide from the bluffs along the Obion River, about 12 km north of Dyersburg, Tennessee (fig. 8). The slide averages 800 m wide by 400 m long and covers approximately 0.3 km². The bluffs in this locality are about 50 m high and their slopes average 20°. The Eocene Jackson Formation, which forms the base of the

bluffs, is overlain here by about 6 m of Pliocene Lafayette gravel and sand, which in turn is overlain by 15 to 20 m of Pleistocene loess. At the Stewart slide, the Jackson dips a few degrees out of the bluff face. Field and drilling evidence indicate that the Stewart slide failed along a weak layer in the Jackson Formation, at a depth of 35 to 40 m.

The broad bowl-shaped scarp forms a notable re-entrant in the local bluff line, and several large horst and graben blocks below the scarp form prominent but discontinuous ridges and troughs that interfinger with one another and create a complex topography. The grabens commonly have sloping bottoms that allow drainage; however, one ephemeral sag pond exists beneath the main scarp in a closed depression on a graben block. Some smaller horst blocks rotated headward as much as 10°, but the larger blocks and most of the smaller ones did not rotate and apparently translated with little internal deformation on a gently sloping basal shear surface. For example, drilling showed that the graben containing the sag pond is displaced downward 15 to 20 m; the horst block immediately downslope from the sag pond, however, is displaced downward only about 3 m and travelled horizontally about 50 m. This indicates that the basal shear surface dips less than 5°.

Below the main landslide blocks is a subdued hummocky toe area. The toe consists of subsidiary slump deposits from the displaced bluff face and compressional features that formed when the landslide blocks moved down and out from the parent slope and compressed the material at the base of the slope.

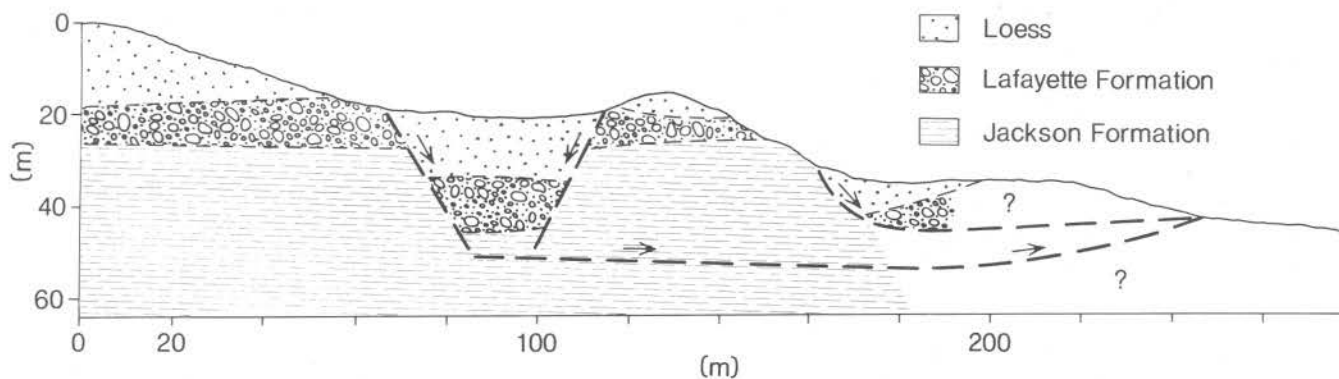


Figure 8 — Cross section of the Stewart translational block slide. The stratigraphic displacements between landslide blocks and the location of the basal shear surface were determined by drilling (Jibson, 1985). No vertical exaggeration.

Jibson (1985) conducted static and dynamic slope-stability analyses to model the conditions needed to cause failure of the Stewart slide. Static slope stability analyses indicate that the modelled pre-landslide bluff at the site is stable in aseismic conditions, even in an unrealistically high ground-water condition modelled as a worst-case bounding situation. In the most probable ground-water condition, the bluff is very stable. Dynamic analyses using Newmark's (1965) method, however, indicate that when subjected to ground shaking of an intensity similar to that produced by the 1811-12 earthquakes, the bluffs would undergo 0.4 to 0.5 m of Newmark displacement, enough to reduce soil shear strengths to residual levels and cause catastrophic failure and continuing large displacements. No earthquakes since the 1811-12 sequence have been large enough or close enough to the Stewart site to produce shaking intensities strong enough to cause significant slope displacement; therefore, Jibson (1985) concluded that the Stewart slide resulted from strong earthquake ground shaking caused by the 1811-12 earthquakes.

STOP F: CAMPBELL LANDSLIDE

Drive to Big Boy Junction, about 5.0 mi west of U.S. 51 on Tennessee 104. Turn right (north) on Tennessee 182. Drive 2.4 mi and pull off at parking lot on right. Note that you are passing over the toe of a large earth flow 1.7 mi north of Big Boy Junction (fig. 5).

The Campbell landslide is representative of earth flows in the area (Jibson, 1985); it is a large coalescing earth-flow complex extending about 4.3 km along the bluffs south of Lenox, Tennessee (fig. 9) and covering about 1.4 km². Individual earth flows

in the complex average about 400 m long. The intact bluff adjacent to the slide has an average slope angle of 15° and is about 55 m high.

The Campbell slide has subtle features: gently hummocky slopes between 5° and 10° are down-slope from a 20° scarp near the top of the bluff. On air photos, discrete lobes are visible on the slide, as is an irregular scarp, which indicates that landsliding began at several places and coalesced to form a continuous complex. All these lobes appear to be the same age; no evidence exists of episodic or recent movement of the slide, except in a few cleared areas where smaller active earth flows are present. Along the base of the bluff the toe of the slide is a gentle ridge, which is a compressional feature formed where material moved downslope to an area flat enough to inhibit movement and cause accumulation. Some larger swales on the complex have been dammed for stock ponds, but no original sag ponds are present. Drilling on the slide showed that the bluff materials dip about 5° out of the bluff face; a disturbed zone of very weak clay, interpreted to be the basal shear surface of the slide, was discovered at the contact between the Jackson Formation and the Lafayette gravel, at a depth of 4 to 5 m.

Static slope stability analyses (Jibson, 1985) indicate that the bluffs at the Campbell site are stable in aseismic conditions, even in an unrealistically high ground-water condition modelled as a worst-case bounding situation. In the most probable ground-water condition, the bluffs are very stable. A dynamic Newmark (1965) analysis, however, indicates that the bluffs are susceptible to major displacements, even at rather low levels of seismic shaking. The Newmark analysis indicates about 2 to 5 m of displacement along the slip surface would have been

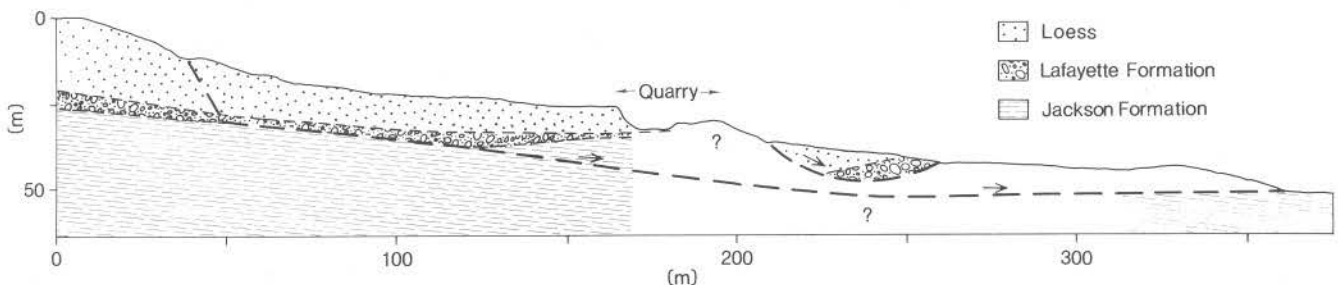


Figure 9 — Cross section of the Campbell earth flow. Stratigraphy and location of basal shear surface were determined by drilling (Jibson, 1985). No vertical exaggeration.

induced by each of the 1811-12 earthquakes in the bluffs at the site. Such displacements would have reduced the shear strength of the soil to residual levels and led to catastrophic failure and consequent large displacements. No earthquakes since 1812 have produced ground shaking at the Campbell site intense enough to cause significant slope displacement; therefore, Jibson (1985) concluded that the Campbell landslide complex resulted from earthquake shaking during the 1811-12 earthquakes.

STOP G: LIQUEFACTION PHENOMENA IN DRAINAGE DITCHES

Stop G can be made anywhere between the Mississippi River on the east and Crowley's Ridge on the west and between the municipalities of Marked Tree, Arkansas, and New Madrid, Missouri, depending upon where drainage ditches are currently being maintained or widened by the U.S. Army Corps of Engineers. As of May 1989, the most recently widened ditch was no. 29, north of Blytheville, Arkansas (fig. 6).

Heyl and McKeown (1978) and Obermeier (1984) used aerial photography and field studies to reexamine the extent of liquefaction during the 1811-1812 earthquakes. They generally confirmed Fuller's (1912) conclusions regarding the extent of liquefaction during the New Madrid events (fig. 2). The correlation between the zone of greatest liquefaction and the New Madrid seismic zone is striking. Figure 10 shows an example of the dense liquefaction deposits visible on aerial photography. At Stop G, subsurface exposures of these deposits will be examined in the late Wisconsinan Mississippi River braided stream terrace.

Recent studies around Charleston, South Carolina show the potential value of studying the geologic record of liquefaction effects to understand the prehistoric record of large earthquakes in a region (Obermeier et al., 1985; Talwani and Cox, 1985). Continuing U.S. Army Corps of Engineers flood-control efforts have resulted in an extensive system of major drainage ditches throughout the Mississippi River alluvial valley in the New Madrid seismic zone. The most recently excavated channels provide an excellent opportunity to search for pre-1811-1812 liquefaction features and to help us understand earthquake-induced liquefaction mechanics.

In the drainage ditches examined so far (Wesnousky et al., 1987), as well as in other geological (Haller and Crone, 1986) and archaeological (Saucier, 1989) excavations, no evidence of earthquakes before 1811 has been observed. The ditches, however, demonstrate the excellent exposure of liquefaction phenomena.

Logs of two sites examined near Big Lake, Arkansas are shown in figure 11. At site 1, the stratigraphy comprises thick soil horizons developed in fine to medium alluvial sand with intercalated clay layers. Impermeable clays are an important factor in the liquefaction process; they impede drainage and limit vertical sand flow, and thus cause sand sills to extend many meters horizontally from a central pipe. Cross-cutting relationships in both logs indicate several phases of sand injection through the same pipe, as was also noted by Saucier (1989) in an archaeological excavation farther south. The liquefied sand at site 1 does not appear to have reached the surface. At site 3, however, sand was extruded onto the surface. The uppermost liquefaction layer, marked L4, may actually comprise several layers separated by lignite or clay (hatches). Saucier (1989) argues that three surface sand layers separated by clays in a similar exposure represent separate 1811-12 New Madrid-sequence earthquakes.

STOP H: THE BOOTHEEL LINEAMENT IN SOUTHEASTERN MISSOURI

Drive 9.5 mi west on Missouri 412 from the I-55 exit. Turn left (south) on County Road C. Drive 5.8 mi and turn left on Pemiscot County farm road 432; continue 0.7 mi, and pull over where convenient (fig. 6).

During a comprehensive examination of the New Madrid seismic zone, using imagery from the French SPOT satellite (similar to our Landsat satellite, but with higher resolution), R.T. Marple (a graduate student at the Center for Earthquake Research and Information at Memphis State University) discovered a discontinuous linear feature, at least 42 km long, that we have named the Bootheel lineament (figs. 2 and 6). Although we do not yet have evidence of structural offset along this feature, its great length, its morphology, and the fact that it separates areas having different surface characteristics all suggest



Figure 10 — Aerial photograph of Bootheel lineament (arrows) and dense sand blows (white patches over entire photograph). Note the difference in the shapes and extent of sand blows on opposite sides of the lineament. Also shown are County Highway C, Pemiscot County Road 432, and stop H.

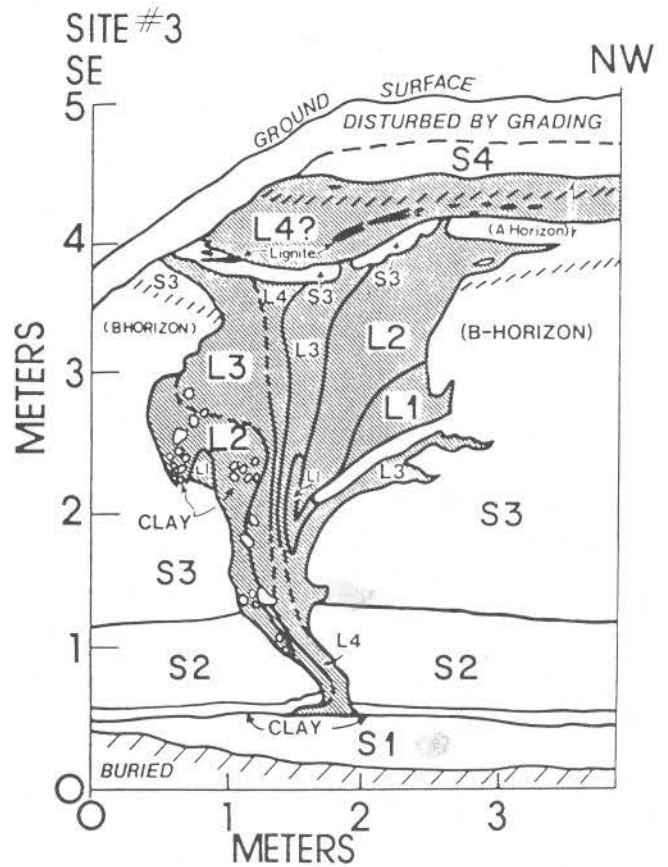
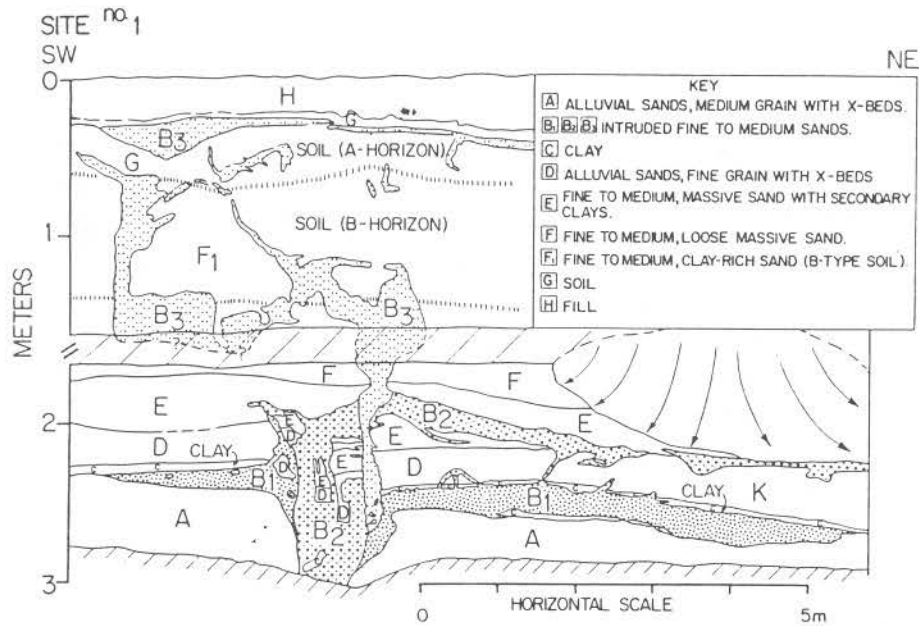


Figure 11 — Logs of exposures of liquefaction features near Big Lake, Arkansas. The log of site no. 1 is after Wesnousky et al. (1987).

that it is a fault. The primary uncertainties are its total extent and its amount and type of offset.

The surface trend of the Bootheel lineament is about N 20° to 25° E through southeastern Missouri and into northeastern Arkansas (fig. 2). It has been traced with confidence from about 15 km west of New Madrid, Missouri, south-southwestward to about 6 km northwest of Blytheville, Arkansas. In areas of incomplete photographic coverage, we have observed features that suggest the Bootheel lineament may extend farther south. The lineament is approximately coincident with the southwestward extension of the northern half of the axial trend of the New Madrid seismic zone, which extends from Charleston, Missouri to New Madrid, Missouri. In Missouri, the Bootheel lineament is west of and oblique to the southern axial trend that extends from Caruthersville, Missouri, southwestward to Marked Tree, Arkansas. Its great length indicates that, if it is a fault, the Bootheel lineament may be capable of generating a large earthquake and may be the surface expression of at least one of the coseismic faults of the New Madrid earthquakes of 1811 and 1812.

With the exception of the 5-km-long Reelfoot scarp in northwestern Tennessee, the Bootheel lineament is, to our knowledge, the first large-scale surface feature, mapped in the New Madrid seismic zone, that may reflect deep-seated faulting, not simply liquefaction-induced subsidence. We are currently (May 1989) mapping the Bootheel lineament in detail and plan to have excavated and logged at least one trench by the time of this field trip. One of our goals is to determine the length of the lineament that ruptured in 1811-12 and the type of displacement. If the Bootheel lineament is indeed a reflection of deep-seated processes, it probably has ruptured in more than one large earthquake in the New Madrid seismic zone. As discussed below, the liquefaction and topographic depression common along this feature create a high potential for the preservation of paleoearthquake features. In addition, the depression increases the likelihood that material datable by ¹⁴C methods may have accumulated.

On satellite images, the Bootheel lineament appears as a subtle linear feature, sometimes darker, sometimes lighter, than the surrounding area; it commonly separates areas of contrasting reflec-

tance. Such contrast is due to different concentrations of liquefied sand vented to the ground surface. The lineament is far more obvious on conventional-scale black-and-white aerial photographs (fig. 10).

The surface trace of the Bootheel lineament consists of a number of very linear segments. Gaps between segments are commonly due to small stream meander scars that obscure the lineament trace. In other areas, the gaps separate segments with slightly different trends; they may represent original discontinuities in the lineament. The nature of the trace, which varies along strike, is represented by some combination of (1) a contrast in sandblow density on opposite sides, generally denser to the southeast; (2) shallow linear depressions, commonly containing standing water; (3) linear continuous or discontinuous sand bodies, presumably liquefaction related; and (4) the apparent truncation of some fluvial features against the lineament, on the southeast side.

Detailed surveying across the Bootheel lineament at two sites generally indicates a 10- to 20-m-wide depression. The area northwest of the lineament is about 0.5 to 1.0 m lower than the area to the southeast. Differences in elevation between the two sides of the lineament could account for the apparent truncation of fluvial features and lack of liquefaction deposits on the northwest side of the lineament; later deposition may have partially covered the surface on the downthrown side. Although topographic irregularities along the Bootheel fault are very subtle, they are visible in the field because they contrast with otherwise extremely flat areas adjacent to the fault zone.

Farmers in several places have used the linear depression as drainage for their fields or to separate acreage with different crops. These ditches are conspicuous on photographs and maps, because they contrast with the otherwise nearly rectilinear drainage ditches and field boundaries in the region. A farmer who has lived 70 yr on the land in the area of Stop H has stated that, before drainage ditches were excavated, the region southeast of the Bootheel lineament always stood above water during minor floods.

Hamilton and McKeown (1988) reported seismic-reflection profiles that revealed a complex anticlinal feature under the southern axial trend of the New

Madrid seismic zone. They named this mostly pre-Late Cretaceous feature the Blytheville arch. Along much of the northern part of the Bootheel lineament, its trace is directly over the faulted western edge of the Blytheville arch. Some seismic-reflection profiles south of the mapped trace of the Bootheel lineament indicate some Tertiary or younger reactivation of the Blytheville arch (R. Hamilton and F. McKeown, oral commun., 1989).

The most recent activity of the Bootheel lineament is of uncertain age. The trace is cut by a few young fluvial meander scars, which indicates only that it

is probably older than this century. Inasmuch as the trace *cuts* many meander scars, it therefore must be younger than 9.5 ka, the age of the earliest meandering streams in the upper Mississippi embayment (R.T. Saucier, oral commun., 1989). Activity probably occurred along the Bootheel lineament during the 1811-12 earthquakes, and it may represent surface faulting from that sequence. Certainly liquefied sand was localized along the lineament at that time. Some microseismicity along its trace (see fig. 2) suggests continuing activity of the Bootheel lineament.

ACKNOWLEDGMENTS

We wish to thank A.J. Crone, R.M. Hamilton, L.R. Kanter, F.A. McKeown, and S.F. Obermeier for thoughtful reviews of this field guide; Tanya George and Pannir Ramaya for drafting maps; and R.G.

Stearns for showing us several stops on this trip. We also thank the many kind landowners and operators for access to their property.

REFERENCES

- Autin, W.J., Burns, S.F., Miller, B.J., Saucier, R.T., and Snead, J.I., 1989, Quaternary geology of the lower Mississippi Valley, *in* Morrison, R.B., ed., Quaternary nonglacial geology; conterminous U.S.: Geological Society of America, Geology of North America, v. K-2 (in press).
- Bickford, M.E., 1988, The formation of continental crust: Part 1. A review of some principles; Part 2. An application to the Proterozoic evolution of southern North America: Geological Society of America Bulletin, v. 100, p. 1375-1391.
- Blythe, E.W., Jr., 1986, Earthquake-related features in the Reelfoot Lake area of the New Madrid fault zone in northwest Tennessee, *in* Neathery, T.L., ed., Southeastern Section: Geological Society of America Centennial Field Guide, v. 6, p. 397-400.
- Braile, L.W., Hinze, W.J., Sexton, J.L., Keller, G.R., and Lidiak, E.G., 1984, Tectonic development of the New Madrid seismic zone, *in* Gori, P.L., and Hays, W.W., eds., Proceedings, Symposium on the New Madrid earthquakes: U.S. Geological Survey Open-File Report 84-770, p. 204-233.
- Braile, L.W., Keller, G.R., Hinze, W.J., and Lidiak, E.G., 1982, An ancient rift complex and its relationship to contemporary seismicity in the New Madrid seismic zone: Tectonics, v. 1, p. 225-237.
- Buschbach, T.C., and Schwalb, H.R., 1984, Sedimentary geology of the New Madrid seismic zone, *in* Gori, P.L., and Hays, W.W., eds., Proceedings, Symposium on the New Madrid earthquakes: U.S. Geological Survey Open-File Report 84-770, p. 64-96.
- Committee on Earthquake Engineering, 1985, Liquefaction of soils during earthquakes: Washington, D.C., National Academy of Sciences, 240 p.
- Conrad, T.A., 1856, Observations on the Eocene deposit of Jackson, Mississippi, with descriptions of 34 new species of shells and corals: Philadelphia Academy of Natural Sciences, Proceedings, 1855, 1st ser., v. 7, p. 257-258.
- Ervin, C.P., and McGinnis, L.D., 1975, Reelfoot rift: reactivated precursor to the Mississippi embayment: Geological Society of America Bulletin, v. 86, p. 1287-1295.
- Fuller, M.L., 1912, The New Madrid earthquakes: U.S. Geological Survey Bulletin 494, 119 p.

- Glenn, L.C., 1933, The geography and geology of Reelfoot Lake: Tennessee Academy of Science Journal, v. 8, no. 1, p. 2-12.
- Haller, K.M., and Crone, A.J., 1986, Log of an exploratory trench in the New Madrid seismic zone near Blytheville, Arkansas: U.S. Geological Survey Miscellaneous Field Studies Map MF-1858.
- Hamilton, R.M., and McKeown, F.A., 1988, Structure of the Blytheville arch in the New Madrid seismic zone: Seismological Research Letters, v. 59, p. 117-121.
- Herrmann, R.B., and Canas, J.A., 1978, Focal mechanism studies in the New Madrid seismic zone: Seismological Society of America Bulletin, v. 68, p. 1095-1102.
- Heyl, A.V., and McKeown, F.A., 1978, Preliminary seismotectonic map of central Mississippi Valley and environs: U.S. Geological Survey Miscellaneous Field Studies Map MF-1011, scale 1:500,000.
- Hildenbrand, T.G., 1985, Rift structure of the northern Mississippi embayment from the analysis of gravity and magnetic data: Journal of Geophysical Research, v. 90, p. 12607-12622.
- _____, Kane, M.F., and Hendricks, J.D., 1982, Magnetic basement in the upper Mississippi embayment region — A preliminary report, *in* McKeown, F.A., and Pakiser, L.C., eds., Investigations of the New Madrid, Missouri, earthquake region: U.S. Geological Survey Professional Paper 1236-E, p. 39-53.
- Jibson, R.W., 1985, Landslides caused by the 1811-12 New Madrid earthquakes [Ph.D. thesis]: Stanford, California, Stanford University, 232 p.
- _____, and Keefer, D.K., 1988, Landslides triggered by earthquakes in the central Mississippi Valley, Tennessee and Kentucky: U.S. Geological Survey Professional Paper 1336-C, 24 p.
- _____, 1989, Statistical analysis of factors affecting landslide distribution in the New Madrid seismic zone, Tennessee and Kentucky: Engineering Geology (in press).
- Johnston, A.C., 1982, A major earthquake zone on the Mississippi: Scientific American, v. 246, no. 4, p. 60-68.
- _____, and Nava, S.J., 1985, Recurrence rates and probability estimates for the New Madrid seismic zone: Journal of Geophysical Research, v. 90, p. 6737-6753.
- Kane, M.F., Hildenbrand, T.G., and Hendricks, J. D., 1981, Model for the tectonic evolution of the Mississippi embayment and its contemporary seismicity: Geology, v. 9, p. 563-568.
- Krinitzky, E.L., and Turnbull, W.J., 1967, Loess deposits of Mississippi: Geological Society of America Special Paper 94, 64 p.
- Lyell, C., 1849, A second visit to the United States, v. 2: New York, Harper Brothers, 287 p.
- McGee, W.J., 1892, A fossil earthquake: Geological Society of America Bulletin, v. 4, p. 411-414.
- Nelson, W.J., and Lumm, D.K., 1985, Ste. Genevieve fault zone, Missouri and Illinois: U.S. Nuclear Regulatory Commission NUREG/CR-4333, 94 p.
- Newmark, N.M., 1965, Effects of earthquakes on dams and embankments: Geotechnique, v. 15, p. 139-160.
- Nuttli, O.W., 1973, The Mississippi Valley earthquakes of 1811 and 1812: intensities, ground motions and magnitudes: Seismological Society of America Bulletin, v. 63, p. 227-248.
- _____, 1982, Damaging earthquakes of the central Mississippi Valley, *in* McKeown, F.A., and Pakiser, L.C., eds., Investigations of the New Madrid, Missouri, earthquake region: U.S. Geological Survey Professional Paper 1236-B, p. 15-20.
- _____, and Herrmann, R.B., 1984, Ground motion of Mississippi Valley earthquakes: American Society of Civil Engineers, Journal of Technical Topics in Civil Engineering, v. 110, p. 54-69.
- Obermeier, S.F., 1984, Liquefaction potential in the central Mississippi Valley, *in* Gori, P.L., and Hays, W.W., eds., Proceedings, Symposium on the New Madrid earthquakes: U.S. Geological Survey Open-File Report 84-770, p. 391-446.

- _____, 1988, Liquefaction potential in the central Mississippi Valley: U.S. Geological Survey Bulletin 1832, 21 p.
- _____, Gohn, G.S., Weems, R.E., Gelinas, R.L., and Rubin, M., 1985, Geologic evidence for recurrent moderate to large earthquakes near Charleston, South Carolina: *Science*, v. 227, p. 408-411.
- O'Connell, D.R., Bufe, C.G., and Zoback, M.D., 1982, Microearthquakes and faulting in the area of New Madrid, Missouri-Reelfoot Lake, Tennessee, in McKeown, F.A., and Pakiser, L.C., eds., *Investigations of the New Madrid, Missouri, earthquake region*: U.S. Geological Survey Professional Paper 1236-B, p. 31-38.
- Owen, D.D., 1856, Report of the geological survey in Kentucky, made during the years of 1854 and 1855: Frankfort, Kentucky, p. 117-119.
- Penick, J.L., 1981, *The New Madrid earthquakes* (revised edition): Columbia, Missouri, University of Missouri Press, 176 p.
- Potter, P.E., 1955, The petrology and origin of the Lafayette gravel, part II, geomorphic history: *Journal of Geology*, v. 63, p. 115-132.
- Russ, D.P., 1979, Late Holocene faulting and earthquake recurrence in the Reelfoot Lake area, northwestern Tennessee: *Geological Society of America Bulletin*, Part I, v. 90, p. 1013-1018.
- _____, 1982, Style and significance of surface deformation in the vicinity of New Madrid, Missouri, in McKeown, F.A., and Pakiser, L.C., eds., *Investigations of the New Madrid, Missouri, earthquake region*: U.S. Geological Survey Professional Paper 1236-H, p. 95-114.
- _____, Stearns, R.G., and Herd, D.G., 1978, Map of exploratory trench across Reelfoot scarp, northwestern Tennessee: U.S. Geological Survey Miscellaneous Field Studies Map MF-985.
- Saucier, R.T., 1974, Quaternary geology of the lower Mississippi valley: *Arkansas Archeological Survey Research Series* 6, 26 p.
- _____, 1977, Effects of the New Madrid earthquake series in the Mississippi alluvial valley: U.S. Army Engineer Waterways Experiment Station Miscellaneous Paper S-77-5, 26 p.
- _____, 1981, Current thinking on riverine processes and geologic history as related to human settlement in the southeast: *Geoscience and Man*, v. 22, p. 7-18.
- _____, 1989, Evidence for episodic sand-blow activity during the 1811-1812 New Madrid (Missouri) earthquake series: *Geology*, v. 17, p. 103-106.
- Stearns, R.G., 1979, Recent vertical movement of the land surface in the Lake County uplift and Reelfoot Lake basin areas, Tennessee, Missouri, and Kentucky: U.S. Nuclear Regulatory Commission NUREG/CR-0874, 37 p.
- Street, R., and Nuttli, O., 1984, The central Mississippi Valley earthquakes of 1811-1812, in Gori, P.L., and Hays, W.W., eds., *Proceedings, Symposium on the New Madrid earthquakes*: U.S. Geological Survey Open-File Report 84-770, p. 33-63.
- Talwani, P., and Cox, J., Paleoseismic evidence for recurrence of earthquakes near Charleston, South Carolina: *Science*, v. 229, p. 379-381.
- Thacker, J.L., and Satterfield, I.R., 1977, *Guidebook to the geology along Interstate-55 in Missouri*: Missouri Department of Natural Resources, Division of Geology and Land Survey, Report of Investigations 62, 132 p.
- Usher, F.C., 1837, On the elevation of the banks of the Mississippi in 1811: *Silliman's Journal (American Journal of Science, First Series)*, v. 31, p. 291-294.
- Varnes, D.J., 1978, Slope movement types and processes, in Schuster, R.L., and Krizek, R.J., eds., *Landslides, analysis, and control*: Washington, D.C., National Academy of Sciences, Transportation Research Board Special Report 176, p. 12-33.
- Weaverling, P.H., 1987, Early Paleozoic tectonic and sedimentary evolution of the Reelfoot-Rough Creek rift system, midcontinent, U.S. [M.S. thesis]: Columbia, Missouri, University of Missouri, 116 p.

- Wesnousky, S.G., Schweig, E.S., and Pezzopane, S.K., 1987, Observations of soil liquefaction in the New Madrid seismic zone, *in* Jacob, K.H., ed., Proceedings, Symposium on seismic hazards, ground motions, soil-liquefaction and engineering practice in eastern North America: National Center for Earthquake Engineering Research Technical Report NCEER-87-0025, p. 494-503.
- White, P.E., 1967, Outline of thermal and mineral waters as related to origin of Mississippi Valley ore deposits, with discussions, *in* Brown, J.S., ed., 1967, Genesis of stratiform lead-zinc-barite-fluorite deposits in carbonate rocks (the so-called Mississippi Valley type deposits), a symposium: Economic Geology Monograph 3. p. 379-382.
- Youd, T.L., 1973, Liquefaction, flow, and associated ground failure: U.S. Geological Survey Circular 688, 12 p.
- Zoback, M.D., 1979, Recurrent faulting in the vicinity of Reelfoot Lake, northwestern Tennessee: Geological Society of America Bulletin, v. 90, p. 1019-1024.
- Zoback, M.L., and Zoback, M.D., 1980, State of stress in the conterminous United States: Journal of Geophysical Research, v. 85, p. 6113-6156.
- _____, 1989, Tectonic stress field of the continental U.S., *in* Pakiser, L., and Mooney, W., eds., Geophysical framework of the continental United States: Geological Society of America Memoir (in press).

Field Trip No. 7

**HYDROGEOLOGY OF
SHALLOW KARST
GROUND-WATER SYSTEMS IN
SOUTHEASTERN MISSOURI**

James E. Vandike and Cynthia Endicott
Missouri Department of Natural Resources
Division of Geology and Land Survey
P.O. Box 250
Rolla, Missouri 65401

and

Paul Blanchard
Department of Geology
University of Missouri-Columbia
Columbia, Missouri 65211

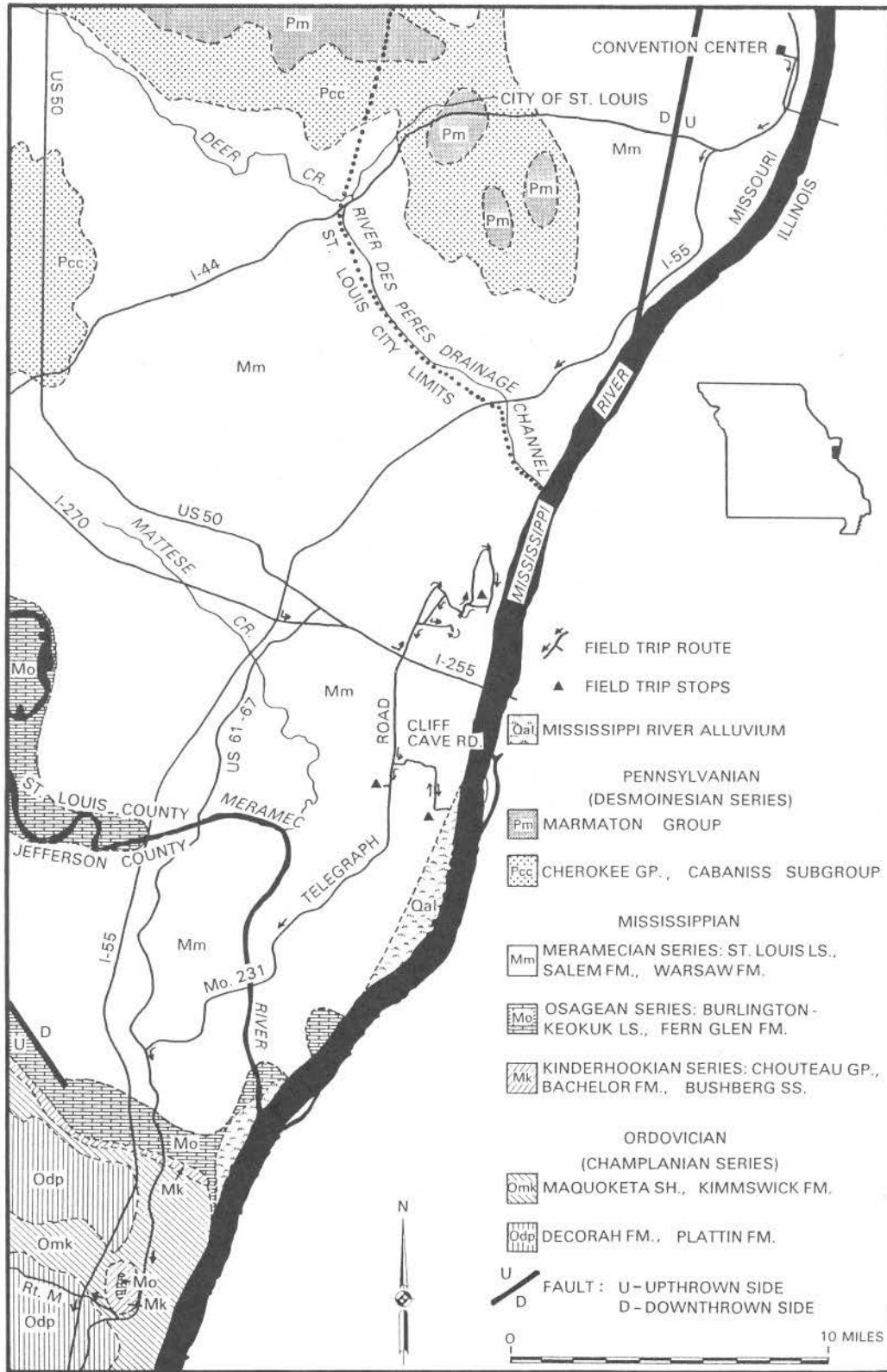


Figure 1 — Generalized geologic map of the St. Louis County portion of the field trip. Geology from Geologic Map of Missouri, 1979.

INTRODUCTION

Ordovician and Mississippian carbonate rocks outcropping in a belt along the eastern flank of the Ozarks uplift in southeastern Missouri and adjacent parts of southwestern Illinois have been intensely karstified. This band of shallow karst development extends from the Florissant karst area in northeastern St. Louis County southeastward to Cape Girardeau, a distance of about 110 mi. Karst features are very common throughout this region, but intense karst development is found primarily in extreme northeast and southeast St. Louis County, eastern Ste. Genevieve County, and eastern Perry County. Large areas of internal drainage, numerous caves, and many springs are found in this region.

Nearly any of the many carbonate formations outcropping in southeastern Missouri show karst development, but intense karst development is limited to specific stratigraphic units. Intense karst development in northeastern and southeastern St. Louis County is primarily in the Mississippian (Meramecian) St. Louis Limestone. In eastern Ste. Genevieve County the Mississippian (Meramecian) Ste. Genevieve Limestone contains many sinkholes and caves. In eastern Perry County, the Ordovician (Champlanian) Joachim Dolomite and Plattin Formation underlie extensive sinkhole plains and contain hundreds of caves including several of the longest caves in Missouri and the United States.

This field trip follows the eastern flank of the Ozark uplift, traversing several of the aforementioned

southeastern Missouri karst regions. The core of the uplift, the St. Francois Mountains, is a subdued mountain range about 75 mi south-southwest of St. Louis. Total structural relief in the Ozarks is greater than 5,000 ft. Dips are steepest on the east and southeast sides of the uplift, averaging about 100 ft/mi, with steeper dips generally associated with faulting, local folds, or solution-induced collapse features. Major fault systems generally reflect the Precambrian basement structure and trend predominantly northwest and to a lesser degree, northeast (Vineyard et al., 1981).

Stops in southeastern St. Louis County in the Jefferson Barracks karst area show landfill development and urbanization effects in karst areas, and how developers contend with karst drainage in new and old subdivisions. Between St. Louis and Perryville the field trip will travel I-55, which roughly follows the Ordovician (Champlanian) St. Peter Sandstone outcrop belt, avoiding the many karst areas developed in dolomites and limestones to the east and west. Just north of the Perry County-Ste. Genevieve County line, I-55 crosses the Ste. Genevieve fault complex, a major structural feature of southeastern Missouri and adjacent Illinois, with up to about 1,800 ft of vertical displacement. Stops in Perryville and the Perryville karst area will explain the complex nature of local subsurface drainage, the interrelationships between many of the karst features, and the problems of urbanization in this unique karst area.

ROAD LOG MILEAGE

0.0 Start at the field trip staging area, proceed east on Convention Plaza to Memorial Drive, and turn right and proceed south to I-55 south/I-44 west.

1.2 Enter I-55 south/I-44 west. The highways separate in one mile; continue south on I-55 to exit 196A.

This portion of the field trip parallels the Mississippi River through downtown St. Louis and passes close to the Gateway Arch. Geology is mostly obscured by urban development, but the area is underlain by Missis-

sippian carbonates and shales. Loess caps the bedrock (fig. 1).

13.6 Intersection I-55, I-270, and I-255. Take exit 196A and proceed east on I-255 to Exit 2.

15.8 Exit 2, Intersection I-255 and Telegraph Road (Mo. 231). Take exit, turn left, and proceed north on Telegraph Road.

17.5 Turn right and proceed east on Jefferson Barracks Road. Jefferson Barracks Road becomes Sherman Avenue; continue east on Sherman Avenue to Worth Road.

- 18.2 Turn left and proceed north on Worth Road. For the next mile, the road follows the western margin of a sinkhole plain. Several sinkholes are adjacent to the road, but most of them were destroyed before the early 1970's when the area was a landfill.
- 19.3 Turn right on Cye road. Large sinkholes are left and right of the road.
- 19.4 Turn right on Grant Road, which parallels Worth Road, about $\frac{3}{8}$ mi to the west. The landfilled area is to the right.
- 20.0 Turn left and stop at Jefferson Barracks Historical Marker and overlook.

STOP 1: JEFFERSON BARRACKS KARST AREA

The Jefferson Barracks karst area is a region of intense sinkhole development adjacent to the Mississippi River, in southeastern St. Louis County. Sinkhole development is in a band up to about 1.5 mi wide, beginning 1 mi north of the stop southward for another 5 mi to just north of the Meramec confluence with the Mississippi River (fig. 2). Karst development is in the Mississippian St. Louis Limestone, which has a maximum thickness of about 100 ft. A thick loess blanket caps the bedrock throughout the area.

The northern portion of the sinkhole plain is part of the St. Louis County parks system, but was formerly part of the Jefferson Barracks military reservation, which still occupies much of the sinkhole plain to the south. Vineyard (1971) reports that landfilling in the northern part of the karst area began in the late 1940's and continued to about 1971. A comparison of the topography shown on the Webster Groves, Missouri-Illinois 7.5-minute Quadrangle with today's topography shows that about 160 acres of the sinkhole plain have been landfilled. Where sinkholes were up to 50 ft deep is now gently rolling topography. It was hoped that vertical drain tiles placed in sinkholes as landfilling progressed would improve drainage in the landfilled area.

Vineyard (1971) reports four springs draining the sinkhole plain in the immediate area (fig. 2); they

discharge from bedding plane or joint openings in the St. Louis Limestone above a rock bench adjacent to the Mississippi River and apparently have low but well-sustained base flows. The southern two springs, both south of the landfill area, discharge relatively good-quality water. The northern two springs, Black Spring and Sewer Spring, do not share these same water-quality characteristics; both discharge heavily contaminated water and have distinctive hydrogen sulfide odors. Water analyses of these two springs show elevated sulfate, iron, and manganese, but very low nitrate. Dye tracing studies have not determined contaminant sources, but the adjacent landfill is strongly suspected of causing poor water quality.

Several sinkholes in the immediate area are modified to improve storm-water disposal. Shallow storm-water disposal wells installed in the sinks differ in construction, but serve to channel storm-water runoff more quickly into the subsurface than did unmodified sinks. Vineyard (1971) reported that one sink equipped with a manhole cover was used by "honey dippers" (septic tank cleaners) for convenient disposal of tank loads of sewage.

- 20.0 Leave overlook, return to, and turn left on Grant Road.
- 20.5 Turn right and proceed west on Hancock Road. Jefferson Barracks military reservation is on the left. Turn left and proceed south on Worth Road. Turn right and proceed west on Sherman Avenue to Boundary Road.
- 21.4 Turn left from boundary Road into Sylvan Spring Park. Turn Left at Sheridan Road.
- 22.5 Turn right into Jefferson Barracks National Cemetery; the brief drive through it perhaps shows a wiser type of land use for this urban karst area. The cemetery began in 1826 as the Jefferson Barracks Military Post cemetery. It became a National Cemetery in 1866 and occupies 309 acres, of which 165 acres are developed. The 95,000 burials include veterans of the American Revolution; the War of 1812; Confederate and Union Civil War soldiers; veterans of WW I, WW II, Korea, and Vietnam; German and Italian prisoners of war (WW II); seven Medal of Honor recipients; and 3,255 unknown United States soldiers. The

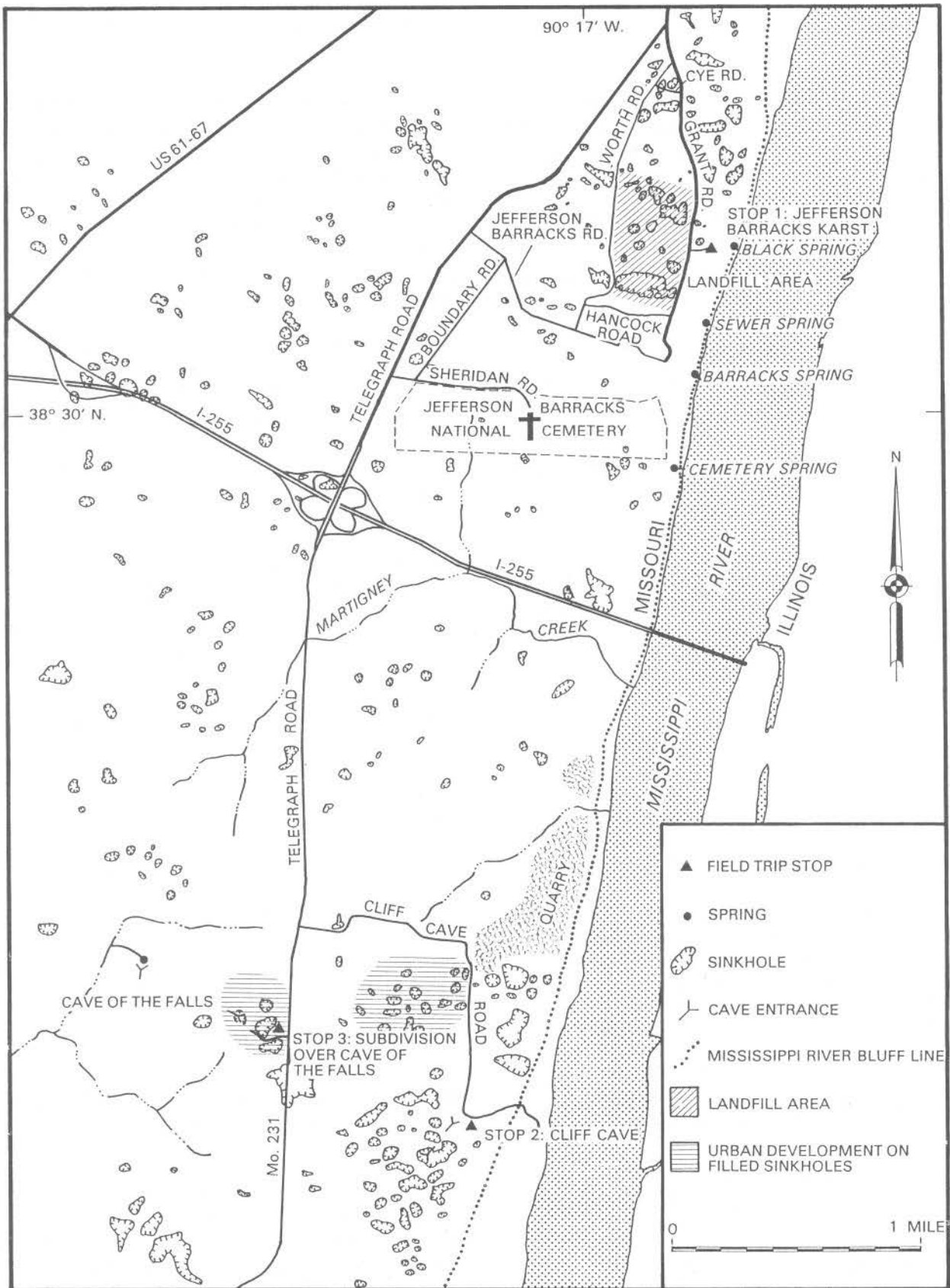


Figure 2 — Field trip route, field trip stops, and karst features in the Jefferson Barracks karst area.

cemetery route passes through burial-site sinkholes. Drainage is apparently good in the sinkholes, as there is no visible evidence of ponding.

- 23.8 Leave Jefferson Barracks National Cemetery, turn left, and proceed west on Sheridan Road.
- 24.3 Turn left and proceed south on Telegraph Road.
- 25.9 A storm-water drainage well can be seen in the bottom of a sinkhole on the west (right) side of Telegraph Road. The well not only channels storm-water runoff into the shallow karst drainage system, but also receives sewage from houses on either side of the sink.
- 26.6 Turn left on Cliff Cave Road. In about 0.75 mi Cliff Cave Road turns south. A large quarry on the left has removed much of the limestone east of Cliff Cave Road. The new subdivision on the right was built on the sinkhole plain. Developers filled some sinks; others were equipped with subsurface storm-water drainage wells that channel street runoff into the underlying conduit systems.
- 28.0 Enter parking area on right at Cliff Cave Park.

STOP 2: CLIFF CAVE

Cliff Cave, also known as Indian Cave, has had a colorful cultural and geologic history. The site reportedly was used by Indians, and in the early to middle 1700's, as a resting place and tavern for French fur trappers. In the 1800's it served as a winery for the Cliff Cave Wine Company and a stop for riverboats on the Mississippi (Marty, 1983). Today, it and the surrounding 231 acres are part of the St. Louis County park system.

Cliff Cave is developed in the St. Louis Limestone about 0.25 mi west of the Mississippi River, in extreme southeast St. Louis County. The St. Louis and other underlying Mississippian carbonates and shale crop out along the Mississippi River valley wall a short distance from the cave.

The 4,700-ft cave can be entered from any of four locations, three of which are through sinkholes. The primary entrance, some 50 ft wide and 20 ft high,

is at the head of a steep ravine about 80 ft above the Mississippi River floodplain. Ruins of a stone wall at the entrance, date from the 1800's, when the cave was used as winery. The entrance room is about 150 ft long and 50 ft wide with a 20-ft ceiling height. The cave trends southwestward from the entrance room with ceiling height and passage dimensions gradually decreasing. The first 700 ft of passage can be easily walked, but much of the remaining passage comprises partly water-filled crawlways. Two side passages enter the main trunk of the cave from the west; both transport water draining from the overlying sinkhole plain through the cave. The second and third entrances are in sinkholes 90 ft apart, about 800 ft southwest of the primary entrance; the fourth entrance is another 500 ft southwest.

Bretz (1956) found excellent examples of phreatic and vadose cave development in Cliff Cave. Phreatic development along two prominent joint sets instituted conduit development. Vadose enlargement followed phreatic development of the conduits. Facetting and fluting can be seen in the floor and walls, about 500 ft from the entrance.

Little flow and no water-quality information are available. Flow likely varies greatly with local rainfall. Water quality appears good, and since recharge to the cave stream is from the sinkhole area above and west of the cave, water-quality changes are probably related to development in the sinkhole plain.

- 28.0 Leave Cliff Cave parking area; return to Telegraph Road on Cliff Cave Road.
- 29.4 Turn left and proceed south on Telegraph Road to England Town Street.
- 29.7 Turn right on England Town Street, and left into parking area at the intersection.

STOP 3: SUBDIVISION DEVELOPMENT IN A SINKHOLE PLAIN ALONG TELEGRAPH ROAD

Most earlier urbanization along Telegraph Road avoided sinkholes; the winding nature of many of the roads attest to this. Roads and older homes are built on rims between adjacent sinkholes. There are exceptions to this, though, and some older homes have been built in sinkholes. Several sinks contain

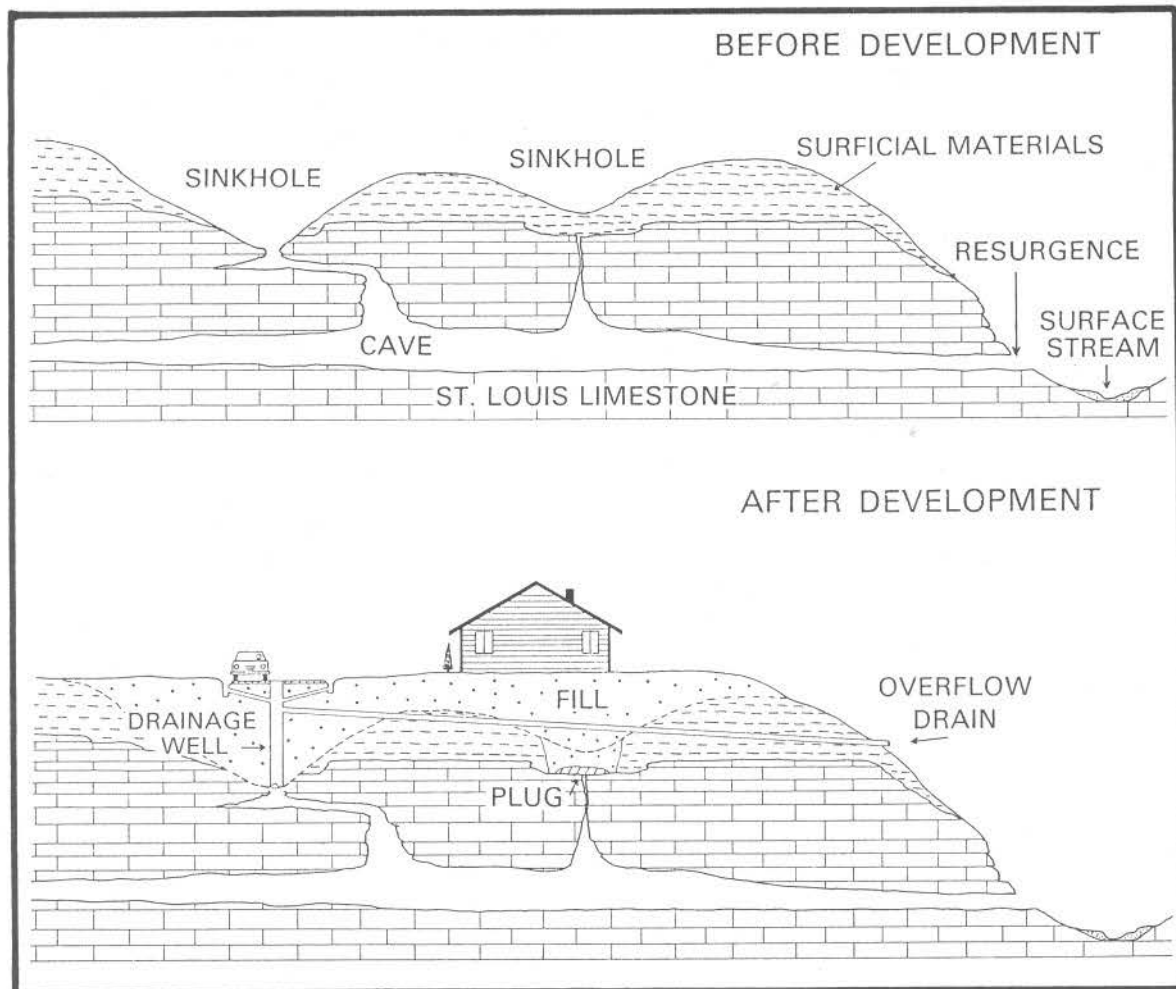


Figure 3 — Diagrammatic cross-section showing subdivision sinkhole modification in south St. Louis County.

storm-water drainage wells, but most are unmodified.

Today, the quest for undeveloped land in the metropolitan area has changed this; even land poorly suited for residential or commercial development is developed because of high land value. The high price of drainage modification is passed to the purchasers by developers.

The subdivision at this location is mostly less than 10 years old. Most of it overlies Cave of the Falls, a major karst feature containing more than a mile of mapped passages. It has three entrances, two in sinkholes in the subdivision, and the spring entrance along a Mattese Creek tributary to the northwest. Before development, four sinkholes, up to 20 ft deep

and 500 ft in diameter, were in the subdivision. Two of them contained entrances to Cave of the Falls; three were filled to allow development. One sink, which contained the main sinkhole entrance to the cave, was equipped with a storm-water drainage well to channel street runoff into the cave. The remaining sink, directly in front of the parking area, is a storm-water retention basin that contains a storm-water inlet that channels runoff into the second sinkhole entrance of the cave. The remaining sinkholes were excavated to bedrock; inlets were plugged with concrete and backfilled to allow development. Figure 3 shows the type of sinkhole modifications typically made during subdivision development in this area.

The County Division of Highways and Traffic, which regulates development in St. Louis County,

requires developers in sinkhole areas who use the karst drainage system to dispose of storm-water runoff to construct overflow drains capable of carrying storm-water runoff from the sinkhole plain to a surface stream, even if the karst drainage system appears adequate.

- 29.7 Leave parking area, turn right, and proceed south on Telegraph Road (Mo. 231).
- 36.5 Junction Mo. 231 and US 61-67. Turn left and proceed south on US 61-67.
- 41.2 Junction US 61-67 and Route M. Turn right and proceed west on Route M.
- 41.9 Junction I-55. Turn left and proceed south on I-55 to Perryville.
- 97.9 Junction Mo. 51 (Exit 129, Perryville). Exit I-55, turn left and proceed north on Mo. 51.
- 98.9 Turn right and proceed west on Edgemont Boulevard.
- 99.3 Turn right and proceed south on Big Spring Boulevard.
- 100.1 Turn into the Perryville Golf Course parking area on the left.

STOP 4: ST. PETER SANDSTONE OUTCROP

Perry County is on the eastern flank of the Ozark uplift. The western part of the county is underlain by lower Ordovician (Canadian) dolomites and sandstones. Dip, generally less than 100 ft/mi, is to the east-northeast. Perryville is in the eastern part of Perry County, where Canadian strata are well below land surface and younger Ordovician (Champlanian) strata crop out (fig. 4). The St. Peter Sandstone, which generally forms the base for karst development in the Perryville karst area, is a fine- to medium-grained quartzose sandstone that is 60 to 200 ft thick, and averages about 75 ft thick at Perryville.

The St. Peter is unconformably overlain by the Joachim Dolomite, which forms the bedrock surface throughout the central part of the Perryville karst area. The Joachim, locally about 250 ft thick, is a yellow-brown silty dolomite containing limestone

interbeds and minor shale. The Plattin Formation, which overlies the Joachim, is about 350 ft thick, and forms the bedrock surface throughout most of the eastern part of the Perryville karst area. It is gray, finely crystalline to sublithographic limestone with minor shale. The Joachim and Plattin both thicken eastward.

Though the Plattin is the youngest bedrock unit exposed in the Perryville karst area, a few miles northeast of Perryville extensive faulting along the Ste. Genevieve fault system has brought Mississippian rocks to the surface, where they abut the Champlanian strata.

Both the Joachim and Plattin contain numerous karst features in the region. The Plattin contains many sinkholes, but the Joachim contains the major caves and springs. Perry County currently has 622 known caves, the majority of them in the Joachim Dolomite. Four major caves in eastern Perry County, all within 5 mi of Perryville, contain more than 70 mi of mapped passages. Figure 5 shows the major caves and springs in the Perryville karst area.

At this stop, the St. Peter Sandstone exhibits sinkhole development, which is unusual for this formation. Most likely, the St. Peter sinkholes are due more to solution and collapse in the underlying Everton Formation than solution in the St. Peter. Big Spring, optimistically named, is one of the smaller springs in the Perryville karst area. It discharges just above the level of the golf course lake. Several dozen acres on the west side of Big Spring Boulevard drain into an ephemeral stream flowing into a conduit in the St. Peter Sandstone; the water is channelled underground a short distance to Big Spring. Drainage through the conduit is somewhat sluggish, however, and water floods over Big Spring Boulevard after heavy rains.

- 100.1 Leave parking area and return to Edgemont Boulevard on Big Spring Boulevard. Turn right and proceed east on Edgemont Boulevard.
- 101.0 Turn left and proceed north on School Street. Several large sinkholes can be seen along School Street.
- 101.6 Turn left and proceed west on Drury Lane. At Bruce Street, turn right and proceed north.
- 101.8 Turn right onto Star Street and park.

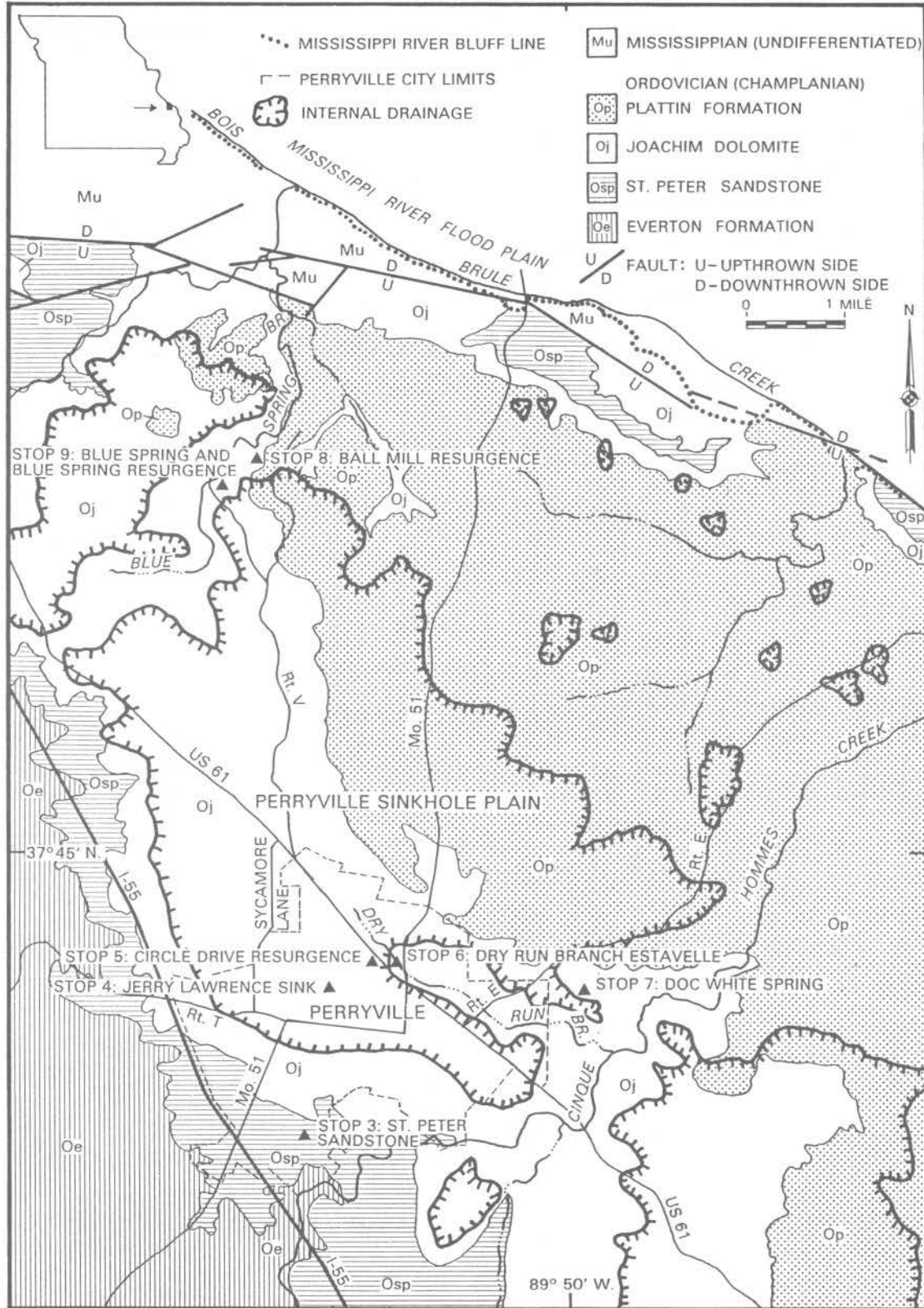


Figure 4 — Geologic map and field trip stops for the Perryville karst area portion of the field trip. Geology compiled from various sources by Kim E. Haas.

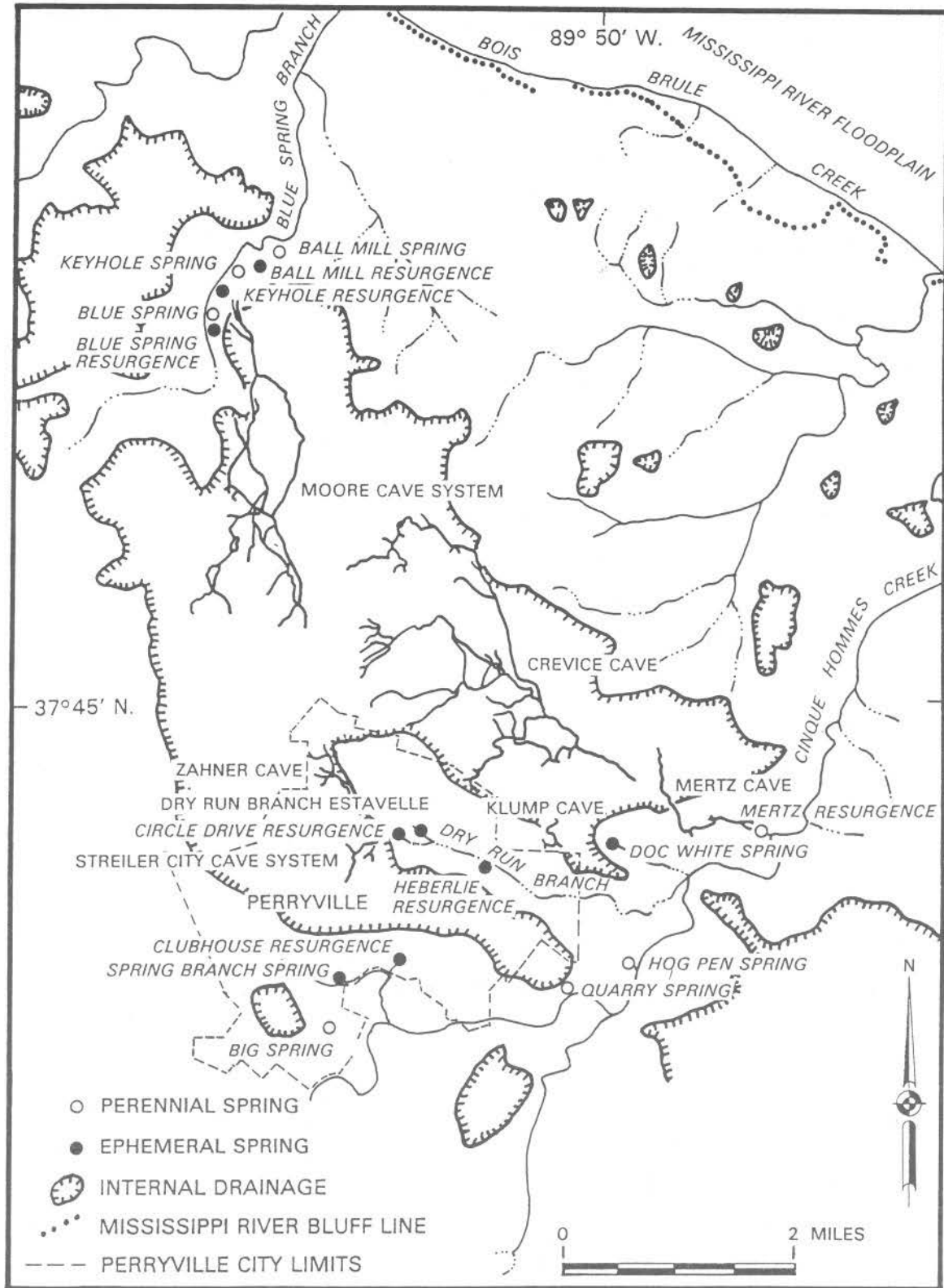


Figure 5 — Major springs, resurgences, and caves in the Perryville karst area (modified from Vandike, 1985).

STOP 5: JERRY LAWRENCE SINK

Jerry Lawrence Sink is an eastward extension of a large shallow uvala developed in the Joachim Dolomite in the western part of Perryville. Before extensive modification and drainage improvement, the sinkhole was subject to flooding after heavy rains. During construction activities in the sinkhole, Streiler City Cave was re-discovered, the entrance of which, choked with accumulated debris and brush, was excavated. Four-foot diameter concrete pipe was laid from the entrance about 200 ft southwest. Two storm-water drainage wells were constructed to channel water from the sinkhole into the upstream reaches of the cave. The pipe leading into the mouth of the cave is an overflow inlet, and only functions when the storm-water drainage wells are overwhelmed by heavy runoff. The area of a planned subdivision that would have been subject to flooding during heavy rainfall is now a storm-water retention and disposal basin. The City plans to build soccer fields or other recreational facilities in the sinkhole.

Jerry Lawrence Sink continues westward to the other side of Bruce Street, an extension that drains nearly 300 acres. Runoff is channelled into the subsurface through a natural throat just west of Bruce Street. Water enters a conduit related to Streiler City Cave, and eventually emerges at several karst resurgences eastward.

The hydrogeology of the Perryville karst area is complex. A hydrogeologic study by Vandike (1985) used extensive dye tracing to determine the outflow points of runoff in the karst area. The Perryville sinkhole plain contains about 16 mi² of continuous internal drainage. Springs and karst resurgences along surface drainages to the northwest and southeast, Blue Spring Branch, and Cinque Hommes Creek, discharge water entering the subsurface through sinkholes in the sinkhole plain. Two major cave systems transport water. The Crevice Cave system, comprising several hydrologically connected caves including Crevice Cave, Mertz Cave, Klump Cave, Streiler City Cave, and Zahner Cave, drains approximately the eastern two-thirds of the Perryville sinkhole plain. The Moore Cave system, which includes Berome Moore Cave, Tom Moore Cave, and other smaller caves, drains approximately the western one-third. These cave systems are among the largest in Missouri. Crevice Cave alone contains

more than 27 mi of mapped passages; the Moore Cave system contains more than 17 mi.

Dye tracing has shown that water entering sinkholes in Perryville mostly drains through a southern branch of the Crevice Cave system, and emerges at several hydrologically connected springs and karst resurgences. The base-flow outlet of the system is Mertz Resurgence on the north side of Cinque Hommes Creek, about 3 mi east of Perryville. Mertz Resurgence discharges much of the runoff entering the karst ground-water system in Perryville, but upstream from Mertz Resurgence are at least four other ground-water outlets that may, depending on hydraulic head in the cave system, discharge a portion of the water. Mertz Resurgence drainage in Perryville is divided into three sub-basins: Circle Drive Resurgence, Heberlie Resurgence, and Dry Run Branch Estavelle. Circle Drive Resurgence and Heberlie Resurgence are essentially overflow outlets for the subsurface drainage network, and discharge water only after heavy rains. Dry Run Branch Estavelle, depending on runoff, can function as either a spring or sinkhole.

Only a portion of the karst recharge discharges from Circle Drive and Heberlie Resurgences and Dry Run Branch Estavelle; the remainder continues downstream in the conduit system toward Mertz Resurgence. Doc White Spring, an intermittent spring between Perryville and Mertz Resurgence, is another overflow outlet for this karst ground-water system. Dry much of the time, it begins discharging water after moderate runoff and before the other overflow outlets in Perryville begin discharging. Like the other upstream resurgences, it discharges only a portion of the water entering the conduit system. The remainder is transported to Mertz Resurgence.

Jerry Lawrence Sink and Streiler City Cave are near the upstream end of this karst drainage system. Dye introduced into Jerry Lawrence Sink can be recovered only at Mertz Resurgence during relatively dry weather. If there is ample runoff to cause discharge at Doc White Spring, dye will also emerge there. After very heavy rains, dye can also be recovered from Circle Drive Resurgence. Figure 6 shows the hydrologic relationships between Jerry Lawrence Sink, Streiler City Cave, and other karst features in northwestern Perryville.

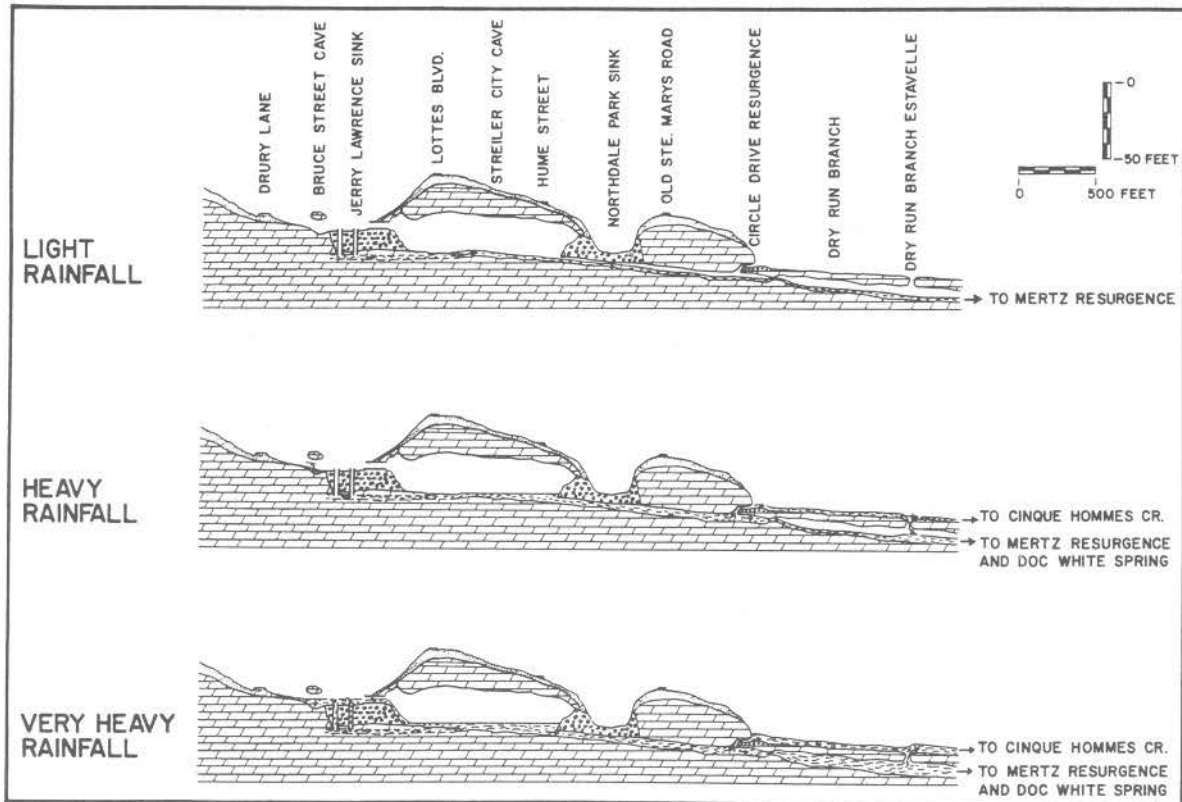


Figure 6 — Diagrammatic cross-section of northwestern Perryville, showing hydrologic relationships of several karst features including Jerry Lawrence Sink, Streiler City Cave, Northdale Park Sink, Circle Drive Resurgence, and Dry Run Branch Estavelle (from Vandike, 1985).

Storm-water drainage wells like those in Jerry Lawrence Sink are a common sight in Perryville. Sinkhole drainage problems date back to the early days of the city. For years, private individuals installed drainage wells in sink bottoms. Today, the city has easements on many of the drainage wells and installs most new ones. Sinkhole modification is controlled by city ordinance that requires a permit for modifications. Most drainage wells are less than 20 ft deep and are typically constructed using large-diameter concrete pipe. Sinkholes are excavated until bedrock openings are encountered. Precast concrete pipe is set over the bedrock openings, a gravel pack is placed around the lower part of the concrete pipe, and the hole is backfilled to original grade. A trash rack completes installation (Vandike, 1987).

Further housing development in sinkholes will soon be limited in the city. In a study funded by

the City of Perryville, Vandike (1988) calculated expected water levels in 58 sinkholes in the city under various rainfall, runoff, and outflow conditions, information that will be used by the city to establish minimum construction elevations for sinkholes in Perryville.

101.8 Leave Jerry Lawrence Sink, turn right, and proceed north on Bruce Street. Turn right on Hume Street and proceed southeast to Northdale Boulevard. Turn left and proceed northeast on Northdale Boulevard. Northdale Park on the left is built in a large sinkhole that, despite several storm-water drainage wells, floods after heavy rains. Part of the problem may be water ascending from the underlying conduit system through the base of the sinkhole.

102.7 Turn left and proceed northwest on St. Marys Street, about 100 ft to the next intersection, then turn right.

102.9 Turn right on US 61. Park on road shoulder 200 ft from last intersection.

STOP 6: CIRCLE DRIVE RESURGENCE

Circle Drive Resurgence, more accurately termed an estavelle, or reversible sinkhole, is in Dry Run Branch watershed. During dry weather, the resurgence appears simply to be a cave entrance, some 3 ft high and 8 ft wide, developed in the Joachim Dolomite. Minor rains will not cause water to discharge from the resurgence. In fact, just the reverse occurs; water draining from the area surrounding the resurgence flows into the cave entrance. During heavy rains, the flow reverses and water discharges from the resurgence, usually for only a brief period of perhaps one or two days, depending, of course, on rainfall amount and duration. Maximum estimated discharge after heavy rains is about 40 ft³/sec (Vandike, 1985).

Circle Drive Resurgence, an upper level overflow outlet for a southern branch of the Crevice Cave system, receives recharge from much of northwestern Perryville, including Jerry Lawrence Sink, but only a portion of the runoff entering the subsurface in the recharge area discharges from the spring. The remaining water continues eastward to Doc White Spring and Mertz Resurgence.

Cavers have had limited success in attempting to explore Circle Drive Resurgence during dry weather. The passage becomes quite small after only a few tens of feet, and considerable excavation would be necessary to continue.

The quality of water discharging from the resurgence is fair. A single analysis shows the water to be a calcium-magnesium-bicarbonate type, reflecting the dolomite bedrock in the recharge area. Sulfate, chloride, and nitrate concentrations are all low. The major water-quality problem is suspended sediment. Discharge occurs only after heavy rains when erosion is usually greatest. High karst groundwater velocities in the conduit systems probably allow little of the suspended solids to settle in the conduits; this results in highly turbid water at all springs draining the Perryville sinkhole plain.

102.9 Continue southeast on US 61 to Mo. 51. Turn left and proceed north on Mo. 51.

103.3 Dry Run Branch bridge. Park at the Intersection Motel parking lot just south of the bridge.

STOP 7: DRY RUN BRANCH ESTAVELLE

Dry Run Branch Estavelle, about 300 ft upstream from Mo. 51, is a sinkhole developed in the channel of Dry Run Branch, which is an intermittent stream. After rain, when there is flow in the stream here, much of the water disappears into the subsurface at Dry Run Branch Estavelle. During very heavy rains, however, the estavelle reverses flow and can channel several cubic feet of water per second from the underlying conduit into Dry Run Branch. Flow reversal is probably brief, lasting only long enough to release the underlying conduit of excess water. When head pressure in the conduit lessens, flow from the estavelle ceases (fig. 7).

Dry Run Branch upstream from the estavelle contains many sinkholes in the valley bottom. Downstream, the channel is on bedrock in many places.

The estavelle looks much different than it did a few years ago. There is an overflow pipe from which water can flow after heavy rains. Before modification, the estavelle was subject to relatively frequent sinkhole collapse. After heavy rainfall, new sinkholes would often form in the stream banks, occasionally threatening a trailer in the adjacent trailer park that was too close to the channel. Sinkholes may have formed by subsurface removal of alluvial material, but probably were formed more by excess water pressure from the underlying conduit; the sinks appeared to blow out rather than collapse. The City of Perryville excavated alluvial materials from the estavelle until solution-enlarged openings in the underlying bedrock were uncovered. Vertical concrete pipe in coarse gravel was placed in the hole before it was backfilled; since installation, the new collapses have decreased.

Dry Run Branch Estavelle, part of the Crevice Cave drainage system, is hydrologically connected with Circle Drive Resurgence but apparently does not share the same recharge area. Dye tracing indicates it is recharged from the area south of the Circle Drive

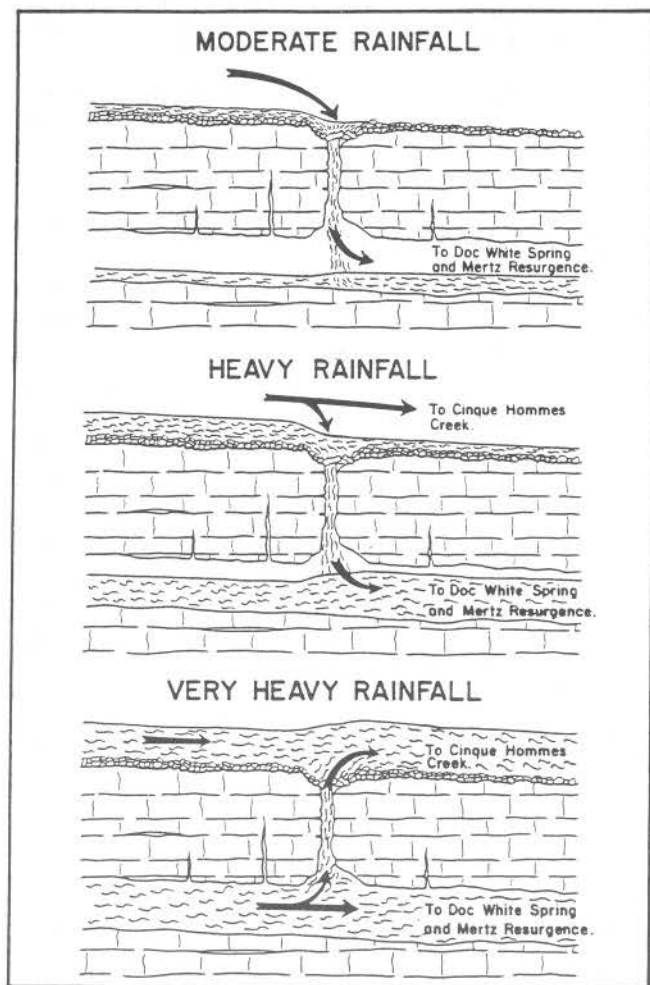


Figure 7 — Diagrammatic longitudinal section of Dry Run Branch Estavelle (from Vandike, 1985).

Resurgence recharge area, and may share recharge with Heberlie Resurgence, another karst ground-water outlet about a thousand feet downstream on Dry Run Branch.

- 103.3 Leave the parking lot and return to US 61 on Mo. 51. Turn left and proceed southeast on US 61 to Route E.
- 104.1 Turn left and proceed northeast on Route E. Dry Run Branch is crossed at the first bridge; Heberlie Resurgence is about 1200 ft upstream from the bridge.
- 105.2 Turn right into a private line; continue to the parking area about 500 ft southeast of Route E.

STOP 8: DOC WHITE SPRING

Doc White Spring is about 1 mi east of Perryville, in the upper watershed of an unnamed tributary of Cinque Hommes Creek. It is intermittent, like other karst ground-water outlets already visited; however, it discharges water more frequently than Circle Drive Resurgence and Dry Run Branch Estavelle. The water rises at the base of a low bluff of Joachim Dolomite from a subvertical cave opening. Water originally flowed through breakdown and other debris. In 1984, a backhoe removed debris blocking the spring opening; it was hoped to find an entrance for exploring and mapping this portion of the Crevice Cave conduit system. The spring was discovered to rise from a submerged opening at the end of an oblong room about 20 ft long and 8 ft wide. Even during dry weather, there is insufficient air space for exploration in the conduit.

Spring discharge is highly variable; flow ceases during dry summer weather, but after heavy rains discharge is estimated to be 40 ft³/sec. Water quality is similar to that of Circle Drive Resurgence.

Perhaps more fascinating than the spring is the geomorphology of the immediate setting. The area near the spring and part of the spring branch are a collapsed cave passage. A bedrock pillar, some hundred feet in diameter, 10 ft high, and only a few feet from the spring, is believed to be a remnant of cave wall between intersecting cave passages. At the base of the pillar, on the spring side, is a small vertical-sided sinkhole about 4 ft in diameter and depth (fig. 8). Even after the spring stops flowing in dry weather, water continues to flow through the bedding-plane opening at the base of the sink. Dye introduced into this small sinkhole was recovered in the cave stream of Mertz Cave, 4,500 ft to the northeast, and Mertz Resurgence, 6,200 ft northeast of Doc White Spring.

Doc White Spring is a middle-level overflow outlet for the conduit system channelling water from the western part of the Perryville sinkhole plain to Mertz Resurgence. Like Circle Drive Resurgence and Dry Run Branch Estavelle, it discharges only part of the water flowing through the conduit system. Mertz Resurgence is the outflow point for the water remaining in the system downstream from Doc White Spring.

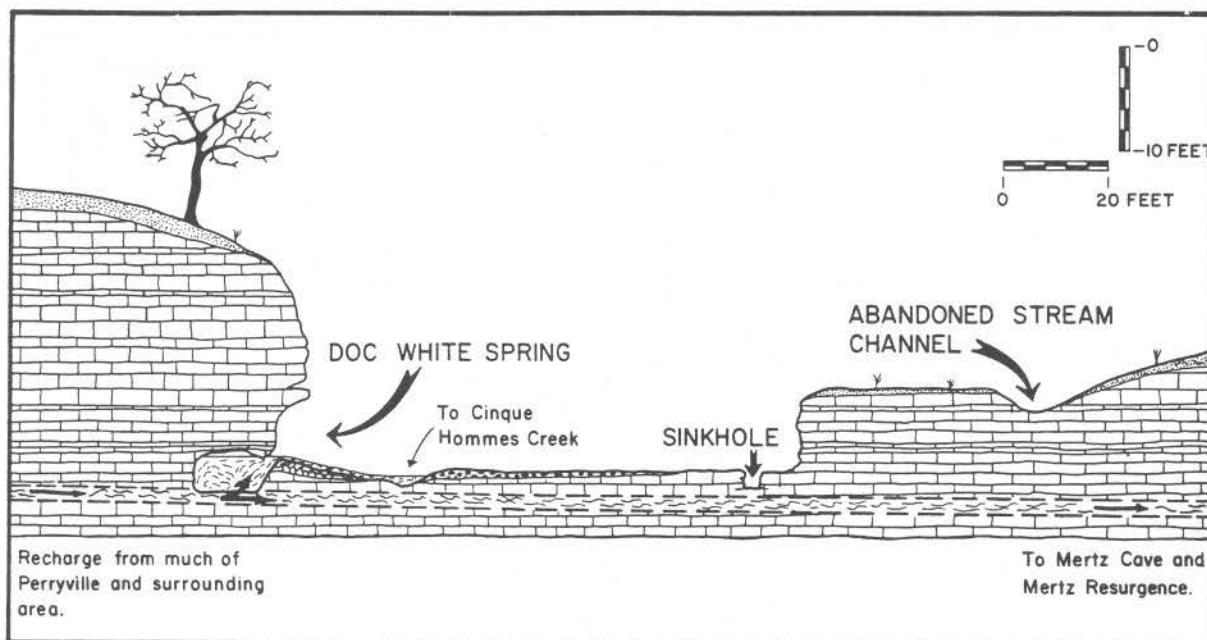


Figure 8 — Diagrammatic cross-section of Doc White Spring, looking north-northeast (from Vandike, 1985).

Mertz Resurgence is the downstream entrance of Mertz Cave. A completely water-filled passage in lower Mertz Cave prevents entry from the resurgence. The only usable entrance to Mertz Cave is through a deep sinkhole 4,100 ft northeast of Doc White Spring. Mertz Cave contains about 2 mi of mapped passages. It is actually a downstream continuation of Crevice Cave. Dye tracing has proved the hydraulic connection, but flooded passage prevents cavers from making a physical connection. Water from the Circle Drive Resurgence-Dry Run Branch Estavelle-Heberlie Resurgence-Doc White Spring recharge area is believed to enter Mertz Cave about 2,200 ft upstream from the sinkhole entrance. Figure 9 shows the recharge areas for many of the springs and resurgences in the Perryville karst area.

At Mertz Resurgence, water flows from a horizontal cave passage developed in the Joachim Dolomite. Plattin Formation caps the hill at the top of the 100-ft bluff above the spring outlet. The cave can be followed upstream only a few tens of feet until the passage siphons. This resurgence is the only perennial spring of the Crevice Cave system. It is about 80 ft lower than Doc White Spring, and 150 ft lower than Circle Drive Resurgence. Flow from Mertz Resurgence during very dry weather may

decline to less than 100 gpm, but after very heavy rains flow has been visually estimated at more than 100 ft³/sec.

- 105.4 Return to US 61 on Route E. Turn right and proceed northwest on US 61 through Perryville.
- 109.1 Turn right and proceed north on Route V.
- 111.9 Road forks, take the right fork.
- 112.5 Road forks again; take the left fork.
- 113.3 Ball Mill Resurgence parking area on left.

STOP 9: BALL MILL RESURGENCE

The Perryville karst area ground-water outlets already discussed drain into Cinque Hommes Creek, which bounds the karst area to the southeast. Blue Spring Branch forms the northwest boundary of the karst area and along its reach are several important and interesting springs and karst resurgences.

The most unusual karst resurgence draining the Perryville sinkhole plain is Ball Mill Resurgence, at

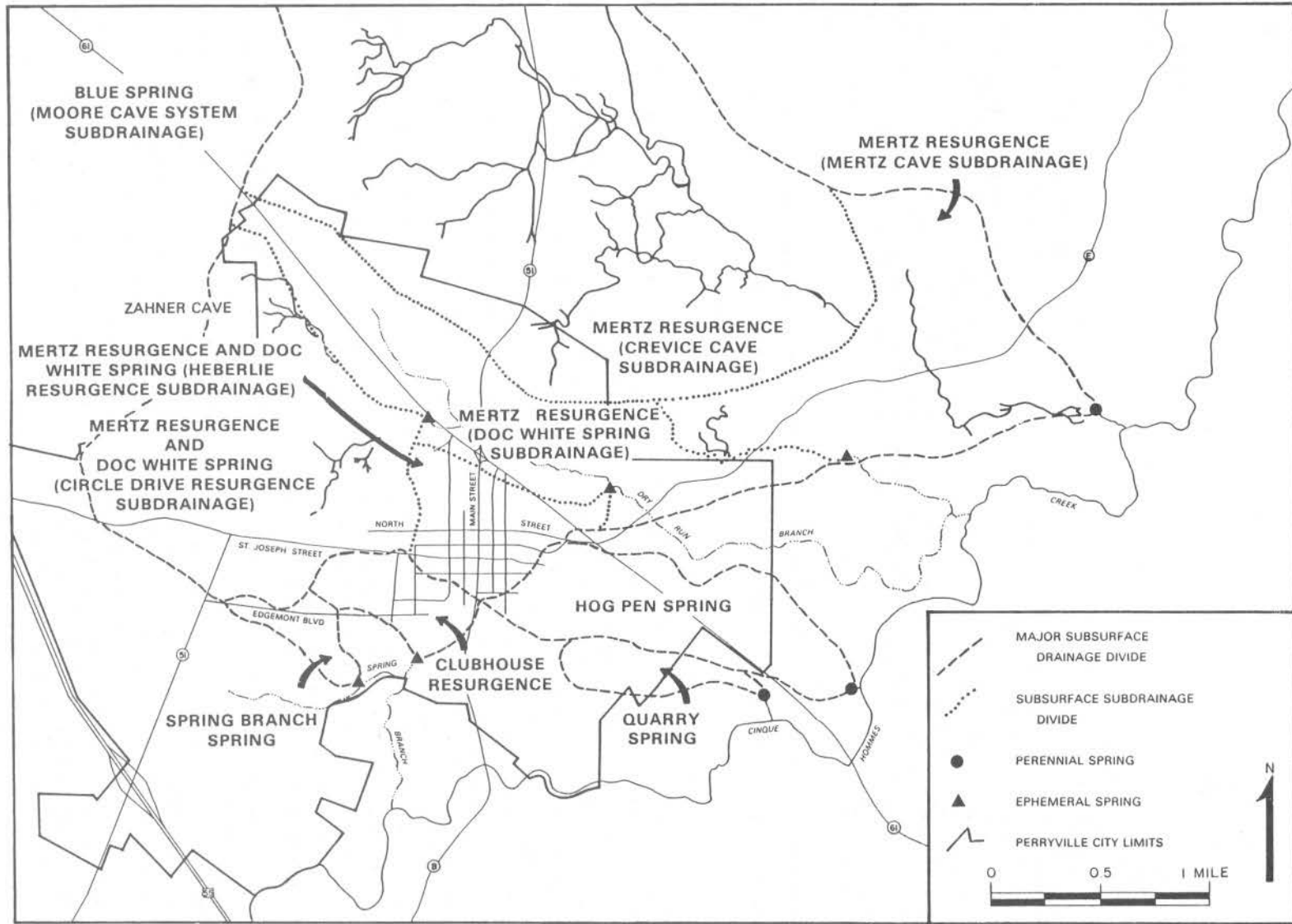


Figure 9 — Recharge area map for major springs and resurgences in the Perryville karst area (from Vandike, 1985).

the base of a 40-ft bluff of Joachim Dolomite, several hundred feet south of Blue Spring Branch. Topographically, the typically dry resurgence looks more like a sinkhole than a spring, and it probably does channel a minor amount of runoff into the ground-water system. After heavy rains, however, its function cannot be mistaken. The rise basin, about 20 ft in diameter and 8 ft deep, neither contains or discharges water most of the time. It functions only briefly after very heavy rainfall when water surges through the well-rounded cobbles covering the basin. The natural milling of rocks striking each other when flood water rushes upward through the cobbles flooring the basin creates the rock "balls" covering the floor of the resurgence. Fresh rock spalling from the bluff above keeps the mill supplied with abrasives and raw materials to replace the dolomite cobbles as they are ground away.

The very brief functioning of the resurgence after heavy precipitation indicates that its recharge area is fairly small but very open and interconnected. Vineyard (1984, personal commun.) visited it after heavy rain in 1968, and observed the resurgence discharging an estimated 60 ft³/sec. Vandike (1985), using high-water marks and channel characteristics, estimated peak flow at over 180 ft³/sec. Ball Mill Spring, another ground-water outlet between Ball Mill Resurgence and Blue Spring Branch, has a well-sustained base flow, and may be a lower level outlet for the conduit system channelling water to Ball Mill Resurgence.

- 113.3 Exit parking area, turn right, and follow the gravel road toward Perryville.
- 114.5 Turn right on Perry County Road 914. The Moore Cave System crosses beneath the county road at several points, and sinkhole entrances to the cave are to the east a short distance from the road.
- 115.7 Park along the county road at the base of the hill.

STOP 10: BLUE SPRING AND BLUE SPRING RESURGENCE

Ball Mill Resurgence and Ball Mill Spring are only two of the groundwater outlets along Blue Spring Branch. Several other ephemeral karst resurgences

and perennial lower-level springs are found near the creek. Most notable are Blue Spring and Blue Spring Resurgence.

These two features are about 500 ft downstream of Perry County Road 914, along the southeastern valley wall. Blue Spring flows from the Joachim Dolomite at the base of a short bluff. Water flows from a solution-enlarged bedding plane opening partly filled with breakdown rubble. Gregory J. (Tex) Yokum, one of the many cavers who worked many years in the Perryville karst area, has shown Blue Spring to be the rising of the cave stream of the Moore Cave System, which lies to the south of the spring. Blue Spring Resurgence, immediately upstream of Blue Spring, is a high-water overflow outlet of the same cave system. When the discharge capacity of lower Berome Moore Cave, or Blue Spring, is exceeded by recharge, Blue Spring Resurgence begins functioning. Like Ball Mill Resurgence, Blue Spring Resurgence looks more like a sinkhole than a spring. In flood stage, water issues from the 20-ft diameter, 5-ft deep pit and flows past Blue Spring to Blue Spring Branch. Like the other ephemeral resurgences along Blue Spring Branch, it functions only briefly until excess water is channelled out of the cave system and Blue Spring can again accommodate the flow.

The Moore Cave System contains more than 17 mi of mapped passages, and drains much of the northern one-third of the Perryville sinkhole plain. Flow through this system after heavy rains may exceed 100 ft³/sec. Part of the recharge is from the area immediately north of Perryville, along U.S. 61, where numerous homes discharge sewage directly into sinkholes. Water quality in the cave and at Blue Spring, especially during low-flow periods, reflects the poor-quality inflow. Much of the problem area has been annexed by Perryville, and will soon be connected to sanitary sewers.

- 115.7 Return to US 61, on Perry County Road 914 and Route V.
- 119.5 Turn right and proceed northwest about 200 ft on US 61, then turn left and proceed south on Sycamore Lane, which is approximately the dividing line between the Crevice Cave system recharge area to the southeast and the Moore Cave system recharge area to the

- northwest. Zahner Cave, 1.9 mi long, is beneath the pasture on the left, about 0.7 mi south of US 61.
- 121.3 Turn left and proceed east on Route T. At Mo. 51, turn right and proceed south to I-55.
- 122.8 Turn right and proceed northwest on I-55 for return to St. Louis.
- 201.6 I-55 and I-44 merge, continue north on I-55/I-44.
- 202.6 Exit I-55/I-44 onto Memorial Drive. Continue north on Memorial Drive to Convention Plaza.
- 203.4 Turn left on Convention Plaza, proceed west for 5 blocks to convention center.
- 203.8 Convention center. End of field trip.

REFERENCES CITED

- Bretz, J Harlan, 1956, Caves of Missouri: Missouri Geological Survey and Water Resources (now Missouri Department of Natural Resources, Division of Geology and Land Survey), vol. 39, 2nd series, p. 436-437.
- Marty, Adam, 1983, Cave report for Cliff Cave, St. Louis County: unpublished report, Missouri Speleological Survey cave files, 4 p.
- Vandike, James E., 1985, Movement of shallow groundwater in the Perryville karst area, southeastern Missouri: Missouri Department of Natural Resources, Division of Geology and Land Survey, Miscellaneous Publication 44, 57 p.
- _____, 1987, Use of storm-water drainage wells in Missouri: International Symposium on Class V injection well technology proceedings, Underground Injection Practices Council, Oklahoma City, Oklahoma, p. 160-178.
- _____, 1988, Using digital watershed modeling to estimate sinkhole-flooding potential at Perryville, Missouri: Missouri Department of Natural Resources, Division of Geology and Land Survey, Open-File Report OFR-88-73-WR, 117 p.
- Vineyard, Jerry D., 1971, Preliminary report on water pollution problems in the Jefferson Barracks karst area, St. Louis County, Missouri: unpublished report, Missouri Department of Natural Resources, Division of Geology and Land Survey, 7 p.
- Vineyard, Jerry D., Vandike, James E., and Hoffman, David, 1981, Guidebook to the karst and caves of the Ozark region of Missouri and Arkansas, in Beck, Barry F., ed., Guidebook to the karst and caves of Tennessee and Missouri: Eighth International Congress of Speleology, Bowling Green, Kentucky, p. 33-68.

Field Trip No. 8
(Guidebook Published Separately)

**"OLYMPIC DAM-TYPE" DEPOSITS
AND GEOLOGY OF
PRECAMBRIAN ROCKS IN THE
ST. FRANCOIS MOUNTAINS TERRANE,
MISSOURI**

Eva B. Kisvarsanyi
Missouri Department of Natural Resources
Division of Geology and Land Survey
P.O. Box 250
Rolla, Missouri 65401

and

V. Max Brown
University of Toledo
Toledo, Ohio 43606

and

Richard D. Hagni
University of Missouri
Rolla, Missouri 65401

FIELD TRIP SUMMARY

This volume was prepared for a field trip sponsored by the Society of Economic Geologists, in conjunction with the 1989 Annual Meetings of the Geological Society of America and its associated societies.

Outcrops of Middle Proterozoic igneous rocks in the St. Francois Mountains, southeastern Missouri, have long interested economic geologists, because of their associated ore deposits. Volcanic-hosted magnetite-hematite-apatite deposits, commonly referred to as "Kiruna-type," have been mined in the region since 1815. Hypo-xenothermal vein deposits of Sn, W, Ag, and Pb, although only of marginal economic value, are interesting because of their similarity to the mineralization at Cornwall, and their apparently unique occurrence at Silver Mine, in the Proterozoic rocks of North America.

The geologic setting and structural relationships of the deposits to their host, the 1.45 Ga St. Francois granite-rhyolite terrane, have become better defined through recent detailed mapping, extensive drill core data, and regional geophysical maps. The volcano-tectonic features identified in the terrane include calderas, cauldron subsidence structures, ring intrusions, and resurgent cauldrons with central plutons. These features are comparable to some of the classic ring complexes of the world, such as the "younger" granites in Nigeria, and Glen Coe in Scotland. They provide the regional geologic framework for the mineral deposits in both the exposed and buried Precambrian rocks of the district.

The discovery in 1975 of the giant Olympic Dam Cu-Au-Ag-U-REE-Fe deposit in South Australia

renewed interest in the Precambrian Fe deposits of the Southeast Missouri district. The Australian and Southeast Missouri deposits share many common features, including age, tectonic setting (rifted continental crust), and close temporal and spatial association with anorogenic, alkalic-silicic rocks; accordingly, current studies concentrate on identification of specific mineralogical and geochemical analogies between the respective ores.

Stops on this field trip feature two of the iron ore mines: Pea Ridge, the only operating underground iron mine in the United States, and Pilot Knob, now inactive, but one of the early producers of iron ore in Missouri. Other stops include the historic Silver Mine district, where complex mineralization can be seen in samples on the old mine dumps, and where one of the ring intrusions in the St. Francois Mountains, the Silvermine Granite, is exposed on the banks of the St. Francis River. The volcanic stratigraphy in the southern St. Francois Mountains, where a caldera has been mapped recently, is highlighted in several stops. The Graniteville Granite, one of the late-stage HHP plutons in the igneous terrane, is the subject of another stop.

In addition to traditional road logs and specific field stop descriptions, this guidebook features several pertinent technical papers. The editors hope to provide both a general overview of and a useful guide to the geology and ore deposits of the St. Francois terrane, the best exposed unmetamorphosed Middle Proterozoic terrane in the midcontinental United States.

Field Trip No. 9
(No Guidebook Published)

**CENTRAL UNITED STATES
EARTHQUAKES AND THE
ST. LOUIS UNIVERSITY
SEISMIC NETWORK**

Sean T. Morissey
Department of Earth and Atmospheric Sciences
St. Louis University
St. Louis, Missouri 63156

FIELD TRIP SUMMARY

Tour the seismic data center for the Central Mississippi Valley Seismic Network, operated by St. Louis University. Methods of retrieving data from approximately 50 stations using analog and digital recording systems will be demonstrated. Seismicity

patterns in the New Madrid Seismic Zone and surrounding regions and recent discoveries concerning the nature of fault-zone properties at New Madrid will be discussed.

Field Trip No. 10
(Guidebook Published Separately)

**THE GEOLOGIC STORY
OF THE
ST. LOUIS RIVERFRONT
(A Walking Tour)**

Arthur W. Hebrank
Missouri Department of Natural Resources
Division of Geology and Land Survey
P.O. Box 250
Rolla, Missouri 65401

FIELD TRIP SUMMARY

St. Louis, like most of the world's great cities, owes much of her success to geography and natural resources. Her advantageous location at the junction of the Mississippi and Missouri Rivers guaranteed prominence throughout the years of westward expansionism and during the glorious steamboat era. The major Mississippi Valley-type lead deposits and Precambrian iron deposits of southeast Missouri also contributed to the city's success, as did nearby Illinois coal.

Construction resources for building the city were also close at hand. Most important in the early years were granite from the St. Francois Mountains; a variety of Ordovician, Silurian, and Mississippian limestones and dolomites from St. Louis and adjacent areas of Illinois; sand and gravel, and the Pleistocene loess and Pennsylvanian clay that brought the city fame as a major brick and clay-products manufacturing center.

Most of the important early history of St. Louis was enacted within a relatively small area near the center of town and extending just 3 or 4 blocks back from the river. In the late 1930's, 40 blocks of blighted buildings were razed to make way for the Jefferson National Expansion Memorial. The razed area included most — but not all — of the historic St. Louis

riverfront district. The historic riverfront district is the subject of this guidebook.

Buildings and structures discussed at the eight guidebook stops include the Old St. Louis Courthouse, Old Cathedral (Catholic), stone-paved levee and streets, Eads Bridge, and several old factories in the Laclede's Landing area. Historical background is provided at each stop, followed by geologic discussion of the stone or industrial mineral products used at that site. In addition to identifying the stratigraphic and geographic source of the stone (where possible), discussions may include mining or milling details, important construction properties or characteristics of the stone, masonry techniques, or evaluation of suitability.

While the field trip area is small, the diversity of geologic materials is great. Twenty different kinds of building, paving, or decorative stone are described, as well as two types of brick, and structural cast iron. Sedimentary and igneous rocks predominate, but a few metamorphic rocks were noted. The Precambrian, all Paleozoic periods except Permian, and the Quaternary are represented. Most of the stone used on the St. Louis riverfront was quarried in Missouri or just across the river in Illinois, but stone from five other states was also used.

Field Trip No. 11

**ENGINEERING GEOLOGY AND
INDUSTRIAL MINERALS ASPECTS
OF THE GREATER
ST. LOUIS-ILLINOIS AREA**

Paul B. DuMontelle and James W. Baxter
Illinois State Geological Survey
615 East Peabody Drive
Champaign, Illinois 61820

and

Alan G. Goodfield
Illinois Department of Transportation
Springfield, Illinois

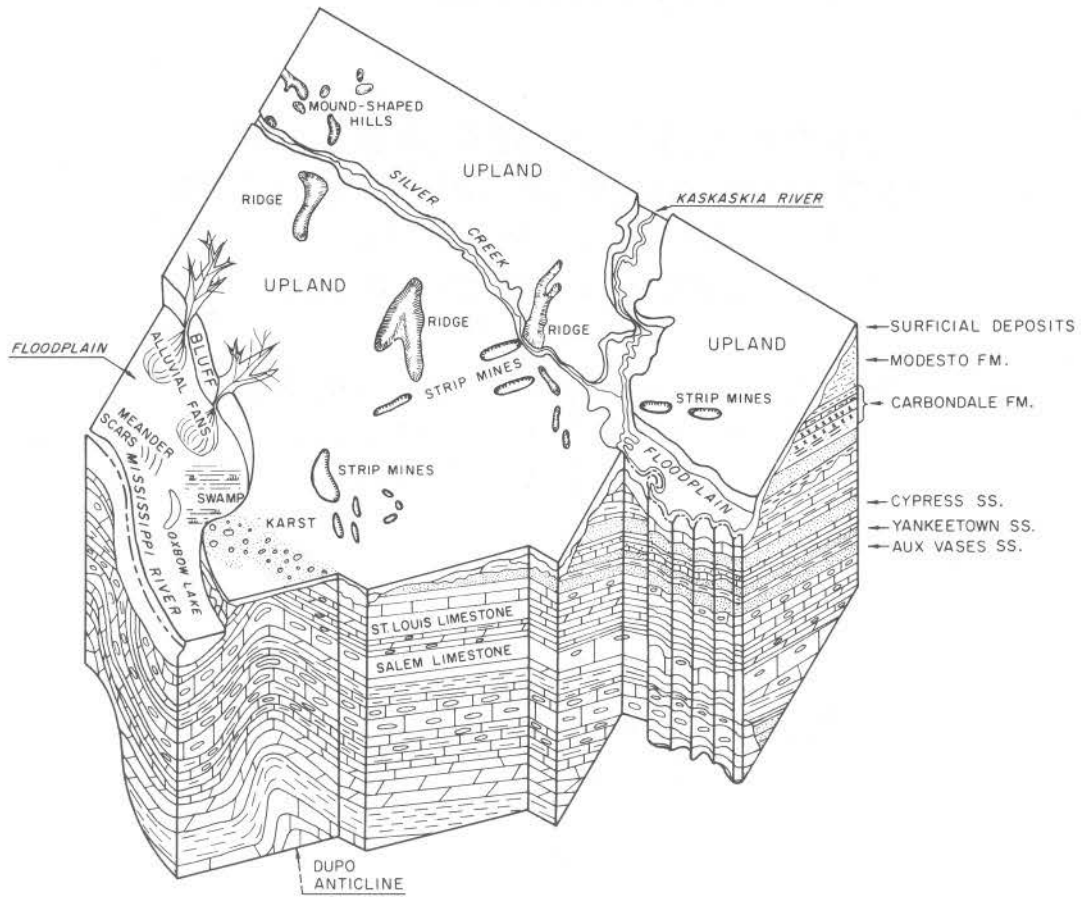


Figure 1 — Three-dimensional geologic view of St. Clair County, Illinois (Jacobs, 1971).

INTRODUCTION

The resources of greater St. Louis-Illinois area played a major role in the development of St. Louis. Plentiful water and coal for heavy industry, fertile agricultural land for truck gardens, and high-purity limestone, and sand and gravel for construction and chemical use were available east of the Mississippi River. Many of these resources were known to the American Indian mound builders that settled this region as early as 600 A.D. (Salzer, 1975).

Many Indians, aware of the natural problems of floodplain occupation, settled the uplands. Those that remained in the floodplain found conditions severe. As Leighton (1928) observed in his studies, some Indian mounds were unstable and prone to slumping. In places, this broad floodplain of the Mississippi River — called the American Bottom (Jacobs, 1971)—extends nearly 8 miles to the bluffs (fig. 1). Deposits of the ancient Mississippi channel are primarily glacial outwash materials comprising coarse sand and gravel. The upper part of the valley fill grades to finer materials, including overbank silts, sands, and organic-rich deposits that are excellent agricultural soils, but are extremely unsuited for foundation construction because of the high water table and local flooding. In some areas, heavy industrial pumping of the ground water lowered the

water table. Levees were constructed to protect the Bottom from major flooding. East St. Louis, Granite City, Cahokia, and many small communities soon occupied the floodplain (fig. 2).

Bedrock bluffs bordering the east side of the American Bottom are capped by Pleistocene glacial deposits. In the northern part of the area, coal seams of the Pennsylvanian Carbondale Formation crop out or lie at shallow depths in the bluffs. Glen Carbon, Maryville, Collinsville, and Belleville were active mining towns of the late 1800's and early 1900's. Natural gas pipelines completed to St. Louis in the 1930's dealt a severe blow to the coal industry in this area. Abandoned headframe foundations, gob piles, and mine subsidence are reminders of the mines. Quarrying and mining are active in Mississippian limestones that crop out in the southern part of the area. Some underground mines may prove valuable for storage and for industries requiring controlled temperatures.

The Illinois minerals industry serves the St. Louis market by providing construction materials and energy; transportation network links them to the market. Both rely on geological investigations, past and present, to solve mining, quarrying, construction, and environmental problems and concerns.

ROUTE GUIDE AND COMMENTARY

Miles

- | | |
|---|--|
| <p>0.0 East side of Convention Center on Convention Plaza. Go east four blocks to Third Street.</p> <p>0.2 Turn right (south) on Third; and follow under and along I-70.</p> <p>0.4 Peabody Coal headquarters on right (west). Begin to merge to left.</p> <p>0.6 The Arch—Jefferson National Expansion Monument—to the left (east).</p> <p>0.7 The Old St. Louis Cathedral on left (east).</p> <p>0.8 Take ramp to left (east) onto Poplar Street Bridge (I-55 & I-70 N/E). The six-span continuous bridge has orthotopic steel deck</p> | <p>on plate girders. The west abutment has spread footings on shallow (27 ft deep) limestone and the east abutment rests on steel H-piles to deep (127 ft) limestone.</p> <p>1.4 Illinois-Missouri State Line—middle of Mississippi River.</p> <p>1.6 Bear left, follow I-55 (north), I-70 (east) and I-64 (east) to East St. Louis.</p> <p>4.0 Bear left; follow I-55 and I-70 east.</p> <p>4.1 Tri-level Pump Station east of the I-55 & 70 east-bound lane is below the level of Mississippi River and pumps ground water to keep the pavement dry.</p> |
|---|--|

5.6 The American Bottom—The Mississippi River floodplain in Illinois.

6.3 Closed municipal dump site on left (north). Note gas flares and other monitoring devices.

8.4 Bridge over Alton & Southern Railroad; an existing five-span continuous structure, recently replaced a bridge about 25 years old, of same length, that had been damaged by negative skin-friction loading resulting from

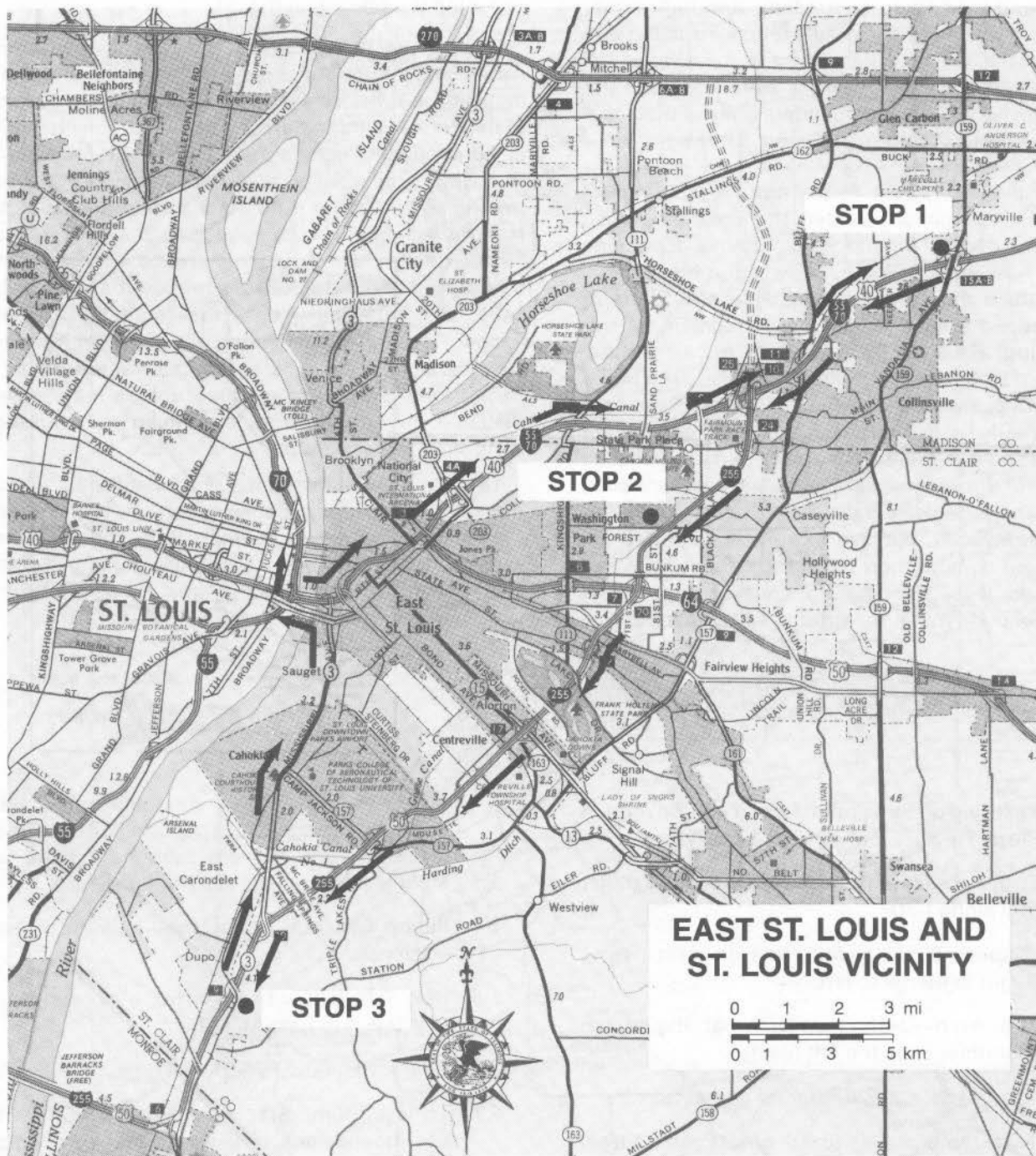


Figure 2 — Map of Greater St. Louis-Illinois area illustrating field trip stops.

large-scale settlement of highway fill in old Mississippi River slough.

- 9.3 Sand Prairie Lane bridge over I-55 and I-70. Note two stages of end-slope stability berms.
- 9.4 The Great Mound of Cahokia Mounds State Park on right (south).
- 10.7 The "Skyhook Bridge"—a 25-year old four-span continuous bridge recently reconstructed by removing two outside piers to permit interchange ramp construction. Large buried H-pile-supported concrete counterweights behind existing pile abutments support post-tensioned ties replacing two old piers.
- 11.0 New I-255 interchange. Continue northeast on I-55 and I-70.
- 14.8 Bridge over IL-157. IL-157 lies along foot of east bluff of Mississippi River Valley. Much of the original bluff (silty loess with buried sand dunes) has been almost totally removed in recent years.
- 16.7 Note vertical slopes in Peoria Loess (Wisconsinan). Similar, north-facing slopes in adjacent area failed in past and were removed.
- 18.6 IL-159 over I-55 and I-70 interchange. Take off-ramp (under bridge) to Maryville (IL-159 north).
- 18.8 IDOT Maintenance Yard on left (west). Coal mine subsidence effects on former adjacent State Police District Office will be viewed and discussed.

STOP 1: ILLINOIS DEPARTMENT OF TRANSPORTATION MAINTENANCE YARD

In May 1980, subsidence damage was noticed at the Illinois State Police District 11 headquarters building and tower, then just north of the IDOT maintenance yard (Wildanger, 1980). The subsidence trough appeared in the west part of the building and progressed generally from the northwest to the south. Efforts to save the building and a 350-ft radio antenna tower were in vain and the

structure was removed. Damage to the maintenance yard building subsequently began on the north side. Tension cracks trending east-west through the structure are monitored periodically. Mine maps indicate a barrier pillar along the southern boundary of the mined-out area, which may have limited the damage to the maintenance building.

The Herrin No. 6 Coal Seam was mined in this area by the Donk Brothers in No. 2 Coal Mine, which was abandoned in 1926. Seven to 8 ft of coal was mined by room and pillar methods; rooms averaged 40 ft wide and were spaced on 60-ft centers. The mine is about 230 to 240 ft below the ground surface here. Mine subsidence is a potential hazard to any structure above an abandoned mine. In 1979 Illinois established an insurance program that covers mine subsidence damage. This is the second program of its kind in the United States. Insurance carriers in Illinois are required to make this coverage available to all property owners.

- 19.0 Return to IL-159/I-55 and I-70 Interchange and take I-55 and I-70 south toward St. Louis.
- 23.9 I-255/I-55 and I-70 Interchange; bear to right to take I-255 south (Memphis). In SE quadrant of interchange note rip-rapped retention basins that are part of interchange to collect and store adjacent storm runoff. Storm water is pumped into the Mississippi after the storm.
- 25.0 Long viaduct over two railroads and Black Lane. Initial interstate plans called for three separate structures; however, results of initial structure borings indicated the presence of low-strength, compressible soils. Additional studies using undisturbed Shelby tube samples indicated that undesirable long-term settlement would occur. Large end and side-slope stability berms were recommended. Analyses indicated that combining structures into one viaduct would be more economical than individual structures. As with most I-255 bridge abutments, these are on high-capacity steel H-piles, with provision for negative skin-friction loading, driven 125± ft to the bedrock floor of the Mississippi Valley.
- 26.8 Sand pit along west side of I-255.

STOP 2: METRO EAST SAND COMPANY

This Metro East Sand Company pit is on a part of the American Bottom. John M. Masters of the Illinois State Geological Survey indicates that the pit overburden comprises about 5 to 10 ft of floodplain and alluvial clay and silt of the Cahokia Formation (Holocene). Sand, about 100 ft thick, and some gravel are mined by hydraulic dredge. The upper part of the section was deposited about 2,000 to 6,000 years ago; the lower part of the section was evidently deposited when the valley was last scoured to bedrock and refilled with sand and gravel by a braid-bar valley train system (Wisconsinan).

A suction pump and cutter-head dredge system pumped sand from a depth of about 50 ft. A new jet pump system being installed will pump the full depth of the deposit and provide a denser, more constant slurry. The raw material is processed with a double deck set of screens and a sand classifier. Jigs are being installed to remove granule-sized lignite or coal grains (less than 1 percent) in the concrete sand product, because they are aesthetically unacceptable to some customers.

- 27.5 I-255/I-64 Interchange; continue south on I-255.
- 29.6 I-255 bridges to left (east) over Harding Ditch. Both structures are supported on point-bearing steel H-piles. I-255 embankments to the south, built on thick low-strength alluvial deposits, are stabilized by extensive use of wick drains.
- 31.6 Note noise barriers along both sides of interstate.
- 32.1 I-255 over local streets and railroad yards. During construction, considerable problems were encountered with large length variations in friction pipe piles at 120-ft piers.
- 34.6 This Cahokia subdivision has experienced severe expansive soil problems.
- 34.9 I-255 bridges over Prairie du Pont Drainage Canal and adjacent levees. Canal is major collector of all east-side runoff in the American Bottom.
- 35.8 Note large limestone quarry in the bluff to left (east).
- 37.1 IL-3 bridges over I-255. Extension of structures to left (south) of I-255 reflects presence of deep, thick organic alluvial deposit that needed bridging until a low enough approach embankment was obtained.
- 38.0 Approximate location of "Range Site," a major archeological dig discovered during preliminary interstate studies.
- 38.2 Columbia Stone Quarry in bluff to east of Dupo.
- 39.3 Embankment on local road to east of interstate was site of "Sand Drain Test Section" during 1970's to test three major types of sand drain installations: jetted, augured, and mandrel-driven.
- 41.3 IL-3 Interchange at Columbia.
- 41.5 Columbia Quarry in the bluff line on the left. About 140 ft of St. Louis Limestone is quarried.
- 41.6 Entrance to Columbia Quarry Company, Dupo Plant (No. 9), on left. Turn left on quarry road. Park on right shoulder.

STOP 3: COLUMBIA QUARRY NO. 9 AND THE DUPO ANTICLINE**Site A. Discussion of the Dupo Anticline**

The Dupo area provides a rare opportunity to examine a major bedrock structure, the Dupo anticline. From this vantage point an almost complete cross section of the anticline is exposed. Along the crest strata have been arched several hundred feet, with a steeply dipping southwest limb and a more gentle dip to the northeast. Dips as great as 50 degrees have been measured on the west limb in the vicinity of Columbia in Monroe County. The Dupo Quarry is on the gentle east flank where approximately 200 ft of Warsaw Shale and the Ullin, Salem, and St. Louis Limestones are exposed and dip about 4 degrees. The Dupo anticline is part of a rather sharp, narrow structure that can be traced from south of Waterloo, past Dupo, to beyond St. Louis, a distance of more than 25 mi. The Dupo and defunct Waterloo Oil fields, with production from the Ordovician "Trenton" pay zone, are over structural

closures along this trend. The Dupo field still produces with waterflooding methods.

Site B. Columbia Quarry Company, Dupo Quarry and Plant.

The St. Louis Limestone quarried here and at other locations between Dupo and Stolle to the north is generally an excellent aggregate source for highway construction and local uses. The Dupo Quarry is developed in a lower part of the St. Louis Limestone, of which approximately 140 ft has been benched

to separate beds that can produce the different qualities required by various state and federal specifications.

The quarry site provides a view of the American Bottom and is a vantage point for further discussion of problems related to I-255 construction, instability of recent alluvial deposits, and the design and installation of vertical sand drains.

50.6 Return to the St. Louis Convention Center via Illinois Route 3 and I-70.

ACKNOWLEDGMENTS

We thank the Illinois Department of Transportation, Jerry Bohnenstiehl, Vice President and Plant Manager of the Metro East Sand Company, and R. L. (Sid) Trexler, Vice President of Operations of the Columbia Quarry Company for their cooperation in

arranging for field trip stops. John M. Masters, James C. Bradbury, and Robert A. Bauer of the Illinois State Geological Survey served as reviewers. Mary Z. Glockner and Barbara Stiff provided editorial and illustration support.

REFERENCES

- Baxter, James W., 1965, Limestone resources of Madison County, Illinois: Illinois State Geological Survey Circular 390, 39 p.
- Jacobs, Alan M., compiler, 1971, Geology for planning in St. Clair County, Illinois: Illinois State Geological Survey Circular 465, 35 p.
- Leighton, Morris M., 1928, The geological aspects of some of the Cahokia (Illinois) Mounds. *in* The Cahokia Mounds: University of Illinois Bulletin, v. 26, No. 4, Pt. 11, p. 109-143.
- Salzer, Robert J., et al., 1975, Cahokia archaeology: field reports: Illinois State Museum Research Series, Papers in Anthropology, No. 3, 64 p.

Field Trip No. 12
(No Guidebook Published)

**DIGITAL CARTOGRAPHY
MAP LIBRARY, AND DATA BASE
MANAGEMENT SYSTEMS OF
WASHINGTON UNIVERSITY'S DEPARTMENT
OF EARTH AND PLANETARY SCIENCES**

Raymond E. Arvidson and Clara McLeod
Department of Earth and Planetary Sciences
Washington University
Campus Box 1169
One Brookings Drive
St. Louis, Missouri 63130

FIELD TRIP SUMMARY

This tour of Washington University's Department of Earth and Planetary Sciences will include (1) an address and discussion on "The Future of Digital Map Catalogs and Digital Cartography in General," especially in terms of procedures for generating, storing, and accessing digital maps; (2) a brief tour of the Earth and Planetary Sciences Library and a hands-on demonstration of its electronic Map Catalog, which utilizes current relational database management technology; and (3) a visit to the NASA

Regional Planetary Image Facility and hands-on demonstration of its Image Retrieval and Processing System (RPIF-IRPS) which was developed jointly by workers at the RPIF, Washington University, and the Astrogeology Branch, U.S. Geological Survey, Flagstaff, Arizona. The system allows researchers to find broad information about raw and derived planetary data, to conduct detailed search and browse sessions for image, mosaic, and map information, and to process image data.

Field Trip No. 13
(No Guidebook Published)

**AEROSPACE CENTER,
U.S. DEFENSE MAPPING AGENCY**

Ron Blouse and Captain Dale Hotzaphel
U.S. Defense Mapping Agency
8900 S. Broadway
St. Louis, Missouri 63118

FIELD TRIP SUMMARY

The Defense Mapping Agency (DMA), was established in 1972, when mapmaking functions of the Defense community were combined into this joint Department of Defense agency. With some 9,500 military and civilian personnel in more than 50 locations around the world, the Defense Mapping Agency provides mapping, charting, and geodetic support to the Armed Forces and other government agencies.

This tour will be conducted through the DMA Aerospace Center's Graphic Arts Department, which

is in south St. Louis, Missouri. Upon arrival at the installation, a 20-minute film covering the Agencies functions will be shown. Following the film, participants will be assigned guides, who will conduct personalized tours through the Graphics Arts Department, where approximately fifteen-million maps and charts are printed, packaged, and distributed each year. This segment of the tour will focus on chart compilation, negative engraving, plate making, and color separation, and the press room's three, four, and five color press operations.

Field Trip No. 14

**ENGINEERING AND
ENVIRONMENTAL GEOLOGY
OF THE ST. LOUIS AREA**

Field trip leaders:

Mimi Garstang and Peter Price
Missouri Department of Natural Resources
Division of Geology and Land Survey
P.O. Box 250
Rolla, Missouri 65401

and

Michael J. Navin
U.S. Army Corps of Engineers
210 Tucker Boulevard
St. Louis, Missouri 63101

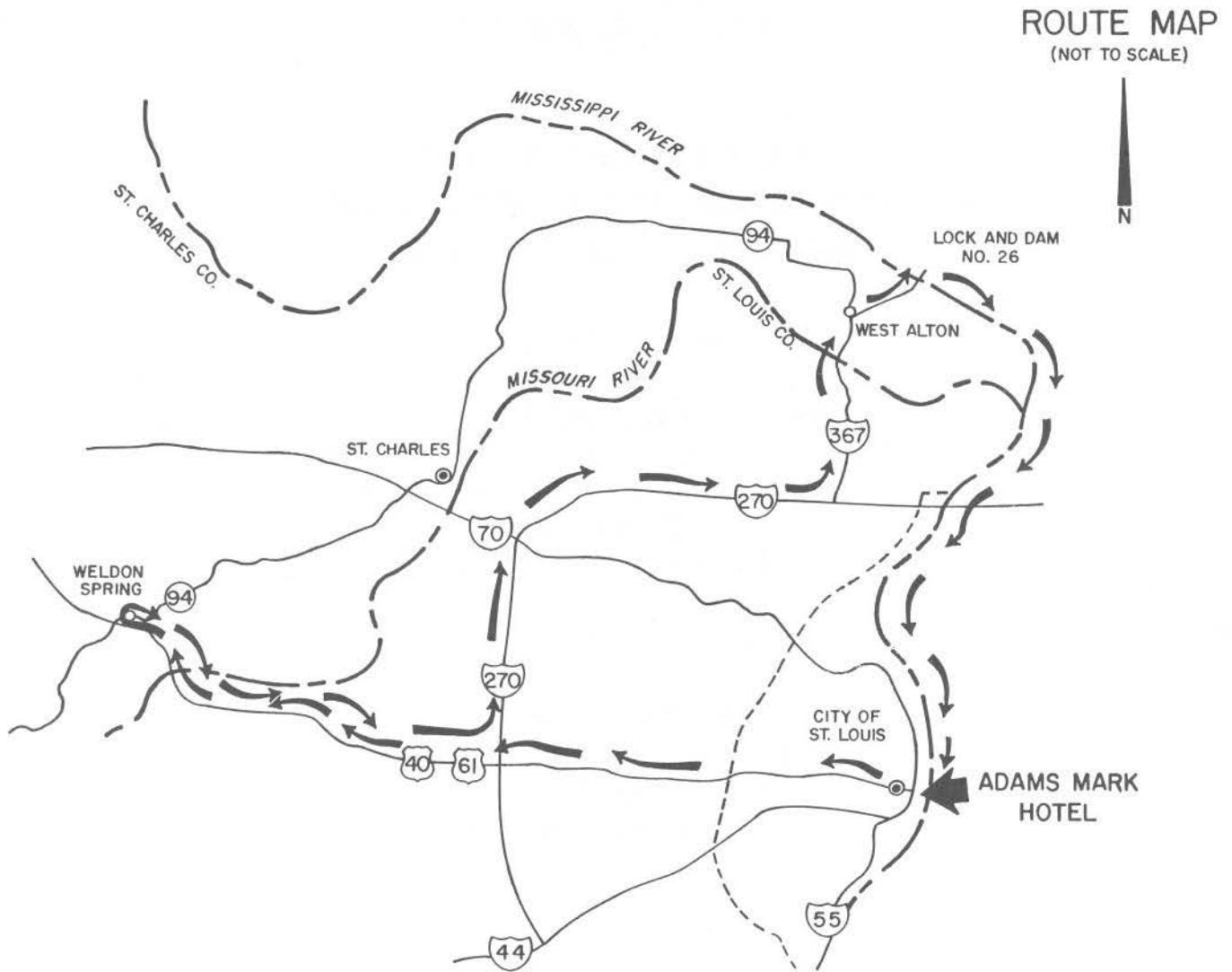


Figure 1 — General route map.

ABSTRACT AND INTRODUCTION

Geologists, engineers, and other construction and environmental professionals cannot ignore the importance of the rivers nor the general concern for surface and subsurface water movement in and around the St. Louis area. The Missouri and the Mississippi Rivers have greatly influenced development in and adjacent to the city of St. Louis. Ancient water activity and weathering have enlarged bedding planes and joints and karstified much of the limestone in the St. Louis area; all this created a complicated ground-water system, a major concern at hazardous waste sites such as Weldon Spring. Recent water activity deposited alluvial sediments along the river's receding banks. Special design considerations are necessary to build competent structures in such material. Complex water movement and river activity in the area have made waste disposal, building construction, and protection of drinking water supplies very important matters. We hope on this trip to combine hydrogeologic characterization of a hazardous waste site in the river uplands with engineering geology features of the Mississippi River lowlands.

At the Weldon Spring Superfund Site, geologists are examining where and why surface water is moving into the subsurface. Hazardous contamination at the site accentuates the concern for how water is transported into the ground and off the site. The hydrology is being thoroughly studied in order to protect the natural springs, river water, river alluvium, and area drinking water supplies. The site is also being considered for on-site disposal of hazardous wastes produced by past activities. Geologists want to insure future contaminant migration will not occur.

A closer look at the alluvial geology of the American Bottoms floodplain will be part of the river boat excursion down the Mississippi River. Delicate engineering geology considerations have been involved with many notable man-made features along the river bank. Construction of the U.S. Army Corps of Engineers lock and dam projects, the bridges spanning the Mississippi River, and even the famous Gateway Arch will be discussed during the river tour. See figure 1 for a general route map.

HYDROGEOLOGY OF THE WELDON SPRING SUPERFUND SITE

SITE HISTORY

Weldon Spring, St. Charles County, Missouri, is about 30 mi west of downtown St. Louis. During World War II the U.S. Army condemned and purchased 17,232 acres near the village of Weldon Spring to build the Weldon Spring Ordnance Works. During the war the Weldon Spring Ordnance Works produced TNT (trinitrotoluene) and DNT (dinitrotoluene) on 18 production lines scattered across a 2,078-acre east-west tract near the center of the ordnance works. The northern portion of the ordnance works was mostly used for TNT and DNT storage. The southern portion of the ordnance works was used for transportation access and as a source of raw materials, mostly water and stone.

After World War II most of the ordnance works were turned over to state and local government. Most of that area is currently included in the August A. Busch Memorial and Weldon Spring Wildlife Areas, administered by the Missouri Department of

Conservation. The Army retained the 2,078-acre tract containing the TNT and DNT production lines as a training facility.

In the mid-1950's a portion of the Army's remaining land was transferred to the Atomic Energy Commission, now the Department of Energy (DOE), for construction and operation of a uranium processing plant. This plant, the Weldon Spring Chemical Plant, was operated from 1957 to 1966 and was mostly used to process uranium ore into pure uranium metal. On the chemical plant tract is a waste-storage area containing four lagoons called raffinate pits. Radioactive waste sludge residues, raffinates, generated by the chemical processing were placed in these pits for temporary storage. These partially sludge- and partially water-filled raffinate pits still exist. The 220-acre chemical plant tract is currently administered by DOE.

The chemical plant is on the eastern end of the former TNT production line tract. The remaining

1,858 acres, still administered by the U.S. Army, are known as the Army Reserve Training Area and are operated by the U.S. Army Engineering Center and Fort Leonard Wood, which are in south-central Missouri.

GEOLOGY

The chemical plant in east-central Missouri, about 35 mi west-southwest of the confluence of the Missouri and Mississippi Rivers, and only about 15 mi southwest of their flood plain confluence, is on the topographic divide between these two major rivers. The Missouri River is approximately 2 mi south of the site. Topography in the Missouri River drainage area near the chemical plant is rugged, as a result of numerous short, steep streams in the river bluffs. The Mississippi River is approximately 15 mi to the north-northeast. Topography in the Mississippi River drainage area near the plant is gently rolling.

The chemical plant is just north of the southern limit of glaciation, consequently, ridgetops and flatter terrane are capped with loess, till, and the Pleistocene Ferrelview Formation, which were deposited on an erosion surface with moderate topographic relief. At the surface, the silty loess varies from a maximum of about 10 ft thick to 0 ft, where erosion has removed it. Beneath the loess in some areas is 0 to 20 ft of the Ferrelview Formation, a silty clay of debatable origin. Beneath the latter is 0 to 40 ft of clayey till. In some steeper terrane areas and in many valleys Pleistocene deposits have been partially to completely eroded.

Beneath the Pleistocene deposits in most areas, a cherty red-clay residuum derived from preglacial weathering of subjacent limestone is 0 to 25 ft thick, depending on its position on the underlying erosion surface and possible removal by glacial action. In some areas residuum is absent and Pleistocene deposits lie on top of the limestone bedrock. In other areas residuum is present and overlying Pleistocene deposits have been removed by postglacial erosion.

Consolidated bedrock beneath the area is mostly limestone with some sandstone, shale, and dolomite at depth. Most to all of the youngest bedrock unit near the site, the Mississippian Warsaw Formation, has been eroded. The lower limestone portion, all that remains of the formation, only exists on

topographically higher positions. The upper portion of the Warsaw, which has been eroded, is mostly shale. Directly under and adjacent to the chemical plant the Warsaw has been completely removed. Some of the red clayey residuum found at the higher elevations may be derived from the Warsaw.

The Mississippian Burlington-Keokuk Limestones, which underlie the Warsaw, are 150 to 200 ft thick; the Keokuk Limestone is the upper 15 to 25 ft. The Burlington Limestone, 135 to 150 ft thick and the principal bedrock of concern in the area, is cherty, white to light gray, coarsely to medium crystalline, and thin to massively bedded. It may contain up to 50 percent chert in the lower 50 ft.

Beneath the Burlington-Keokuk Limestones are 40 to 55 ft of Fern Glen Formation, 10 to 20 ft of Chouteau Group, 0 to 1 ft of Bachelor Formation, and 5 to 20 ft of Bushberg Sandstone; all these units are Mississippian. The Fern Glen and the Chouteau are limestones; the Bachelor, a sandstone. Unconformably underlying the Mississippian units are the upper Devonian and upper and middle Ordovician units, which are 0 to 2 ft of Glen Park Limestone, 0 to 15 ft of Maquoketa Shale, 100 ft of Kimmswick Limestone, 30 ft of Decorah Formation (shale and limestone), 80 to 135 ft of Plattin Limestone, 60 to 80 ft of Joachim Dolomite, and over 100 ft of St. Peter Sandstone (see fig. 2).

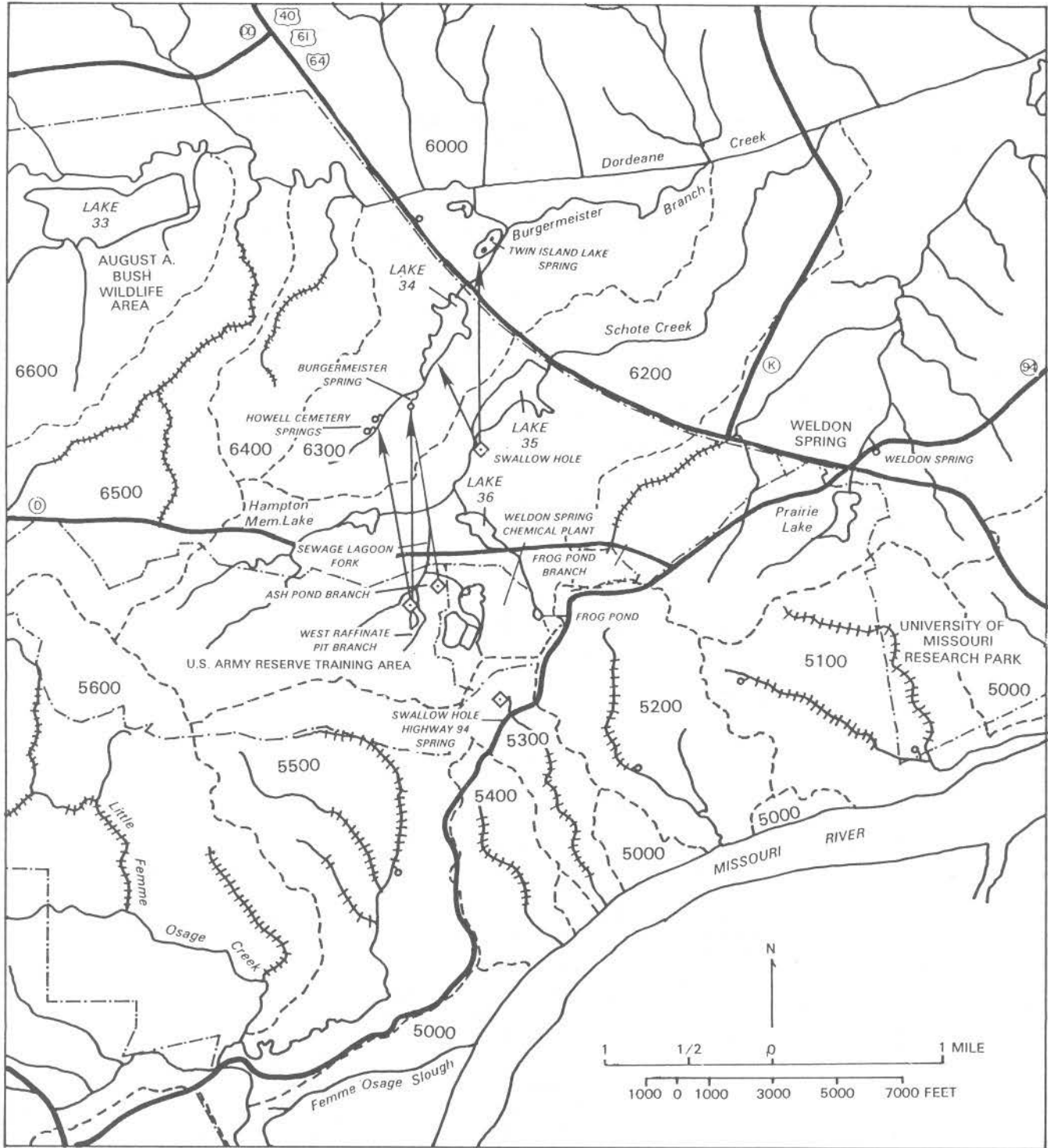
The area is structurally influenced by the Ozark uplift centered in southeastern Missouri; this results in an east-northeast dip of about one degree near Weldon Spring. An east-west fault with 40 to 80 ft of vertical displacement was mapped about 5 mi northeast of the chemical plant. Joint patterns and lineaments are common in the area; northwest-southeast and northeast-southwest trends are most abundant.

HYDROLOGY

Surface water from the chemical plant drains to the Mississippi and Missouri Rivers. The surface water divide crosses the southern edge of the plant, so most plant drainage is northward to the Mississippi River. Three drainage channels collect runoff from the north portion of the plant: Frog Pond Branch drainage on the east, Ash Pond Branch drainage to the northwest, and West Raffinate Pit Branch drainage to the west (see fig. 3).

System	Formation	Geologic Description	Thickness in Feet
Pennsylvanian	Pleasanton	Sandstone, channel-fill	0-100
	Marmaton	Shale; some limestone, minor sandstone	75
	Cherokee	Shale; with some clay and sandstone, very little limestone	50-150
	Cheltenham	Clay, plastic, refractory	0-25
	Ste. Genevieve	Limestone, sandy, oolitic, coarsely crystalline, white	30-60
Mississippian	St. Louis	Limestone, fine grained to lithographic, medium to massive bedded, white to gray breccia beds common	80
	Salem	Limestone, dolomitic, cherty, gray to light brown, becoming shaly at base	100-160
	Warsaw	Limestone and shale; limestone is coarse grained, crinoidal; upper portion is shaly	70-100
	Burlington-Keokuk	Limestone, coarse grained, olive-gray to brownish-gray, massive, crinoidal, cherty	200
	Fern Glen	Limestone and shale; grayish-green to red limestone; green to red shales, fossiliferous; upper unit cherty	60+
	Bushberg	Sandstone; yellowish-brown, fine to coarse grained, "dirty" appearance	5-50
Devonian	Glen Park	Limestone, oolitic, shaly, pale yellow, fossiliferous, contains quartz sand	0-30
	Maquoketa	Shale, silty, calcareous	0-100+
Ordovician	Kimmswick	Limestone, coarse-grained, massive, brownish-gray	25-125
	Decorah	Shale and limestone; interbedded, fossiliferous	25
	Plattin	Limestone, fine-grained to lithographic, gray to light tan, evenly bedded; burrowed appearance	80-150
	Joachim	Dolomite, argillaceous, shaly, yellowish-brown	60-125
	St. Peter	Sandstone, orthoquartzitic, grains medium size, rounded and frosted	50-150+

Figure 2 — Generalized stratigraphic section of St. Louis Area.



- - - - - BOUNDARY LINE
 ——— HIGHWAY
 - - - - - DRAINAGE BOUNDARY
 5000 AND BASIN NUMBER
 ~~~~~ STREAM

- - - - - LOSING STREAM REACH  
 ———> DYE TRACE  
 ~~~~~ SPRING  
 ◆ DYE INJECTION LOCATION

Figure 3 — Weldon Spring Chemical Plant and vicinity showing drainage basins and other hydrologic features.

Ash Pond Branch and West Raffinate Branch are losing streams in which amounts of flow decrease downstream, because flow sinks into openings in underlying materials. Most commonly, losing streams are associated with soluble rocks, such as limestones, which contain fractures and solution features such as caves and springs. In a "normal" stream, called a gaining stream, the amount of flow increases downstream, because contributions from tributary streams normally increase downstream.

Ash Pond Branch and West Raffinate Pit Branch join about 700 ft west of the northwest corner of the chemical plant. The drainage below this confluence, called Sewage Lagoon Fork, continues as a losing stream. Sewage Lagoon Fork drains into Schote Creek, a losing stream along this reach. Schote Creek drains into Lake 35, which also loses water from its basin. Frog Pond Branch drains through Lake 36 and into Schote Creek along the losing stream reach between Sewage Lagoon Fork and Lake 35. The downstream end of Frog Pond Branch, including Lake 36 and below, is a losing stream reach.

Except during major runoffs, all surface-water flow from the chemical plant is diverted into karst conduits and the shallow ground-water system within a short distance from the plant boundary. Water tracing tests with fluorescent dyes have shown that most sinking water from north-flowing drainages moves northward under the normally dry bed of Schote Creek, underneath a ridge, and resurfaces at springs along the next drainage to the north, Burgermeister Branch. Burgermeister Spring system, the largest known spring system in the area, is a discharge point for the water lost near the plant. Nearby Howell Cemetery springs also discharge some losing water flow.

A swallow hole in the headwaters of Lake 35 diverts water from a downstream reach of Schote Creek to Lake 34 and Twin Island Lake Spring, both in a reach of Burgermeister Branch downstream of Burgermeister Spring. The swallow hole in Lake 35 operates intermittently, sometimes becoming plugged with sediment. Frequently, Lake 35 water level is significantly below the spillway elevation and the swallow hole elevation, because of lake bed leakage and lack of inflow.

Surface-water drainage from a small portion of the chemical plant on the south and east flows to

the Missouri River. Most of this drainage is through Valley 5300, also known as the Southeast Drainage. A very small portion of the plant drainage to the Missouri River is through Valley 5200; Valley 5300 and Valley 5200 contain losing streams. Water tracing shows that water lost in a swallow hole in the upper part of Valley 5300 resurges and loses sequentially down the valley. The spring farthest downstream, almost to the Missouri River, is in the Fern Glen Limestone.

The ground-water divide in the uppermost aquifer is under the chemical plant and nearly coincides with the surface-water divide. The potentiometric surface gradient is low to the north, averaging about 60 ft per mi, or 1.1 percent, and moderate to the south, averaging about 125 ft per mi, or 2.3 percent. Most ground-water flow from the plant originates there and moves northward.

The Burlington Limestone, the shallow aquifer under and near the plant, is an aquifer with high secondary permeability. Water tracing tests have indicated ground-water flow velocities of up to 0.5 mi per day. These high-rate flows occur in conduits, developed along bedding planes and fractures, which lead to springs where ground water becomes surface water. The limestone permeability is heterogeneous. The primary permeability of the intact rock is very low. The horizontal distribution of the secondary permeability is quite variable. The vertical distribution of secondary permeability is from high in the upper part of the aquifer to very low in the aquifer base. Most flow appears to occur near the water table; video camera inspection of drillholes and packer-test results support this concept.

Surficial materials control the precipitation that enters the shallow aquifer and where it enters. Residuum typically has relatively high permeability and can allow rapid recharge to occur to the shallow aquifer. Glacial till and the Ferrelview Formation have very low permeability. In areas covered by these Pleistocene materials, shallow aquifer recharge is generally low. Most recharge that occurs through till or the Ferrelview enters the aquifer through discrete discontinuities in these Pleistocene deposits, such as vertical fractures. Loess is moderately to highly permeable but only has a minor effect on recharge, because it is underlain by till or the Ferrelview and till, a combination that results in

patchy and sometimes intermittent perched water tables on the till or the Ferrelview.

Many of the fifty springs and seeps within a 3-mi radius of the chemical plant are small and are believed to be supplied by a local small ground-water basin. About 10 springs are larger and are believed to be supplied by the larger ground-water basins in the area.

To the south the springs in Valley 5300 appear to be the ground-water and diverted surface-water outlets for a small area at the south edge of the plant. To the north, the Burgermeister Spring system appears to be the ground-water and diverted surface-water outlet for most of the chemical plant.

The Burgermeister Spring complex contains several outlets, the main one of which, called Burgermeister Spring, is a perennial spring. During high flow conditions, three nearby outlets begin to function and appear to act as relief valves. Flow from the three intermittent outlets can greatly exceed that of the main outlet. Howell Cemetery Spring and Howell Cemetery Wet Weather Spring are believed, based on water tracing tests, to be hydrologically connected to Burgermeister Spring and are considered parts of the Burgermeister Spring complex.

The ground-water hydrology of the shallow aquifer near the chemical plant is being investigated by several methods. Water tracing, the method being emphasized, involves injecting a fluorescent dye into a volume of ground water at a known location such as a losing stream or monitor-well drillhole. Monitoring at ground-water discharge points, usually springs, determines where the ground-water flow has taken the dye; hence, ground-water flow direction and travel time can be measured. Direct water labeling is a very powerful tool in sorting out the complex nature of ground-water flow in a conduit flow aquifer.

Another investigative method used is stream and spring gaging. Gaging of gaining and losing stream reaches and spring gaging, along with water tracing, provides data for a water balance study. The portion of ground water flowing from a spring, that originated as discrete recharge, is estimated. The remaining portion of spring flow is assumed to originate as diffuse recharge, i.e., slow seepage through the unsaturated zone.

Other methods used are spontaneous-potential geophysical surveys, tracking of monitoring well water levels, video camera observation of drillholes, and review of historical data and reports. Geophysical surveys attempt to locate and track ground-water conduits. Monitoring well water levels reflect aquifer response to precipitation. Video camera observations were used to assess the characteristics of the aquifer and to help decide which drillholes to use for water tracing tests.

ENVIRONMENTAL CONCERNS

Two kinds of contaminants are present at the chemical plant. A variety of chemicals were left behind as a result of production of TNT and DNT at the former ordnance works, of which a group of compounds collectively called nitroaromatic compounds is of greatest concern. They include 2,4,6-TNT (trinitrotoluene), 2,4-DNT (dinitrotoluene), 2,6-DNT, 1,3,5 TNB (trinitrobenzene), 1,3-DNB (dinitrobenzene), and NB (nitrobenzene).

During the mid-1950's to mid-1960's, when uranium ore was processed to uranium metal at the plant, the chemical extraction process resulted in contamination by a variety of radioactive isotopes and chemicals. Radioactive isotopes and some of the other heavy metals are of greatest concern.

Access is strictly controlled at the chemical plant, where most of the radioactive materials are present. Plans are being developed to raze the plant and remediate the hazardous materials to a safe condition. Some radioactive material and nitroaromatic compounds have been detected outside the plant boundary. Surface-water transport is assumed to be the most important mechanism moving contaminants from the plant. Contaminants have been detected in some surface-water drainages and some springs. Low levels of uranium and nitroaromatic compounds have been detected in a few monitoring wells and high levels of sulfates and nitrates in numerous monitoring wells.

Radioactive materials and heavy metals have been detected at Burgermeister Spring. Nitroaromatic compounds have been detected in several wells north of Lake 34. Transport to those locations is assumed to be through karst conduits that divert water from one drainage basin to another. Figure 3 shows the inferred direction of this flow.

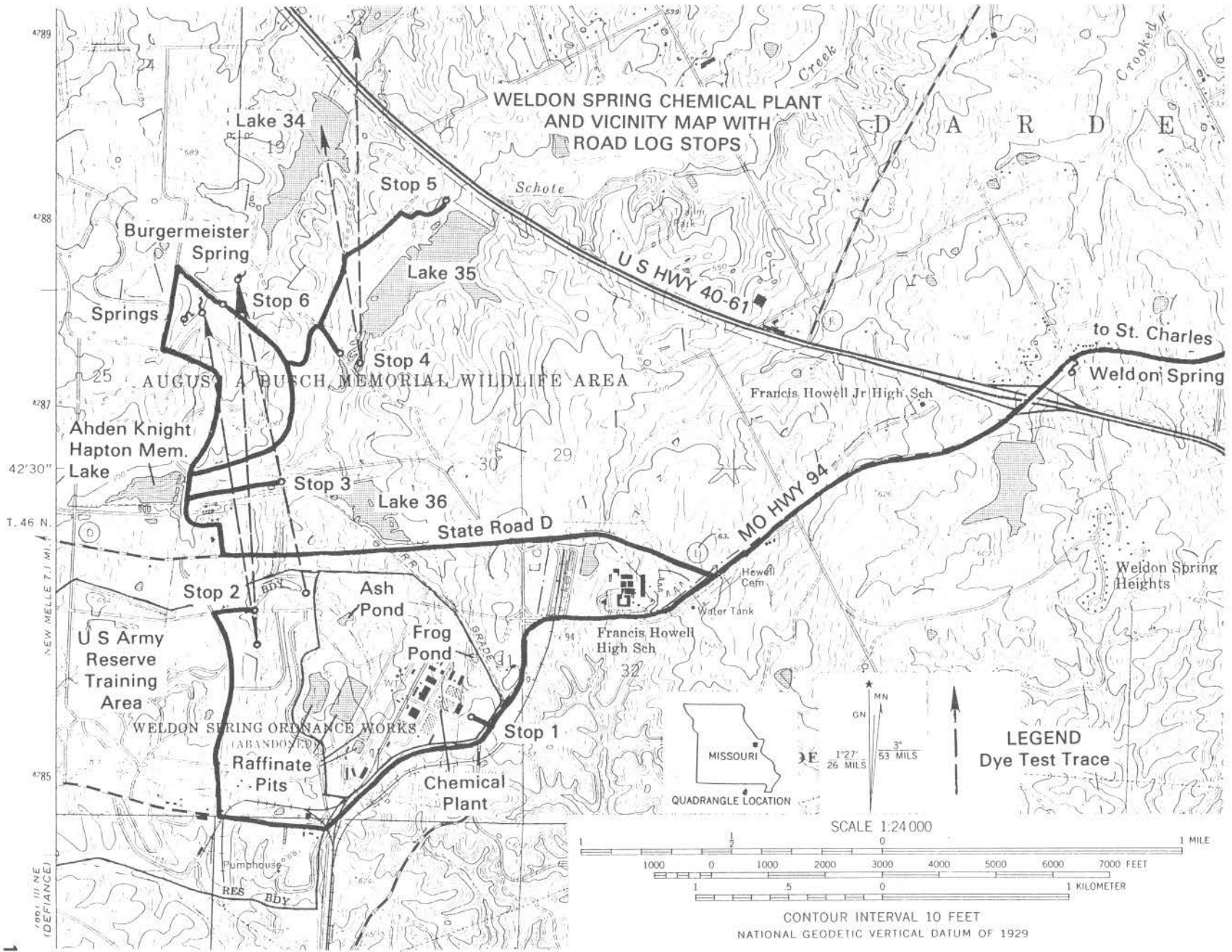


Figure 4 — Weldon Spring Chemical Plant and vicinity with road log stops.

**ROAD LOG FOR THE ENGINEERING AND
ENVIRONMENTAL GEOLOGY
OF THE ST. LOUIS AREA FIELD TRIP**

Mileage

0.0 Start at the front entrance (Chestnut Street) of the Adam's Mark Hotel. Go a half block (east) to Memorial Drive. Turn right (south) onto Memorial Drive and stay in right lane. Go one block on Memorial Drive to Market Street. Turn right (west) on Market Street and go two blocks, merging into left lane.

Turn left (south) onto Broadway and go four blocks (0.3 mi), merging into right lane, to entrance ramp of west-bound U.S. Hwy. 40.

Turn right onto entrance ramp of west-bound U.S. Hwy. 40 and proceed west through the greater metropolitan St. Louis area 28.4 mi to Missouri Hwy. 94 exit (first interchange after crossing the Missouri River).

Turn left at the head of the exit ramp onto Missouri Hwy. 94 south and proceed 2.3 mi to the front gate of the abandoned Weldon Spring Chemical Plant (7295 Hwy. 94 S.). Turn right into front gate.

31.3 STOP 1. Abandoned Weldon Spring Chemical Plant. During World War II this area was a U.S. Army explosives manufacturing facility. In 1955 part of the property was turned over to the Atomic Energy Commission; they built and operated this plant until 1966 to process uranium ore into uranium metal. Waste residues from the uranium processing plant, called raffinate, were disposed in waste lagoons, now called raffinate pits. Radioactive materials remain throughout the processing facility and in the raffinate pits. Ground-water monitoring at and around the facility has indicated that low-level contaminants are locally present in the ground water. Nitroaromatic contaminants remain from explosives production.

The plant is on a surface-water and ground-water divide. Surface water draining from the facility, after flowing over low

permeability Pleistocene deposits, often enters the subsurface and recharges ground water rapidly through high permeability bedrock and bedrock-derived residuum.

At the entrance gate of the Weldon Spring Chemical Plant, turn right on Missouri Hwy. 94 and go south 0.1 mi. Turn right onto access road to U.S. Army Reserve Training Area. Main gate to training area is 0.7 mi down entrance road. Enter main gate and continue on main road an additional 0.4 mi. Turn right on gravel road (small red brick building on right) and go 0.7 mi.

Turn right, passing through cable gate and proceed 0.1 mi to creek crossing; monitor wells to left. Stop here.

33.1 STOP 2. West Raffinate Pits Branch of Sewage Lagoon Fork of Schote Creek. This upland tributary of Schote Creek carries surface drainage from the raffinate pits area. A short distance downstream of this point all surface flow is lost to the subsurface; water tracing experiments have shown that at least some lost water resurges (discharges) at springs (Stop 6) not in the Schote Creek drainage, but in the next surface drainage to the north.

Turn around and retrace route to Missouri Hwy. 94. Turn left at cable gate and go 0.7 mi on gravel road. Turn left onto main training area road and proceed to main gate and then to Missouri Hwy. 94.

Turn left onto Missouri Hwy. 94 north and go 1.1 mi to State Road D.

Turn left onto State Road D and go 1.6 mi to entrance road of August A. Busch Memorial Wildlife Area.

Turn right onto the entrance road to the wildlife area and go 0.1 mi.

Turn left in front of wildlife area office and lodge and pass through fence gate.

Turn right onto wildlife area road A (just past gate) and go 0.1 mi.

Turn right onto gravel road and go 0.3 mi toward lake 36 and to the first creek crossing. Stop.

- 38.1 STOP 3. Sewage Lagoon Fork of Schote Creek. This point is directly downstream from the last stop (STOP 2). The only regular flow observed here is a trickle that disappears a short distance downstream, from discharge of the small wildlife-area sewage lagoon. There is significant flow only during and immediately after rainfall. These features illustrate typical losing-stream characteristics.

Turn around and return to wildlife area road A. Turn right onto road A and go 0.1 mi. Turn right onto road C and go 0.5 mi towards Lake 35. Turn right towards Lake 35 and go 0.2 mi. Turn right and go 0.1 mi to parking area (on left) at upstream end of Lake 35. Turn left into parking area and stop.

- 39.4 STOP 4. Swallow hole at upper end of Lake 35. Walk down road beyond parking area. About 100 ft beyond the old bridge over Schote Creek, turn left and walk out beside the easternmost finger at the upstream end of the lake. About 100 ft from the road a swallow hole can be seen if the lake level is low; it first appeared in the fall of 1986 and drained several feet of lake water. A water-tracing dye introduced into it was recovered about one mile north in a spring and in the spillway of Lake 34, just upstream, both in an adjoining drainage. Return to vehicles.

Turn right out of parking area and go 0.1 mi to road junction. Turn right and go 0.2 mi towards lower end of Lake 35. Road forks; take right fork towards Lake 35 and go 0.3 mi. Road forks again; take left fork towards dam of Lake 35. Proceed 0.2 mi to end of dam of Lake 35. Stop.

- 40.1 STOP 5. Exposure of Burlington-Keokuk Limestone bedrock. Walk across dam of Lake 35, to its east end, to the dam's emergency spillway blasted into bedrock, one of

the few bedrock exposures in the area. The Burlington-Keokuk, a medium- to coarse-grained gray fossiliferous limestone with interbedded chert seams and nodules, is typically highly fractured, and has high secondary permeability. Solution weathering of fractures also creates high permeability and a very uneven weathered bedrock surface. During periods when the emergency spillway is unused, lake seepage can be seen emerging from bedding plane fractures in the spillway rock. The bright orange iron staining at the base of the spillway also indicates lake leakage. These leakage examples attest to the permeable character of the bedrock.

Turn around and return to road C. Turn right at first fork in road (0.1 mi) and turn left at second fork (0.3 mi). Go 0.5 mi to rejoin road C. Turn right on road C and go 0.3 mi. Stop.

- 41.0 STOP 6. Burgermeister Spring. Walk NE through field to right (about 500 ft) to find Burgermeister Spring, just inside the wooded area; the spring is marked by an old concrete foundation around it. The spring flows perennially and is the discharge point for much of the surface drainage lost to the subsurface from the chemical plant area. Water-tracing experiments have demonstrated the hydrologic connection between this spring and West Raffinate Pits Branch (Stop 2) and Ash Pond Branch to the east. Above-background concentrations of nitrates and radionuclides in the spring water also suggest a hydrologic connection. Because Burgermeister Spring has been identified as an important ground-water discharge point, instruments were installed by parties studying the hydrogeology around the chemical plant. The U.S. Geological Survey installed a weir and automatic water level recorder to measure the spring's discharge and an automatic temperature/conductivity recorder to record water quality elements. The Missouri Department of Natural Resources installed an automatic water sampler to assist in water tracing experiments; they also installed a gridwork of grounding rods, for use of the self-

potential method, around the spring in an attempt to determine the location of the conduit feeding the spring. Return to vehicles.

Continue on road C to tee-road junction. Turn left and go 0.1 mi to junction of road A. Go straight ahead on road A 0.2 mi to another tee junction. Turn left to follow road A back through wildlife area gate and past office.

Turn right onto wildlife area entrance road to return to State Road D.

Turn left onto State Road D and go 1.6 mi to Missouri Hwy. 94. Turn left onto Missouri Hwy. 94 north and go 1.1 mi to entrance ramp onto eastbound U.S. Hwy. 40-61.

45.1 Turn right onto U.S. Hwy. 40-61. Travel east 2.3 mi on U.S. Highway 40-61 to Daniel Boone Bridge, and cross the Missouri River. Continue eastward 12.4 mi to entrance ramp onto northbound I-270.

59.8 Follow ramp onto I-270 North. The trip will circle the greater St. Louis area on I-270. There will be a lunch stop at Furrs Cafeteria on Dorsett Road, 6.3 mi north of the U.S. Hwy. 40-61/I-270 interchange.

66.1 Lunch Stop — Continue north on I-270 off Dorsett Road 15.1 mi to Hwy. 367 northbound.

81.2 Exit to the right and circle left (north) on Hwy. 367.

86.6 Approximately 5.4 mi from the I-270/Hwy. 367 interchange, the trip will use the Lewis Bridge to cross the Missouri River again. Immediately before crossing the river, two quarries mining the Mississippian Ste. Genevieve and St. Louis limestones can be observed. North of the Missouri River, before reaching Alton, Illinois and Lock and Dam 26, Hwy. 367 crosses the common flood plain of the Missouri and Mississippi Rivers.

90.3 The trip will use the Clark Bridge to cross the Mississippi River into Alton, Illinois. Turn right on East Broadway as you exit off the

bridge and travel 0.1 mi. Turn right on Henry Street and travel southward 0.3 mi. At the levee turn right and travel west to Riverfront Park.

91.8 At Riverfront Park is a visitors area for the U.S. Army Corps of Engineers Lock and Dam #26, which is undergoing serious foundation problems. The lock and dam is at river mile 202.9, where we will board the U.S. Army Corps of Engineers boat, the Blankenship.

River
Mile
201 Melvin Price Locks and Dam is a new structure that will soon replace the original Locks and Dam No. 26 completed in 1938. Very detailed subsurface exploration helped site this structure; completion date is 1992.

River
Mile
195.3 The Missouri River flows into the Mississippi River. The area is part of the American Bottoms flood plain.

River
Mile
194.1 We will enter Chain of Rocks Canal, which is 8.4 mi long. Construction began on the canal in February 1949, in order to provide a deeper navigation route for river traffic. The "chain of rocks" on the main river channel is a bedrock high which restricts travel in low water periods.

River
Mile
190.3 U.S. Army Corps of Engineers Dam No. 27 is located on the main river channel. It was constructed to restrict water flow in the natural channel in order to increase navigable depths in the man-made canal. This is the most southern of the 29 dams and locks on the Mississippi River. We will pass through Lock 27 on the canal to allow us to reenter the main river channel at River Mile 183.7.

River
Mile
183.2 We will pass beneath the Merchants Bridge (Terminal Railroad).

River
Mile
182.5 We will pass beneath the McKinley Bridge. Many St. Louis City Municipal Docks are south of this bridge.

River
Mile
180.2 We will pass beneath the Veterans Memorial Highway Bridge.

River Mile 180.0 The Eads Bridge was a tremendous engineering feat for its time. Construction began in 1867 and was completed in 1874. Piers were sunk to depths of 136 ft, the deepest pneumatic caisson ever constructed.

River Mile 179.8 The Gateway Arch is a symbol of St. Louis' historic position. Foundation construction began in 1961. The two arch legs are

founded over 60 ft deep through 30 ft of alluvium and 30 ft of St. Louis Limestone. The arch, 630 ft high, was completed in 1965.

The river trip ends at the Gateway Arch. By walking directly west from the structure, the field trip will end at the Adam's Mark Hotel.

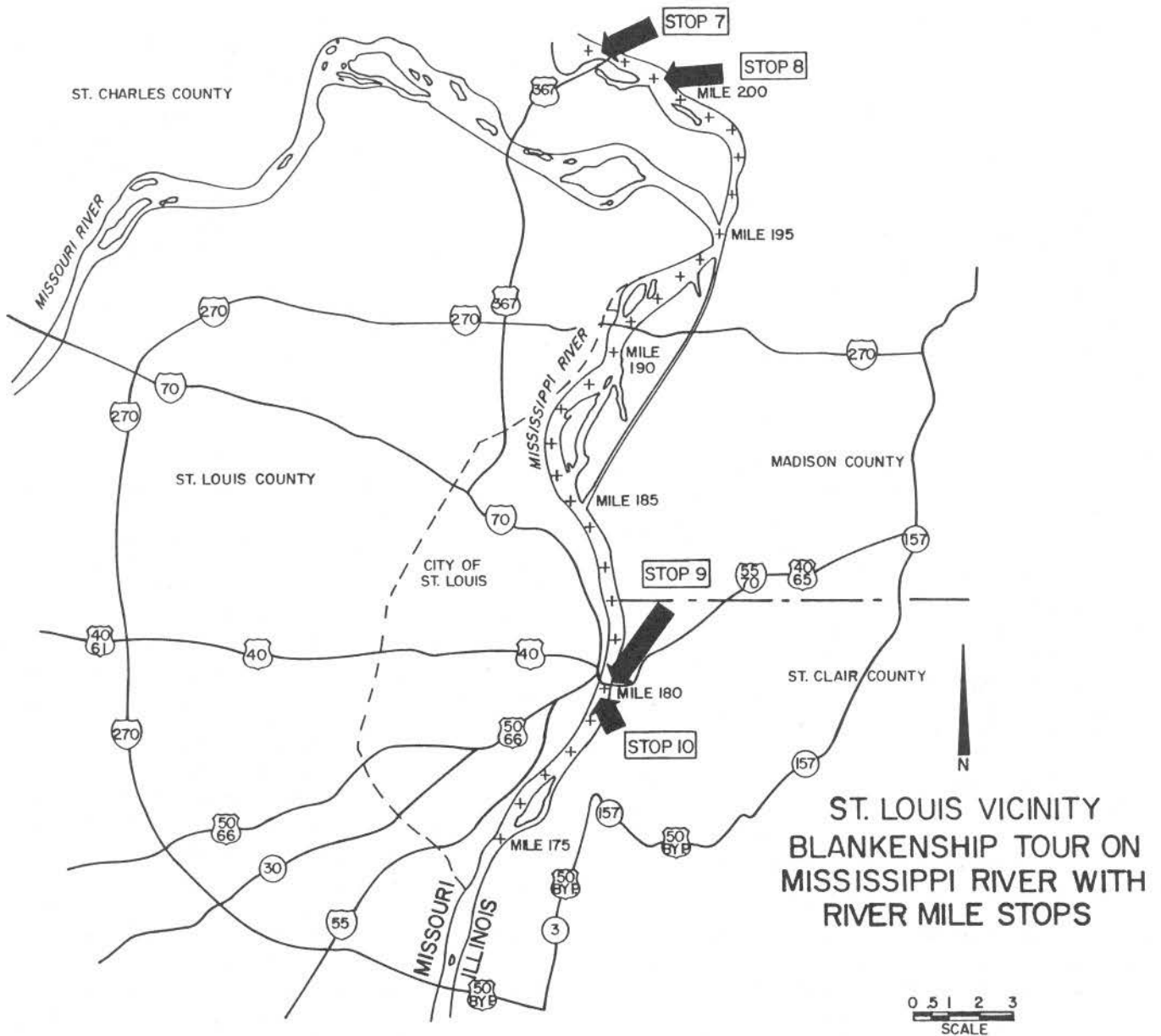


Figure 5 — St. Louis Vicinity showing boat tour route on Mississippi River and river mile stops.

PHYSIOGRAPHY OF THE MISSISSIPPI RIVER FLOOD PLAIN

This section of the Mississippi River Valley from Melvin Price Locks and Dam at river mile 201, downstream to the St. Louis riverfront at river mile 179, is in two physiographic provinces, the Ozark plateau to the west and the Central lowland to the east. The Missouri side lies in the easternmost extremity of the Salem plateau. The Illinois side is in the Springfield till plain.

The Mississippi River flood plain, 150 to 200 ft below the upland crests and 4 to 12 mi wide, is separated from the uplands by an abrupt bluff line. Only the Missouri bluffs are visible from the river. The low hills and broad divides of the Missouri side are underlain by Mississippian limestones. Several feet of sandy, gravelly clay till (Kansan?) overlies bedrock and is covered by 10 to 25 ft of silt and silty clay loess (Peoria Loess and Roxana Silt).

Repeated cycles of vertical incision, aggradation, and lateral migration by the Mississippi River are

responsible for the formation of the present flood plain. Advances and retreats of Pleistocene ice sheets were accompanied by aggrading of the river bed and development of a braided channel pattern during the glacial stages. Degradation of the river bed and return to a meandering channel form was common during interglacial stages. As the river migrated laterally, the periodic channel abandonment occurred and former meanders became arcuate oxbow lakes (Smith and Smith, 1984).

The Mississippi River, is in a deep bedrock valley that is 100 ft or more beneath the present valley surface. The bedrock valley has steep sides along bluff lines but is relatively level to slightly undulating in the middle. Valley fill is Recent alluvium and underlying glacial valley-train deposits. Modern river scour and fill has reworked much of the lower glacial deposits and identification of contacts is thereby difficult. River bed scour near the St. Louis riverfront has been estimated to be as much as 80 ft.

MELVIN PRICE LOCKS AND DAM

The Melvin Price Locks and Dam, under construction by the U.S. Army Corps of Engineers, St. Louis District, is a current project that will span the Mississippi and benefit both national transport and commerce. This river control structure, about 20 river miles upstream of downtown St. Louis, is needed to replace the original Locks and Dam No. 26 completed in 1938. The existing structure, which has serious foundation problems, has only a 600-ft (183 m)-long main lock that is a serious bottleneck to modern river-traffic demands.

The replacement structure, when completed in 1992, will be a non-navigable gated dam and two medium-lift navigation locks. In addition, a 114 megawatt low-head hydroelectric plant may be added to the structure, if approved by Congress.

This three-stage project comprises construction of 6½ gatebays of the main dam in the first stage; the 1200-ft (366 m) lock and 2½ gatebays in the second stage; and a 600 ft (183 m) lock, 1½ dam gatebays and closure structure during the third stage. Dam and locks are reinforced concrete structures founded on steel H-piles driven to bedrock.

In 1967 the Corps of Engineers began extensive subsurface explorations for the replacement structure. More than 200 exploratory borings were completed in the site area to define engineering and geologic foundation characteristics. Early overwater explorations encountered boulder and cobble deposits at isolated places along the initial dam axis; it was recognized that these could hinder the proposed construction of a driven pile foundation.

After additional exploration, the proposed dam site was moved 350 ft (107 m) downstream to its final location. During initial explorations a hard, compact, basal till (Illinoian) was also encountered at some places. The potential for encountering such problem deposits during foundation construction greatly increased the scope of subsurface investigations. Routine geotechnical sampling methods, consisting of drive sampling with 2-in. (50 mm) o.d. (SPT) and 3-in. split-spoon samplers, were augmented with borehole geophysical logging, diamond coring of the clay and till deposits, cross-hole shear-wave determinations, dredging for large diameter boulders, overwater seismic reflection surveys using

both "pinger" and "boomer" systems, and in situ soil pressuremeter testing. Investigations revealed

a highly varied site stratigraphy comprising alluvial and glacial deposits on Mississippian bedrock.

EADS BRIDGE

The Eads Bridge is a most notable St. Louis structure. Fittingly, it is immediately north of the Arch and is the northern boundary of the memorial. Although almost one hundred years older than the neighboring Arch it shows the same engineering design and construction pioneering and was, in a practical sense, an early gateway to the west. Many new and controversial design aspects were involved in bridge construction, which began in August 1867. It was the largest bridge constructed at that time, the first important structural application of steel, and used an arch design that was radically different from the prevailing long-span bridge construction. The most interesting aspect of the bridge from a geotechnical perspective was the use of pneumatic caissons in river pier construction.

James Eads began his engineering work on the Mississippi at the age of 22. He convinced investors to back a salvage operation to reclaim the sunken vessels that littered the river at that time. As part of his work Eads walked the river bottom in a crude diving bell, in search of salvage. His first diving bell was comprised of a modified 40-gallon whiskey keg with one end knocked out and the closed end fitted with an air line. From his explorations Eads learned much about the river and its fill and scour processes. The personal observations of 80 ft (24 m) of river scour would prove important in his later endeavor to construct a bridge and its foundations across the great river.

During a European trip in 1868, Eads became convinced that the pier-sinking system he had observed in the construction of a small bridge over the Allier River in France would perfectly suit his project. This pneumatic caisson procedure would allow the bridge to be founded on bedrock that Eads

realized would be necessary to withstand the river's force and structural loads. Instead of an open cofferdam, this method employed a caisson sunk to the river bed. The caisson was watertight and ended in a pressurized air chamber enclosed in a strong bulkhead. Air locks permitted workmen to enter and exit the work area without losing air pressure. These "sandhogs" shoveled the river bottom material into sand pumps that discharged it into the river. As the caisson sank, masons working in open air laid the outer stone pier blocks, leaving a hollow core for stairwells, elevators, and piping. As the masonry rose, the caisson sank to the bedrock, its rate of descent controlled by the excavation and the buoyancy of the air chamber. Once on bedrock, the air chamber and access shaft were filled with concrete.

In October 1869, only 8 months after the first stone was laid for the east river pier, both it and the west river pier were completed above water line. Over 40,000 tons of stone and concrete were placed during this time. Construction of these piers had been so effective that the east abutment pier was also founded with the caisson method. With a total depth of 136 ft (41 m) this east pier became the deepest pneumatic caisson ever constructed. By April 1871, all four piers were completed. And on May 24, 1874 the highway deck of the completed bridge was opened to pedestrians.

This tremendous engineering feat was marred by the effects suffered by the air chamber workers. The physiological effects of working for extended periods in pressures almost three times atmospheric were not well understood at the time. As a result of inadequate decompression times, 119 of the 600 sandhogs or submariners were stricken and 14 died.

GATEWAY ARCH

The famed "Gateway Arch" (Frontpiece) is one of the most interesting engineered structures in the St. Louis area. It has become a symbol of the historic position of St. Louis as the "Gateway to the West" and has spurred a regrowth in downtown development and civic pride.

The St. Louis riverfront was selected in 1935 as the site for a national monument to commemorate the westward expansion of the United States. A nationwide competition was held in 1947 to select a design for the yet unnamed Jefferson National Expansion Memorial. Eero Saarinen won the

competition with his submittal of a memorial park dominated by a 630 ft (192 m)-high stainless steel arch, which was to be in the shape of an inverted catenary curve with the distance between the legs at its base equaling its height. Each leg section therefore forms an equilateral triangle, 54 ft (16 m) on a side at ground level and 17 ft (5 m) at the apex.

Foundation construction began in April 1961, with the excavation of about 30 ft (9 m) of soil overburden to the St. Louis Limestone. Excavation for the two arch legs were carried another 30 ft (9 m) into rock by drill and blast method. To prepare the visitor center site beneath the arch, over 10,000 cubic yards of soil and rock were excavated for the foundations. Following the two triangular excavations, approximately 13,000 cubic yards of steel reinforced concrete was placed. Over 200 tons of reinforcement were used in the foundations. In addition to the conventional concrete reinforcing bars, 252 steel tendons were also added to the foundation. These 35-ft (11 m)-long, 1.25-in (32 mm) tendons were preassembled into groups of 21 each; they could be shipped and erected as a unit. The tendons, made of a high-strength alloy steel have an ultimate strength of 145,000 psi. Three bar assemblies, each with 63 bars, were placed in each of the four outside corners of the arch legs. Welded steel tubing, each with an inside diameter of 1.50 in. (38 mm), covered each bar in the assembly. The tendons were post-tensioned following concrete placement and 7 to 10 days of curing. The bars were post-tensioned to a load of 71 tons using a 100-ton center pull hydraulic jack. The annular space between the bar and sleeve

was then pressure injected with cement grout. Adjacent tendons were linked at their base with 1-in. (25 mm) steel grout tubes that connected the two sleeves and acted as bleeder tubes and allowed the grouting of two bars in one operation. No significant problems or delays were experienced during the foundation construction.

In cross section, each arch leg is a double-walled equilateral triangle with a hollow core 40 ft (12 m) wide at the base and 15.5 ft (4.7 m) wide at the top. The inner skin is constructed of 0.37 in. (10 mm)-thick A-7 carbon steel, except at the corners where it is 1.75 in. (45 mm) thick to provide additional stiffness. The outside surface was fabricated from 0.25 in. (6 mm)-thick polished stainless steel. The space between outer and inner skins is filled with post-tensioned concrete from the base to a height of 300 ft (91 m). From 300 ft (91 m) to the top of the Arch at a height of 630 ft (192 m) the two skins are reinforced by a steel diaphragm.

After almost 4 years of construction and nearly 20 years of planning the Gateway Arch was topped out on October 29, 1965. Since its opening to the public the Arch has become a popular visitor attraction, even fostering claims that only Lenin's tomb and the Disney theme parks draw more attendance than the Arch. In 1976, the 42,000 sq ft (3,880 sq m) Western Expansion Museum was opened; it is the largest museum operated by the U.S. Park Service and continues to welcome visitors to the "Gateway to the West."

REFERENCES

- Jensen, J.E., 1968, The construction of the Arch, Jefferson National Expansion Memorial: National Park Service, U.S. Department of the Interior, Washington, D.C., 9 p.
- Smith, L.M., and Smith, F.L., 1984, Engineering geology of selected areas: U.S. Army Engineer Division, Lower Mississippi Valley; Report 1, The American Bottom Area, MO-IL; vol. 1, 38 p.
- Williams, W.J., 1977, James Eads and his bridge: Civil Engineering-Association of Civil Engineers, October 1977, p. 102-107.
- Woodward, C.M., 1881, A history of the St. Louis Bridge: St. Louis.

Field Trip No. 15

**TRANSITION FROM
PASSIVE MARGIN TO FORELAND
BASIN SEDIMENTATION:
THE ATOKA FORMATION OF THE
ARKOMA BASIN,
ARKANSAS AND OKLAHOMA**

**David W. Houseknecht, Marvin O. Woods,
and Paul H. Kastens**
Department of Geology
University of Missouri-Columbia
Columbia, Missouri 65211

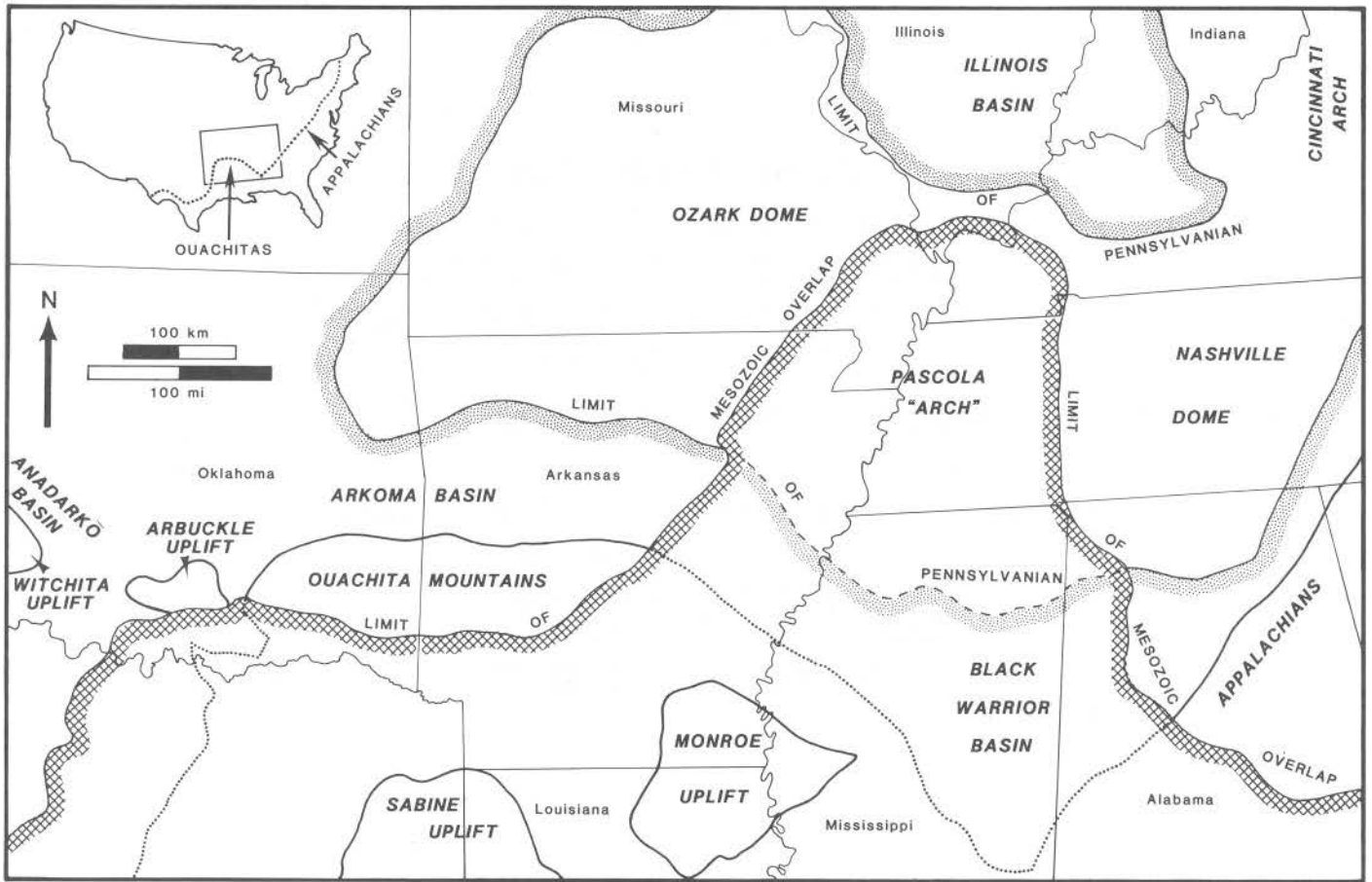


Figure 1 — Major structural elements of southern midcontinent region and limits of Pennsylvanian and Mesozoic strata (Houseknecht, 1986).

INTRODUCTION

The Arkoma is one of a series of foreland basins that formed along the North American side of the Ouachita mountain belt during Carboniferous orogenesis. Atokan strata of the basin record the remarkably rapid transition from sedimentation on a marine shelf of a passive continental margin to sedimentation in a foreland basin formed in response to convergent tectonism along the Ouachita orogenic belt. Basal Atokan strata were deposited along a tidally swept coastline on a tectonically stable shelf that had prevailed since the late Cambrian. The remainder of Atokan strata were deposited during the breakdown of that shelf by normal faults, apparently induced by obduction of the Ouachita accretionary prism onto the southern margin of North American continental crust. The resulting sediment wedge represents progressive basin filling by submarine fan, marine slope, and deltaic facies that record the dynamic evolution of tectonic style, sediment distribution patterns, and sediment

composition, as the orogenic belt pushed northward onto the continent. By the end of Atokan time, flexural subsidence and deposition of coal-bearing molasse characterized the final phase of foreland basin development.

This field trip illustrates vertical and lateral variations in depositional facies, sediment dispersal patterns, and sandstone petrofacies that reflect the three major phases of tectonics and sedimentation summarized in the preceding paragraph. The trip emphasizes Atoka Formation strata that accumulated during the most dynamic phase of basin development, but also includes Morrowan and Desmoinesian strata for comparison of strata deposited during contrasting tectonic phases. Because continuity and quality of exposures are not outstanding in this region, we rely heavily on subsurface data for documentation of tectonic features and for stratigraphic correlation.

GEOLOGIC SETTING

The Ouachita Mountains, extending from central Arkansas into southeastern Oklahoma (fig. 1), represent the largest exposure of an orogenic belt that is mostly buried beneath Mesozoic and Cenozoic strata of the Gulf coastal plain. The foreland region along the entire length of the Ouachita orogenic belt generally shared a common history of rifted margin sedimentation during the early through middle Paleozoic, followed by foreland basin development induced by convergent tectonism during the late Paleozoic (Flawn et al., 1961; Graham et al., 1975; Thomas, 1985). Only during final phases of Ouachita orogenesis was the foreland region segmented into individual structural basins, one of which is the Arkoma.

The Arkoma basin, an arcuate synclinorium extending from east-central Arkansas to southeastern Oklahoma (fig. 1), lies immediately north of the Ouachita orogenic belt, to which it is intimately related genetically. Although the southern margin of the basin is historically defined as the northern edge of the Ouachita frontal thrust belt, it is now clear that Atokan strata exposed in the frontal thrust belt were deposited in continuity with Arkoma basin

strata and that older Arkoma basin strata extend southward significantly far beneath the thrust belt.

STRATIGRAPHY

Figure 2 schematically summarizes Paleozoic stratigraphy of the Arkoma basin and Ouachita Mountains. Upper Cambrian through basal Atokan strata in the basin comprise shallow marine carbonates, shales, and quartzose sandstones whose maximum aggregate thickness along the southern part of the basin is about 1.5 km. They represent only 16 percent of Paleozoic strata thickness in the basin, yet they represent 93 percent of the time in which Paleozoic sediments accumulated in the basin and on the precursor shelf (fig. 2). In the Ouachitas, Cambrian through earliest Mississippian strata are deep water carbonates, siliceous shales, and cherts (novaculite) that have been called "starved basin strata," whereas Mississippian and Morrowan strata are submarine fan and basin plain facies constituting a flysch sequence.

In the Arkoma basin, basal Atokan strata are overlain by the Atoka Formation (fig. 2), comprising

shales and sandstones displaying complex stratigraphic and facies characteristics detailed in the following text. Deposited during a mere 5 million years, the Atoka attains a maximum thickness of more than 5.5 km along the southern margin of the basin, representing 58 percent of Paleozoic strata thickness in the basin, yet representing only 2 percent of the time in which Paleozoic sediments accumulated! In the Ouachitas, the Atoka Formation, present as the youngest part of the Carboniferous flysch pile, is estimated to attain a maximum

thickness of about 5 km, although its original thickness is probably not preserved.

Conformably overlying the Atoka Formation in the Arkoma basin, coal-bearing Desmoinesian formations attain a maximum aggregate thickness of about 2.5 km (fig. 2). They represent 26 percent of the cumulative Paleozoic section and 5 percent of the time in which Paleozoic strata accumulated. There are no equivalent strata present in the Ouachita Mountains, perhaps due to erosion, but more likely due to non-deposition because of orogenic belt uplift near the end of Atokan time.

Figure 3 is a summary of sediment accumulation rates for strata of the Arkoma basin and Ouachitas. Significant slope breaks in the two sediment accumulation curves indicate onset of the orogenesis. In the deep water (off-the-shelf) Ouachitas realm, the contact of the Arkansas Novaculite and the overlying Stanley Formation represents onset of orogenically influenced sedimentation, apparently induced by initiation of subduction and initial uplift of the orogenic belt to the east. In the Arkoma basin (on-the-shelf), the contact of the Spiro (Cecil-Spiro in Arkansas) sandstone and overlying lower Atoka shales represents tectonic breakdown of the passive margin shelf and the initial development of the Arkoma foreland basin.

These slope breaks (fig. 3) also represent abrupt transitions in sandstone and kerogen compositions. Before slope breaks, sandstones are mostly quartz arenites to subarkoses, and shales contain mostly types I and II (sapropelic) kerogen. Following slope breaks, sandstones are mostly sublithic to lithic arenites, and shales contain mostly type III (humic) kerogen. The abrupt shift in sandstone compositions reflects rapid changes in provenance and sediment dispersal patterns, whereas the shift in kerogen compositions reflects rapid transition from predominantly clear water sedimentation to turbid conditions that accompanied onset of synorogenic sedimentation.

STRUCTURE

In the Arkoma basin, broad synclines separated by narrow anticlines dominate the surface structure (fig. 4). Fold axes generally parallel the overall arcuate trend of the basin and that of the Ouachita

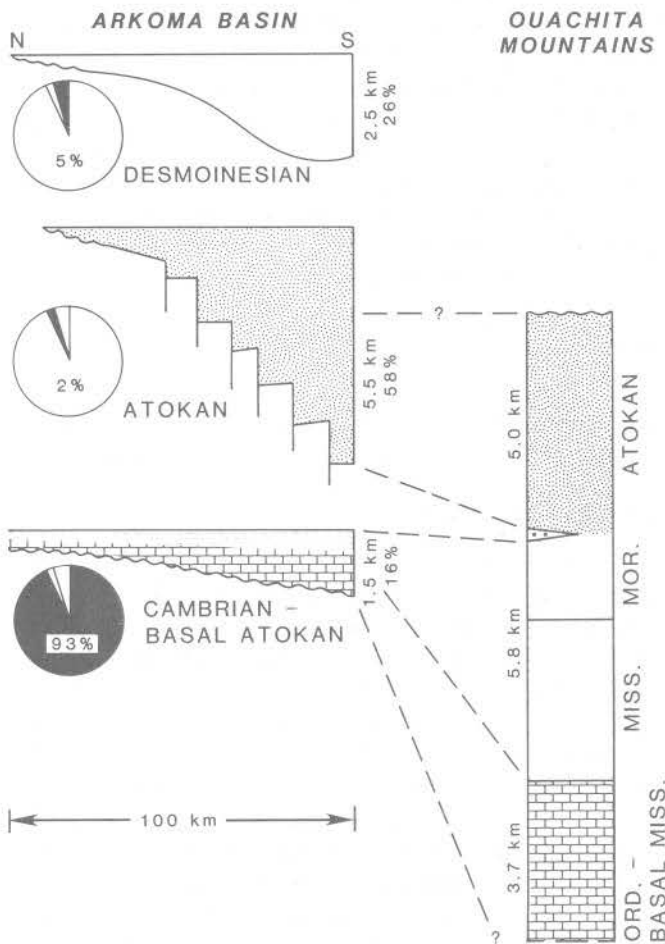


Figure 2 — "Tectonic stratigraphy" of the Arkoma basin and Ouachita Mountains, showing overall geometry of Arkoma basin strata deposited in various tectonic settings depicted in figure 5. Symbols denote genetically related strata and do not imply lithologies. Pie diagrams illustrate the time represented by each genetic package of strata, expressed as a percentage of total Paleozoic time during sedimentation (Houseknecht, 1987).

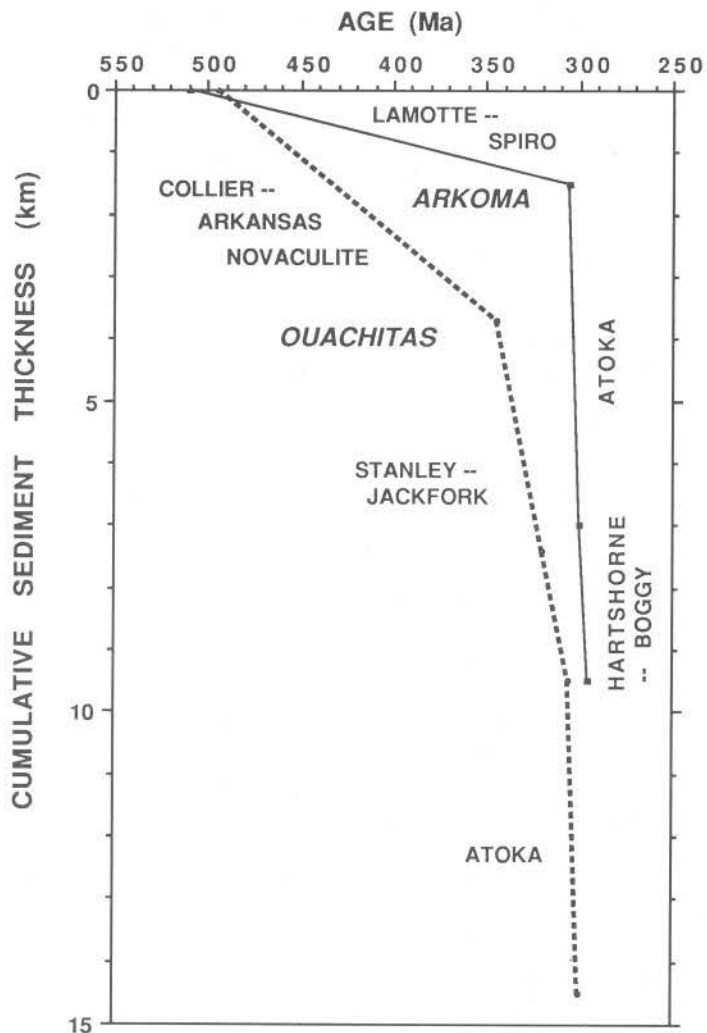


Figure 3 — Sediment accumulation curves for Arkoma basin and Ouachita strata (not corrected for compaction).

frontal thrust belt. Listric thrust faults underlie much of the folded section and ramp to the surface along many anticlinal crests (fig. 4). Beneath thrust fault horizons, the structural style is dominated by normal faults that offset the Precambrian basement and the entire sub-Atoka sedimentary section (fig. 4). These faults, most of which dip southward, were active during deposition of lower through middle Atokan strata, as indicated by significant thickening of those strata across the faults.

The Ouachita Mountains represent a collisional orogenic belt displaying complex thrust fault and fold geometries. The origin of specific Ouachita structural features is still hotly debated, but recent work

suggests the presence of both accretionary and foreland deformational features (Underwood and Viele, 1985; Houseknecht and Underwood, 1988).

TECTONIC HISTORY OF THE ARKOMA BASIN

Recent tectonic interpretations of Ouachita orogenic belt origins involve consumption of oceanic lithosphere via southward-dipping subduction and consequent collision between a passive continental margin (the southern margin of North America) and either an island arc or continental plate (commonly called Llanoria) (see Houseknecht, 1986, 1987).

According to this interpretation, a rifting event resulted in opening an ocean basin during the latest Precambrian or earliest Paleozoic (fig. 5A). It is unclear if the Arkoma continental margin developed as an Atlantic-type rifted margin or as a transform margin as suggested by Thomas (1985). In either case, the southern margin of North America evolved into a passive continental margin that persisted through the middle Paleozoic (fig. 5B). The sediment prism that accumulated along this passive margin includes Cambrian through lowermost Mississippian strata deposited in shelf and deeper water environments (figs. 2 and 3). Shelf facies are mostly carbonates with subordinate shale and quartzite sandstone. Although their original southward extent is unknown, they occur throughout the Arkoma basin; the lower Paleozoic portion extends southward beneath the core of the Ouachitas (Lillie et al., 1983; Thomas, 1985; Leander and Legg, 1988).

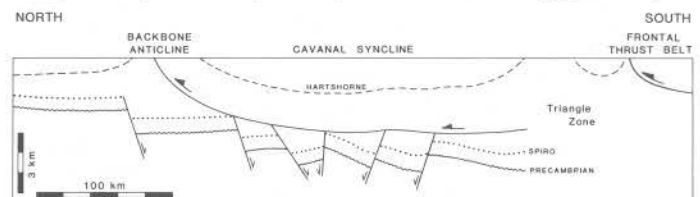


Figure 4 — Generalized tracing of a seismic line extending from north of Backbone anticline southward to Ouachita frontal thrust belt (see fig. 6). Wavy line is approximate Precambrian-Cambrian unconformity; dotted line is approximate horizon of basal Atoka Spiro sandstone; dashed line is approximate horizon of basal Desmoinesian Hartshorne Sandstone; and heavy solid lines are faults, with displacements indicated by arrows. Upper parts of syndepositional normal faults are displaced northward by thrust fault, but are not shown on this figure (Houseknecht, 1986).

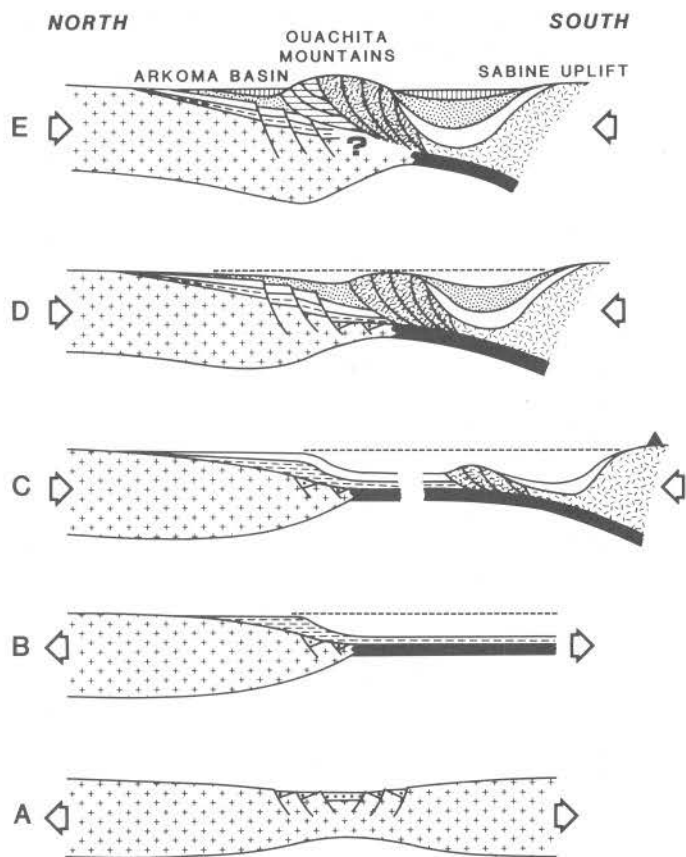


Figure 5 — Hypothetical cross sections depicting tectonic evolution of southern margin of North America during (A) late Precambrian-earliest Cambrian, (B) late Cambrian-earliest Mississippian, (C) early Mississippian-earliest Atokan, (D) early-middle Atokan, and (E) late Atokan-Desmoinesian. Key to patterns: crosses = continental crust (undifferentiated in A, North American in B-E); straw hachures = "Llanorian" crust; black = oceanic crust; heavy dots = basal Paleozoic strata; horizontal hachures = upper Cambrian-basal Mississippian strata; white = Mississippian-basal Atokan strata; sand stippling = lower-middle Atokan strata; vertical lines = upper Atokan-Desmoinesian strata; mottled = Ouachita accretionary prism; wavy lines = Ouachita foreland thrust belt; black triangle = magmatic arc volcanoes (Houseknect, 1986).

Deep-water facies, exposed only in allochthonous positions in the Ouachita core, are mostly dark colored shales and subordinate limestone, quartzose sandstone, and bedded chert. Known collectively as the "Ouachita facies," these strata are believed to represent slope, rise, and abyssal sediments.

During the Devonian or early Mississippian, the ocean basin began to close, accommodated by southward subduction beneath Llanoria (fig. 5C). Although it is impossible to determine when subduction began, orogenic detritus (Morris, 1974), locally abundant volcanic detritus in the Stanley Formation, and a significant increase in sediment accumulation rates in the Ouachita basin (fig. 3) indicate it was under way during the Mississippian. Carboniferous volcanic rocks encountered in the subsurface south of the Ouachitas, along the flanks of the Sabine uplift (fig. 1) (Nicholas and Waddell, 1982), probably are vestiges of a magmatic arc that developed on Llanoria (fig. 5C). In this convergent tectonic setting, the incipient Ouachita orogenic belt began to form as an accretionary prism associated with the subduction zone (fig. 5C).

Throughout the Mississippian, into the earliest Atokan (culminating with deposition of the basal Atoka Spiro and Cecil-Spiro sandstones), the shelf along the southern margin of North America was a site of relatively slow sedimentation in shallow marine through nonmarine environments (figs. 2 and 3). Carbonates, shales, and quartzose sandstones continued to be deposited in much the same environment that had characterized the region since the late Cambrian; however, the trench and remnant ocean basin became the site of rapid flysch deposition. Derived primarily from the east, where collision orogenesis had already resulted in uplift along the Ouachita trend (Thomas, 1985), sediment poured into the deep basin where it was dispersed longitudinally westward and ultimately deposited on submarine fans and in associated abyssal environments. Additional sediment, apparently dispersed southward through the Mississippi embayment during deltaic progradation in the Illinois basin, resulted in deposition of more than 5 km of flysch during the Mississippian and Morrowan in the deep Ouachita basin (Stanley, Jackfork, and Johns Valley Formations, figs. 2 and 3).

By early Atokan time, the remnant ocean basin had been consumed by subduction and the northward advancing accretionary prism was being obducted onto the rifted continental margin of North America (fig. 5D). Partly as a result of attenuated continental crust entering the subduction zone and partly because of vertical loading by the overriding accretionary prism (Dickinson, 1974, 1976), the

southern margin of the North American continental crust was subjected to flexural bending, which apparently induced widespread normal faulting in the foreland. These faults generally strike parallel to the Ouachita trend, are mostly downthrown to the south, and offset both crystalline basement and overlying Cambrian through basal Atokan strata of the rifted margin prism. Subsurface and seismic evidence suggests most of these faults broke undeformed continental crust, although it is likely that some of them may represent reactivation of faults formed during early Paleozoic rifting (fig. 5D). The shelf-slope-rise geometry prevailing along the passive continental margin since the early Paleozoic was broken down by the tectonically induced normal faults; subsidence and sediment accumulation rates increased markedly (figs. 2 and 3). Fault movement, contemporaneous with lower through middle Atokan shale and sandstone deposition, resulted in abrupt thickness increases across the faults (fig. 5D). Sediment dispersal became predominately strike-oriented during this phase of sedimentation in the Arkoma basin. Sediment transported through the Black Warrior basin to the east and the Illinois basin to the north was distributed through the basin by westward prograding depositional systems, including deltas, tectonically localized slope channels, and submarine fans. These Atokan strata, which

represent a critical transition between passive margin sedimentation and foreland basin sedimentation, are discussed in more detail in subsequent sections.

By late Atokan time (fig. 5E), foreland thrusting became predominant as the subduction complex pushed northward against strata deposited in environments illustrated by figure 5C-D. Resulting uplift along the Ouachita frontal thrust belt completed formation of a peripheral foreland basin (Dickinson, 1974) in which flexural subsidence replaced the normal fault-controlled subsidence active during the Atokan. Such flexural subsidence in a foreland basin is commonly induced by thrust fault loading at the orogenic side of the basin, as described by Jordan (1981). Sedimentation occurred in shallow marine, deltaic, and fluvial environments, with continuation of longitudinal sediment dispersal established during the Atokan. Upper Atokan and Desmoinesian strata in the Arkoma basin constitute a typical coal-bearing molasse, characterized by sediment accumulation rates lower than those of the early and middle Atokan (figs. 2 and 3). At that time, gross structural features of the Arkoma-Ouachita system were essentially the same as at present, although relatively minor folding and thrusting continued after the Desmoinesian.

SYNDEPOSITIONAL NORMAL FAULTS

INFLUENCE ON STRATIGRAPHY

From a depositional edge along the northern margin of the basin, Atokan strata thicken to more than 5.5 km (18,000 ft) along the northern edge of the Ouachita frontal thrust belt. Most of this thickness increase is accommodated by abrupt expansion of the lower through middle part of the Atoka Formation across syndepositional normal faults, which are shown in figure 6. Earlier workers suggested these faults are analogous to Gulf Coast type "growth faults," which are restricted to the unconsolidated sediment pile (Koinm and Dickey, 1967); however, well and seismic data clearly demonstrate that they break continental crust not previously broken, and they offset the entire section of passive margin strata (Houseknecht, 1986). These normal faults are therefore fundamental tectonic features related to convergent tectonism, and the

expansion ("growth") of Atokan strata across them resulted from sediment accumulation during tectonically induced faulting.

Houseknecht (1986) documented that displacements measured at the level of the Spiro sandstone (base of Atoka Formation) range from less than 500 to more than 2000 m (1500-7000 ft). He also documented the geometry of these syndepositional normal faults and demonstrated that they decrease in age northward and result in a step-like onlap lithofacies sequence in the Atoka Formation. Surprisingly, there is no evidence of erosion of the Spiro sandstone or overlying strata on upthrown sides of faults. Throughout the basin, overlying the Spiro sandstone, a 100- to 200-m thick, dark-gray shale is apparently the stratal equivalent of expanded sections downthrown to major faults.

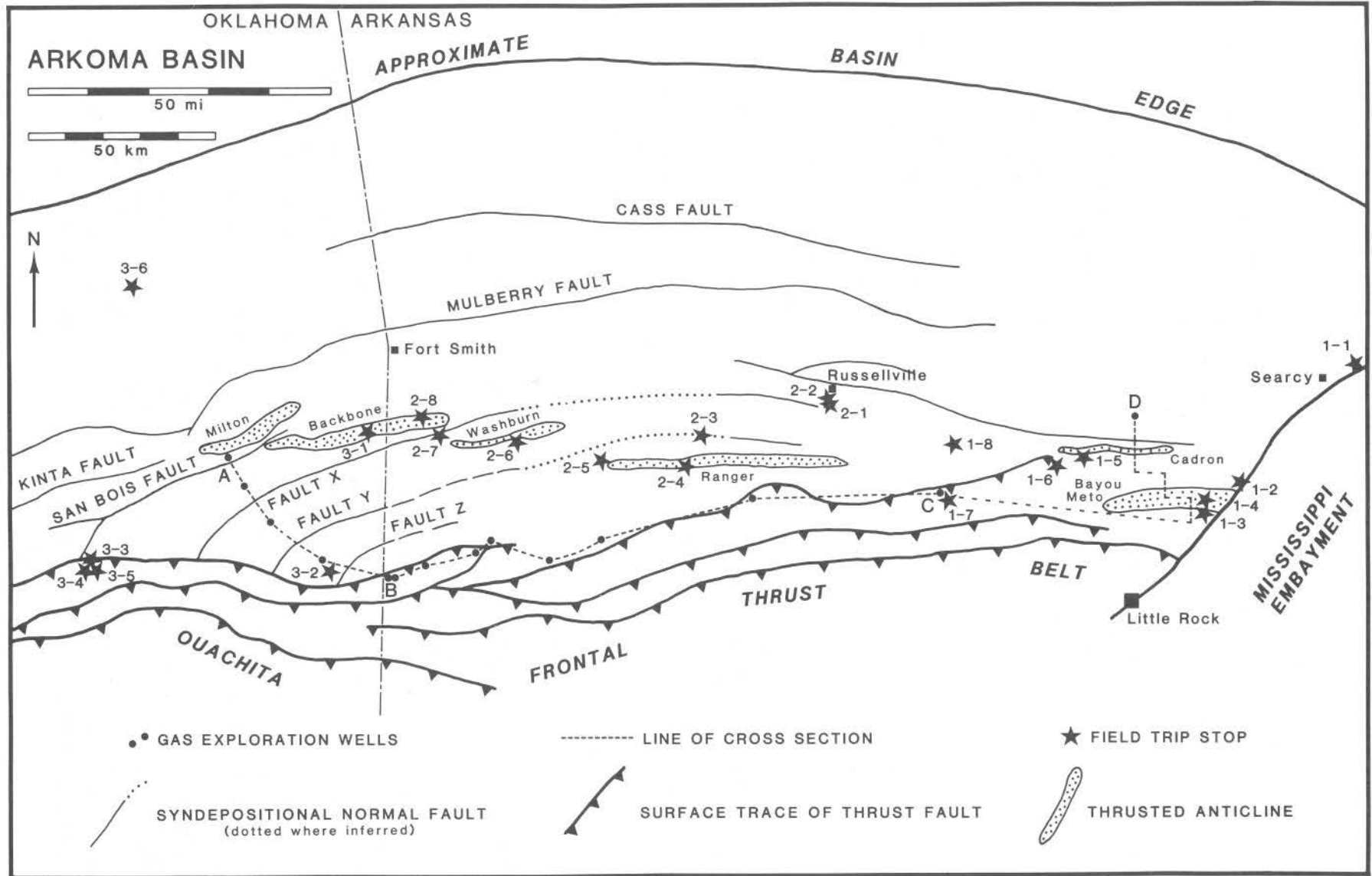


Figure 6 — Base map of Arkoma basin showing known syndepositional normal faults, major thrust anticlines exposed at surface, lines of cross section, and field trip stops.

In contrast to the Atoka section, neither older strata nor overlying Desmoinesian strata show evidence of abrupt thickening across normal faults. The basal Atokan Spiro sandstone displays nearly constant thickness along numerous north-south cross sections that traverse the syndepositional normal faults. The Desmoinesian section (including the Hartshorne Formation overlying the Atoka) gradually thickens north to south and thereby suggests flexural subsidence induced by foreland thrust loading of the basin's southern margin (Houseknecht, 1986).

In summary, syndepositional normal faults fundamentally control the distribution and thickness of Atoka strata throughout the basin. Neither the basal Atokan Spiro sandstone nor the basal Desmoinesian Hartshorne Sandstone shows evidence of syndepositional fault movement, facts that limit the duration of normal faulting to less time than the Atokan age (approximately 5 million years). Active normal faulting migrated northward and resulted in a step-like onlap stratigraphic sequence in the Atoka Formation. Northward advance of the Ouachita orogenic front undoubtedly caused this northward migration of faulting.

INFLUENCE ON FACIES DISTRIBUTION

Figures 7, 8, and 9, stratigraphic cross sections constructed from wire-line logs and measured outcrop sections (see table 1), illustrate the active influence that syndepositional normal faults exerted on distribution of depositional facies in the Atoka Formation. Cross section A-B (fig. 7) is more detailed than the other two, because it is in a part of the basin where subsurface control is more abundant and where more precise correlations are possible in the Atokan section (cross section A-B is the same line of section as cross section B-B' of Houseknecht, 1986).

Cross section A-B is schematic in that it shows no structural dip on any strata; nevertheless, it illustrates stratigraphic and facies implications of four syndepositional normal faults (San Bois, X, Y, and Z). Southward along the line of section, the Atoka Formation thickens from less than 1,200 to more than 5,500 m (estimated by projecting the Hartshorne Sandstone to well 5, fig. 7); displacement on syndepositional normal faults accounts for this

thickness increase. Displacements at the horizon of the Spiro are as follows: San Bois, 1,300 m; fault X, 500 m; fault Y, 2,100 m; no displacement can be calculated for fault Z because the Spiro has not been penetrated on that structural block.

The influence of syndepositional faulting on depositional facies is clearly illustrated in figure 7. The thick pile of submarine fan facies deposited on the bathymetric floor of the basin are present only south of fault Y. There is no evidence of erosion on the upthrown side of fault Y, yet that fault obviously acted as a bathymetric barrier to deposition of unconfined turbidites. This suggests that a slope break corresponded to the seafloor trace of fault Y during deposition of the lower part of the Atoka section; north of fault Y the basin was a slope on which hemipelagic mud was deposited, whereas south of fault Y the basin was a relatively level floor on which unconfined turbidites were deposited.

Following deposition of the thick submarine fan facies on the basin floor, three different syndepositional normal faults (fault Y, fault X, and the San Bois fault) all acted as northern limits of slope mud

| Well # | Company | Lease | Location | TD (feet) |
|--------|---------------------------------|--------------|------------------|-----------|
| 1 | Pan Am | Birkel | 29-8N-23E | 5,953 |
| 2 | Sun | Reed | 23-7N-23E | 12,183 |
| 3 | Humble | Thompson | 20-6N-24E | 14,607 |
| 4 | Hunt | Pebsworth | 23-5N-25E | 17,496 |
| 5 | Arkla | Edwards "B" | 6-2N-32W | 15,060 |
| 6 | Hunt | U.S.A. 1-3 | 3-2N-32W | 12,873 |
| 7 | Jones & Pellow | U.S.A. | 28-3N-31W | 9,583 |
| 8 | Arkla/Santa Fe | Jones | 14-3N-30W | 12,350 |
| 9 | Arkla | Fronterhouse | 7-3N-29W | 8,604 |
| 10 | El Paso | Cheesman | 22-3N-28W | 11,670 |
| 11 | Hunt | U.S.A. 1-1 | 1-3N-27W | 17,033 |
| 12 | Arco | Peeler Gap | 32-5N-22W | 13,914 |
| 13 | Santa Fe/Arco | Deltic | 32-5N-17W | 11,800 |
| 14 | <i>outcrop measured section</i> | | 4 ---> 29-4N-10W | |
| 15 | <i>outcrop measured section</i> | | 33---> 20-5N-11W | |
| 16 | <i>outcrop measured section</i> | | 36---> 25-6N-14W | |
| 17 | Lone Star | Moore | 22-7N-12W | 10,476 |

Table 1. List of wells and outcrop measured sections used in constructing stratigraphic cross sections. Section A-B (fig. 7) comprises wells 1-5; section B-C (fig. 9) comprises wells 5-13; and section C-D (fig. 8) comprises wells and measured sections 13-17.

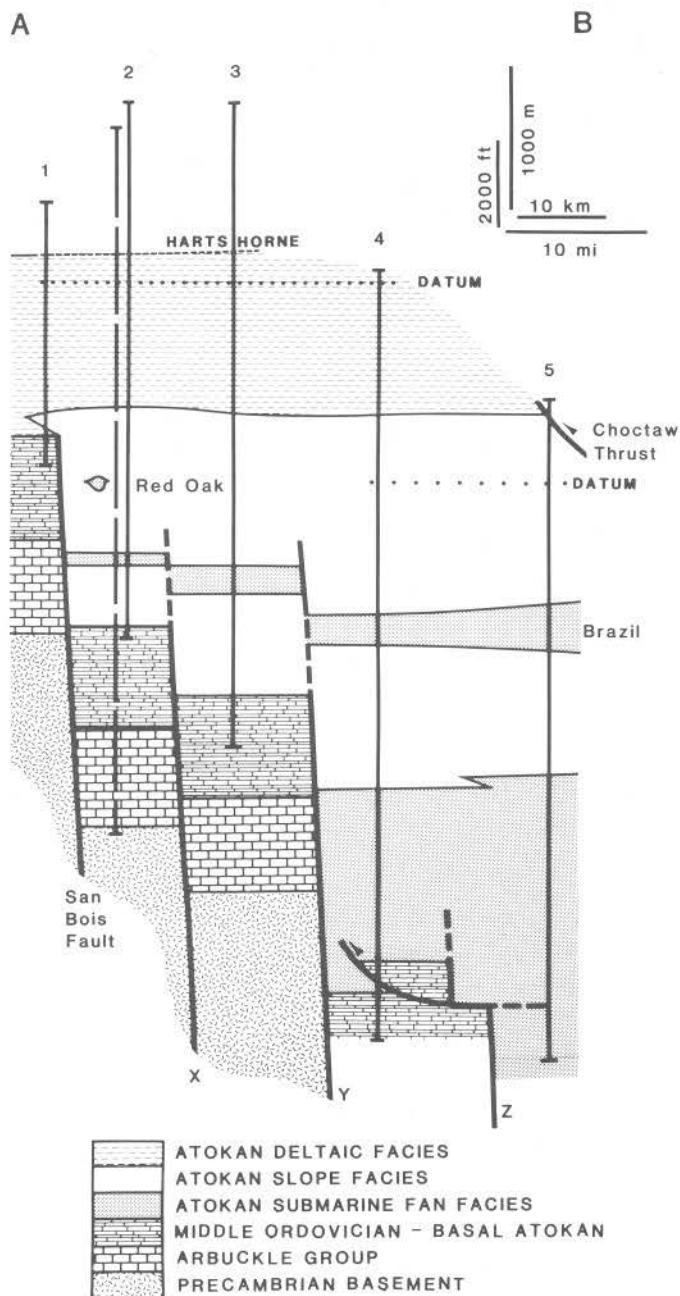


Figure 7 — Stratigraphic cross section A-B constructed from wire-line logs from five wells; well locations are indicated by vertical lines. Dashed vertical line beside well #2 is projected into line of section to provide control on sub-Atoka formations and Precambrian basement.

deposition, as active faulting migrated northward (fig. 7). During this time, a widespread section of submarine fan facies was also deposited (Brazil sandstone of Oklahoma subsurface terminology, fig. 7). The Brazil pinches out against the San Bois fault and shows significant thickness increase across fault X (fig. 7), indicating that both faults were active during Brazil deposition. In contrast, the Brazil displays little or no thickness increase across fault Y (fig. 7), indicating that movement on fault Y had ceased by the time the Brazil was deposited. Tectonically localized, slope channel sands were also deposited immediately downthrown to some of these syndepositional normal faults during deposition of the thick slope muds. One such example is the Red Oak sandstone (localized downthrown to the San Bois fault, fig. 7), whose depositional characteristics suggest deposition in fault-controlled "sags" that obliquely traversed the muddy slope (Houseknecht, 1986).

As the basin filled with detrital sediment, deltaic environments prograded over the slope muds. The upper 700 to 11,000 m of the Atoka Formation comprise such deltaic facies, which display no obvious expansion across syndepositional faults (fig. 7). These upper Atoka deltaic facies grade upward into coal-bearing deltaic and fluvial facies of the Desmoinesian Series (e.g., the Hartshorne Formation).

In summarizing the information illustrated in figure 7, the syndepositional faults thus far documented in the Arkoma basin were active during a limited interval of Atokan time. In the area of the field trip, faulting caused abrupt water-depth increase and breakdown of the pre-existing shelf-slope-rise geometry. The basin floor rapidly evolved into a site of submarine fan deposition and the area of most active faulting accumulated a thick mantle of slope muds. Some of the more basinward syndepositional normal faults acted as subtle bathymetric and/or slope breaks and thereby formed rather abrupt barriers to deposition of unconfined turbidites on the bathymetric basin floor. Other, more cratonward syndepositional normal faults (e.g., San Bois), acted as bathymetric barriers to unconfined turbidite deposition at certain times (e.g., deposition of the Brazil sandstone) and localized turbidite deposition into slope channel "sags" at other times (e.g., deposition of the Red Oak sandstone).

Figure 8 is a similar cross section across the Cadron and Bayo Meto anticlines, where we will spend most of the first day of the trip. Even though this figure is more generalized than figure 7, it nevertheless illustrates that a syndepositional normal fault beneath Cadron anticline acted as the northern limit of submarine fan and younger slope facies during Atokan deposition in the eastern part of the basin. Displacement across the Cadron normal fault is estimated to be at least 2,500 m.

Figure 9, a cross section constructed from widely spaced wells that penetrate the Atoka Formation in the deepest part of the basin, is somewhat distorted relative to figures 7 and 8, because the top of the submarine fan facies is used as a stratigraphic datum, whereas deltaic facies in the upper part of the Atoka Formation are used as stratigraphic data

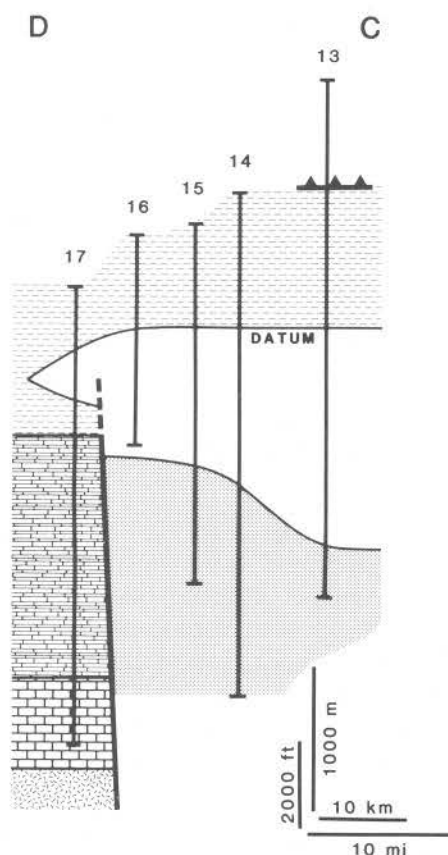


Figure 8 — Stratigraphic cross section D-C constructed from wire-line logs and measured outcrop sections. Top of Precambrian basement was estimated from seismic section. Symbols same as those on figure 7.

in the other two cross sections. Figure 9 illustrates the longitudinal continuity of submarine fan (basin floor) and muddy slope facies across the basin; moreover, it provides tentative documentation of the longitudinal facies relationships that have been inferred within the Atoka Formation (fig. 10). West to east, the Brazil submarine fan facies pinch out up depositional dip into muddy slope facies, which in turn grade into sandy deltaic facies at the eastern end of the cross section (fig. 9).

SANDSTONE COMPOSITION AND DEPOSITIONAL FACIES

A primary objective of the field trip is to allow participants to examine the sedimentary facies suite that records the transition from passive margin to foreland basin sedimentation. The planned field trip stops are summarized in table 2. The petrofacies and depositional facies we will see on the trip are outlined and briefly described below.

PASSIVE MARGIN STRATA: MORROWAN AND BASAL ATOKAN SANDSTONES

Late Cambrian through earliest Atokan strata in the Arkoma basin are mostly carbonates with subordinate shale and sandstone, deposited on a tectonically stable shelf. Morrowan and earliest Atokan sandstones examined on this trip represent the final phase of passive margin sedimentation before tectonic breakdown of the shelf.

Morrowan and earliest Atokan sandstones are fine- to medium-grained quartz arenites that contain small amounts of K-feldspar and chert. Paleocurrent data indicate generally southward sediment dispersal. These compositional characteristics and paleocurrent trends suggest derivation of sand from older sedimentary strata and perhaps basement sources on the craton. Facies characteristics suggest deposition in deltaic and associated shallow marine environments. In addition, fluvial facies have been documented in Morrowan sandstones north of the basin, along the southern rim of the Ozark dome (Zachry, 1979).

In the easternmost portion of the Arkoma basin, Morrowan sandstones (field trip stop 1-1) are probably distal equivalents of thick deltaic and fluvial facies exposed along the southern rim of the Illinois basin, which was open-ended to the south until post-

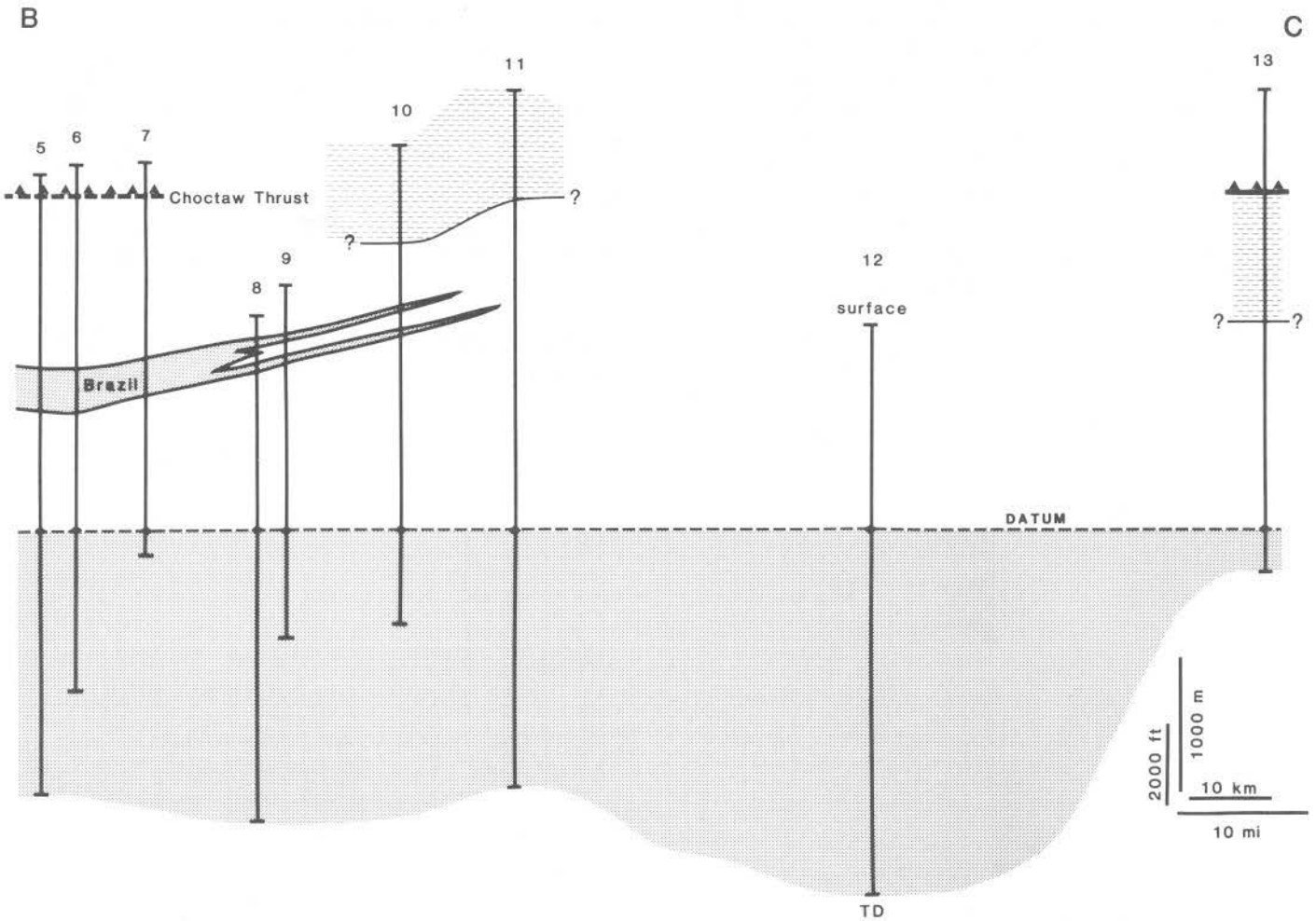


Figure 9 — Stratigraphic cross section B-C constructed from wire-line logs in the structurally deepest part of the Arkoma basin. Note that datum is top of submarine fan facies; this may result in distortion of stratigraphic relationships up section. Symbols same as those on figure 7.

Atokan uplift of the Pascola "arch" (fig. 1). Morrowan sediment was transported southward through the Illinois basin, through the Mississippi embayment, into the deep Ouachita basin. Sandstones exposed at stop 1-1 are typical of Morrowan strata in the easternmost portion of the basin; they show a coarsening-upward deltaic facies sequence, southward dipping cross-bed sets, and a quartz-rich composition.

Farther west in the basin, Morrowan and basal Atokan sandstones show more evidence of marine influence. Quartz-rich sand, apparently eroded from older Paleozoic strata on the Ozark dome and Nemaha ridge, was transported to the basin by fluvial systems and deposited along a tidally swept coastline

on the shelf of the passive margin (Houseknecht, 1986). The Spiro sandstone exposed at stop 3-3 is a typical example of a fossiliferous, cross-bedded quartz arenite that was deposited in a delta front or shallow marine environment. Stop 3-6 illustrates Morrowan marine strata, including sandstones, shales, and carbonates deposited in clear-water shelf environments.

FORELAND BASIN STRATA: ATOKA FORMATION

Tectonic breakdown of the passive margin shelf was accompanied by an abrupt change in sediment dispersal patterns and in framework grain compo-

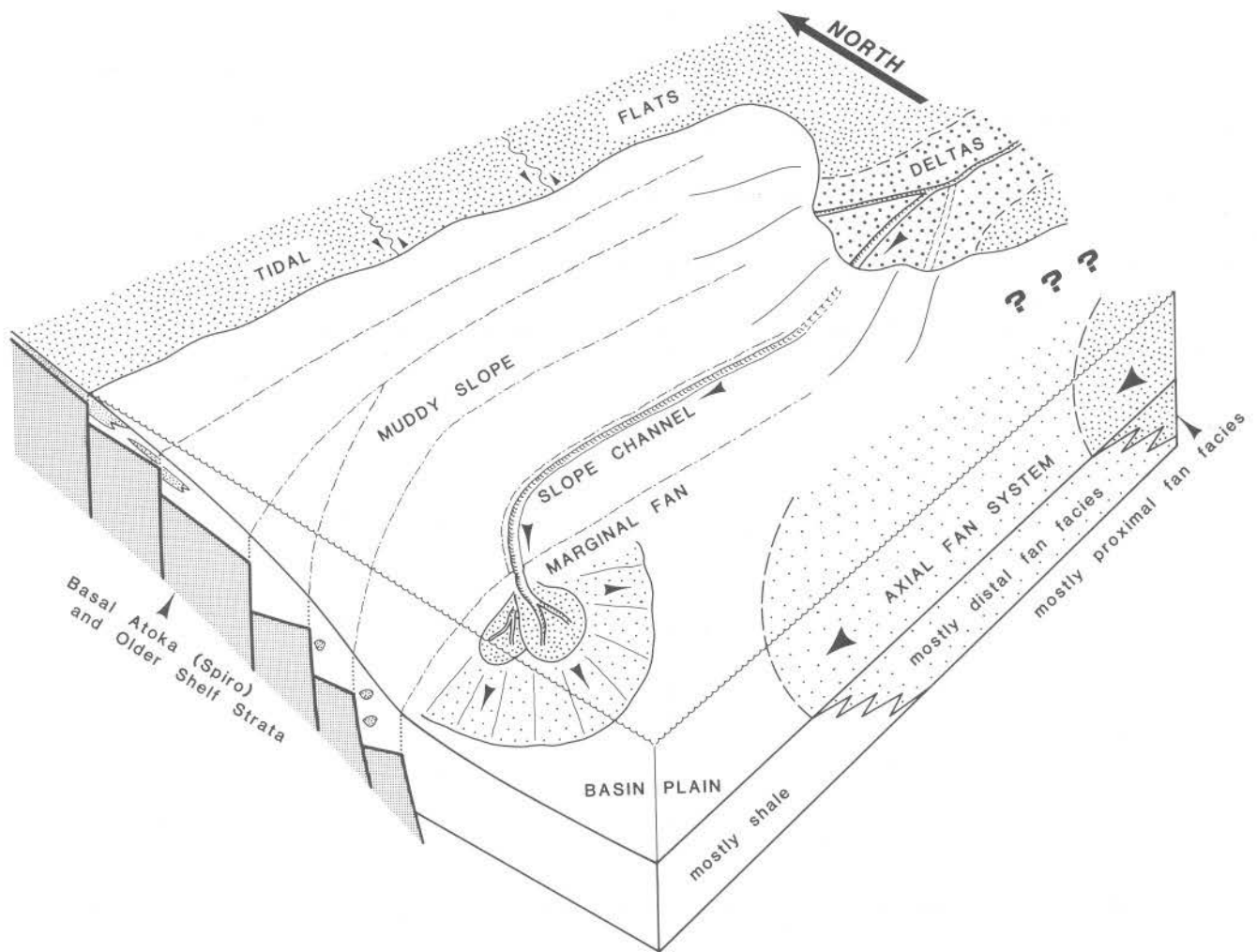


Figure 10 — Reconstruction of depositional system in which post-Spiro-Atokan strata were deposited. Dash-dot lines represent sea floor traces of syndepositional normal faults. The spatial relationship between deltaic facies and axial fan facies in the eastern portion of the basin is not well documented (as denoted by question marks), and should be considered schematic (Houseknecht, 1986).

sition of sand delivered to the Arkoma basin. Paleocurrent data from the Atoka Formation (excluding Spiro sandstone) reveal a mostly westward sediment dispersal in the basin proper. Atoka Formation sandstones (excluding the Spiro) are mostly fine-grained lithic arenites that contain metamorphic, volcanic, and sedimentary lithic fragments, and plagioclase grains. Regional paleocurrent patterns and sandstone compositions indicate that most of the Atoka Formation sand was derived from the uplifted Ouachita orogenic belt to the east (southwest of the Black Warrior basin, fig. 1), with some contribution from deltaic sediment dispersal systems in the Illinois basin. This sand entered the

eastern portion of the basin and was transported longitudinally westward to depositional sites (fig. 10). Throughout the Atokan, a relatively small amount of quartzose sand continued to enter the basin from the north; most of it was deposited near the northern edge of the basin.

As illustrated in figure 10, the Atoka Formation (for the sake of convenience, this discussion excludes the Spiro and Cecil-Spiro sandstones from the Atoka Formation) shows complex facies relationships throughout the Arkoma basin. The following sections briefly summarize the main characteristics of these facies.

| Morrowan | Atokan | | | Desmoinesian |
|------------------------|---------------------------|--------------|---|-----------------------|
| Passive Margin | Foreland Basin | | | |
| | <i>Normal Fault Phase</i> | |  | <i>Flexural Phase</i> |
| Marine Shelf - Deltaic | Submarine Fan | Marine Slope | Deltaic | Deltaic |
| 1-1 | 1-4
1-7 | | 1-2
1-3
1-5
1-6
1-8 (opt) | |
| | | 2-4 | 2-5
2-6
2-8 | 2-1
2-2
2-7 |
| 3-3
3-6 | 3-4
3-5 | 3-4
3-5 | 3-1
3-2 | 3-2 |

Locations:

- | | | |
|--------------------------------|------------------------------|---|
| 1-1 Rte. 67, 32-8N-6W | 2-1 Rte. 7, 20-7N-20W | 3-1 Rte. 112, 31-9N-27E |
| 1-2 Rte. 67, 27-5N-9W | 2-2 quarry, 19-7N-20W | 3-2 Rte. 59, 31-5N-26E |
| 1-3 quarry, 21-4N-10W | 2-3 Magazine Mtn., 24-6N-25W | 3-3 Wilburton golf course, 21 & 22-5N-19E |
| 1-4 Rte. 5, 3 & 4-4N-10W | 2-4 Blue Mtn. Dam, 15-5N-25W | 3-4 Rte. 2, 29-5N-19E |
| 1-5 I-40, 35 & 36-6N-14W | 2-5 Rte. 109, 6-5N-26W | 3-5 drill pad, 26-5N-19E |
| 1-6 Toad Suck L & D, 18-5N-14W | 2-6 Rte. 60, 35-6N-29W | 3-6 Webbers Falls L & D, 33-13N-20E |
| 1-7 Rte. 9, 34-5N-17W | 2-7 Rte. 71, 22-6N-31W | |
| 1-8 Rte. 9, 16 & 20-6N-16W | 2-8 Rte. 71, 5-6N-31W | |

Table 2. Field trip stops listed according to age of the strata, the phase of basin evolution represented by the strata, and the gross depositional environment recorded by the strata. Approximate outcrop locations are listed at the bottom; the first two days' stops are located in Arkansas, while the third day's stops are in Oklahoma.

DELTAIC AND ASSOCIATED FACIES

The upper 700 to 1,000 m of the Atoka Formation comprises shallow marine, deltaic, and tidal flat facies. In Arkansas, deltaic facies predominate and will be the subject of several field trip stops (table 2). In most deltaic sequences, marine shales grade upward rather abruptly into sand-rich delta front subfacies, which display an abundance of ripple-scale crossbedding and mud drapes. Such subfacies are locally interbedded with trough cross-bed sets. Together, these sedimentary structures indicate interacting fluvial and marine processes at distributary channel mouths. Delta-front subfacies are typically overlain by distributary channel deposits, which show conspicuous trough crossbedding and horizontal bedding. In outcrops where paleocurrent data can be collected from distributary channel subfacies, westward to southwestward paleoflow is indicated. Significantly, the oldest deltaic facies in the Atoka Formation show evidence of marine (tidal) domination. An up-section gradation to fluvial domination in deltaic facies at the top of the Atoka probably resulted from the basin becoming more restricted as it was tectonically closed during the Atokan.

The northern limit of marine sedimentation in the Oklahoma portion of the basin is indicated by the presence of tidal flat shoreline facies (fig. 10), whose southernmost extent occurs in the subsurface just south of the Milton and Backbone anticlines (fig. 6). Marine shales grade upward by increasing number and thickness of sandstone beds into sand-dominated tidal flat facies; the entire sequence shows a rich and diverse, shallow marine trace fossil assemblage (Chamberlain, 1978). The tidal flat facies comprise fining upward sequences, in which sand-flat, mixed-flat, and mud-flat subfacies are recognized. A well-developed vertical sequence through such progradational tidal-flat shoreline facies is exposed at stop 3-1.

Slope Facies

In that part of the Arkoma basin where the section thickens significantly across syndepositional faults, the Atoka Formation comprises dark gray shale, which is unfossiliferous except for macerated and obviously transported plant debris. Subsurface data indicate that despite significant syndepositional

displacement along many normal faults, numerous widespread key beds show continuity across the faults and there is absolutely no evidence of erosional truncation of strata upthrown to the faults (fig. 7). It is also apparent that these mostly pelitic facies form a transition from tidal flat and deltaic facies in the north and east to deep marine facies in the south and west. Such characteristics suggest deposition as a mantle of slope muds over the area of most active faulting.

Because of extensive weathering, slope facies are not well exposed in the Arkoma basin or Ouachita frontal thrust belt. Field trip stop 2-4 is the best example of probable slope facies in the region. Silty shales displaying rotational slump structures and local bioturbation are well exposed along the spillway of Blue Mountain Dam. These silty shales are overlain by both channelized and unconfined turbidites of a marginal submarine fan (see next section).

Submarine Fan Facies

Numerous workers have published details of submarine fan facies deposited on the deep basin floor and now exposed in the Ouachita frontal thrust belt. These are illustrated schematically and labeled "axial fan system" in figure 10. However, smaller submarine fan sequences were also apparently deposited at the toe of the slope as distal facies equivalents of slope channels; these are labeled "marginal fan" in figure 10. In outcrops along the frontal thrust belt, these two types of submarine fan facies can be distinguished in three ways. First, the marginal fan facies are composed of "cleaner" sandstones than the axial fan facies. Petrographic analysis reveals that the framework grain compositions of sandstones in the two facies are identical, but samples of the axial fan system contain significantly more matrix and are more poorly sorted than samples of the marginal fan system. Secondly, deposits associated with the axial fan system invariably show westward directed paleocurrent indicators, whereas marginal fan facies display southward to southwestward indicators. Thirdly, the marginal fan deposits display internal facies architecture that suggests north-to-south progradation. For example, channelized proximal lobe facies grade both westward and eastward along the strike of the frontal thrust belt into more distal lobe facies

characterized by beds deposited by unconfined sediment gravity flows. Dimensions of such lateral facies sequences are typically 14 to 25 km, suggesting the original size of the marginal fans. As indicated in figure 10, abundant evidence for interfingering of marginal and axial fan facies suggests that the two systems evolved simultaneously, but were supplied by different sediment dispersal systems. An example of such interfingering will be observed at stop 3-5.

Proximal facies of the axial fan system will be observed at stops 1-4 and 1-7, and distal facies of the axial fan system will be observed at stops 3-4 and 3-5. Examples of marginal fan lobes will be observed at stops 2-3, 2-4, and 3-5.

FORELAND BASIN STRATA: HARTSHORNE FORMATION

The basal Desmoinesian Hartshorne Sandstone conformably overlies the Atoka Formation and represents a continuation of deltaic depositional conditions established during the late Atokan. The Hartshorne comprises a fluvial dominated deltaic facies assemblage, described by Houseknecht et al. (1983) and Houseknecht (1988). It was deposited during the flexural subsidence phase of basin development and represents the lowest of several coal-bearing deltaic sequences in the Desmoinesian section. Hartshorne facies will be observed at stops 2-1, 2-2, 2-7, and 3-2 as a basis for comparison with Atoka facies.

REFERENCES

- Chamberlain, C.K., 1978, Trace fossils and paleoecology of the Ouachita geosyncline: Society of Economic Paleontologists and Mineralogists Guidebook, 68 p.
- Dickinson, W.R., 1974, Plate tectonics and sedimentation, *in* Dickinson, W.R., ed., *Tectonics and Sedimentation: Society of Economic Paleontologists and Mineralogists, Special Publication 22*, p. 1-27.
- _____, 1976, Plate tectonics and hydrocarbon accumulations: American Association of Petroleum Geologists, Course Notes No. 1, 62 p.
- Flawn, P.T., Goldstein, A., Jr., King, P.B., and Weaver, C.E., 1961, The Ouachita System: Bureau of Economic Geologists, University of Texas, Publication 6120, 401 p.
- Graham, S.A., Dickinson, W.R., and Ingersoll, R.V., 1975, Himalayan-Bengal model for flysch dispersal in the Appalachian-Ouachita system: *Geological Society of America Bulletin*, v. 86, p. 273-286.
- Houseknecht, D.W., 1986, Evolution from passive margin to foreland basin: the Atoka Formation of the Arkoma basin, south-central U.S.A., *in* Allen, P.A., and Homewood, P., eds., *Foreland Basins: International Association of Sedimentologists, Special Publication 8*, p. 327-345.
- _____, 1987, The Atoka Formation of the Arkoma basin: Tectonics, sedimentology, thermal maturity, sandstone petrology: *Tulsa Geological Society Short Course Notes*, 72 p.
- _____, 1988, Deltaic facies of the Hartshorne Sandstone in the Arkoma Basin, Arkansas-Oklahoma border, *in* Hayward, O.T., ed., *Geological Society of America, Centennial Field Guide*, v. 4, p. 91-92.
- _____, and Underwood, M.B., 1988, Depositional and deformational characteristics of the Atoka Formation, Arkoma basin, and Ouachita frontal thrust belt, Oklahoma, *in* Hayward, O.T., ed., *Geological Society of America, Centennial Field Guide*, v. 4, p. 145-148.
- Houseknecht, D.W., Zaengle, J.F., Steyaert, D.J., Matteo, A.P., Jr., and Kuhn, M.A., 1983, Facies and depositional environments of the Desmoinesian Hartshorne Sandstone, Arkoma basin, *in* Houseknecht, D.W., ed., *Tectonic-sedimentary evolution of the Arkoma basin: Society of Economic Paleontologists and Mineralogists Midcontinent Section*, v. 1, p. 53-82.
- Jordan, T.E., 1981, Thrust loads and foreland basin evolution, Cretaceous, western United States: *American Association of Petroleum Geologist*, v. 65, p. 2506-2520.

- Koinm, D.N., and Dickey, P.A., 1967, Growth faulting in McAlester basin of Oklahoma: American Association of Petroleum Geologists Bulletin, v. 51, p. 710-718.
- Leander, M.H., and Legg, T.E., 1988, Potential for subthrust gas fields: Results of recent deep drilling in the Ouachitas (abs.): American Association of Petroleum Geologists Bulletin, v. 72, p. 211.
- Lillie, R.J., Nelson, K.D., deVoogd, B., Brewer, J.A., Oliver, J.E., Brown, L.D., Kaufman, S., and Viele, G.W., 1983, Crustal structure of Ouachita Mountains, Arkansas: A model based on integration of COCORP reflection profiles and regional geophysical data: American Association of Petroleum Geologists Bulletin, v. 67, p. 907-931.
- Morris, R.C., 1974, Sedimentary and tectonic history of the Ouachita Mountains, *in* Dickinson, W.R., ed., Tectonics and sedimentation: Society of Economic Paleontologists and Mineralogists, Special Publication 22, p. 120-142.
- Nicholas, R.L., and Waddell, D.E., 1982, New Paleozoic subsurface data from the north-central Gulf Coast (abs): Geological Society of America, Abstracts with Programs, v. 14, p. 576.
- Thomas, W.A., 1985, The Appalachian-Ouachita connection: Paleozoic orogenic belt at the southern margin of North America: Annual Review of Earth and Planetary Sciences, v. 13, p. 175-199.
- Underwood, M.B., and Viele, G.W., 1985, Early Pennsylvanian tectonic transition within the frontal Ouachitas of Arkansas (abs.): Geological Society of America, Abstracts with Programs, v. 17, p. 195.
- Zachry, D.L., 1979, Early Pennsylvanian braided stream sedimentation, northwest Arkansas, *in* Hyne, N.J., ed., Pennsylvanian sandstones of the Mid-Continent: Tulsa Geological Society, Special Publication 1, p. 269-281.

Field Trip No. 16
(Guidebook Published Separately)

**QUATERNARY LOESS AND
GLACIAL RECORD OF
SOUTHWESTERN ILLINOIS**

Leon R. Follmer and E.D. McKay, III
Illinois State Geological Survey
615 East Peabody Drive
Champaign, Illinois 61820

and

Edwin R. Hajic
Department of Geology
University of Illinois
Urbana, Illinois 61801

FIELD TRIP SUMMARY

During this Quaternary field trip we will visit outcrops and exposures that are best for understanding geologic processes and stratigraphic relationships. We will visit five exposures that best show the current relationships of loesses, tills, and paleosols in southwestern Illinois. Several key exposures have recently been lost to construction; others have been lost for a variety of reasons, including mass wasting and vegetation cover.

The East St. Louis area has been an important region in past studies of loess formations and their relation to Illinoian and older tills. The most significant locality was the Pleasant Grove School Section where three loess formations (overlying an Illinoian till) were described including the controversial mid-Wisconsinan Roxana Silt (Willman and Frye, 1970). This section was designated the type section for the Roxana and served as a benchmark for about 20 years until it was mined away for road construction in 1988.

As new studies were completed in the region a more detailed stratigraphic picture evolved (McKay, 1979; Graham et al., 1986). Older loesses have been identified and problems with Illinoian interpretations arose, such as number and distribution of till members. This trip will emphasize the examination of stratigraphic relationships used to interpret the loess record in Illinois, and to discuss current work on the evolution of the lower Illinois River Valley.

STRATIGRAPHY OF THE FIELD TRIP STOPS LISTED FROM THE TOP DOWN

Stop 1. Powdermill Creek borrow pit. Peoria Loess,

Roxana Silt, Sangamon Geosol (soil) in Illinoian till, and Chinatown silt.

Stop 2. Maryville stream cuts. Peoria Loess, Roxana Silt, Sangamon in Berry Clay/Teneriffe Silt/till, Chinatown silt with weak soil, Maryville silt with strong soil ("Yarmouth"), pre-Illinoian till, and loess.

Stop 3. Paddock Creek cut. Peoria Loess, Roxana Silt, Sangamon Geosol in Illinoian till over a strong soil developed in pre-Illinoian till.

Stop 4. Williams Hollow borrow pit. Peoria Loess showing zonation, including a clay bed, over a Farmdale Geosol developed in Roxana Silt.

Stop 5. Pancake Hollow stream cut. Peoria, Roxana, Sangamon in Loveland Loess, weathered gravel over a strongly weathered Chinatown (lower Loveland?), and a sequence of weathered loesses and alluvium.

Limited results from radiocarbon, thermoluminescence, amino acid ratios, and magnetic susceptibility measurements have given promising results for correlations, but the details are not yet clear. The lithostratigraphic record of the Wisconsinan has three parts: early — poor sediment record (cool climate soil formation), middle — Roxana Silt, and late — Peoria Loess. The record of the Illinoian is not clear; it may have up to four lithostratigraphic parts, and apparently spans two glacial stages. The pre-Illinoian appears to be middle Pleistocene. The Illinois River Valley has late Wisconsinan and Holocene terraces and stratigraphic features that record major glacial events in the upper Illinois and Mississippi River basins.

REFERENCES

Graham, et al., 1986, Quaternary records of SW Illinois and adjacent Missouri: preprint for 1986 AMQUA Trip 4; in preparation, Illinois State Geological Survey Guidebook 23.

McKay, E.D., 1979, Stratigraphy of Wisconsinan and

older loesses in SW Illinois: Illinois State Geological Survey Guidebook 14.

Willman, H.B., and Frye, J.C., 1970, Pleistocene stratigraphy of Illinois: Illinois State Geological Survey Bulletin 94, 204 p.

Note: The 1989 GSA Field Trips 1 and 16 draw most of their information from Graham et al., 1986, and McKay, 1979. A guidebook that summarized Trip 1 (Archaeological geology and geomorphology in the central Mississippi-lower Illinois Valley region, Illinois and Missouri) and Trip 16 will be prepared and distributed by the Illinois State Geological Survey, 615 East Peabody Drive, Champaign, Illinois 61820.

Field Trip No. 17

**CYCLIC STRATA OF THE
LATE PENNSYLVANIAN OUTLIER,
EAST-CENTRAL ILLINOIS**

C. Pius Weibel

Illinois State Geological Survey
615 East Peabody Drive
Champaign, Illinois 61820

and

R.L. Langenheim, Jr. and D.A. Willard

University of Illinois
Urbana, Illinois 61801

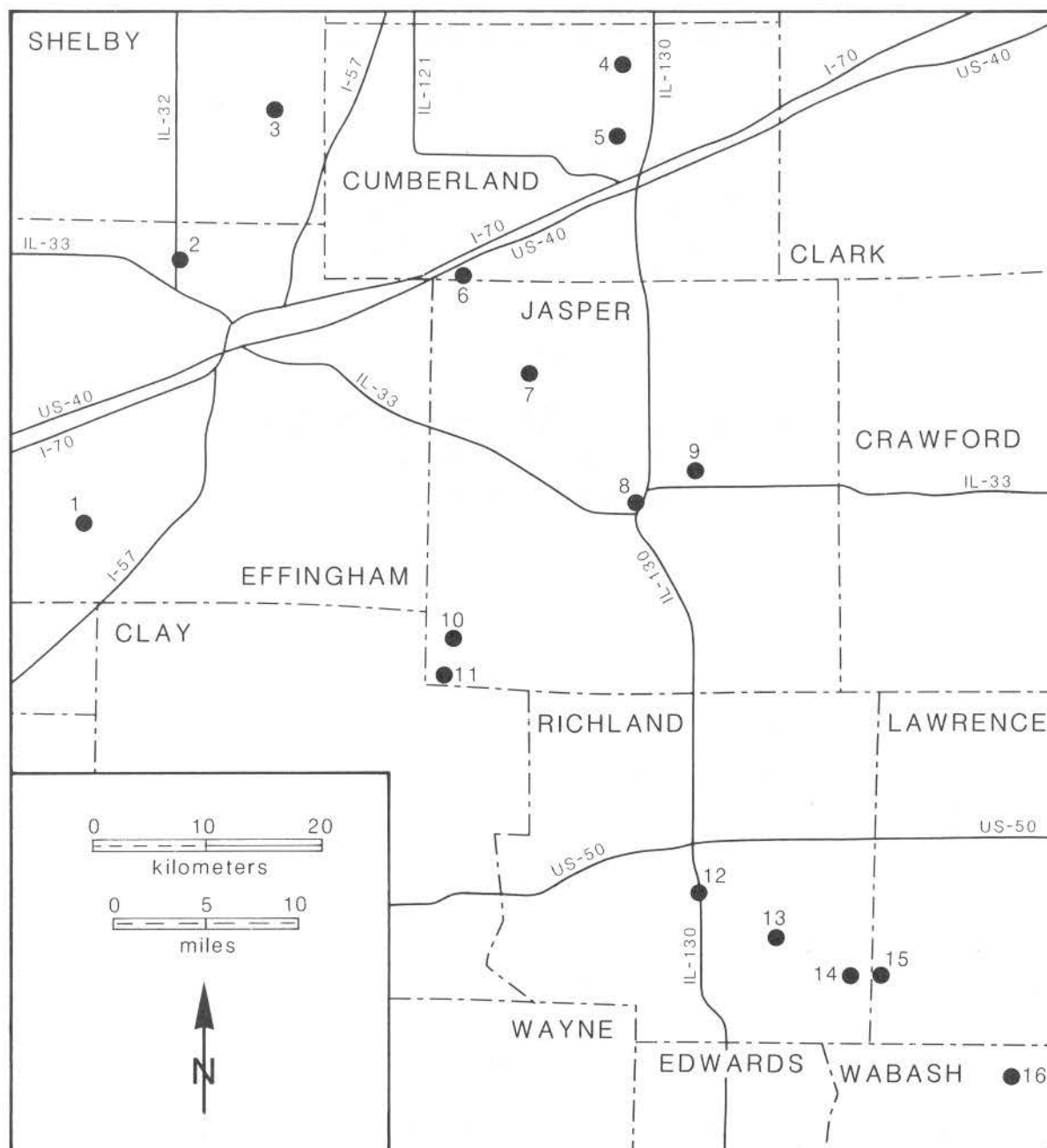


Figure 1 — Index map with field trip stop locations.

INTRODUCTION

Virgilian rocks in east-central Illinois constitute an outlier of intermediate lithology, paleontologic character, depositional environment, and paleogeographic position between nearly wholly terrestrial Appalachian Basin sequences and largely marine midcontinent basin rocks. Although older Pennsylvanian Illinois Basin strata have been extensively studied, the Virgilian sequence is largely neglected. Our purpose on the first field trip to examine these rocks is to discuss (1) current and "proposed" lithostratigraphic classifications, including application of a genetic stratigraphic sequence (modified

cyclothem) as the basis for revising the stratigraphic column, (2) depositional and diagenetic histories, particularly at marine-terrestrial transitions, (3) lithostratigraphic and biostratigraphic correlation with equivalents in the Appalachian Basin, the midcontinent, and north-central Texas, and (4) autocyclic- versus allocyclic-controlling factors that resulted in repeated cycles, including glacial-eustatic sea level changes, PACs, and rhythmic tectonism. Because of limited space, these topics are only partly covered in the guidebook text.

VIRGILIAN STRATIGRAPHY

The field trip region (fig. 1) has little topographic relief and is covered by Pleistocene deposits; exposures are largely restricted to stream-cut banks. We will examine strata from the latest Missourian (?) Friendsville Coal Member to the late Virgilian Woodbury Limestone Member (fig. 2), all currently assigned to the Mattoon Formation of the McLeansboro Group, except the Friendsville Coal (Kosanke et al., 1960).

Worthen (1875) first investigated the geology of the region, but did not recognize the rocks as cyclic deposits. Udden (1912) recognized cyclic deposits in middle Pennsylvanian strata near Peoria and selected underclay/coal surfaces as "subdivision" boundaries. Weller (1930) rejected this boundary, and suggested two alternative boundaries: (1) surfaces that mark the end of peat accumulation and are succeeded by transgressive units, and (2) unconformities beneath sandstones deposited after regression. Weller considered the first boundary unsuitable, because marine strata do not always succeed coals, and selected the second because these unconformities "may be present....in areas not subjected to marine submergence" and "mapping them reveals....features that would otherwise escape notice." Wanless and Weller (1932) later defined a cyclothem, a terrestrial-marine-terrestrial sequence. Newton and Weller (1937) recognized cyclothem and proposed the first stratigraphic column for the field trip region. Subsequent studies, using diverse data, resulted in at least 13 different proposed stratigraphic successions (Weibel, 1986). Wanless

(1956) introduced a cyclothem-based stratigraphic classification of the entire Illinois Pennsylvanian, but Kosanke et al. (1960) rejected it because of cyclothem-sequence variations and difficulty in mapping the basal sandstone. They replaced cyclothem formations with much thicker key-bed-bounded formations, such as the Mattoon Formation, but retained a separate, informal cyclical classification, ostensibly because it was considered "useful in geologic interpretation" (*ibid.*, p. 9). However, the Illinois State Geological Survey (ISGS) ended its use of cyclothem for lithostratigraphic classification or geologic interpretation with that publication.

Weibel (1988) indicated that modified cyclothem are mappable lithostratigraphic units and are therefore potential formational units. The modified cyclothem boundary is at the top of the coal or at the base of the marine portion, delineating a marine-terrestrial sequence. Boundary recognition is greatly simplified because the terrestrial to marine transition is in a relatively thin portion of the sequence and generally is marked by abrupt lithologic change. If the transition is gradational, the boundary is placed at the base of the lowest significant marine unit. Coal and marine units are readily recognizable at the surface and on most geophysical logs. Marine units lack thickness irregularities characteristic of basal sandstones; in addition, basal sandstones typically are not exposed in the Virgilian outcrop area and may be laterally restricted. These sandstones may also be at different stratigraphic positions in the terrestrial portions of cyclothem; therefore, such

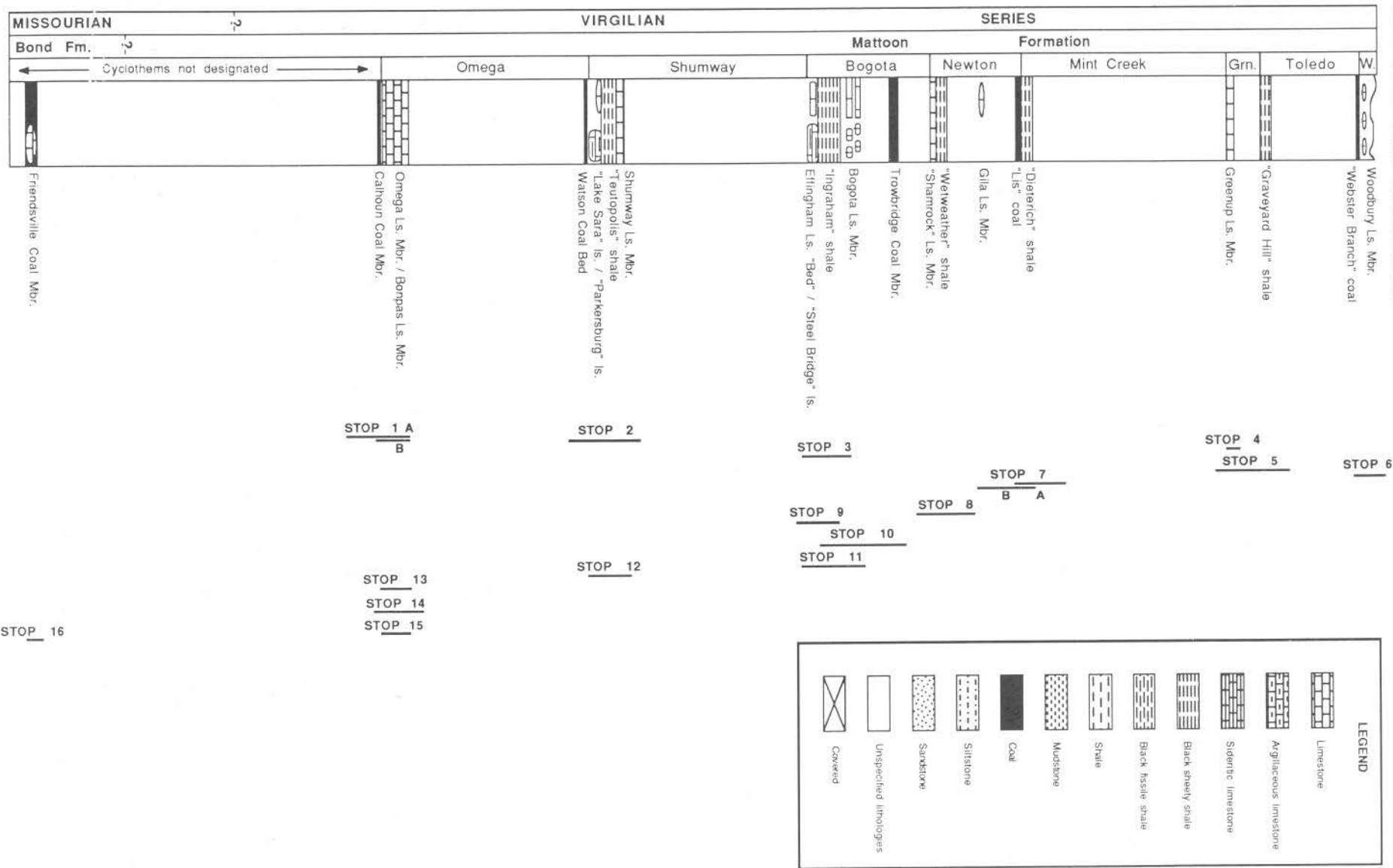


Figure 2 — Generalized stratigraphic column of uppermost Missourian through Virgilian strata of east-central Illinois, with cyclothems as modified herein. Stratigraphic position of exposures viewed at field trip stops are shown. Grn. = Greenup, W. = Woodbury.

sandstones are disqualified as consistent key boundary units. The modified cyclothem boundary used herein is more consistently identified in the Illinois Virgilian and is similar to one of the horizons originally suggested by Weller (1930) when cyclothem were first advanced as formational units.

The modified cyclothem, like Udden's (1912) subdivisions and Wanless and Weller's (1932) original cyclothem, is a genetic-stratigraphic sequence bounded by the surface recording the first marine sediments deposited in the overall marine-terrestrial sequence. This genetic approach has an advantage over the seismic stratigraphic treatment by Vail et al. (1984); their depositional sequences are bounded by unconformities or correlative conformities. Applying their approach to the Virgilian strata would result in radically dissimilar sequences because unconformity positions differ from cyclothem to cyclothem. The genetic sequence is inherently more significant for formational use, because each cyclothem is defined uniformly. Much of the terminology of Vail et al. (1984), however, is applicable; for example, the genetic Virgilian stratigraphic unit is bounded by a transgressive surface, contains a regressive surface, and is a depositional system roughly comprising a transgressive-systems tract, a highstand systems tract, and a lowstand systems tract.

We are not here formally proposing a revised Illinois stratigraphic classification. Weibel (1988) first suggested that the Illinois Basin Virgilian could

be readily classified using both single and groups of modified cyclothem(s) as either formations or as members. Such a classification differs from that of Wanless (1956), because not every individual cyclothem would be considered a single formal lithostratigraphic unit. This field trip provides a format to discuss this approach. Weibel's revisions in the stratigraphic succession are included, but space prevents complete substantiation; thus, all newly named or newly applied units are informal and bracketed by quotations. The stratigraphic column (Weibel, 1988) is based on detailed outcrop examination supported by newly available subsurface data. Unlike previous studies, Weibel's study included examination of Virgilian exposures throughout the region. In most cases, correlations combined methods that resulted in a well-substantiated stratigraphic succession. Local correlation is possible, despite few outcrops, because the marine portion of each cyclothem is typically a distinct lithologic sequence of black fissile shale and/or limestone. The black sheeted shales are distinctive in relative thicknesses and in the presence or absence of large calcareous concretions. Several cyclothem contain distinct marine fossil assemblages. Regional structural trends and physical tracing of cyclothem also were used to determine stratigraphic succession. Subsurface correlations, although not presented here in detail, are based on stratigraphic succession, thicknesses of the black shales and the intervals between them, and correlation with outcrops.

PALEOBOTANY AND PALYNOLOGY

Structurally preserved peat (coal balls) and abundant spores and pollen have been recovered from Illinois Basin upper Pennsylvanian coals. Five Missourian coals and the basal Virgilian coal have coal balls (Phillips et al., 1985); coal-ball sites in the Friendsville and Calhoun Coal Members will be examined on this field trip. Upper Pennsylvanian coals of the Illinois Basin typically are dominated by *Psaronius* tree ferns; seed ferns, primarily *Medullosa*, are subdominant. Sphenopsids, cordaites, and lycopods also occur, but arborescent lycopod taxa differ from those in the middle Pennsylvanian. *Sigillaria* was the only arborescent lycopod in upper Pennsylvanian coals, whereas *Lepidophloios*,

Lepidodendron, *Diaphonodendron*, and *Paralycopodites* also were common in middle Pennsylvanian coals. *Lycospora* is absent in Illinois Basin upper Pennsylvanian coals but is present in contemporaneous coals of Europe and Russia, although less abundant than in the middle Pennsylvanian; this indicates some members of this group persisted through the Stephanian east of the Appalachians (*ibid.*). Upper Pennsylvanian coals also differ from their middle Pennsylvanian counterparts in lateral extent, thickness, and tissue/organ composition. Illinois Basin upper Pennsylvanian coals generally have a maximum thickness of less than 0.91 m (3 ft) and cover a very limited region (Nance and

Treworgy, 1981). Upper Pennsylvanian coals were formed mostly from aerenchymatous (air-chambered) roots and other parenchymatous organs that were much more compactable and easily decayed than middle Pennsylvanian components, mostly periderm (bark) and cortical tissues (Phillips et al., 1985).

Coal-ball and palynological data from these coals give a general picture of some late Pennsylvanian coal-swamp vegetational composition and structure. Coal balls provide excellent overviews of vegetational composition and abundance at particular swamp localities, but they reflect localized conditions.

Spores, however, because of their excellent preservability and wide dispersability, are preserved throughout the coal; therefore, they provide a more regional picture of vegetation and allow analysis of changes in vegetational composition and abundance throughout the coal. Data from the two sources provide more accurate estimates of conditions throughout the swamp than either source alone. The three stops at which paleobotanical investigations were made provide information on community composition and structure and on lateral and vertical variation in late Pennsylvanian coal-swamp plant communities (Willard, 1985).

ROAD LOG

First Day:

- | | | | |
|-------|---|-------|--|
| 0.0 | Altamont exit off I-70. Proceed south. | 34.00 | Private residence. Park and walk north (0.25 mi/400 m) on abandoned road to exposures along Shoal Creek west of condemned bridge. STOP 2. Retrace route back to IL-32. |
| 4.0 | Turn left (E) on 500N. | 34.80 | Turn right (N) on IL-32 (+5.8 mi to east edge of Stewardson). |
| 6.0 | Turn right (S) at 500E/500N. | 44.30 | Turn right (E) on Neoga Road. |
| 6.8 | Fulfer Creek. Park along road. Walk east (0.1 mi/160 m) along creek toward railroad trestle to outcrop on north side of creek. STOP 1A. Proceed straight (S). | 49.80 | Turn right (S) toward Trowbridge. |
| 7.1 | Turn left (E) on 400N. | 50.30 | Cross abandoned NF&W Railroad in Trowbridge. Note icons. |
| 7.8 | Quarry on left. Park along road. Walk north (0.15 mi/240 m) to exposure in Fulfer Creek. STOP 1B. Retrace route back to Altamont. | 51.20 | Little Wabash River. Park along road. Walk along south bank to exposures in ravines east of bridge. STOP 3. Retrace route back to Neoga Road. |
| 15.6 | I-70 overpass, continue straight (N) through Altamont. | 52.55 | Neoga/Trowbridge roads intersection. Turn right (E). |
| 24.5 | Turn left (W), correction line jog. | 53.40 | Little Wabash River. Vicinity of Trowbridge Coal Member type section. |
| 24.6 | Turn right (N) on 300E. | 55.70 | Neoga village limits. |
| 25.65 | Turn right (E) on IL-33. | 56.20 | Cross IC Railroad, US-45. Continue straight (E-SE). |
| 29.90 | Road bears left, proceed straight on 1900N through edge of Shumway. | 56.70 | Turn right (S) at "T" intersection (Wilson St.). |
| 32.75 | Turn right (S) at "Y" junction with IL-32. | 56.80 | Turn left (E) on 5th St. |
| 33.20 | Turn left on 1850N (E). | | |
| 33.70 | Turn left on 1050E (N). | | |

- 60.25 Turn right (S) on IL-121.
- 63.05 Road curves to left (E).
- 69.70 Toledo village limits.
- 70.20 Turn left (N) at Missouri Street (Janesville Road).
- 73.70 Turn right (E) toward Bradbury.
- 77.10 Tippet Hollow Cemetery to right.
- 77.35 Turn left (N).
- 78.70 "T" intersection, turn right (E).
- 79.25 Ryan Bridge on Embarras River. Turn left (N) just east of bridge on private lane.
- 79.65 End of lane. Turn around, proceed straight (S).
- 79.85 Park along lane. Walk to river bank. STOP 4. Retrace route back to intersection east of Tippet Hollow Cemetery.
- 81.75 Intersection east of Tippet Hollow Cemetery. Proceed straight (S).
- 84.30 Turn left (E).
- 84.80 Sharp turn to right (S).
- 85.00 Park along road at farm. Walk west past barn and up ravine (about 0.25 mi/400 m). STOP 5. Proceed straight (S).
- 86.30 Sharp turn to right (W).
- 86.55 Turn left (S).
- 87.05 Sharp turn to left (E).
- 87.15 Sharp turn to right (S).
- 87.55 Turn left (S) on IL-121. Poorly exposed type locality of Greenup Limestone Member is about 0.25 mi (400 m) west-northwest. (+0.2 mi to Embarras River).
- 87.80 Poorly exposed Greenup Limestone on east side of road. Enter Greenup.
- 88.10 Turn left (E), proceed through Greenup on the "National Road."
- 89.00 Turn right (S) on IL-130.
- 89.15 Turn right (W) on US-40 (+1.95 mi to Embarras River).
- 98.10 Turn left (S), enter Woodbury and cross Conrail Railroad.
- 98.70 Sandstone crops out on right; road turns left (E).
- 98.90 Webster Branch. Argillaceous sandstone outcrop to right is in Toledo cyclothem. Road turns right (S).
- 99.75 Road turns right (W).
- 100.00 Road turns left (S).
- 100.60 Turn right (W) at 2160N/375E.
- 101.85 Turn right (N) on private lane.
- 102.10 Park near house. Walk to left of house, following farm road to Webster Branch tributary (0.2 mi/320 m). STOP 6. Retrace route to 2160N/375E.
- 103.15 Turn right (S) on 375E.
- 103.80 Road turns right (S).
- 104.00 "T" intersection, 2100N/420E, turn left (E).
- 105.80 Turn right (S) at 600E/2100N (+3.0 mi to Gila).
- 107.00 Mint Creek. Park along road near cemetery. Walk northeast to west-facing cut bank (about 500 ft/152 m). STOP 7A. Return to road and walk south to edge of wooded area, turn east to Mint Creek (about 900 ft/274 m) and continue downstream (about 400 ft/122 m) to east-facing cut bank east of private residence. STOP 7B. Return to vehicles. Proceed straight (S).
- 107.55 Road turns right (W) on 1625N.
- 107.90 Road turns left (S) on 550E.
- 110.25 "T" intersection, 550E/1400N, turn right (W).
- 110.50 Turn left (S) on 525E.
- 110.60 Slate Creek. "Dieterich" black shale crops out just to right (W) of bridge.

- 111.50 "T" intersection, turn right (W) on 1500N.
 111.75 "T" intersection, turn left (S) on 500E.
 112.45 Turn left (SE) on IL-33 (+1.2 mi to Lis).
 117.60 Newton village limits.
 118.65 Turn left (N) on Van Buren Street.
 118.80 Turn right (E) on Marion Street.
 119.10 Turn left (N) on Third Avenue, just west of cemetery.
 119.15 Park at riverside. Walk east to exposure (about 450 ft/137 m). STOP 8. Return to Marion Street.
 119.20 Marion Street. Turn left (E).
 119.45 Turn left (N) on Peterson Drive and proceed through park.
 119.80 Exit park, cross IL-130 to River Park Motel. Sweet Dreams.

Second Day:

- 0.0 Turn right (N) on IL-130 (+0.05 mi to Embarras River).
 1.0 Bear right on IL-33 (+0.8 mi to Sam Parr State Park).
 4.6 Turn left (N) at 1600E/1100N.
 5.05 Turn left (W) at 1600E/1150N.
 5.30 Road jogs north.
 5.40 Road jogs west.
 5.90 Road jogs north at tank battery and continues west down to Crooked Creek floodplain.
 6.00 Park at foot of hill near pumping jack. Walk northeast to creek (about 100 ft/30.5 m). STOP 9. Retrace route to Embarras River.
 11.95 Embarras River, enter Newton. Continue on IL-33.
 20.20 Turn left (S) on CIPS Road (500E).
 25.20 Turn right (W) on 750N.

- 26.60 Road turns left (S).
 27.00 Road turns right (W).
 27.45 Road turns left (S) on 300E.
 27.85 Turn right (W) on 300N.
 28.35 Proceed straight on gravel road at 250E/300N.
 28.65 Big Muddy Creek. Park near bridge. STOP 10. Walk south along creek to bend (about 0.25 mi/400 m). Return to paved road.
 28.95 Turn right (S) on paved road (250E).
 29.95 Turn right (W) on 200N.
 30.55 Lower Bogota cyclothem exposure to left. Bogota Limestone Member type locality.
 30.95 Turn left (S) at 150E/200N.
 31.65 Limestone Creek. Basal Bogota cyclothem to left in cut bank.
 32.45 Turn left (E) at 150E/50N.
 32.60 Big Muddy Creek. Park near bridge. Walk south along east bank (about 0.1 mi/160 m). STOP 11. Proceed straight (E).
 32.90 Turn right (S) on 200E.
 34.45 Ingraham. Turn left (E) at 1600N/2000E (+4.05 mi to Wendelin) (+0.25 mi to Wet Weather Creek).
 45.10 Fox River.
 46.30 Turn right (S) on IL-130.
 52.60 Olney. Continue on IL-130.
 54.50 Park north of Big Creek bridge. Walk to exposures on south bank on both sides of bridge, and then northeast upstream (about 0.3 mi/480 m). STOP 12. Proceed straight (S).
 57.15 Turn left (E) on Calhoun Road (550N).
 59.15 Jog to right (S).
 59.20 Cross IC RR, enter Calhoun and continue straight (E).

- 59.50 Road turns left (N).
 59.55 Road turns right.
 60.55 Turn right (S) on 1500E.
 61.05 Turn left (E) on 500N.
 62.15 500N/1600E. To right, just south of bridge and on west side of road, is poorly exposed Bonpas Limestone Member type locality. Turn left (N).
 62.90 Turn right (E) at 1600E/575N.
 63.40 Park near house. Walk south to "New Calhoun" coal ball exposure (about 0.2 mi/320 m). STOP 13. Proceed straight (E).
 64.40 Turn left (N) at "T" intersection.
 64.65 Right turn (E) at 600N/1750E. Continue on paved road.
 65.65 Turn right (S) on 1850E.
 67.15 Turn left (E) on 450N.
 68.65 Turn right (S) at 2000E/450N.
 69.40 Park along road. Walk down ravine to right (W) and then upstream (N) to west-facing cut bank (about 0.35 mi/560 m). STOP 14. Turn around, proceed straight (N).
 69.65 Turn right (E) on 400N.
 70.65 2100E/400N. Park along road. Walk southeast down ravine (about 0.3mi/480 m). STOP 15. Proceed south on county line road.
 72.65 Turn left (E).
 73.60 Turn right (S).
 73.85 Turn left (E).
 75.35 Turn right (S).
 78.65 Lancaster intersection. Turn right (E).
 80.20 Road bears right (S-SE).
 80.80 Road bears left (E).
 84.05 Turn left (N) at 1150E/2200N.
 84.45 Park along road at mine gate. Walk west (about 0.25 mi/400 m) to abandoned coal mine. STOP 16. Retrace route back to 1150E/2200N. Turn left (E).
 84.95 Turn right (S) at 1200E/2200N to IL-1 (4.5 mi), then to I-64 (24 mi). Take I-64 west to St. Louis, Missouri. End of log.

FIELD TRIP STOP DESCRIPTIONS

STOP 1A: Upper unnamed cyclothem, basal Omega cyclothem.

Location: South cut bank, Fulfer Creek, just west of railroad trestle, 600 ft FWL, 1,400 ft FSL, 12-T6N-R4E, Effingham County.

The Omega cyclothem, as originally defined by Wanless (1956) contained only one named unit, the Omega Limestone Member; neither upper nor lower boundaries were specified. The succession underlying the Omega limestone is of terrestrial origin; it is the uppermost part of the marine-terrestrial sequence of an unnamed (or unidentified) modified cyclothem. The limestone is the marine portion of the succeeding marine-terrestrial sequence; the Omega cyclothem is therefore modified herein to include strata from the base of the Omega Limestone

(fig. 3) to the base of the Shumway cyclothem. The limestone is not well studied but appears to be mostly phylloid algal limestone with abundant well-preserved, pelmatozoan fragments, fusulinids, and numerous brachiopods. Unpublished ISGS field notes described a gray to brown shale with siderite nodules overlying the limestone in this area.

The Omega lithology appears very similar to that of the younger Greenup Limestone Member (Stop 4), and therefore probably caused Weller et al. (1942) to correlate tentatively the two units. Cooper (1946), however, asserted that no ostracode species were common to the Greenup and Omega Limestones and tentatively correlated the Omega with the Bonpas Limestone Member (Stops 13, 14, and 15), a correlation still not substantiated. Dunbar and

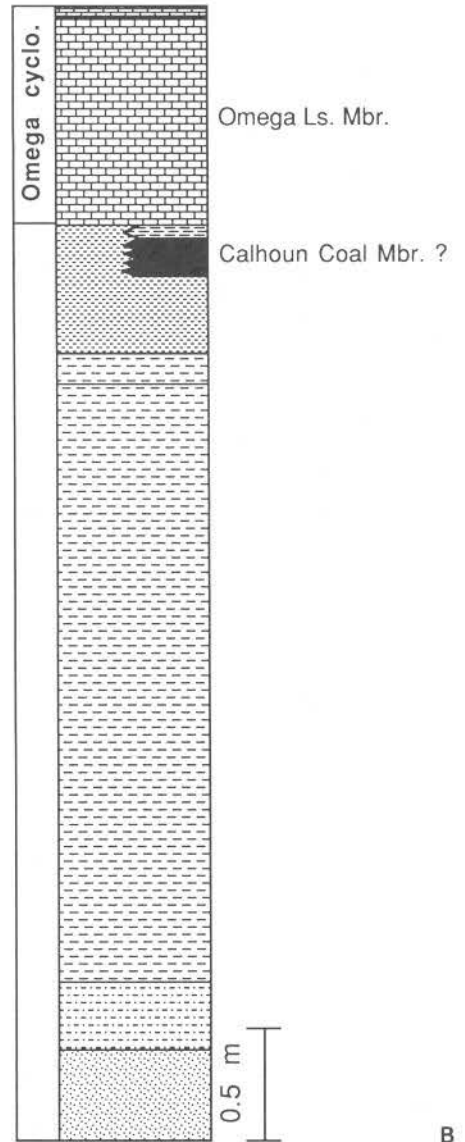


Figure 3 — A. Lowermost Omega cyclothem and underlying strata at Stop 1A. Hand is at base of Omega Limestone Member, Calhoun Coal Member?, not shown in this photograph, is present just to left of view. B. Composite stratigraphic column of rocks exposed at Stops 1A and 1B.

Henbest (1942) collected *Triticites venustus* and *T. ohioensis* from the Omega just west of the road, and poorly preserved *T. venustus* from the Bonpas; this suggests equivalence. Palynological study of the coal underlying the Omega and the Calhoun Coal Member, which underlies the Bonpas, indicates probable, but not conclusive, equivalence (R. Peppers, personal commun.). The Omega and Bonpas crop out similarly close to the Shumway cyclothem, also suggesting equivalence. Neither

limestone has been traced in the subsurface far from its outcrop area; thus both have little potential as key beds for regional stratigraphic control.

Because of the general endemism of Virgilian fusulinids in the Illinois Basin and poorly understood field relationships, Weller et al. (1942) correlated the Illinois Virgilian limestones to only the group level in Kansas; the Omega was correlated with the Lansing Group. Cooper (1946) correlated the Omega

with the Deer Creek Limestone of Kansas. Range overlap of the fusulinids and correlation based on lithological and genetic sequences indicate that the Omega probably is equivalent to the Haskell Limestone Member of the Lawrence Formation of Kansas (Weibel, 1988). Boardman and Heckel (1989) correlated the lower Colony Creek cycle of north-central Texas with the midcontinent Haskell-Cass cycle; thus the Omega cyclothem presumably is equivalent to the lower Colony Creek. Black "core" shales, however, are present in the lower Colony Creek and the Haskell-Cass cycles, but absent in the Omega; either the cycles are miscorrelated or a regional facies change is present.

STOP 1B: Basal Omega cyclothem and underlying coal bed.

Location: Streambed, Fulfer Creek, just north of abandoned quarry, 1,200 ft FEL, 800 ft FSL, 12-T6N-R4E, Effingham County.

This excellent Omega Limestone exposure was used as a ford to access the quarry and consequently not excavated. Erosion removed most of the sideritic cap on the limestone and revealed less altered surfaces. Brachiopods, fusulinids, and grazing trails are common but difficult to extract. The underlying coal is separated from the limestone by a thin dark-gray bituminous shale, apparently nonmarine, that caps the terrestrial portion of the underlying unnamed modified cyclothem.

STOP 2: Uppermost Omega cyclothem and basal Shumway cyclothem.

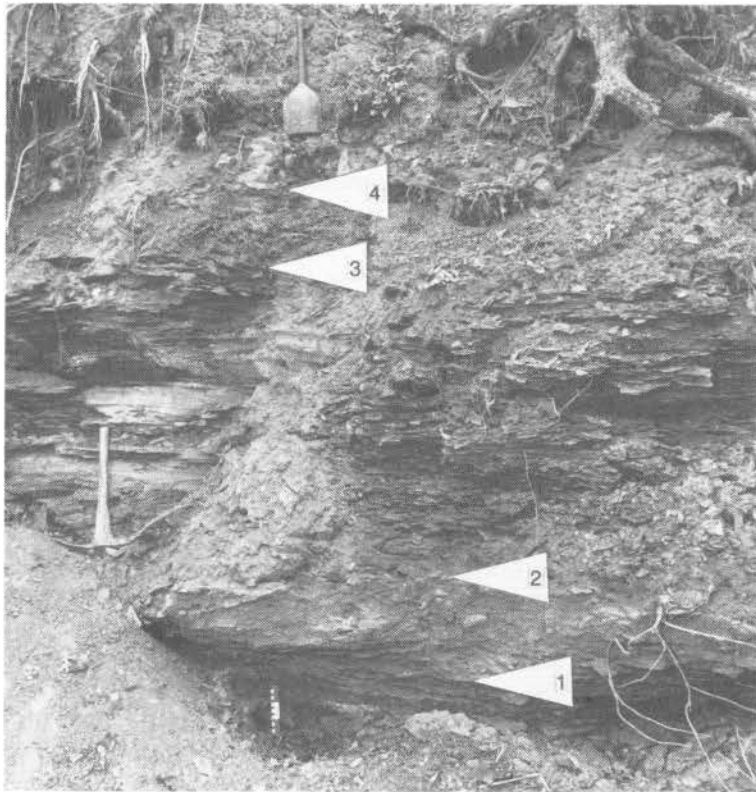
Location: South bank, Shoal Creek, directly west of derelict steel truss bridge on abandoned road, 50 ft FEL, 150 ft FSL, SW/4, 26-T9N-R5E, Effingham County.

This outcrop (fig. 4) consists of a terrestrial-marine-terrestrial sequence, equivalent to the Shumway cyclothem originally described by Weller and Bell (1941). The lower terrestrial succession is the top of the modified Omega cyclothem. The succeeding marine-terrestrial sequence is the lower and middle portions of the Shumway cyclothem, herein modified to include strata from the base of the lowest of the "Lake Sara" limestone, the

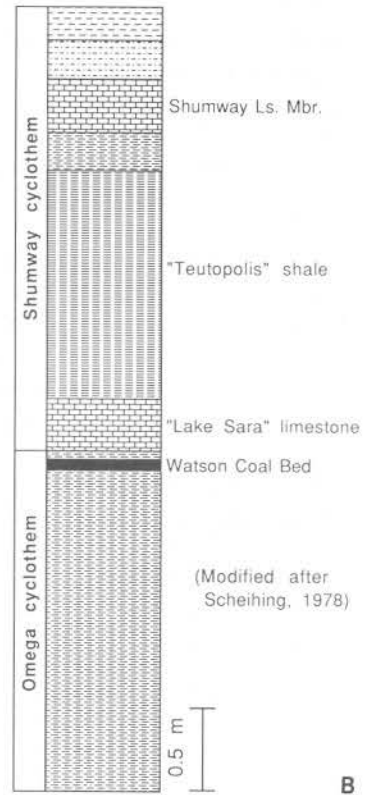
"Parkersburg" limestone, or the "Teutopolis" shale, to the base of the Bogota cyclothem.

The uppermost Omega cyclothem here consists of an upward sequence of burrowed laminated siltstone and sandstone, dark-gray to variegated shale containing abundant plant debris, green-gray, very fine-grained limestone (containing fecal pellets, corroded ostracodes and bivalves, and birds-eye texture), gray claystone (underclay) with *Stigmaria* rootlets, and the Watson Coal Bed (Kosanke, 1950), which contains fossiliferous and carbonaceous limestone lenses. The Watson Coal, formerly referred to as the "Shumway Coal," here is only a few centimeters below the "Lake Sara" limestone. It is palynologically correlated (R. Peppers, personal commun., in Scheihing, 1978) with the Watson Coal at its type locality about 2.4 km (1.4 mi) to the south, where it is about 2 m (6.6 ft) below the "Lake Sara" limestone. The coal here is succeeded by a thin gray to black calcareous shale containing coal fragments and sand-sized bioclasts.

The Shumway cyclothem here consists of, in upward order, "Lake Sara" limestone, "Teutopolis" shale, Shumway Limestone Member, shale, and sandstone. The basal 3 cm (0.1 ft) of the "Lake Sara" limestone are argillaceous and abundantly fossiliferous and contain carbonaceous and coaly material. The middle portion is a massive, bioturbated limestone with well-preserved, unabraded shells. The top 3-4 cm (0.1-0.13 ft) are a grain-supported fossil hash in a silty, calcareous to carbonaceous matrix. The basal 37 cm (1.2 ft) of the succeeding black "Teutopolis" shale are blocky to poorly fissile and contain abundant shell fragments, dominated by inarticulate and productoid brachiopods. The upper 63 cm (2.1 ft) are fissile and contain sparse fish scales and conodonts. The Shumway Limestone was informally amended by Weibel (1988) to include the lenticular gray shale between the limestone bed and the overlying "Teutopolis" black shale. The gray shale is calcareous and fossiliferous (brachiopods, pectinoids, and plant debris). The lower 16 cm (0.52 ft) of the limestone are a massive, mud-supported fossiliferous calcilutite. The upper 8 cm (0.26 ft) are a thin-bedded, grain-supported calcarenite with an argillaceous micritic matrix. Brachiopod and pelmatozoan debris are the dominant fossils. The limestone is succeeded by a slightly silty gray shale containing siderite concretions. The shale is unconformably



A



B

Figure 4 — A. Uppermost Omega cyclothem and lowermost Shumway cyclothem at Stop 2. Watson Coal Bed crops out at centimeter scale. "Lake Sara" limestone is delineated by pointers 1 and 2. "Teutopolis" shale by pointers 2 and 3, and Shumway Limestone Member by pointer 4 and base of trenching shovel. **B.** Stratigraphic column of rocks at Stop 2.

overlain by a fine to medium grained sandstone that filled channels eroded into the shale.

Scheihing and Langenheim (1978a, 1978b, 1980) described 43 invertebrate taxa from the lower Shumway cyclothem. Their work, coupled with descriptions of fusulinids by Dunbar and Henbest (1942), ostracodes by Cooper (1946), nautiloids by Tucker (1976) and a conulariid by Tucker and Paukstis (1977), make the Shumway fauna (more than 100 species) one of the most thoroughly described and illustrated normal marine faunas from the Illinois Basin.

The "Teutopolis" shale, the most widespread member of the Shumway cyclothem, has been recognized in many coal exploratory wells in the region (Weibel, 1988). The "Ingraham" shale of the overlying modified Bogota cyclothem is also widely recognized in the subsurface. Because these shales are readily recognized on gamma ray logs while adjacent limestones are not, the shales delineate

the bases of the Shumway and Bogota cyclothem in the subsurface. Thus the Shumway cyclothem is a strong candidate as either a member or a formation.

Scheihing and Langenheim (1985) compared the sequence with "Kansas-type" cycles described by Heckel (1977). This exposure also represents a symmetrical succession of environments. The uppermost Omega cyclothem records successively an alluvial channel, a floodplain, a floodplain lake or an interdistributary bay, and a coal swamp. The lower Shumway cyclothem records inundation of the swamp, a progressively deepening marine shelf, offshore and anoxic marine conditions, restored aeration on a marine shelf, marine limestone accumulation, encroachment of fluvial clays, and fluvial channels.

Correlation of the Shumway marine sequence with the midcontinent sequences has varied from the uppermost Missourian Stanton Limestone through the middle Virgilian Topeka Limestone. Weller et al.

(1942) correlated the Shumway with the Douglas Group, based primarily on two fusulinid species considered unique to the Shumway. Cooper (1946), using ostracodes, concluded the Shumway is equivalent to the upper Shawnee Topeka Limestone. However, because Cooper incorrectly correlated the Shumway with the Newton ("Shamrock"), this correlation is suspect. The NRC correlation chart (Moore et al., 1944) correlated the Shumway with the Stanton Limestone, but quoted Weller as tentatively supporting correlation with the Topeka Limestone. Siever (*in* Wanless, 1956, pl. 1), Kosanke et al. (1960, pl. 1), and Hopkins and Simon (1975) placed the Shumway at the base of the Virgilian in Illinois and, in the first two references, correlated the Shumway with the Stanton. Wanless (1975) correlated the Shumway to the lower Shawnee Lecompton Limestone. Moore (1959) published a correlation diagram, closely resembling that of Moore et al. (1944), showing the Shumway Limestone as an eastward extension of the Oread Limestone. Sturgeon and Hoare (1968) correlated the Shumway with the Iatan Limestone of Kansas and the Gaysport Limestone of Ohio; they also placed the Shumway at the base of the Virgilian. Scheihing and Langenheim (1980) and Langenheim and Scheihing (1983), using brachiopods and considering other paleontologic data, concluded that the Shumway best correlates with the Oread Limestone. Scheihing and Langenheim (1978b) quoted Wanless (personal commun., 1962), who correlated the Shumway black shale ("Teutopolis" shale) with the Heebner Shale of the Oread cyclothem. Finally, Weibel (1988) correlated the Shumway cyclothem with the Oread on the basis of "similarity of lithologies, particularly the black shale, similarity of lithologic successions, and both cyclothem succeeding a thick interval of strata.....devoid of black shale-bearing cyclothem." Boardman and Heckel (1989) correlated the Oread cyclothem with the Finis cycle of north-central Texas. Presumably the Finis is equivalent or nearly equivalent to the Shumway cyclothem.

In summary, based on biostratigraphic data and physical stratigraphy, particularly black shale distribution, the Shumway cyclothem correlates well with the Oread cyclothem of Kansas. This correlation is compatible with more securely supported correlations of Illinois Pennsylvanian rocks below this stratigraphic level and is based on substantially more

data than are available for most rocks in the later part of the Illinois Basin Pennsylvanian succession.

STOP 3: Basal Bogota cyclothem.

Location: South bank and small ravines along Little Wabash River, just east of bridge, 2,400 ft FEL, 1,900 ft FNL, 22-T10N-R6E, Shelby County.

This outcrop is the marine portion of the Bogota cyclothem, as modified at Stop 10. The transition from the terrestrial portion of the largely covered underlying Shumway cyclothem to the Bogota marine portion is more gradational than at previous stops. The cyclothem base at this exposure (fig. 5) is the "Steel Bridge" limestone (Nance and Treworgy, 1981) which is of marginal-marine origin and is succeeded by the more marine "Ingraham" shale. The "Steel Bridge" is a light-gray to gray, fine-grained, argillaceous, carbonaceous limestone. Carbonaceous plant impressions are the only prevalent macroscopic fossils. The bed is lens-shaped and the rock readily splits into thin plates. Petrographically, the limestone is a sparsely fossiliferous, argillaceous calcisiltite. The basal part is dominated by algal fragments and disseminated plant debris; quartz silt is prevalent and ostracodes rare. Disarticulated ostracodes are most abundant and small (possibly juvenile) pelecypods, gastropods, and thin-shelled brachiopods are also common. Scattered algal clusters are present. Small horizontal burrows are conspicuous, but vertical burrows are rare.

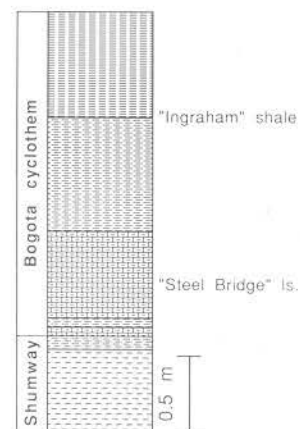


Figure 5 — Stratigraphic column of rocks at Stop 3.

The fissile black shale above the "Steel Bridge" limestone is the "Ingraham" shale; it will be examined and discussed at Stops 9, 10, and 11. Strata above the "Ingraham" are not exposed here, but near the railroad trestle upstream the Bogota Limestone Member crops out above the shale. The Trowbridge Coal Member (Cady, 1948), about 8.2 m (27 ft) above the Bogota, crops out in only a few places because shallow-shaft and small strip mines obliterated most exposures. The type locality could not be found and is either overgrown or has been mined.

STOP 4: Basal Greenup cyclothem.

Location: East bank, Embarras River, 0.32 km (0.2 mi) north of Ryan Bridge, 1,500 ft FWL, north edge, 2-T10N-R9E, Cumberland County.

The Greenup cyclothem of Newton and Weller (1937) herein is modified to include strata from the base of the Greenup Limestone Member up to the base of the "Graveyard Hill" shale of the Toledo cyclothem (fig. 6A). The marine portion of the Greenup cyclothem is exposed here, whereas the terrestrial portions of both the Mint Creek cyclothem

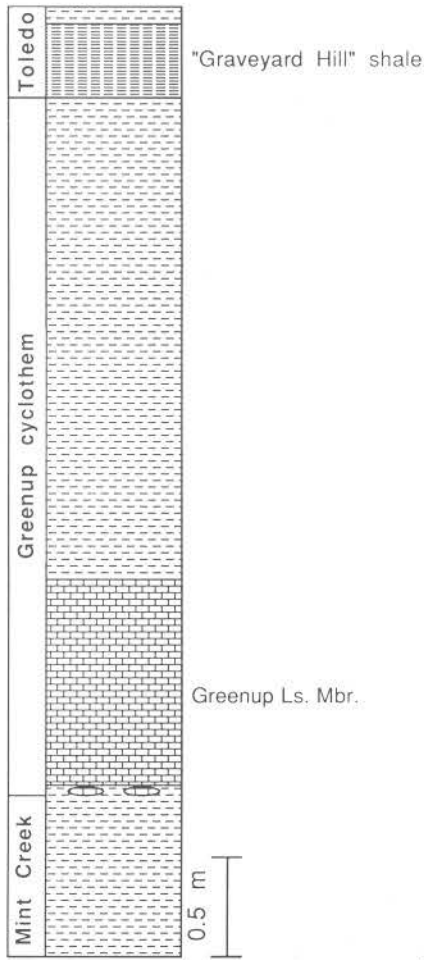


Figure 6 — A. Stratigraphic column of rocks at Stops 4 and 5. B. Uppermost Greenup cyclothem and basal Toledo cyclothem at Stop 5. Base of "Graveyard Hill" shale at top of machete.

(as described at Stop 7), below the limestone, and the Greenup cyclothem, above the limestone, are not well exposed. The Greenup Limestone is a gray, moderately fossiliferous, phylloid algal limestone. Fusulinids are dominant in the upper and lower parts; brachiopods, corals, and gastropods are dominant in the middle. The limestone nodules in shale at the very base of the Greenup are *Osagia*-encrusted, pelecypod, pelmatozoan, grain-supported biocalcarenes. The succeeding massive portion is a complex association of three microfacies: (1) a clastic microfacies grading from biocalcissiltite containing scattered bioclasts, into matrix-supported biocalcarenite, and into grain-supported biocalcarenite; (2) a compacted phylloid algal, bioaccumulated limestone; and (3) a phylloid algal, bioconstructed limestone. The top of the unit is an intraclastic, pisolitic, neomorphosed limestone, having features diagnostic of a paleosol. Weibel (1988) recognized the Greenup Limestone in only the northern half of his study area; thus it has poor potential for regional stratigraphic control.

Dunbar and Henbest (1942) collected *Triticites* from the Greenup Limestone (at a different locality) and Weller et al. (1942) correlated the Greenup with the midcontinent Shawnee Group. The range of the equivalent Kansas fusulinids is from the Plattsburg Group up into the lower Permian (Dunbar and Condra, 1927). Weibel (1988) tentatively correlated the Greenup Limestone with the midcontinent Burlingame Limestone Member of the Bern Limestone. Like the Greenup, this limestone is a phylloid algal bank containing fusulinids, brachiopods, and molluscs (Moore, 1936; Heckel et al., 1979). Cooper (1946) correlated the limestone with the Willard Shale, upper Wabaunsee Group, using ostracodes.

STOP 5: Uppermost Mint Creek cyclothem, Greenup cyclothem, and lower Toledo cyclothem.

Location: East-trending ravine, west side of Embarras River valley, 50 ft FEL, 600 ft FNL, 27-T10N-R9E, Cumberland County.

The succession in this ravine consists of the terrestrial portion of the Mint Creek cyclothem (as described at Stop 7), the complete marine-terrestrial sequence of the Greenup cyclothem, and the marine

portion of the Toledo cyclothem. The fine-grained argillaceous sandstone in the Mint Creek cyclothem at the ravine mouth has a composition typical of nonchannel sandstones in the upper portion of Virgilian modified cyclothem. Succeeding strata are covered or poorly exposed up to the resistant Greenup Limestone. Approximately 2.5 m (8.2 ft) of gray shale separate the Greenup Limestone top from the base of the Toledo cyclothem. The Toledo cyclothem, named for the village, comprises strata from the base of the "Graveyard Hill" shale to the top of the "Webster Branch" coal. As defined herein, the Toledo cyclothem includes the lower part of the Woodbury cyclothem of Newton and Weller (1937). The black, blocky to sheety basal shale, the "Graveyard Hill" (fig. 6B), is named for a nearby prominence on the Embarras River floodplain. Sparse fossils consist of scattered fish debris and ostracodes in the upper part. The "Graveyard Hill," which crops out at only one other place, a ravine just north of here, is recognized in only a few coal exploration wells in the area and is not useful for regional stratigraphic control.

Heckel et al. (1979) described a thin, widespread, conodont-rich shale in the lower part of the Wakarusa Limestone Member of the Bern Limestone in Kansas. Heckel (1984) suggested this shale is a lateral facies of a "core" shale and Weibel (1988) suggested it may be equivalent to the "Graveyard Hill" shale.

STOP 6: Uppermost Toledo cyclothem and Woodbury cyclothem.

Location: Cut bank, Webster Branch tributary, 1,400 ft FEL, 600 ft FSL, 32-T9N-R8E, Cumberland County.

The interval between the "Graveyard Hill" shale and the "Webster Branch" coal is estimated at 7.6 m (25 ft). The coal, formerly the "Woodbury coal" of Newton and Weller (1937), herein is called the "Webster Branch" coal because of homonymy with the Woodbury Limestone Member; it caps the terrestrial portion of the Toledo cyclothem unit. Newton and Weller erroneously correlated the "Lis" coal (Newton cyclothem) with the "Webster Branch" coal.

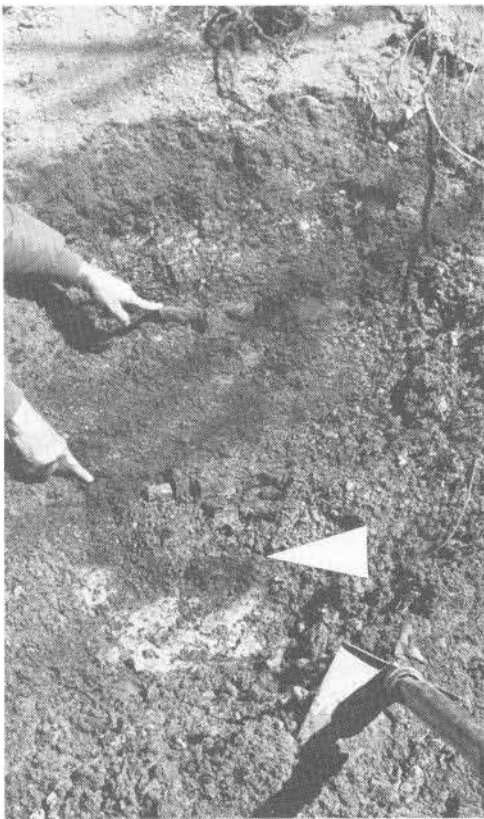
The overlying strata consist of the marine portion of the Woodbury cyclothem of Newton and Weller

(1937), herein modified to include all Pennsylvanian strata above the top of the "Webster Branch" coal. This cyclothem and the "Webster Branch" coal crop out only along this creek (fig. 7) and have not been recognized on subsurface logs. Post-Pennsylvanian erosion has reduced the lateral continuity and extent of the coal and succeeding strata in the region.

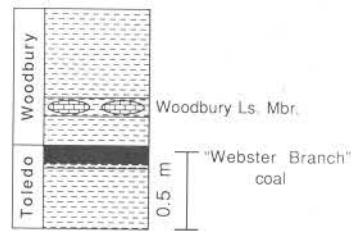
At the Woodbury cyclothem base, a semi-fissile variegated shale separates the lower shaly part of the Woodbury Limestone Member from the coal. The shale is transitional from the terrestrial uppermost Toledo cyclothem to the marine Woodbury Limestone, which is composed of calcareous concretions having ferruginous weathering rinds in a light-gray shale. The limestone and shale are moderately fossiliferous; gastropods and brachiopods are dominant, pelmatozoans, pelecypods, and ostracodes, common, and trilobites, rare. Newton and

Weller (1937) also reported a rugosan coral and a nautiloid. The limestone is a bioturbated neomorphosed calcisiltite with scattered bioclasts. The poorly sorted, unevenly distributed bioclasts vary from whole fossils to fine sand-sized fragments. The youngest Virgilian bed of east-central Illinois is gray to gray-brown shale overlying the Woodbury Limestone.

The Woodbury cyclothem is difficult to correlate because of its undistinctive lithological sequence. Weibel (1988) suggested that on the basis of its relative stratigraphic position in the Illinois section, possible midcontinent equivalents of the Woodbury could be the Emporia and Zeandale Limestones. Using ostracodes, Cooper (1946) correlated the Woodbury cyclothem of Newton and Weller (1937) with the lower Admire Group.



A



B

Figure 7 — A. Uppermost Toledo cyclothem and basal Woodbury cyclothem at Stop 6. "Webster Branch" coal is bracketed by pointer (bottom) and right index finger (top). Left index finger points at Woodbury Limestone Member. B. Stratigraphic column of rocks at Stop 6.

STOP 7A: Uppermost Newton cyclothem and lower Mint Creek cyclothem.

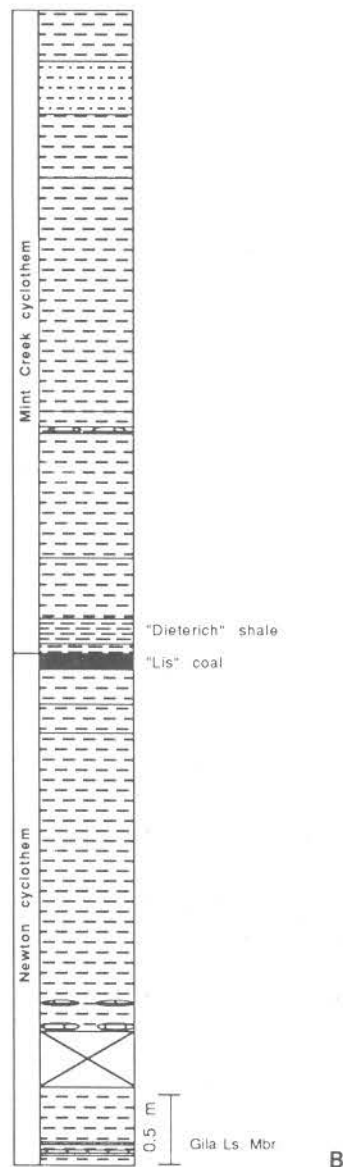
Location: West-facing cut bank, Mint Creek, 350 ft F WL, 1,200 ft FNL, 31-T8N-R9E, Jasper County.

The "Lis" coal (fig. 8) at the base of the cut bank caps the terrestrial portion and is the highest unit in the modified Newton cyclothem, as described at Stop 8. The coal crops out along creeks in the Gila-

Mint Creek area and creeks to the south and southeast toward Newton. The coal was formerly called the "Brush Creek" (Needham, 1931; Weibel, 1985) and "Gila" (Peppers, 1984). Nance and Treworgy (1981) suggested correlation of the "Lis" with the Trowbridge Coal of the underlying Bogota cyclothem, but the "Lis" is equivalent to their "unnamed" coal.



A



B

Figure 8 — A. Uppermost Newton cyclothem and lowermost Mint Creek cyclothem at Stop 7A. Pointer 1 marks base of "Lis" coal and pointer 2 marks contact of coal and "Dieterich" shale. B. Stratigraphic column of rocks at Stops 7A and 7B. M. Cr. = Mint Creek.

Strata above the "Lis" coal up to the base of the Greenup Limestone Member are defined herein as the Mint Creek cyclothem, named for the creek. The thin marine portion of the Mint Creek cyclothem consists only of the "Dieterich" shale and is succeeded by terrestrial deposits (fig. 8). The "Dieterich" shale is black, sheety, and well-indurated; near the base, it locally includes calcareous laminae and flattened clasts that are bioaccumulated, bituminous, algal limestone. The upper part is a softer, fissile, black shale. Fossils are sparse and consist of fish fragments and carbonaceous plant fragments. The succeeding unit is a fissile, weakly calcareous, gray to brown shale, that locally contains fossils, mostly molluscs.

The "Dieterich" shale has been recognized in most coal exploratory wells in the outcrop area (Weibel, 1988). The shale is the highest Virgilian stratum that is mappable throughout the region; it is a good candidate for the lower boundary bed of a member or formation consisting of the package of the four youngest cyclothem: Mint Creek, Greenup, Toledo, and Woodbury. The base of the shale could also be used to mark the upper contact of a member or formation consisting of the Bogota and Newton cyclothem.

The lower Mint Creek cyclothem lithologically correlates with the midcontinent Topeka cyclothem (Weibel, 1988). The "Dieterich" shale is equivalent to the lithologically similar Holt Shale Member of the Topeka Limestone. A possible equivalent shale in north-central Texas is the Wayland Shale Member of the Graham Formation, but Boardman and Heckel (1989) correlated the Wayland with the midcontinent Deer Creek cyclothem.

STOP 7B: Uppermost Newton cyclothem and basal Mint Creek cyclothem.

Location: East-facing cut bank, Mint Creek, 900 ft FWL, 2500 ft FNL, 31-T8N-R9E, Jasper County.

The Gila cyclothem of Newton and Weller (1937) consists of strata of nonmarine origin. The marine strata underlying this outcrop are the "Shamrock" Limestone Member and the "Wetweather" shale of the Newton cyclothem of Newton and Weller (1937). This marine strata and the Gila cyclothem are combined to form a marine-terrestrial sequence, the

modified Newton cyclothem, as described at Stop 8. The Gila Limestone Member (fig. 8B) probably should be abandoned because of its extreme thinness and limited lateral extent (a single exposure); absence of biostratigraphically useful fossils precludes nonspeculative extra-basinal correlations.

The Gila Limestone consists of two thin, gray to brown, fine-grained limestone beds, each 2-3 cm (0.07-0.1 ft) thick, separated by 2 cm (0.07 ft) of soft, poorly fissile, dark-gray shale with carbonaceous laminae. The bed is overlain by dark-gray shale and underlain by a thin layer of dark-gray to black soft shale, which succeeds a gray shale. The limestone is a sparsely fossiliferous calcilutite in which ostracodes are dominant, plant debris common, and fish scales rare. The Gila is separated from the "Lis" coal by 3.7 m (12.1 ft) of gray shale with a few siderite nodules and a few thin calcareous and micaceous sandstones. The "Dieterich" shale of the Mint Creek cyclothem is at the top of this exposure.

STOP 8: Uppermost Bogota cyclothem and lower Newton cyclothem.

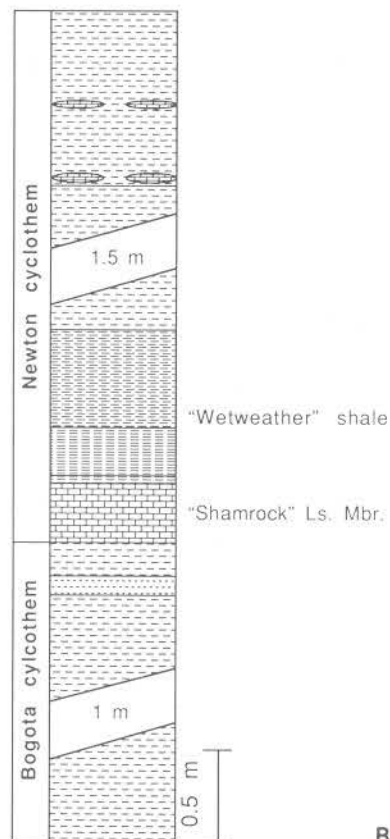
Location: South bank, Embarras River, just north of cemetery in Newton, 850 ft FEL, 100 ft FNL, 1-T6N-R9E, Jasper County.

The lower 1.5-2.5 m (4.9-8.2 ft) of strata at this exposure comprise the upper terrestrial portion of the modified Bogota cyclothem (fig. 9), as described at Stop 10. These strata are mostly gray shale interbedded with siltstone and very fine-grained sandstone. The top of the Bogota cyclothem is a dark-gray weakly calcareous mudstone containing myalinid pelecypods.

The overlying strata consist of a marine-transitional marine to terrestrial sequence (fig. 9) and comprise the upper portion of Newton and Weller's (1937) Newton cyclothem, herein modified to include strata from the base of the "Shamrock" Limestone Member up to the base of the "Dieterich" shale. The modified cyclothem therefore includes the upper part of the Newton cyclothem and the entire Gila cyclothem of Newton and Weller (1937). Needham (1931) defined the "Shamrock" Limestone



A



B

Figure 9 — A. Uppermost Bogota cyclothem and lower Newton cyclothem at Stop B. Top of icicle in center marks base of "Shamrock" Limestone Member. "Wetweather" shale is bracketed by hands. B. Stratigraphic column of rocks at Stop 8.

as a gray fossiliferous limestone cropping out near the village of Shamrock, in southwestern Jasper County; the name has priority over the "Newton" Limestone (Newton and Weller, 1937) and the "Reisner" Limestone (Kosanke et al., 1960). The "Shamrock" is a bioturbated mud-supported (locally grain-supported) biocalcarene with an argillaceous neomorphosed matrix. Brachiopods, encrusting foraminifers, and pelecypods are abundant; gastropods, pelmatozoans, and ostracodes are prevalent, and trilobites and foraminifers are rare. Most bioclasts are encrusted by *Osagia*.

The succeeding unit, the black sheety "Wetweather" shale, herein named after Wetweather Creek (southwest of Newton), is generally less than 1 m (3.3 ft) thick. The shale lacks large calcareous concretions and characteristically contains abundant pelecypods and brachiopods at the base. The middle and upper portions are sparsely fossiliferous,

containing poorly preserved pelecypods, coalified plant fragments, and fish fragments. Contact with the underlying "Shamrock" Limestone ranges from sharp (at this exposure) to intergradational. Unlike other Illinois Virgilian black shales, the "Wetweather" has been recognized on only a few of the numerous coal exploration well logs of Virgilian strata in the region; thus, it probably has little potential as a regional stratigraphic key bed. The interval between the "Wetweather" shale and the Gila Limestone is about 4-7 m (13-23 ft) thick and is mostly shale and fine-grained sandstone.

A coal mined southeast of Newton was correlated by Nance and Treworgy (1981) with the Trowbridge Coal of the underlying Bogota cyclothem. However, since the "roof rock," reportedly a black shale, was probably the "Dieterich" shale of the younger Mint Creek cyclothem, the coal probably was the "Lis" coal (Weibel, 1988).

Cooper (1946), using ostracodes, considered the Newton ("Shamrock") Limestone biostratigraphically equivalent to the Shumway Limestone, but noted differences "in physical character and in stratigraphic association." The lower part of the modified Newton cyclothem lithologically correlates with the middle part of the midcontinent Deer Creek cyclothem (Weibel, 1988). Boardman and Heckel (1989) correlated the Wayland cycle of north-central Texas with the midcontinent Deer Creek cycle; thus, the Newton cyclothem presumably is equivalent to the lower Deer Creek.

STOP 9: Uppermost Shumway cyclothem and lower Bogota cyclothem.

Location: South bank, Crooked Creek, 1,200 ft FWL, 2350 ft FNL, 27-T7N-R10E, Jasper County.

The lower 0.85 m (2.8 ft) of strata at this exposure constitute the top terrestrial portion of the Shumway cyclothem, as described at Stop 2; however, these strata are now under water. This interval includes the thin transitional zone between the Shumway cyclothem terrestrial portion and the Bogota cyclothem marine portion, and consists of gray, fissile shale with a 7 cm (0.23 ft) thick layer of calcareous septarian nodules in the upper portion. The shale also contains a few scattered sideritic nodules and is sparsely to moderately fossiliferous, containing brachiopods, gastropods, and pelecypods. Although deposited in a marine to marginal-marine environment, the shale is placed in the uppermost terrestrial portion of the Shumway cyclothem because it is thin and not lithologically distinctive.

The overlying marine strata constitute the lower portion of the modified Bogota cyclothem (fig. 10), as described at Stop 10. The Bogota cyclothem base at this exposure is the "Ingraham" shale, the thickest (1.2-3 m/3.9-9.8 ft) Virgilian black shale. The "Ingraham" is characterized by large, gray, calcareous concretions and locally at the base, locally abundant poorly preserved shells and shell fragments, chiefly brachiopods. In the middle part pectinoids are abundant, fish fragments prevalent, and brachiopods and gastropods rare, whereas the upper part contains only sparse fish fragments and pectinoids.

The Bogota Limestone Member here comprises two limestone beds 30-40 cm (1.0-1.3 ft) thick, separated and underlain by 50-60 cm (1.6-2.0 ft) of fossiliferous shale. The lower bed is a grain-supported, fine-grained biocalcarenite with a neomorphosed matrix. Pelmatozoans are abundant; brachiopods and trilobites are prevalent throughout, but ostracodes are prevalent only at the base. Foraminifers, fusulinids, corals, bryozoans, fish scales, and plant debris are rare. *Osagia* encrusts larger bioclasts. Angular to subangular quartz silt is rare, except at the top, where it is abundant. The upper bed, similar in most respects to the lower, is arenaceous throughout.

The "Ingraham" shale is widespread; like the underlying "Teutopolis" shale (Weibel, 1988), it is recorded on almost all coal exploration logs of Virgilian strata in the region. The marine limestones that underlie the "Ingraham" and the "Teutopolis" are rarely recorded on geophysical logs; the shales thus are the basal key beds for these modified cyclothem in the subsurface. The "Ingraham" shale base is used in the subsurface to separate the Shumway cyclothem below from the Bogota-Newton cyclothem succession above; both of which are strong candidates as potential members or formations.

STOP 10: Lower Bogota cyclothem (fig. 11).

Location: Southeast bank at bend, Big Muddy Creek, 800 ft FWL, 2,300 ft FNL, 9-T5N-R8E, Jasper County.

These strata, deposited in environments ranging from open marine at the base to coal swamp at the top, represent a marine-terrestrial sequence of the modified cyclothem. This outcrop shows the complete transition from the marine portion to the terrestrial portion, an interval usually poorly exposed.

The Bogota cyclothem, originally the "upper Bogota" cyclothem of Newton and Weller (1937), is modified herein to include strata from the top of the Shumway cyclothem up to the base of the "Shamrock" Limestone Member. The cyclothem therefore includes the upper part of the "upper Bogota" cyclothem and the lower part of the Newton cyclothem of Newton and Weller (1937). The Bogota cyclothem base is either the "Steel Bridge"

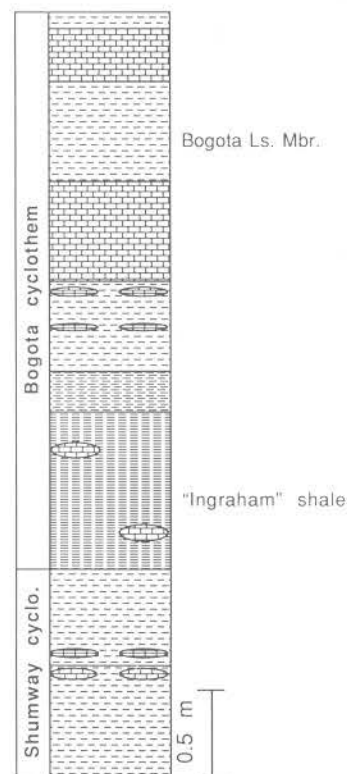


Figure 10 — A. Lower *Bogota cyclothem* at Stop 9. Upper portion of "Ingraham" shale exposed just above creek; pointers 1 and 2 bracket two limestone beds in Bogota Limestone Member. B. Stratigraphic column of rocks at Stop 9.

limestone, Effingham Limestone, or "Ingraham" shale, which all form resistant ledges. The "lower Bogota" cyclothem of Newton and Weller (1937), which includes strata ranging from within the Shumway cyclothem up to the Newton cyclothem, is herein rejected. The black sheety shale at the base of this outcrop is the "Ingraham" shale, with its characteristic large gray calcareous concretions. In this area, it also contains several alternating resistant and less resistant layers, each 20-35 cm (0.66-1.15 ft) thick.

The "Ingraham" shale is overlain by the Bogota Limestone. The Bogota here is about 1.5 m (4.9 ft) thick and consists of a fossiliferous shale with two fossiliferous nodular limestone layers. The lower nodular bed is a neomorphosed calcisiltite with scattered sand-sized bioclasts. The bioclasts include

abundant brachiopods, pelmatozoans, ostracodes, and trilobites, and prevalent encrusting and unattached foraminifers, gastropods, pelecypods, and carbonized plant debris. The upper nodular bed is a grain-supported biocalcarenite with neomorphosed bioclastic matrix and interparticle cement. Sand- to rudite-sized brachiopods, pelecypods, and pelmatozoans fragments are abundant; gastropods, encrusting and unattached foraminifers are prevalent, and bryozoans, corals, trilobites, fish scales, and plant debris are rare.

The Bogota Limestone is overlain by a conformable sequence of thick, gray, soft shale (underclay), thin, dark-olive calcareous shale, and very argillaceous limestone. The coal near the top of this exposure, tentatively correlated with the Trowbridge Coal, consists of interbedded coal and calcareous laminae.

complete large fossils occur at the top. A 3.2-m (10.5 ft) thick interval of shale separates the Effingham Limestone from the black sheety "Ingraham" shale at this exposure. The succeeding Bogota Limestone Member is poorly exposed, but fossils are weathering out of the limestone into the soil.

STOP 12: Lower Shumway cyclothem (fig. 12).

Location: South bank, Big Creek, from east of Illinois Highway 130, 200 ft FWL, 200 ft FSL, to 1,350 ft FWL, 1,000 ft FSL, SE/4, 15-T3N-R10E, Richland County.

The strata cropping out along the creek are the marine portion of the Shumway cyclothem, except for the sandstone at the top of the exposure. The sandstone was deposited in a fluvial channel that eroded down into the marine portion of the cyclothem and presumably represents the basal sandstone of the Wanless and Weller (1932) cyclothem.

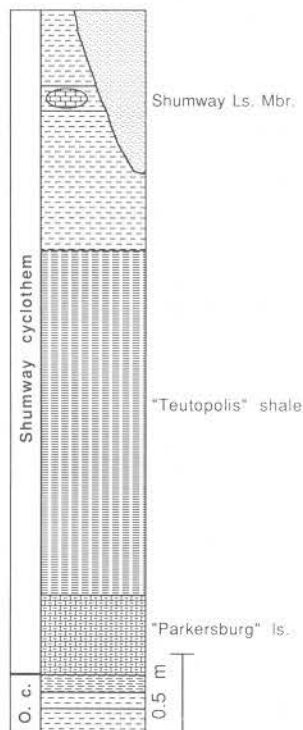


Figure 12 — Stratigraphic column of rocks at Stop 12.
O. c. = Omega cyclothem.

The "Parkersburg" limestone, the base of the modified Shumway cyclothem at the eastern edge of this exposure, is a dark-gray, sparsely fossiliferous argillaceous and carbonaceous limestone that is strikingly similar to the "Steel Bridge" limestone. Carbonaceous plant impressions are the only common macroscopic fossil. The limestone is thickest (53 cm/1.7 ft) at this outcrop, but thins abruptly and pinches out within 1.6 km (1 mi). It is an argillaceous calcisiltite containing sparse ostracodes. Thin-shelled small brachiopods, fish scales, and elongate algal clusters are rare. Silt-sized carbonized plant debris is scattered throughout and quartz silt is rare. The base of the unit is marked by alternating bitumen and bioclast laminae. The "Parkersburg" limestone is a facies equivalent of the "Lake Sara" limestone, which is absent in this area. The overlying black sheety "Teutopolis" shale, thicker here than at Stop 2, is succeeded by the Shumway Limestone Member, which here consists of fossiliferous limestone nodules in gray shale.

STOP 13: Lowermost Omega? cyclothem and underlying Calhoun Coal Member.

Location: East-trending ravine, 2,300 ft FNL, 2,800 ft FEL, 32-T3N-R14W, Richland County.

This locality is within an abandoned strip mine that operated prior to 1950. The exposures of the Calhoun Coal Member, with associated coal balls, and the overlying Bonpas Limestone Member probably were not mined because of the large coal-ball concentration. The stratigraphic column for Stop 14 (fig. 13) is also applicable to this site.

Coal balls have been collected from the Calhoun Coal since about 1937 (Phillips, Pfefferkorn, and Peppers, 1973), and because of their exquisite preservation, Calhoun specimens have been the basis for most paleobotanical studies of upper Pennsylvanian Illinois Basin coals (Galtier and Phillips, 1985). This locality ("New Calhoun") has been rigorously sampled over the past decade. In the outcrop, coal balls grade from marble-sized nodules at the top to massive intergrown sheets near the coal base. Ten profiles of coal balls from this site were used to test vertical trends in vegetation and determine how much variation occurs in this relatively small area. Coal samples for palynology

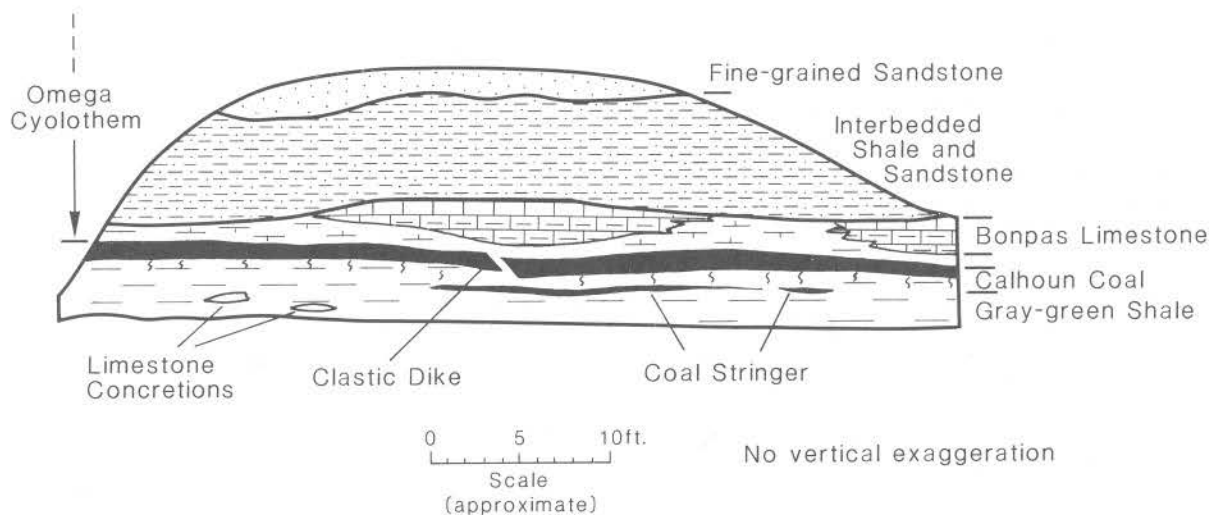


Figure 13 — Diagrammatic sketch of the exposure at Stop 14. Modified after Sweet (1983) and W.J. Nelson (unpublished IGS field notes, 1988).

also were taken from this site and elsewhere within the Calhoun Coal for comparison with megafossil evidence. Coal-ball peels were quantified using the techniques of Phillips et al. (1977); after coal maceration using Kosanke's (1950) methods, 300 spores per coal sample were identified and counted.

Ferns, mostly *Psaronius* tree ferns, averaged 58 percent of the biomass, dominating every coal-ball profile at the "New Calhoun" site. *Sigillaria*, an arborescent lycopod, is subdominant (25 percent), pteridosperms rank third (12 percent), sphenopsids are common (4 percent), but cordaites are rare (0.3 percent). Most of the peat is root material (44-76 percent), and stems are common (19-42 percent). Less than 10 percent and 5 percent of the peat are foliage and fructifications, respectively. Among the profiles, little consistent lateral variation exists; no successional trends were evident, although the sigillarian lycopods appear more abundant in the central part. Detection of vertical trends is difficult because profile zones are not laterally continuous or of similar thickness.

The Calhoun Coal spore flora is dominated by tree ferns (88 percent). Other fern spores are present (4 percent), as are sphenopsid spores (2.5 percent) and cordaite pollen (2 percent). Lycopod spores are absent, which is surprising because *Sigillaria* is subdominant in the coal-ball flora.

The roof shale and underclay also were palynologically studied. Tree ferns and small ferns, nearly

co-dominant in the roof shale flora, constitute 36 percent and 32 percent of the flora, respectively. Lycopod spores also are abundant; *Crassispora* (from *Sigillaria*) contributes 17 percent and *Endosporites* (from *Chaloneria*) 4 percent of the flora. *Calamospora* (sphenopsids) and *Florinites* (cordaites) also are present. Tree ferns dominate the underclay flora (66 percent), and spores of smaller ferns are subdominant (15 percent). Sphenopsid spores rank a close third (12 percent), cordaite pollen and lycopod spores are rare. Future consideration of compression and megaspore evidence from enclosing clastics in conjunction with palynological and petrification evidence should allow a much more complete understanding of vegetational history of the area before, during, and after the life of the Calhoun coal swamp.

STOP 14: Lowermost Omega? cyclothem and underlying Calhoun Coal Member.

Location: West-facing cut bank, Higgins Creek, 1,000 ft FEL, 1,100 ft FNL, 11-T2N-R14W, Richland County.

This locality, part of the abandoned Silas Bell strip mine, has an excellent exposure of the boundary between the marine portion of the Omega? cyclothem and the terrestrial portion of the underlying unnamed (or identified) cyclothem.

The Calhoun Limestone, described and named by Noe (1934), was renamed the Bonpas Limestone

Member by Kosanke et al. (1960). The Bonpas Limestone occurs only in Richland County and western Lawrence County (Nance and Treworgy, 1981). As discussed at Stop 1, we consider the Bonpas equivalent to the Omega Limestone Member on the basis of lithologic similarities, stratigraphic and geographic relationships to the Shumway cyclothem, and biostratigraphy (albeit inconclusive). This outcrop (fig. 13), about 1.6 km (1 mi) east of the type locality, is the best currently accessible Bonpas Limestone exposure. The following description incorporates observations made by Sweet (1983) and W.J. Nelson (unpublished ISGS field notes, 1988). The sequence of shale, claystone, coal, and mudstone beds beneath the limestone constitute the top of the unnamed cyclothem. At the bottom, the green-gray to gray shale is slightly silty and well laminated, and contains sideritic concretions and veins. The overlying soft, poorly laminated, olive-gray mudstone contains carbonaceous plant debris and a coal stringer near the base. The bright-banded Calhoun Coal Member is 0.33 m (1.1 ft) thick. At the top of the sequence is a gray calcareous mudstone containing scattered sideritic nodules.

The basal Omega? cyclothem here consists of the Bonpas Limestone, shale, and sandstone. The lower portion of the Bonpas is an argillaceous biocalcar-enite; the proportion of mud matrix increases towards the base (the basal contact is gradational), locally producing an argillaceous matrix-supported biocalcic siltite and shaly partings. The mud matrix is predominantly micrite, but contains clay and silt. The upper portion is a bioaccumulated brachiopodal-pelmatozoan limestone with coarse sparite cement. The limestone is lenticular, comprising a major lens about 4.6 m (15 ft) long near the middle of the exposure and another lens, partially exposed, at the southern end.

The overlying gray to brown micaceous shale is interbedded with fine-grained micaceous quartz sandstone or siltstone. The sandstone laminae have ripple marks on the top and tool marks on the base. The shale has soft-sediment deformation features and horizontal and vertical burrows. The contact with the overlying buff, fine- to medium-grained (fining upward) sandstone is sharp and apparently of erosional origin.

Bedding appears slightly arched over lenses of Bonpas Limestone and markedly depressed below.

Upper lens surfaces appear to be distinct bedding planes, but the lower contacts seem to grade into the underlying calcareous mudstone. A 3 cm (0.1 ft) wide clastic dike cuts the Calhoun Coal directly below the principal limestone lens.

Sweet (1983) suggested a Missourian age for the Bonpas Limestone, based on a fusulinid, *Triticites venustus* (Dunbar and Weller), and conodonts. *T. venustus* ranges from middle to late Missourian according to Sturgeon and Hoare (1968). The conodont taxa are also relatively long-ranging, but are similar to the *Spathognathodus minutus-S. ellisoni* fauna described by Merrill (1973) and considered Missourian. Whether the Bonpas is late Missourian or early Virgilian (as postulated by Weibel and Langenheim), can only be answered by further study.

STOP 15 (Optional): Calhoun Coal Member and basal Omega? cyclothem.

Location: Northeast-facing bank along southeast-trending ravine, 1,300 ft FWL, 1,150 ft FNL, 7-T2N-R13W, Lawrence County.

Unpublished ISGS field notes described a well-exposed succession, including the Calhoun Coal and Bonpas Limestone Members, in this ravine. A large concentration of coal balls locally replaced the entire coal bed. Over-zealous collecting of the coal balls about 20 years ago, including the reported use of dynamite and a bulldozer, has destroyed much of the outcrop. Presently the outcrop consists of an ascending sequence of gray claystone (76 cm/2.5 ft), Calhoun Coal (48-56 cm/1.6-1.8 ft), and a partly exposed Bonpas Limestone block that may have slumped. A large lens of coal balls, enveloped by thin coal layers, crops out; numerous displaced coal balls are present nearby in the streambed and on banks.

At this locality ("Berryville"), coal-ball samples (randomly collected) are dominated by *Psaronius* tree ferns, ranging from 64-74 percent biomass; seed ferns, mostly *Medullosa*, are subdominant (12.5-24 percent biomass). Sphenopsids comprise up to 9 percent of the peat biomass, and lycopods, primarily *Sigillaria*, represent up to 10.5 percent of the flora. Cordaites are rare, making up less than 1 percent of the biomass.

STOP 16: Friendsville Coal Member.

Location: Abandoned strip pit, approximately 1,100 ft FEL, approximately 2,000 ft FSL, SW/4, 5-T1N-R12W, Wabash County.

The Allendale Coal Corporation operated this mine from 1958 to 1965, working the Friendsville Coal Member. Unpublished ISGS field notes of outcrops just to the west described the following section, in upward order: underclay; coal, 0.86 m (2.8 ft); black shale, 2.5 cm (0.1 ft); and sandy shale, 0.88 m (2.9 ft).

The large aggregation of intergrown coal balls near the mine site is ideal for a small-scale study of lateral and vertical variations in vegetational composition of a Missourian coal. A 20-square-meter grid system was superimposed on the mass, and vertical profiles were collected from most of the grid blocks. Coal

samples for palynological analysis also were collected near the coal-ball mass and elsewhere within the Friendsville Coal.

The Friendsville flora, averaged from all samples, is strongly dominated by ferns (69 percent), mostly *Psaronius*, with medullosan pteridosperms subdominant (15 percent). Calamites were common (4 percent), and lycopods were rare (0.5 percent); however, cordaites, at 9.5 percent biomass, were more abundant than in any other paralic, late Pennsylvanian coal swamp studied thus far (Galtier and Phillips, 1985). Roots are the major biomass contributors (76 percent), foliage second, stems third, and fructifications last (Willard, 1985).

No successional patterns were detected in coal-ball profiles, but lateral variation was marked (fig. 14). The grid system allowed the adequacy of single profiles to be evaluated for representation of entire

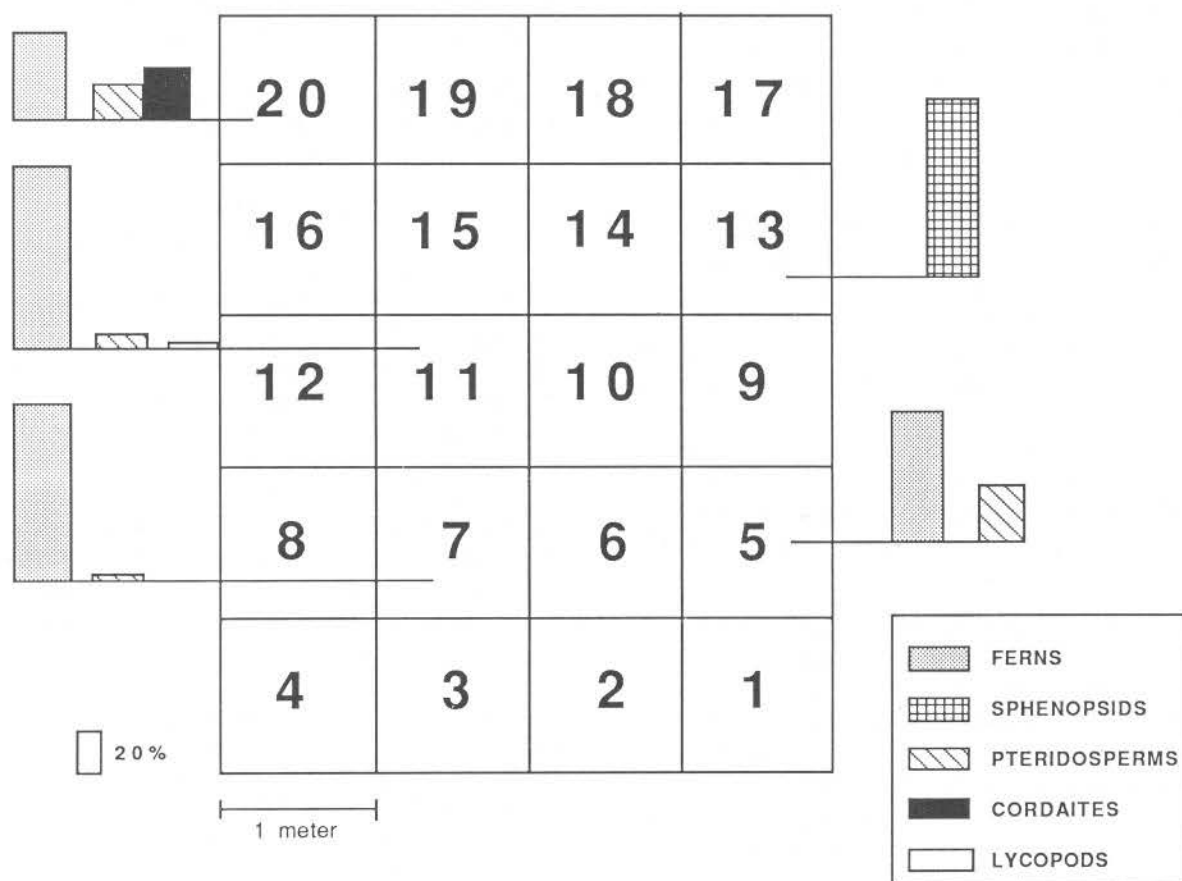


Figure 14 — Relative abundance of major plant groups from coal-ball profiles collected in grid in the Friendsville Coal Member at Stop 16.

plant communities. Block 7 was strongly dominated by tree ferns; two semi-erect *Psaronius* trunks were found in blocks 6 and 7. The largest calamite stem known from the Illinois Basin had fallen across the area of blocks 13 and 14; calamite wood comprised 98 percent of the peat biomass from those blocks. The abundance of cordaite wood in and around block 20 also suggests preservation of the roots of one tree. The strong influence of individual plants on quantitative results emphasizes the need for laterally extensive collections of coal balls and exposes biases that must be considered in quantitative data interpretation.

Spore flora of the Friendsville Coal Member corresponds fairly well with the average floral composition of all coal-ball samples. The seed ferns, however, are unrepresented because their prepollen is too large to be included in standard palynological

preparations. Like the peat data, vertical trends in vegetational composition or abundance were not evident from the palynological studies. Tree fern spores average 86 percent of the spore flora and other fern spores comprise 7 percent of the flora. Sphenopsid spores, mostly *Calamospora*, rank third (4 percent), and lycopod spores, mostly *Crassispora* and cordaite pollen are rare.

Paleobotanical and palynological evidence indicate low floristic diversity and dominance of tree ferns in the Friendsville coal-swamp flora. Subdominant pteridosperms were scattered rather regularly among the tree ferns, but calamites, cordaites, and sigillarian lycopods were interspersed more sparsely throughout the ancient forest. Understory plants, including small ferns, lycopods, and seed ferns, are better represented in the spore record than in the coal-ball peat.

REFERENCES

- Boardman, D.R., and Heckel, P.H., 1989, Glacial-eustatic sea-level curve for early Upper Pennsylvanian sequence in north-central Texas and biostratigraphic correlation with curve for midcontinent North America, in Boardman, D.R., Barrick, J.E., Cocke, J., and Nestell, M.K., eds., Middle and Late Pennsylvanian chronostratigraphic boundaries in north-central Texas: glacial-eustatic events, biostratigraphy, and paleoecology (Part II-contributed papers): Texas Tech University Studies in Geology 2, p. 63-73.
- Cady, G.H., 1948, Analyses of Illinois coals: Illinois State Geological Survey Bulletin, supplement to v. 62, 77 p.
- Cooper, C.L., 1946, Pennsylvanian ostracodes of Illinois: Illinois State Geological Survey Bulletin, v. 70, 177 p.
- Dunbar, C.O., and Condra, G.E., 1927, The Fusulinidae of the Pennsylvanian System in Nebraska: Nebraska Geological Survey Bulletin, 2nd series, v. 2, 135 p.
- Dunbar, C.O., and Henbest, L.G., 1942, Pennsylvanian Fusulinidae of Illinois: Illinois State Geological Survey Bulletin, v. 67, 218 p.
- Galtier, J., and Phillips, T.L., 1985, Swamp vegetation from Grand' Croix (Stephanian) and Autun (Autunian), France, and comparisons with coalball peats of the Illinois Basin, in Dutro, J.T., Jr., and Pfefferkorn, H.W., eds., Compte Rendu, Neuvième Congrès International de Stratigraphie et de Géologie du Carbonifère, v. 5: Paleontology, Paleocology, Paleogeography, p. 13-24.
- Heckel, P.H., 1977, Origin of phosphatic black shale facies in Pennsylvanian cyclothems of midcontinent North America: American Association of Petroleum Geologists Bulletin, v. 61, p. 1045-1068.
- _____, 1984, Factors in mid-continent Pennsylvanian limestone deposition, in Hyne, N.J., ed., Limestones of the mid-continent: Tulsa Geological Society Special Publication 2, p. 25-50.
- _____, Brady, L.L., Ebanks, W.J., Jr., and Pabian, R.K., 1979, Field guide to Pennsylvanian cyclic deposits of Kansas and Nebraska: Kansas Geological Survey Guidebook, series 4, p. 4-60.
- Hopkins, M.E., and Simon, J.A., 1975, Pennsylvanian System, in Willman, H.B., et al., Handbook of

- Illinois Stratigraphy: Illinois State Geological Survey Bulletin, v. 95, p. 163-201.
- Kosanke, R.M., 1950, Pennsylvanian spores of Illinois and their use in correlation: Illinois State Geological Survey Bulletin, v. 74, 128 p.
- _____, Simon, J.A., Wanless, H.R., and Willman, H.B., 1960, Classification of the Pennsylvanian strata of Illinois: Illinois State Geological Survey Report of Investigations, v. 214, 84 p.
- Langenheim, R.L., Jr., and Scheihing, M.H., 1983, Detailed biostratigraphic correlation, Shumway "cyclothem," Virgilian, Illinois Basin [abs.]: Geological Society of America Abstracts with Programs, v. 15, no. 4, p. 265.
- Merrill, G.K., 1973, Pennsylvanian nonplatform genera, I: *Spathognathodus*: Journal of Paleontology, v. 47, p. 289-315.
- Moore, R.C., 1936, Stratigraphic classification of the Pennsylvanian rocks of Kansas: Kansas Geological Survey Bulletin 22, 256 p.
- _____, 1959, Geological understanding of cyclic sedimentation represented by Pennsylvanian and Permian rocks of northern Midcontinent Region, in Moore, R.C., and Merriam, D.F., Twenty-third Field Conference Guidebook, Kansas Geological Society and State Geological Survey of Kansas, p. 41-50.
- Moore, R.C., et al., 1944, Correlation of Pennsylvanian formations of North America: Geological Society of America Bulletin, v. 55, p. 657-706.
- Nance, R.B., and Treworgy, C.G., 1981, Strippable coal resources of Illinois, part 8—central and southeastern counties: Illinois State Geological Survey Circular, v. 515, 32 p.
- Needham, C.E., 1931, Notes on the Pennsylvanian rocks of Jasper County, Illinois: Transactions of the Illinois Academy of Science, v. 23, p. 426-429.
- Newton, W.A., and Weller, J.M., 1937, Stratigraphic studies of Pennsylvanian outcrops in part of southeastern Illinois: Illinois State Geological Survey Report of Investigations, v. 45, 31 p.
- Noe, A.C., 1934, Our present knowledge of American coal ball plants: Transactions of the Illinois Academy of Science, v. 26, no. 3, p. 103.
- Peppers, R.A., 1984, Comparison of miospore assemblages in the Pennsylvanian System of the Illinois Basin with those in the Upper Carboniferous of Western Europe, in Sutherland, P.K., and Manger, W.L., eds., Compte Rendu, Neuvième Congrès International de Stratigraphie et de Géologie du Carbonifère, v. 2: Biostratigraphy, p. 483-502.
- Phillips, T.L., Kunz, A.B., and Mickish, D.J., 1977, Paleobotany of permineralized peat (coal balls) from the Herrin (No. 6) Coal Member of the Illinois Basin, in Given, P.N., and Cohen, A.D., eds., Interdisciplinary studies of peat and coal origins: Geological Society of America, Microform Publication, no. 7, p. 18-49.
- Phillips, T.L., Peppers, R.A., and DiMichele, W.A., 1985, Stratigraphic and interregional changes in Pennsylvanian coal-swamp vegetation: environmental inferences: International Journal of Coal Geology, v. 5, p. 43-109.
- Phillips, T.L., Pfefferkorn, H.W., and Peppers, R.A., 1973, Development of paleobotany in the Illinois Basin: Illinois State Geological Survey, Circular 480, 86 p.
- Scheihing, M.H., 1978, A paleoenvironmental analysis of the Shumway Cyclothem (Virgilian, Effingham County, Illinois) [unpublished M.S. thesis]: Urbana, University of Illinois, 186 p.
- _____, and Langenheim, R.L., Jr., 1978a, Mollusca and a trilobite from the Shumway Cyclothem, Mattoon Formation, Pennsylvanian, Illinois: Transactions of the Illinois Academy of Science, v. 71, no. 1, p. 2-23, 124 [Published in 1979].
- _____, 1978b, Lingulid, rhynchonellid and spiriferid brachiopods from the Shumway Cyclothem, Mattoon Formation, Pennsylvanian of Illinois: Transactions of the Illinois State Academy of Science, v. 71, p. 165-182 [Published in 1979].
- _____, 1980, Brachiopods of the suborder Strophomenidina from the Shumway Cyclothem,

- Mattoon Formation, Virgilian of Illinois: *Journal of Paleontology*, v. 54, p. 1019-1034.
- _____, 1985, Depositional history of an Upper Pennsylvanian cyclothem in the Illinois Basin and comparison to Kansas cyclothem sequences, in Dutro, J.T., Jr., and Pfefferkorn, H.W., eds., *Compte Rendu, Neuvième Congrès International de Stratigraphie et de Géologie du Carbonifère*, v. 5: Paleontology, Paleogeology, Paleogeography, p. 373-382.
- Sweet, M.L., 1983, A paleoenvironmental analysis of the Late Missourian (Pennsylvanian) Bonpas Limestone Member, Mattoon Formation, east-central Illinois [unpublished M. S. thesis]: Urbana, University of Illinois, 63 p.
- Sturgeon, M.T., and Hoare, R.D., 1968, Pennsylvanian brachiopods of Ohio: *Ohio Geological Survey Bulletin*, v. 63, 95 p.
- Tucker, J.K., 1976, A coiled nautiloid fauna from the Mattoon Formation (Pennsylvanian) of Illinois: *Transactions of the Illinois Academy of Sciences*, v. 69, p. 57-77.
- _____, and Paukstis, G.L., 1977, An Upper Pennsylvanian *Paraconularia* (Coelenterata: Conulariina): *Transactions of the Illinois Academy of Sciences*, v. 69, p. 501-502.
- Udden, J.A., 1912, Geology and mineral resources of the Peoria Quadrangle, Illinois: *United States Geological Survey Bulletin*, v. 506, 103 p.
- Vail, P.R., Hardenbol, J., and Todd, R.G., 1984, Jurassic unconformities, chronostratigraphy, and sea-level changes from seismic stratigraphy and biostratigraphy, in Schlee, J.S., ed., *Interregional unconformities and hydrocarbon accumulation: American Association of Petroleum Geologists, Memoir 36*, p. 129-144.
- Wanless, H.R., 1956, Classification of the Pennsylvanian rocks of Illinois as of 1956: *Illinois State Geological Survey Circular*, v. 217, 14 p.
- _____, 1975, Illinois Basin region, in McKee, E.D., and Crosby, E.J., eds., *Paleotectonic investigations of the Pennsylvanian System in the United States; Part 1, Introduction and regional analysis of the Pennsylvanian System: United States Geological Survey Professional Paper 853-E*, p. 71-95.
- _____, and Weller, J.M., 1932, Correlation and extent of Pennsylvanian cyclothem: *Geological Society of America Bulletin*, v. 43, no. 4, p. 1003-1016.
- Weibel, C.P., 1985, Three Virgilian coal beds, Mattoon Formation, east-central Illinois [abs.]: *Geological Society of America Abstracts with Programs*, v. 17, no. 5, p. 331.
- _____, 1986, Resolution of stratigraphic disarray (Virgilian of Illinois Basin) [abs.]: *Geological Society of America Abstracts with Programs*, v. 18, no. 4, p. 330.
- _____, 1988, Stratigraphy, depositional history, and brachiopod paleontology of Virgilian strata of east-central Illinois [unpublished Ph.D. Thesis]: Urbana, University of Illinois, 228 p.
- Weller, J.M., 1930, Cyclical sedimentation of the Pennsylvanian Period and its significance: *Journal of Geology*, v. 38, no. 2, p. 97-135.
- _____, and Bell, A.H., 1941, Explanation and summary, in Newton, W.A., *Surface structure map of Shelby, Effingham, and Fayette Counties: Illinois State Geological Survey Report of Investigations*, v. 76, p. 5-21.
- Weller, J.M., Henbest, L.G., and Dunbar, C.O., 1942, Stratigraphy of the fusuline-bearing beds of Illinois, in Dunbar, C.O., and Henbest, L.G., *Pennsylvanian Fusulinidae of Illinois: Illinois State Geological Survey Bulletin*, v. 67, p. 9-34.
- Willard, D.A., 1985, Upper Pennsylvanian coal-swamp vegetation of the Illinois Basin coal field [unpublished M.S. thesis]: Urbana, University of Illinois, 97 p.
- Worthen, A.H., 1875, *Geology and palaeontology: Geological Survey of Illinois*, v. 6, 532 p.

Field Trip No. 18

**SELECTED
ECONOMIC MINERAL DEPOSITS
OF CENTRAL ARKANSAS**

**J. Michael Howard, Charles G. Stone,
and Benjamin F. Clardy**
Arkansas Geological Commission
3815 West Roosevelt Road
Little Rock, Arkansas 72204

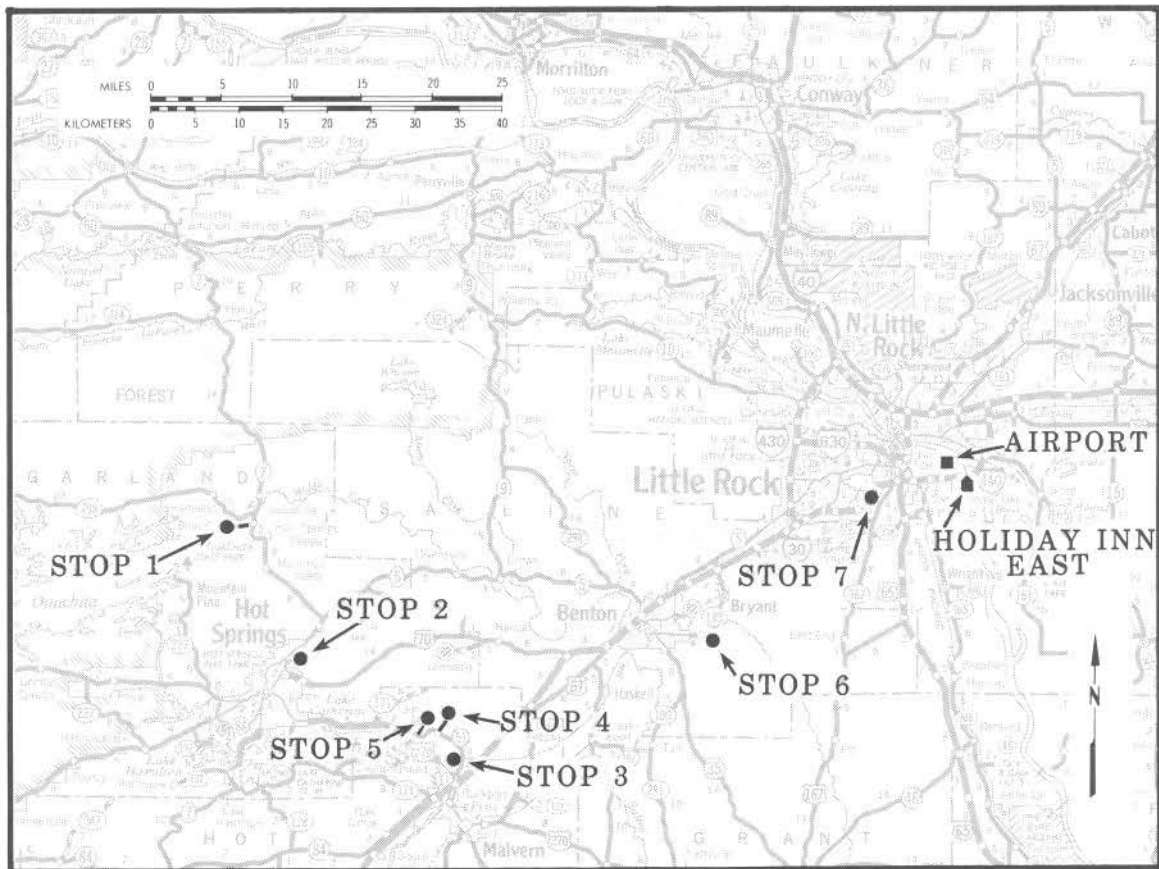


Figure 1 — Field trip stops.

INTRODUCTION

Central Arkansas geology is both complex and varied. The formation of the Ouachita Mountains, hydrothermal vein systems, igneous intrusives, and Cenozoic Gulf Coastal Plain sedimentation and weathering have all played a part in forming mineral

deposits. The purpose of this trip is to examine some economic mineral deposits in central Arkansas and their relation to regional geology (fig. 1). Each site description was revised and updated from one or more guidebooks listed in the references.

DAY 1

Milky quartz veins, abundant in the complexly deformed Paleozoic rocks in the core of the Ouachita Mountains, occur in a wide belt extending from Little Rock, Arkansas to near Broken Bow, Oklahoma. They are up to 100 ft wide, and typically may contain adularia, chlorite, calcite, and dickite, and occasionally rectorite, pyrophyllite, and cookeite. Certain metals, including lead, zinc, silver, copper, antimony, and mercury, are associated with the veins.

The milky quartz and associated minerals are hydrothermal deposits of tectonic origin. Veins formed during the closing stages of the Late Pennsylvanian-Early Permian orogeny in the Ouachita Mountains commonly fill rock fractures and joints and are often closely associated with thrust faults. Smoky quartz crystals occur with vanadium, titanium, and lithium mineralization in the contact-metamorphosed Paleozoic rocks adjacent to Magnet Cove and are considered Late Cretaceous.

Some milky quartz veins have cavities containing crystal clusters suitable for mining. Individual quartz crystals up to 5 ft long, weighing over 400 pounds, and crystal clusters 15 ft long, weighing over 5 tons, have been produced from various mines. Most mined crystals are from fracture-filling veins in the Ordovician Crystal Mountain and Blakely sandstones near Mount Ida, central Montgomery County, and near Jessieville, northern Garland County, respectively. Because of the aesthetic beauty of many of the crystals and crystal clusters, the principal market over the years has been for mineral specimens. Other uses have been oscillators in communications equipment during World War II, for fusing quartz, and as lasca—the chemical feedstock for vitreous silica or for growing cultured quartz. Some crushed milky quartz has been used as aggregate in precast concrete.

It should be noted that “Hot Springs Diamonds” in local rock shops and jewelry stores are Arkansas quartz crystal, not diamonds from the Crater of Diamonds State Park at Murfreesboro.

STOP 1: QUARTZ CRYSTAL MINE

We thank Mr. Ron Coleman for permitting us access to the Coleman Quartz Mine and for invaluable assistance in examining this deposit, approximately 2 mi west of Blue Springs, Garland County, Arkansas.

The Coleman Quartz Mine is also known as the Geomex Mine, West Chance Area, Dierks No. 4 Mine and Blocker Lead (fig. 2). The quartz crystals are in veins in limy sandstone and conglomeratic sandstone beds of the probable Blakely Sandstone (Middle Ordovician). Beds of conglomeratic sandstone exposed in the pit contain abundant weathered meta-arkose and granitic boulders, cobbles, and pebbles, and some clasts of limestone, chert, and shale. These sediments were probably deposited in submarine fan channels and were derived from a granite-rich terrane to the north-northeast. It has been postulated that the exotic boulders are mostly Precambrian. This area contains many thrust-faulted sequences; at least two major periods of folding resulted in differing attitudes in fold hinge lines and axial planes. The mine is on the nose of a large, complexly deformed syncline.

The quartz crystal veins are fracture fillings; the larger and more productive cavities are at the intersection of two veins. Mining operations are relatively simple, consisting initially of removing overburden and loose rock with a bulldozer to expose crystal-filled cavities. The quartz crystals are removed with hand tools.

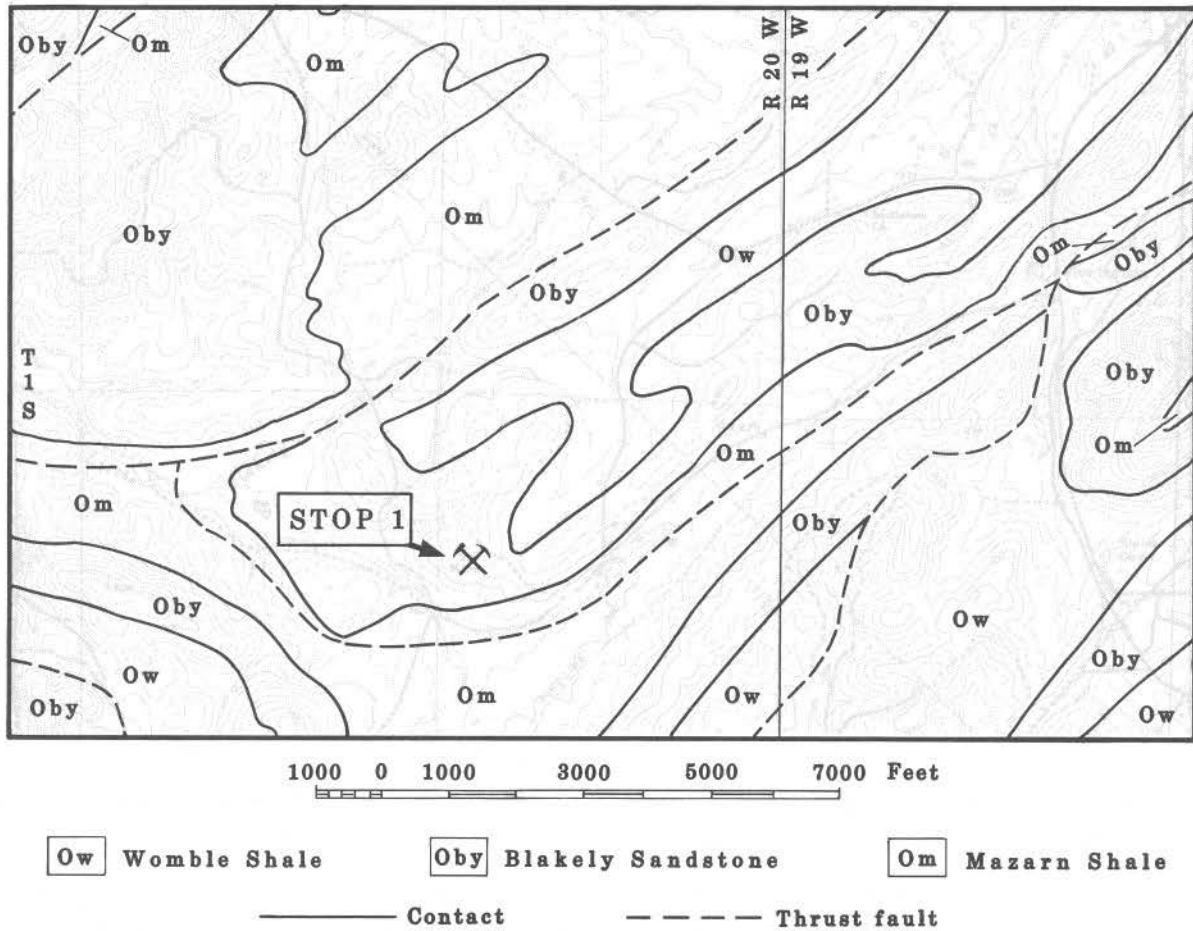


Figure 2 — Coleman quartz mine, west of Blue Springs, Garland County, Arkansas.

Geomex Mine Services, Inc. produced 2.5 million pounds of lasca in 1984, placing Arkansas as the world's leader in lasca production. Geomex ceased production in 1985. In 1988 Ron Coleman Mining Company bought Geomex's plant and property and began lasca production. The six grades of quartz produced are the feedstock for a variety of commercial applications, including cultured quartz, fiber optics, and vitreous silica.

The outlook of quartz mining in Arkansas looks bright. Demand is steady for specimen and commercial quartz production. In over 100 years of mining approximately 5 percent of the quartz that is estimated to be available by open pit methods has been mined.

STOP 2: SMITH WHETSTONE COMPANY'S PLANT

We thank Mr. Richard Smith and Mr. Murray Harding for permission to visit the Smith Whetstone factory, 1500 Sleepy Valley Road, Hot Springs, Arkansas (fig. 1).

Most companies that produce whetstones from the Arkansas Novaculite are in the Hot Springs area. The Hiram J. Smith Company of Hot Springs has been in business since 1885.

Indians were the first known to use Arkansas novaculite. They came from afar to get the rock, and took it as rough blocks to their camps, where they shaped it into arrowheads, spear points, knives,

plows, scrapers, and other implements; thus, novaculite chips may be found over a large region. "Novaculite" is from a Latin word meaning "sharp knife"; the conchoidal fracture of the rock makes it possible to shape it to a thin, keen edge.

The more modern use of novaculite is for whetstones, the finest honing stones available, sold the world over as Arkansas oilstones. It has been quarried in the Hot Springs area since 1832 by only a few families or groups. One of these, the Hiram Smith family, is now represented by a fourth generation of whetstone men. The company, founded in 1885 by Mr. James A. Smith, was turned over in 1905 to James' son, Archer. Archer's son, Mr. Hiram Smith, entered the business in 1938, at the age of 18. Up to 1962 the Smiths quarried the stone and shipped it in rough blocks to manufacturers in eastern United States, Europe, and Japan for finishing. In 1962 Hiram learned the meticulous technique of finishing the stones himself and found a ready demand. Mr. Richard Smith, Hiram's son, presently owns and operates Smith's Whetstone Company.

A Smith brochure describes novaculite block processing as follows:

"The rough Novaculite is cut by diamond saws, using large amounts of degradable lubricant as a coolant. Each stone is cut individually by hand, so the quality of each stone is graded many times during the cutting process. To properly cut whetstones, it often takes many, many months to learn the technique of diamond saw operation.

"Each stone is lapped (smoothed) on horizontal grinding wheels using industrial grit as an abrasive. This process removes any ridges or saw marks on the stones. The edges of each stone are beveled on vertical grinding wheels to smooth any rough edges the stones may have. During this finishing process each stone is again graded for quality. Due to the hand cutting and finishing of each individual stone, tolerances will be plus or minus $1/16$ of an inch."

Smith's produces four grades of whetstones. *Washita* stone, the fastest cutting grade, with the lowest specific gravity, is used by commercial knife sharpeners, butchers, sportsmen, wood carvers, and others who desire a quick keen edge; much of this stone is of the rainbow type. *Soft Arkansas* grade, a general purpose stone for kitchen cutlery, hunting

knives, and pocket knives, produces a polished as well as keen edge; most of this stone is gray or gray marbled. *Hard Arkansas* grade, white or almost so, produces a fine polished edge; it is used by gunsmiths, dentists, surgeons, watchmakers, precision toolmakers, and finicky sportsmen. *Hard Arkansas* stones are the only stones for the precision sharpening and polishing of surgical instruments. Densest of all grades, the *Black Hard Arkansas* stone, is used for polishing the final finish on edges already extremely sharp.

STOP 3: BUTTERFIELD NOVACULITE QUARRY

We thank Mr. Gary Coleman for permission to visit this active quarry. The Butterfield Quarry is approximately one-half mile west of Arkansas Highway 51, near the Butterfield community, Hot Spring County.

Arkansas novaculite is an unusual type of rock, to which Schoolcraft, as early as 1819, gave the name "novaculite," a term now in general use. Although this kind of rock is uncommon in most areas, it is widely distributed in the Ouachita Mountains, where it crops out in an almost unbroken trend from around Little Rock, in Pulaski County, Arkansas, westward about 200 mi, to McCurtain County, Oklahoma. Its greatest outcrop extent, north to south, is in the eastern Ouachitas, where it is more than 30 mi between the northernmost and southernmost outcrops. Because of the resistance of the rock, novaculite stands out as steep, narrow ridges; the younger and the older beds form the adjacent valleys. Novaculite is thickest in southern outcrops, where it averages about 700 ft, but thins northward rather rapidly. Novaculite rock is dense, homogeneous, highly siliceous, translucent on thin edges, and is commonly bluish white; its color may be red, green, brown, yellow, and even black, the various shades resulting from carbonaceous matter or iron and manganese oxides. As it weathers the rock loses calcium and manganese carbonate and becomes white and porous. The Arkansas Novaculite is Mississippian-Devonian; the formation's shales often contain conodonts and other fossils.

Butterfield quarry (fig. 3) is one of several quarries in the lower division of the Arkansas Novaculite, in Garland and Hot Spring Counties, Arkansas, that

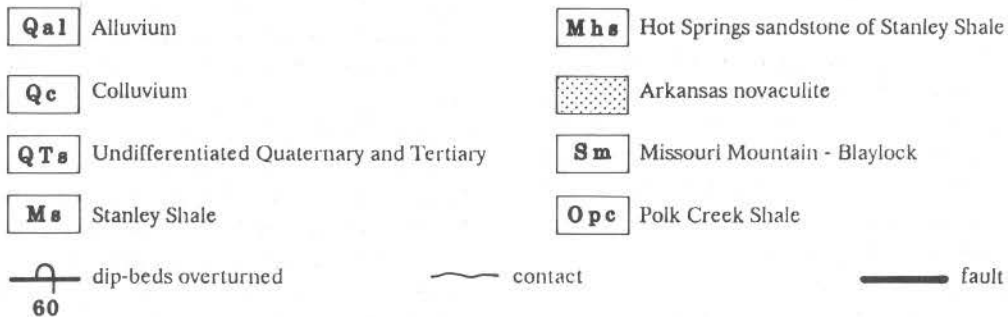
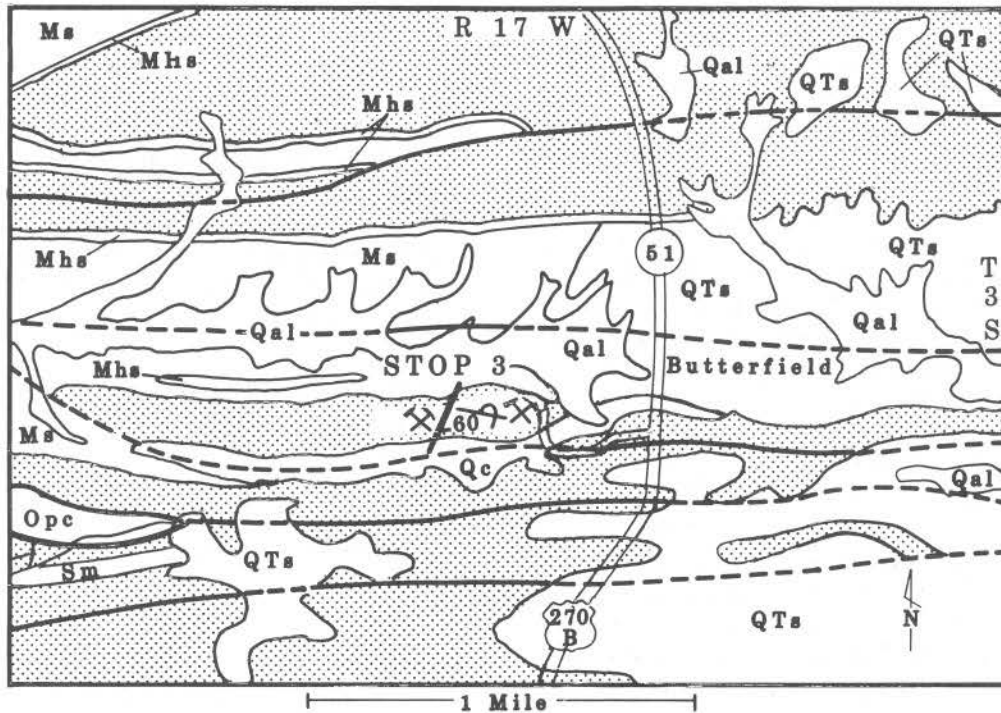


Figure 3 — Butterfield quarry, west of Butterfield, Hot Spring County, Arkansas.

produce novaculite, which is quarried from rather thin, even beds of slightly weathered, white to light gray novaculite near the base of the lower division of the formation. This particular quarry produced crushed stone. Present operations are for high silica raw material.

STOP 4: N.L. BAROID'S CHAMBERLAIN CREEK BARITE DEPOSIT

We thank Mr. John Firestone, Operations Superintendent, for permission to examine this mine. The Chamberlain Creek mine is 2 mi northeast of Magnet

Cove, Hot Spring County. The barite deposit is currently inactive, but ore still remains in deeper portions of the syncline to the west.

The two companies formerly operating this mine produced over 9 million tons of barite from this deposit. Exploitation began in 1939 when the Magnet Cove Barium Corporation started to mine and mill, concentrating the ore by flotation. The Baroid Division of National Lead Industries started mining and milling barite in 1942.

The office and mill of Baroid Division of National Lead Industries (now N.L. Baroid) was on the

southern limb of the syncline, from along which they originally stripped the shallow ore. By pit mining, Baroid Division then took the main body of ore in Chamberlain syncline, but later, the depth of the ore forced them to go exclusively to underground mining. Mining at the deposit ceased several years ago. For a short time the mill processed ore from deposits in Montgomery County, but it was recently sold for scrap.

During milling the ore was ground to 325 mesh and processed by froth flotation. The concentrates contained about 98 percent BaSO_4 with a loss of only about 10 percent of the original values. All barite produced from this deposit was used as a weighting agent in oil well drilling muds.

The Chamberlain Creek barite deposit (fig. 4), a stratiform deposit at the base of the Mississippian Stanley Shale, is essentially conformable with the bedding of the enclosing sediments and averages 60 ft thick. The deposit was in an asymmetrical syncline, which plunges southwest toward the Magnet Cove intrusive 1 mi westward; erosion has truncated it at its eastern end, thereby making the orebody spoon-like. The maximum length of the orebody was 3,200 ft; its maximum width was 1,800 ft. Some ore was nodular, but most had a dark-gray dense appearance resembling limestone. The barite was intimately mixed with minor amounts of fine-grained quartz, pyrite, and shale. High-grade ore was 85 percent BaSO_4 , 11 percent SiO_2 , and 3 percent iron oxide and alumina. The average mill feed was about 60 percent BaSO_4 .

Origin of Arkansas barite has been subjected to many investigations, including two Ph.D. dissertations: B.J. Scull, University of Oklahoma, 1956 (published 1958, Arkansas Geological and Conservation Commission, Information Circular 18) and R.A. Zimmermann, University of Missouri at Rolla, 1964. Scull postulated that all Arkansas barite deposits were lower Upper Cretaceous, derived from the sub-silicic Upper Gulf Coastal Plain igneous suite and, with the sulfide deposits in the Ouachita Mountains, represent a minerogenetic province. Zimmermann concentrated on the deposits in the Stanley Formation (several thousand times greater in volume than the combined other types of deposits) and postulated that they are of sedimentary origin, and thus Mississippian.

GRANDE (GAMMA RAY AND NEUTRINO DETECTOR), AN ASTROPHYSICAL PROJECT TO UTILIZE AN ABANDONED BARITE MINE.

In March of 1987 the High Energy Group, headed by scientists from the University of California, Irvine, and comprising astrophysicists from several other universities, initiated a search for a site to construct the world's largest Gamma Ray and Neutrino Detector (GRANDE). Detector design required a lake or large water-filled pit; the detector will be below water level.

The Arkansas Geological Commission (AGC) suggested the abandoned Chamberlain Creek barite pit owned by N.L. Baroid, a location that seemed to meet all requirements of the High Energy Group. By October of 1987 it was determined that the Arkansas site was the most suitable. N.L. Baroid agreed to donate the pit to the University of Arkansas system if the project was funded.

The detector is designed to have two functions. As a neutrino telescope it is designed to study point sources of high-energy extraterrestrial neutrinos and very high energy neutrino interaction. The gamma ray telescope will detect and study very high energy and ultra high energy gamma ray sources. The project needs such a large body of water, because GRANDE will be 100 times larger than any existing detector of its type. It will open new frontiers in the study of high-energy physics.

The AGC agreed to cooperate with the U.S. Geological Survey Water Resources Division to study pit and surrounding area hydrology. A magnetic survey of the pit, completed in 1988, assisted in detector design.

The High Energy Group submitted a funding proposal to the Department of Energy; it is estimated that it will cost over \$30 million to construct and to begin operating the facility. The University of Arkansas at Little Rock and the University of Arkansas system, now part of the High Energy Group, are responsible for the section of the funding proposal concerned with site preparation.

This has been an unusual experience for the AGC but a very rewarding one. If funding is successful and the detector is built it will probably result in a most unique reclamation project.

DAY 2

STOP 5: CHRISTY VANADIUM-TITANIUM MINE

We thank Mr. Dan Harris of Stratcor, Inc. for permission to visit this mine.

The Christy deposit is on the east rim of Magnet Cove, Hot Spring County, about a half mile northwest of the community of Magnet Cove (fig. 5). The U.S. Bureau of Mines in 1949 established the extent of the titanium mineralization (brookite-rutile) by drilling the deposit, which is partly on top and partly

on the south slope of an east-west ridge of metamorphosed Arkansas Novaculite. The ridge, the south limit of the Chamberlain Creek syncline, is overturned so that the sediments dip about 45° south. A few hundred feet westward of the deposit a coarse-grained nepheline syenite intrusive truncates the syncline. USBM core sample analyses varied from less than 1 percent to a maximum of 26 percent TiO_2 , averaging about 5 percent TiO_2 for the orebody. Appreciable percentages of V_2O_5 (1 to 2 percent) occur in several core samples. Union Carbide Corporation leased this property during their vanadium-titanium exploration program in Arkansas in the mid-1960's; the deposit was drilled out by Union Carbide. A developmental test pit, dug in 1975, allowed testing the ore for amenability to their present mill at Wilson Springs and blendability of Christy ore with those of Wilson Springs. The Christy vanadium ore is a goethite-rich clay and brookite; it averages slightly less than 1 percent V_2O_5 . In December 1981 ore-stockpile sites and water-control ponds were selected. Overburden stripping began in fall 1983; the mine operated until fall 1985. Mining operations by Stratcor, Inc. resumed in early February 1989.

Besides brookite, minerals with the vanadium ores include smoky quartz, taeniolite, rutile, anatase, siderite, pyrite, and rarely eggonite ($ScPO_4 \cdot 2H_2O$).

Fryklund and Holbrook (1950) suggested that the Christy deposit formed by the introduction of mineralizing fluids from the Magnet Cove intrusion into the folded and metamorphosed Arkansas Novaculite, with subsequent erosion and weathering of mineralized rock. In a recent investigation of TiO_2 polymorph-bearing vein deposits adjacent to the Magnet Cove intrusion, Viscio (1981) discovered adularia at the Hardy-Walsh brookite deposit (approximately 2 mi to the NNW) on the northern limb of the Chamberlain Creek syncline, a fact suggesting that the brookite deposits adjacent to Magnet Cove may be an aborted initial phase alkali metasomatism (fentization) by late fluids from the Magnet Cove intrusion.

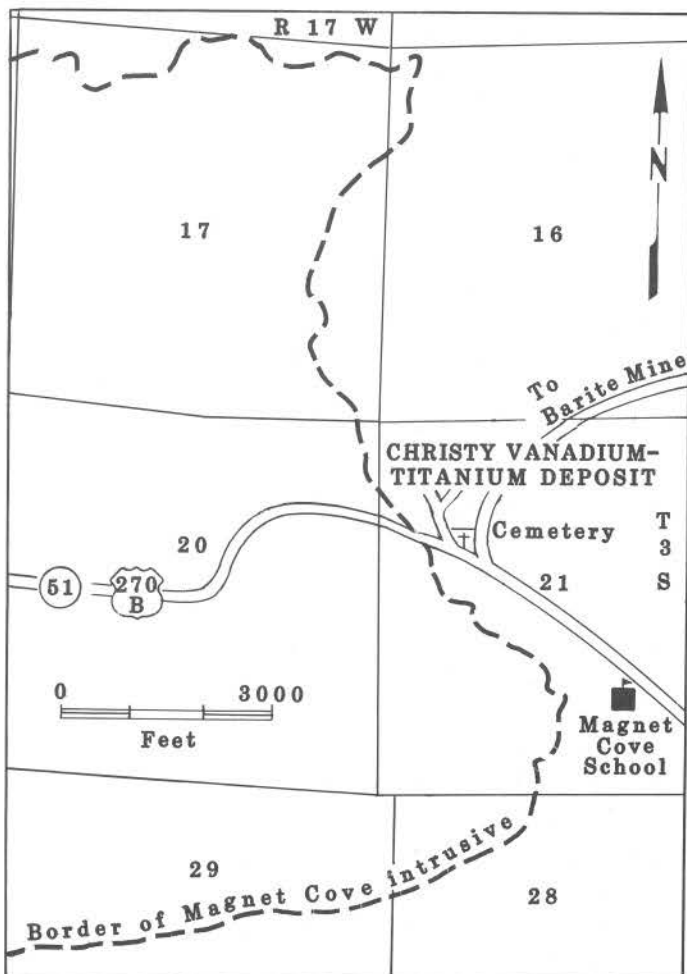


Figure 5 — Christy vanadium-titanium deposit, near Magnet Cove, Hot Spring County, Arkansas.

STOP 6: ALCOA BAUXITE MINE, SALINE COUNTY, ARKANSAS

We thank Miss Clarenda Eaton for permission to visit ALCOA'S property in Saline County, Arkansas.

Bauxite, the major aluminum ore was first identified in Arkansas by State Geologist John C. Branner, in 1887; it has been mined commercially since 1899. Arkansas bauxite production in 1972 was over 2 million tons. For many years Arkansas has produced more than 90 percent of domestic bauxite. Arkansas bauxite is now mostly used for making alumina chemicals; other important uses are for abrasives, refractories, and alumina cements.

In addition to ALCOA, there are three smaller bauxite producers. American Cyanamid Company and Stauffer Chemical mine and ship high-grade dried bauxite and kaolinite clay to the chemical and abrasive industry; Porocel Corporation processes bauxite for the chemical industry. Reynolds Company, a former major Arkansas bauxite producer, is now closed.

Bauxite deposits (fig. 6) are centered around nepheline syenite intrusives. Nepheline syenites and related Late Cretaceous igneous rocks were intruded into highly folded Paleozoic beds. Subsequent erosion subjected parts of the intrusives to weathering and to partial burial later by Tertiary sediments. Central Arkansas bauxite deposits resulted from early Eocene lateritic weathering of the nepheline syenites.

According to Gordon, Tracey, and Ellis (1958), the bauxite deposits can be classified into four types:

- (1) Residual deposits on the upper slopes of partly buried nepheline syenite hills.
- (2) Colluvial deposits at the base of the Berger Formation (lowermost formation of the Eocene Wilcox Group).
- (3) Stratified deposits in the Berger Formation.
- (4) Conglomeratic deposits at the base of the Saline Formation (in the Wilcox Group just above the Berger Formation).

Bauxite in the various mines differs considerably in its character and physical properties. Most of it is pisolitic, and varies from very hard to soft and earthy. Generally, it is hard at the top of a deposit, firm to mealy in the middle, and clayey, though not

plastic, at the base. It varies from light gray through tan and brown to red. Color is not necessarily an index of grade nor of the amount of iron present; some brick-red bauxite has very little iron. The principal mineral in bauxite is gibbsite (aluminum trihydrate); the chief impurities are silica, iron, and titanium. Gallium is present in significant amounts and has been recovered as a by-product. Other by-products of alumina production and other alumina sources in the bauxite region may be utilized in the future.

Briefly these possibilities are the following:

- (1) Recovery of titanium, iron, and columbium from the black sands and red muds that are currently waste products from alumina production.
- (2) Recovery of iron and alumina from large high-iron bauxite deposits.
- (3) Recovery of alumina from the vast deposits of high-alumina clay associated with bauxite deposits (estimated to total over 100 million tons).

A.P. Green Refractories Company mines kaolinite clay associated with the bauxite deposits, for production of high heat duty clay refractories.

Bauxite reserves in the region are estimated to be about 60 million long tons, averaging 50 percent alumina and 10 percent silica; no cutoff on iron is assumed. Of this total about 56 million tons occur in Saline County and 4 million tons in Pulaski County.

STOP 7: SYENITE QUARRY, PULASKI COUNTY, ARKANSAS

We thank Mr. George Dumont, mining engineer and quarry supervisor, for permission to visit this quarry. You are requested not to take photographs.

3M's Big Rock Quarry (fig. 7) is in the largest sure of Arkansas igneous rock (syenite), covering some 6 square miles south of Little Rock. This area, shown on the Little Rock 7.5-minute Quadrangle as Granite Mountain, and in older literature as Fourche Mountain, is the dome or boss of a buried large Late Cretaceous batholith intruded into intensely folded Paleozoic sedimentary rocks. Paleocene (Midway Group) and Eocene (Wilcox Group) sediments cover low-lying portions of the batholith. Bauxite deposits

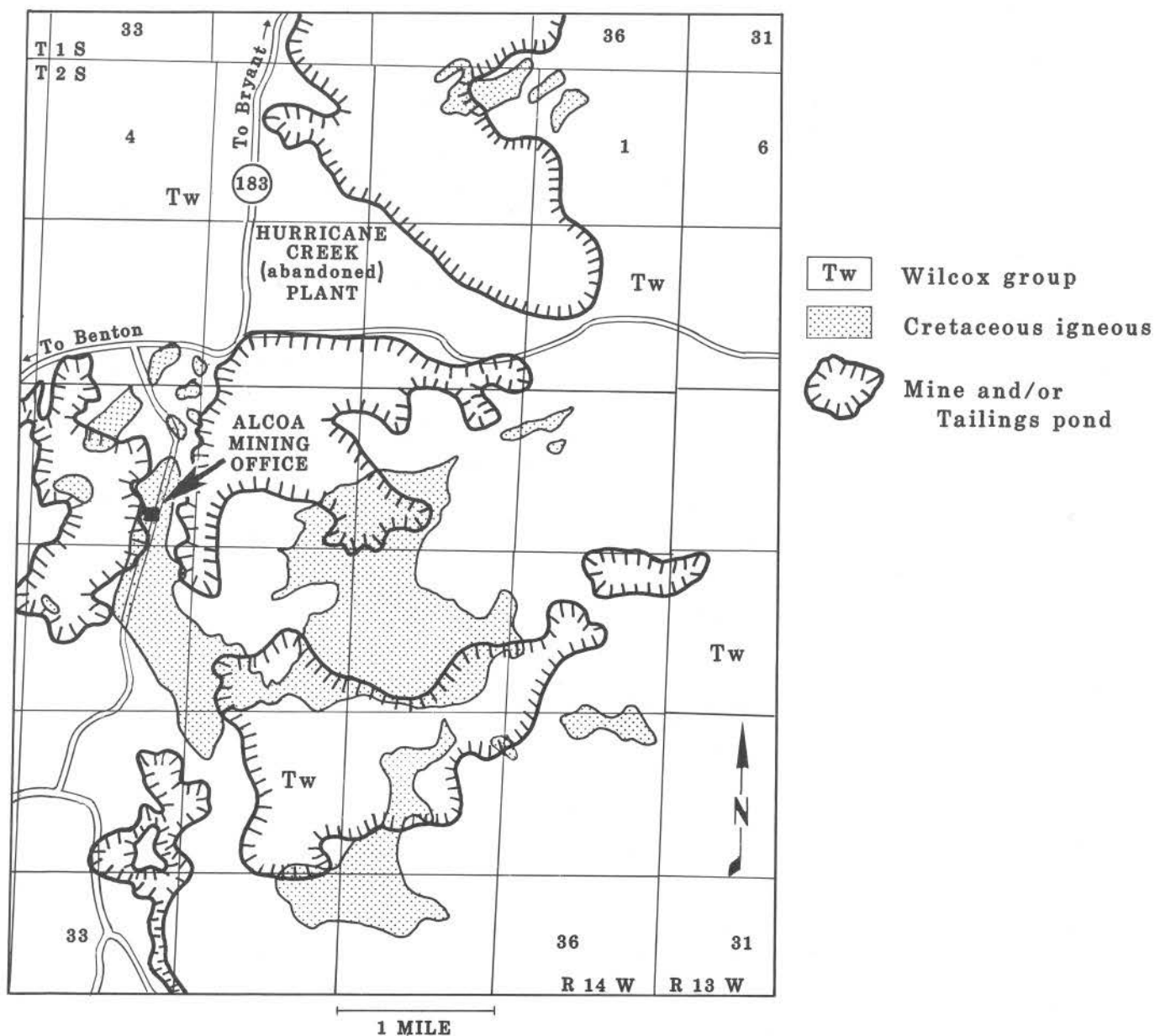


Figure 6 — Bauxite mines, east of Bryant, Saline County, Arkansas.

mined in Pulaski and Saline Counties resulted from lateritic weathering of syenite (Gordon et al., 1958).

Notable features in the quarry are jointing and spheroidal residual boulders formed by weathering along joints, small segregation veins, rare xenoliths and gas cavities, fracture-filling fluorite, trachytic textures, and subtle zones of flow banding. Collectable rock types are "blue" syenite (pulaskite) and "gray" syenite (nepheline syenite).

Williams (1891) described pulaskite as a rock made up of orthoclase, pyroxene (var. diopside and aegirine), amphibole (var. arfvedsonite), and a little eleolite (nepheline) or its decomposition product analcime. Johannsen (1938) defined pulaskite as "a granular to trachytoid rock of Family 2113, and as consisting essentially of a potash-feldspar, usually cryptoperthite, and a small amount of nepheline and pyribole." These rocks are now classified as foid-bearing alkali-feldspar syenite and foid syenite in the

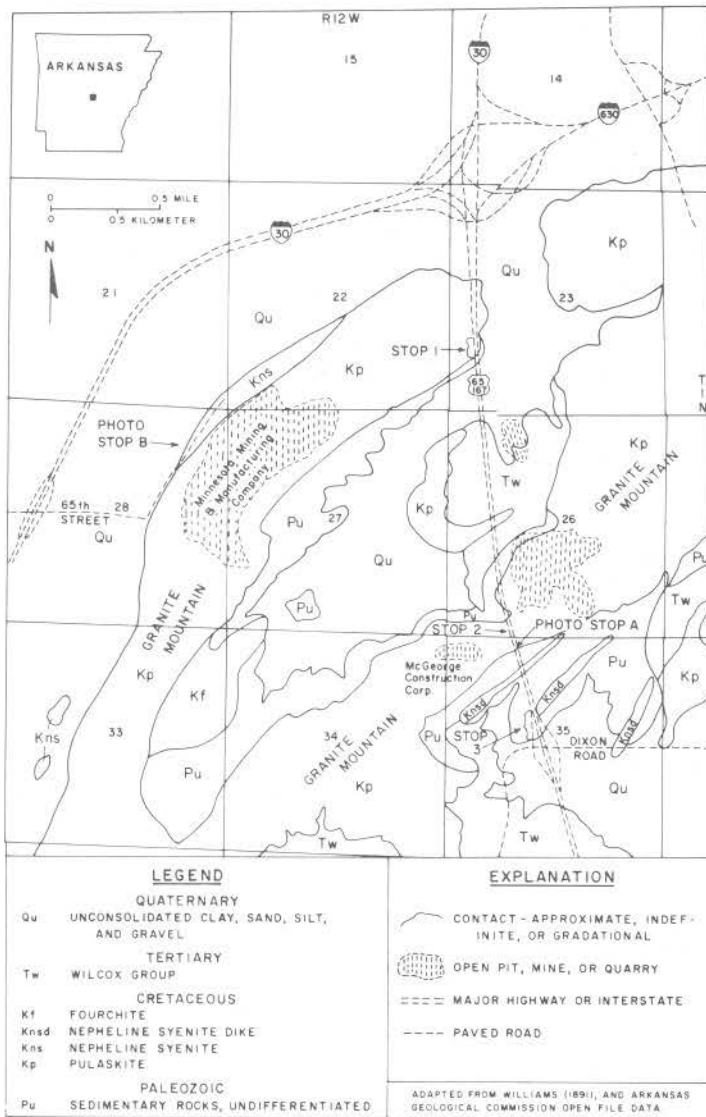


Figure 7— Granite Mountain area, southeast of Little Rock, Pulaski County, Arkansas.

nomenclature of Streckeisen et al. (1973). Mega-
 scopically, the rock is gray, varying from dark bluish
 gray to light gray. The structure is semi-porphyr-
 itic; large feldspars form the principal part of the rock.
 Between the larger feldspars is a finer grained
 second generation of feldspar and an occasional
 biotite flake or crystal of hornblende or augite.
 Microscopically, the texture is between hypauto-
 morphic-granular and granito-porphyr-
 itic. This rock makes up the greater part of Granite Mountain,
 particularly the ridges and higher slopes. Spher-
 oidally weathered boulders are in the upper parts of
 the quarry. Rare miarolitic cavities containing zeo-
 lites are sometimes formed, most frequently along
 the west highwall near the contact with the Paleo-
 zoic sediments.

3M Company produces large tonnages of stone
 for roofing granules. A private contractor also pro-
 duces some aggregate rock from this quarry.

REFERENCES

- Gordon, Mackenzie, Jr., Tracey, J.I., Jr., and Ellis, M.W., 1958, Geology of the Arkansas bauxite region: U.S. Geological Survey Professional Paper 299, 268 p.
- Howard, J.M., and Steele, K.F., 1988, Igneous rocks at Granite Mountain and Magnet Cove, Arkansas, *in* Hayward, O.T., ed., South central section of the Geological Society of America: Geological Society of America Centennial Field Guide, Vol. 4, p. 259-262.
- Howard, J.M., and Stone, C.G., 1988, Quartz crystal deposits of the Ouachita Mountains, Arkansas and Oklahoma, *in* Colton, G.W., ed., Proceedings of the 22nd Forum on the Geology of Industrial Minerals: Arkansas Geological Commission Miscellaneous Publication MP-21, p. 63-71.
- Stone, C.G., and Bush, W.V., 1982, Guidebook to the geology of the eastern Ouachita Mountains: Arkansas Geological Commission Guidebook 82-2, 24 p.
- Stone, C.G., Howard, J.M., and Haley, B.R., 1986, Sedimentary and igneous rocks of the Ouachita Mountains of Arkansas; A guidebook with contributed papers — Part 1: Arkansas Geological Commission Guidebook 86-2, 151 p.
- Stone, C.G., Howard, J.M., and Holbrook, D.F., 1982, Field guide to the Magnet Cove area and selected mining and mineral collecting localities in central Arkansas: Arkansas Geological Commission Guidebook 82-1, 31 p.

Field Trip No. 19
(Guidebook Published Separately)

**MISSISSIPPI VALLEY-TYPE
MINERALIZATION OF THE
VIBURNUM TREND, MISSOURI**

Richard D. Hagni
Department of Geology
125 McNutt Hall
University of Missouri
Rolla, Missouri 65401

and

Raymond M. Coveney, Jr.
University of Missouri
Kansas City, Missouri 64110

FIELD TRIP SUMMARY

This volume was prepared for a field trip sponsored by the Society of Economic Geologists, in conjunction with the 1989 annual meeting of the Geological Society of America. The volume contains descriptions of the geology of four mines in the Viburnum Trend, descriptions of mine stops, articles on selected aspects of the geology of the Trend, and road logs.

The Viburnum Trend is the world's largest lead producer, and it is an important producer of zinc, copper, and silver. In the past few years, there have been significant new mining developments and geological discoveries in the Trend. The new Casteel (or Viburnum 35) and West Fork mines have been opened by Doe Run Company and ASARCO Incorporated. The Sweetwater (or Milliken or Ozark Lead) mine has been purchased and reopened by ASARCO. The Magmont West orebody, a new mining development about 2 mi west of the main orebodies at the Magmont mine, has been opened by Cominco American. In addition to these new mines and deposits, production continues at the Viburnum 28 and 29 mines, Magmont, Buick, and Fletcher mines.

The accessibility of these new and reopened mines and the previously operating mines provides the opportunity to obtain new geological information. Unusually large amounts of copper have been discovered to occur with the lead-zinc ores at the Casteel mine; Bob Dunn and Bill Grundmann discuss those ores. Well-developed metal zoning discovered at the West Fork mine is the topic discussed by Rick Dingess. Bud Walker gives a new understanding of the structural conditions that favor and control ore

deposition at the Sweetwater. Milt Bradley describes the unusually zinc-rich ores controlled by narrow fracture zones in the Magmont West orebody.

Collaborative studies by the U.S. Geological Survey and the Missouri Department of Natural Resources, Division of Geology and Land Survey contribute to a better understanding of the regional aspects of the ore deposits. Viets and Leach summarize some of those results in a paper in this volume. Research studies by professors and graduate students at various universities provide new information about mineralogy, temperatures of deposition, and regional aspects. Ray Coveney has contributed a paper on the possible relationships among metal-rich Pennsylvanian black shales, minor occurrences of sphalerite in Paleozoic carbonates, and ores in the main MVT mining districts. Dick Hagni reviews the mineralogy and other geologic aspects of the Viburnum Trend.

Ernie Ohle and Paul Gerdemann review the complicated, but fascinating history of discovery of the ore deposits of the Viburnum Trend in this volume. Gregg and Gerdemann discuss the Bonneterre Formation's varied facies that control ore deposition. Hagni reviews the application of ore microscopy and other process mineralogy techniques to a variety of metallurgical problems in the Viburnum Trend.

Each field trip participant will visit one of several operating properties: the Casteel, West Fork, Sweetwater, or the Magmont mine. Participants will also have the opportunity to examine the varied facies of the host rock Bonneterre Formation in outcrops.

*Richard D. Hagni
Raymond M. Coveney*

MISSOURI DEPARTMENT OF NATURAL RESOURCES

G. Tracy Mehan, III, Director

DIVISION OF GEOLOGY AND LAND SURVEY

*James Hadley Williams, Ph.D., Director and State Geologist

Sarah Hearne Steelman, M.A., Deputy Director

Tami Allison, Division Secretary

ADMINISTRATION AND GENERAL SUPPORT PROGRAM

*James A. Martin, M.S., Principal Geologist and Acting Program Director

*Wallace B. Howe, Ph.D., Adjunct Professor and Research Geologist

Personnel/Fiscal Management

Carolyn Ellis, Executive I
Barbara Kennedy, Accountant I
Terry Brenner, Clerk-Typist III
Susan Davault, Clerk-Typist II

Computer Services

+Cathy Primm, B.A., Prog. Analyst III

Buildings and Grounds

Luther Fryer, Labor Supervisor
Gene Lewis, Maintenance Worker I
Carl Kuelker, Laborer I
Ellis Humphrey, Custodial Worker II

Geographic Information Systems

Gregory L. Easson, M.S., Geologist III
Kim E. Haas, Geology Technician II

Information Services

*W. Keith Wedge, Ph.D., Chief
Arthur W. Hebrank, B.S., Geol. III
Robert H. Hansman, Ph.D., Editor
Barbara Miller, Clerk III
Jane Lea, Pub. Dist. Mgr.
Kayla Brockman, Clerk-Typist II

Gary Clark, B.S., Graphics Supvr.
Susan C. Dunn, B.F.A., Artist III
Billy G. Ross, Artist II
Phillip Streamer, Artist II
Betty Harris, Clerk-Typist II

GEOLOGICAL SURVEY PROGRAM

*Jerry D. Vineyard, M.A., Program Director and Deputy State Geologist

*James A. Martin, M.S., Principal Geologist
Sharon Krause, Clerk-Typist II**Engineering Geology**

James W. Duley, B.S., Chief
James Vaughn, B.S., Soil Scien. III
David Hoffman, P.E., M.S., Geol. III
*James C. Brown, Jr., B.S., Geol. III
Mimi Garstang, B.S., Geol. III
Gary St. Ivany, B.A., Geol. II
Peter Price, B.S., Geol. II
Myrna Reiff, B.A., Geol. II
Jim B. Fels, B.S., Geol. I
Ben Pendleton, B.S., Geol. Tech. II
Danny Sherman, Geol. Tech. I
Deborah Breuer, Clerk-Steno III

Economic Geology

Ira R. Satterfield, M.S., Chief
Laurence M. Nuelle, M.S., Geol. III
Ardel W. Rueff, B.A., Geol. III
Bruce Netzler, M.S., Geol. III
Kenneth L. Deason, B.S., Geol. III
Joy L. Bostic, B.S., Geol. II
Michael C. McFarland, B.S., Geol. II
Evan A. Kifer, B.S., Geol. I
Jerry Plake, Lab. Tech.
Hairl Dayton, Jr., Lab. Tech.
Lois Miller, Clerk-Typist III
Rita Brasure, Clerk-Typist II
Jeffrey C. Jacques, Lab Helper

Geologic Investigations

Charles E. Robertson, M.A., Chief
Thomas L. Thompson, Ph.D., Geol. IV
Eva B. Kisvarsanyi, M.S., Geol. IV
John W. Whitfield, B.A., Geol. III
*David C. Smith, B.S., Geol. III
James R. Palmer, B.S., Geol. III
Mark A. Middendorf, B.S., Geol. II
David M. Work, B.S., Geol. II
Cheryl M. Seeger, M.S., Geol. Tech. II
Sandra Miller, Clerk-Typist II

WATER RESOURCES PROGRAM

Steve McIntosh, M.S., Program Director

Mary Woodland, Clerk-Steno III

Leila Johnson, Clerk-Typist II

Groundwater Geology

Don E. Miller, M.S., Chief
James E. Vandike, M.S., Geol. III
Rex Bohm, B.S., Geol. II
Cynthia Endicott, B.S., Hydrologist II
Debbie Elliott, Clerk-Typist III

Well Driller's Support

Artney Lewis, B.S., Geol. II
Beth Marsala, Eng. Tech. II
Gary Penny, Eng. Tech. I
Edith Starbuck, M.S., Geol. Tech. I
Jerrri Bixler, Geol. Tech. I
Vacant, Clerk-Typist II
Kathy Ragan, Clerk III

Floodplain Management

Richard Gaffney, M.A., Planner III
Herman Skaggs, B.A., Planner II

Economics and Water Use

Robert Clark, M.A., Planner II
Jeanette Barnett, B.S., Planner I
Mary Jo Horn, Clerk-Typist II

Surface Water

John Drew, B.S., Hydrologist II
Vacant, Hydrologist II
Charles DuCharme, B.S., Hydrologist I

River Basin Policy

Charles Michael, B.A., Chief

Water Quality

Steve McIntosh, M.S.

LAND SURVEY PROGRAM

Robert E. Myers, P.E., L.S., Program Director

and State Land Surveyor

Glenda Henson, Clerk-Steno III

Bruce Wilson, B.S., Drafter II

Land Survey Projects

J. Michael Flowers, L.S., Chief
O. Dan Lashley, L.S., Project Surveyor
Robert L. Wethington, P.E., L.S., Proj. Surv.
Michael Cape, Eng. Tech. I
+Darrell Pratte, L.S., Surveyor-Parks
+Bruce D. Carter, Land Surv. Tech. II-Parks
+Richard Bates, Park Maint. Worker I-Parks

Land Corner Maintenance

Norman L. Brown, P.E., L.S., Chief
Jack C. McDermott, County Surveyor Coord.
John D. Paulsmeyer, L.S., Project Surv.
Michael Lloyd, Land Survey Tech. I
Ruth Allen, Corner Registration Clerk

Survey Document Processing

James L. Matlock, Chief
Linda Miller, Clerk-Typist III
Jane Dunakey, Clerk-Typist I

Survey Document Distribution

Diane R. Hess, Chief
Ruth A. Booker, Clerk-Typist II
Mary Davis, Clerk II

DAM AND RESERVOIR SAFETY PROGRAM

Brian J. Swenty, Ph.D., P.E., Program Director and Chief Engineer

Marge Paulsmeyer, Clerk-Typist III

Russell C. Adams, P.E., Civil Engineer
James L. Alexander, P.E., Civil Engineer
Robert A. Clay, P.E., Engineer
Ralph P. Hess, Eng. Tech. III

S.P. 5

**GEOLOGICAL SOCIETY OF AMERICA
1989 FIELD TRIP GUIDEBOOK**



**MISSOURI DEPARTMENT OF NATURAL RESOURCES
DIVISION OF GEOLOGY AND LAND SURVEY**

James H. Williams, Director and State Geologist
P.O. Box 250, Rolla, MO 65401